

**Final Research Report**

**ANALYSIS AND DESIGN OF  
WIRE MESH/CABLE NET SLOPE PROTECTION**

**Balasingam Muhunthan**

**Shanzhi Shu**

**Navaratnarajah Sasiharan**

**Omar A. Hattamleh**

Department of Civil and Environmental Engineering  
Washington State University  
Pullman, Washington 99164-2910

**Thomas C. Badger and Steve M. Lowell**

Washington State Department of Transportation  
P.O. Box 47365  
Olympia, Washington 98504-7365

**John D. Duffy**

California Department of Transportation  
50 Higuera Street  
San Luis Obispo, California 93401

Prepared for  
**Washington State Transportation Commission**  
Department of Transportation  
And in cooperation with  
**U.S. Department of Transportation**  
Federal Highway Administration

April 2005

## TECHNICAL REPORT STANDARD TITLE PAGE

1. REPORT NO. <b>WA-RD 612.1</b>	2. GOVERNMENT ACCESSION NO.	3. RECIPIENT'S CATALOG NO.	
4. TITLE AND SUBTITLE <b>ANALYSIS AND DESIGN OF WIRE MESH/CABLE NET SLOPE PROTECTION</b>		5. REPORT DATE <b>April 2005</b>	
		6. PERFORMING ORGANIZATION CODE	
7. AUTHOR(S) <b>Balasingam Muhunthan, Shanzhi Shu, Navaratnarajah Sasiharan, O.A. Hattamleh, Tom C. Badger, Steve M. Lowell, John D. Duffy</b>		8. PERFORMING ORGANIZATION REPORT NO.	
9. PERFORMING ORGANIZATION NAME AND ADDRESS <b>Washington State University Dept. of Civil and Environmental Engineering Pullman, Washington 99164-2910</b>		10. WORK UNIT NO.	
		11. CONTRACT OR GRANT NO.	
12. SPONSORING AGENCY NAME AND ADDRESS <b>Research Office Washington State Department of Transportation Transportation Building, MS 47372 Olympia, Washington 98504-7372 Kim Willoughby, Project Manager, 360-705-7978</b>		13. TYPE OF REPORT AND PERIOD COVERED <b>Final Research Report</b>	
		14. SPONSORING AGENCY CODE	
15. SUPPLEMENTARY NOTES <b>This study was conducted in cooperation with the U.S. Department of Transportation, Federal Highway Administration.</b>			
16. ABSTRACT  <p style="text-align: justify;">Since the 1950s, heavy gage wire mesh has been used along North American highways to control rockfall on actively eroding slopes. More robust fabrics, such as cable nets, have more recently been introduced to improve the capacity of these rockfall protection systems. To date, however, the design of these systems has been based primarily on empirical methods, engineering judgment, and experience. This report summarizes research that characterized existing performance, tested critical system components, back-analyzed system failures, evaluated typical loading conditions, and developed analytical models to refine engineering design of these systems. Finally, guidelines were developed to support the design of these systems for a variety of loading conditions. Specifically, the report provides design guidance on site suitability, characterizing external loads, fabric selection, anchorage requirements, and system detailing.</p>			
17. KEY WORDS <b>Rockfall, wire mesh, cable net, slope hazard mitigation, snow load, anchor, interface friction</b>		18. DISTRIBUTION STATEMENT <b>No restrictions. This document is available to the public through the National Technical Information Service, Springfield, VA 22616</b>	
19. SECURITY CLASSIF. (of this report)  <b>None</b>	20. SECURITY CLASSIF. (of this page)  <b>None</b>	21. NO. OF PAGES	22. PRICE

# TABLE OF CONTENTS

<b>CHAPTER 1 INTRODUCTION .....</b>	<b>1</b>
1.1 Problem Statement.....	1
1.2 Background.....	3
1.2.1 General Applications .....	3
1.2.2 System Elements.....	6
1.2.3 Loading Conditions .....	7
1.3 Literature Review .....	8
1.4 Research Objectives .....	9
<b>CHAPTER 2 FIELD PERFORMANCE .....</b>	<b>11</b>
2.1 Gaviota Pass, California .....	12
2.1.1 Problem Description .....	12
2.1.2 Installation Description.....	13
2.1.3 System Performance .....	14
2.2 Malibu Highway, California.....	15
2.2.1 Problem Description .....	15
2.2.2 Installation Description .....	16
2.2.3 System Performance .....	18
2.3 Rain Rocks, California .....	18
2.3.1 Problem Description .....	18
2.3.2 Installation Description.....	20
2.3.3 System Performance .....	20
2.4 Franklin Falls, Washington.....	25
2.4.1 Problem Description .....	25
2.4.2 Installation Description .....	26
2.4.3 System Performance .....	27
2.5 West Snowshed, Washington .....	28
2.5.1 Problem Description .....	28
2.5.2 Installation Description .....	29
2.5.3 System Performance .....	30
2.6 Tumwater Canyon, Washington.....	32
2.6.1 Problem Description .....	32
2.6.2 Installation Description .....	32
2.6.3 System Performance .....	34
2.7 State-of-Practice .....	35
2.7.1 Anchors.....	37
2.7.2 Support Cables.....	38
2.7.3 Fabric.....	38
2.7.4 Load-Influencing Factors .....	40
<b>CHAPTER 3 TESTING AND MONITORING DATA.....</b>	<b>42</b>
3.1 Fabric Testing.....	42
3.1.1 Objectives .....	42
3.1.2 Methodology.....	44

3.1.3 Test Specimens.....	45
3.1.4 Results .....	49
3.2 Seam Testing for Double-Twisted Hexagonal Mesh .....	51
3.2.1 Objectives .....	51
3.2.2 Methodology.....	52
3.2.3 Results .....	53
3.3 Tumwater Canyon Instrumentation .....	55
3.3.1 Objectives .....	55
3.3.2 Methodology.....	55
3.3.3 Results .....	57
3.4 Anchor Testing .....	61
3.4.1 Objectives .....	61
3.4.2 Methodology.....	62
3.4.3 Results .....	66
<b>CHAPTER 4 SNOW LOADS.....</b>	<b>75</b>
4.1 Snow Load on Avalanche Structures.....	75
4.2 Snow Load on Mesh Systems.....	78
4.2.1 Snow Load below Freezing .....	79
4.3.2 Snow Load above Freezing .....	80
4.3 Performance of Mesh Systems .....	82
4.3.1 Upper Tumwater Canyon Site #1 .....	84
4.3.2 Upper Tumwater Canyon Site #2 .....	86
4.3.3 Instrumented Tumwater Canyon Site.....	88
4.3.4 Daggett Pass, Nevada .....	89
4.3.5 Franklin Falls Site.....	91
4.3.6 US 20 Rainy Pass Site .....	92
4.4 Summary of Performance Analysis.....	95
<b>CHAPTER 5 LOCAL STABILITY OF MESH SYSTEMS.....</b>	<b>97</b>
5.1 Deformation and Strength Analysis .....	97
5.1.1 Free Sides .....	98
5.1.2 Fixed Sides .....	102
5.2 Local Failure Analysis.....	103
5.2.1 Transverse Failure .....	103
5.2.2 Seam Failure .....	105
5.3 Puncture Failure.....	107
5.3.1 Field Test Data.....	107
5.3.2 Finite Element Analyses for BCMoT.....	109
5.3.3 Back-analyses of Impacts to Mesh Systems.....	110
5.3.4 Anticipated Performance from Impact Loads .....	113
<b>CHAPTER 6 GLOBAL STABILITY OF MESH SYSTEMS.....</b>	<b>114</b>
6.1 Limit Equilibrium Model.....	114
6.1.1 Anchor Capacity .....	116
6.1.2 Interface Friction .....	116
6.1.3 Mesh Weight.....	118
6.1.4 Debris Load .....	118

6.1.5 Parametric Study of Overall System Performance .....	119
6.2 Finite Element Analysis.....	123
6.2.1 Overview .....	123
6.2.2 FE Model.....	125
6.2.3 Description of Field Tests.....	125
6.2.4 Verification of FE Analysis.....	127
6.2.5 Parametric Studies .....	131
6.3 Modeling Results.....	136
6.3.1 Anchorage and Top Connection .....	136
6.3.2 Support Cables.....	139
6.3.3 Verification of Interface Friction.....	142
6.3.4 Limiting Conditions on Global Stability .....	143
<b>CHAPTER 7 DESIGN GUIDELINES .....</b>	<b>148</b>
7.1 Site Suitability and Characterization .....	151
7.1.1 Block/Event Size .....	152
7.1.2 Slope Conditions .....	153
7.1.3 Interface Friction .....	155
7.1.4 Debris Loads.....	158
7.1.5 Impact Loads .....	159
7.1.6 Snow Loads .....	160
7.2 Design Methodology .....	162
7.2.1 Fabric Selection.....	162
7.2.2 Anchor Capacity and Spacing.....	165
7.3 Design Details and Specifications .....	168
7.3.1 Slope Coverage.....	168
7.3.2 Anchors.....	170
7.3.3 Support Ropes.....	172
7.3.4 Fabric Seaming and Fastening.....	174
7.4 Aesthetic Concerns and Mitigation .....	175
7.4.1 Limiting Coverage Area .....	176
7.4.2 Increasing Mesh Contact .....	177
7.4.3 Colorizing System Components .....	179
7.5 Construction Considerations.....	179
7.6 Maintenance.....	181
7.7 Future Work.....	182
<b>ACKNOWLEDGMENTS .....</b>	<b>183</b>
<b>REFERENCES.....</b>	<b>185</b>
<b>APPENDICES</b>	
Appendix A Survey of State-of-Practice for DOT's .....	A-1
Appendix B Fabric Test Reports .....	B-1
Appendix C Anchor Load Test Data .....	C-1
Appendix D Anchor Spacing/Load Charts.....	D-1
Appendix E Plan Sheets .....	E-1

## LIST OF FIGURES

<i>Figure</i>		<i>Page</i>
1-1	Schematic drawing shows basic elements of a drape mesh system.....	2
1-2	Typical rock anchors include (A) deformed steel threaded bar, and (B) a wire rope tendon .....	6
1-3	Typical soil anchors include (A) hollow core drillable-groutable bars and (B) MANTA RAY® .....	6
2-1	Gaviota Pass, CA, slope condition before mesh installation .....	13
2-2	Malibu Highway, CA, slope condition after the slope was covered with a cable net .....	16
2-3	Rain Rocks, CA, slope condition after the mesh installation .....	19
2-4	Slope condition after slope instabilities destroyed the hexagonal wire mesh installation at Pitkins Curve adjacent to Rain Rocks chute .....	22
2-5	Franklin Falls, WA, slope configuration for the western portion of the 1998 cable net installation .....	25
2-6A	Failure in the eastern portion of the 1982 chainlink installation .....	27
2-6B	Localized rupture by a 3- to 4-foot-diameter boulder that initiated from the bouldery talus shown at the top of photograph.....	27
2-7A	Failure of the cable net system in the western portion of the site in July 1999.....	28
2-7B	Deformation of the ground where loads exceeded passive earth pressure, causing 8 inches of anchor deflection.....	28
2-8	Looking west of the West Snowshe, WA, slope, active raveling near the crest of the cut slope and a large percentage of boulders within the debris .....	29
2-9	Note the large accumulation of debris at the juncture of the underlying support ropes and the midslope anchor.....	30
2-10	Rupture of the vertical seam and fabric; the midslope horizontal support cable was also damaged. ....	31
2-11	Tumwater Canyon, WA, slope condition before cable net installation; note the rockfall-related damage to the concrete barrier .....	33
3-1	Testing apparatus with TECCO® mesh .....	44
3-2	Setup for <i>Mac Double Galv1</i> mesh with bolts extended above the loading plates .....	47
3-3	Setup for (A) Geobruigg square grid cable net and (B) Geobruigg diagonal grid cable net.....	48
3-4	Setup for Maccaferri diagonal grid cable net utilizing modified test apparatus .....	48
3-5	Setup for Maccaferri diagonal grid cable net utilizing modified test apparatus .....	50
3-6	Tested seams included (A) butted seam with 6-inch fastener spacing, (B) single-cell overlap with 3-inch fastener spacing, and (C) two-cell overlap with doubled fasteners on 3-inch spacing.....	52
3-7	Testing/clamping apparatus and failed specimen of bulk material (no seam).....	53

3-8	Dimensions and configuration of the cable net system and layout of the instrumentation .....	56
3-9	Normalized values of load for vertical (longitudinal) strain gauges, temperature, and snow depth .....	60
3-10	Normalized values of load for horizontal (transverse) strain gauges, temperature, and snow depth .....	61
3-11	A boring log depicts the subsurface conditions in which the anchors were founded.....	63
3-12	Layout of anchors and the depths to which they were installed .....	63
3-13	The tested anchors included (A) Manta Ray <sup>®</sup> ; (B) single-strand cable; (C) deformed steel threaded bar; (D) HI-TECH (drillable-groutable); and (E) Geobruigg double-strand cable .....	64
3-14	Setup for vertical loading.....	65
3-15	Setup for horizontal loading.....	66
3-16	Load versus displacement plot for all vertical anchor tests .....	67
3-17	The data from Anchor 7 in Figure 3-16 are plotted as a hyperbolic relation .....	69
3-18	Ground cracking (white painted lines) that developed around Anchor 17 (double cable anchor) during vertical loading .....	70
3-19	Load-displacement plot for horizontal test of a Manta Ray <sup>®</sup> anchor (#4).	72
3-20	Load-displacement plot for horizontal test of a double-strand cable anchor (#16).....	73
3-21	Load-displacement plot for horizontal test of a single-strand cable anchor (#20).....	73
4-1	Stress components of snowpack upslope of an avalanche structure.....	76
4-2	A cross-section of snowpack upslope of an avalanche structure illustrates the distribution of drag force and velocity along the slope.....	77
4-3	The force components of the mesh and snowpack when the snow is bonded to both to the mesh and ground.....	79
4-4	The force components of the mesh and snowpack when the snow is bonded to the mesh but uncoupled from the ground.....	81
4-5	The force components of the mesh and snowpack snow, including the contribution of interface friction.....	82
4-6	Upper Tumwater Canyon Site #1 mesh installation (yellow line) on a planar and relatively smooth slope segment upslope of the steep bedrock exposures at roadway level .....	84
4-7	Cross-section of installation with slope configuration and area of snow accumulation .....	85
4-8	Upper slope area before 1997 installation and the area where snow accumulates.....	86
4-9	Slope area in (A) 1997 before and (B) 2002 five years after mesh installation and just after repair of the system .....	87
4-10	Upper Tumwater Canyon Site #2, cross-section of installation shows approximate slope configuration.....	88

4-11	Daggett Pass, NV, eastern half of the damaged installation still partially suspended on the slope, held in place mostly through interface friction and the few remaining intact anchors .....	90
4-12	Cross-section through failed cable net shows the portion of the installation that accumulated snow.....	91
4-13	US 20 Rainy Pass Site slope conditions; snow accumulation occurs on the upper portion of the slope .....	93
4-14	Cross-section shows upper and lower slope segments .....	94
4-15	View looking downslope; note numerous boulders protruding into the mesh.....	94
5-1	Displacement of single hexagonal cell at centerline of an impact cone ....	98
5-2	Deformation and movement of a single hexagonal cell.....	99
5-3	Pullout displacements versus pullout resistance assuming free sides.....	101
5-4	Deformation of single hexagonal cell with two sides fixed.....	102
5-5	Applied load versus displacement of a cell assuming fixed sides .....	103
5-6	Forces on a circular membrane .....	104
5-7	Assumed circular cross-sectional shape of the mesh and the conditions that would result in seam failure.....	106
5-8	US 12 White Pass Site #1, modified cable net installation, upslope source of rockfall, and typical range of block sizes that impact the installation in a sub-perpendicular orientation.....	111
5-9	US 12 White Pass Site #2, (A) Configuration of slope and installation. (B) Enlarged view of top of mesh, downslope of chute. ....	113
6-1	Mesh installation and loads that act on the system.....	115
6-2	Effects of debris accumulation ( $H$ = height of debris) on anchor load as a function of slope angle with an assumed interface friction angle ( $\delta$ ) of $36^\circ$ and debris accumulation angle ( $\phi_{cs}$ ) of $35^\circ$ .....	121
6-3	The effects of interface friction angle ( $\delta$ ) on anchor load for 30-m (100-ft) slope heights for a range of debris heights on a $50^\circ$ slope.....	122
6-4	The effects of interface friction angle on anchor load for a 30-m (100-ft) high slope with no external load on the system.....	122
6-5	Finite element discretization shows loads ( $P$ ) and forces ( $F$ ) acting on mesh.....	124
6-6	Test setup and locations of load cells .....	126
6-7	The direction of loading of the TECCO <sup>®</sup> mesh by the steel beam and the load transfer to perimeters (support ropes and anchors) of the mesh pane .....	126
6-8	Stress- strain relationship for TECCO <sup>®</sup> G65 mesh .....	128
6-9	FE model setup shows locations of anchors and beam .....	129
6-10	Stress contours for Test 1 .....	130
6-11	Logarithmic strain contours for Test 1 .....	130
6-12	Anchor arrangements that were investigated for a mesh system of 50 ft (18 m) wide by 100 ft (30 m) long.....	132
6-13	Stress contours for arrangement 1.....	134
6-14	Strain contours for arrangement 1.....	134
6-15	Stress contours for arrangement 6.....	135

6-16	Strain contours for arrangement 6.....	135
6-17	Anchor load v. spacing for double-twisted hexagonal wire mesh for a vertical slope (no interface friction) ranging in height from 50 to 300 ft (15 to 90 m).....	137
6-18	Anchor load v. spacing for TECCO® G65 mesh for a vertical slope (no interface friction) ranging in height from 50 to 300 ft (15 to 90 m).....	138
6-19	Anchor load v. spacing for cable nets for a vertical slope (no interface friction) ranging in height from 50 to 300 ft (15 to 90 m).....	138
6-20	Mesh without support ropes.....	139
6-21	Mesh with top horizontal support rope.....	140
6-22	Mesh with top horizontal and vertical support ropes.....	140
6-23	Mesh with top and interior horizontal support ropes.....	140
6-24	Mesh with both vertical and horizontal support ropes.....	141
6-25	The arrangement for verification of assigned friction includes a top horizontal cable and the inclusion of an internal point of support to simulate a protrusion on the slope.....	143
6-26	Load distribution in the top horizontal support rope.....	146
7-1	Recommended design approach for wire mesh/cable net systems.....	150
7-2	Cross-sections show typical (A) concave and (B) convex slopes and the areas of mesh contact, debris accumulation, and rockfall impacts.....	154
7-3	Ongoing erosion threatens a wire mesh system installed in the late 1980s in the North Cascades of Washington.....	155
7-4	Rough slopes exhibit a high degree of surface roughness with planar, uniform profiles.....	157
7-5	Undulating slopes exhibit profiles with (A) somewhat uniform particle distribution with limited overall roughness, and (B) numerous localized protrusions.....	157
7-6	These planar slopes exhibit little surface roughness or slope irregularity.....	158
7-7	Coverage area depicted by stationing and slope length.....	169
7-8	Testing setup of anchors in a sub-horizontal direction.....	171
7-9	(A) The mesh was carefully installed to closely conform to this moderately inclined slope. (B) On a steep to overhanging slope where mesh conformance is generally more difficult to achieve, the mesh can become more visually apparent.....	178

## LIST OF TABLES

<i>Table</i>		<i>Figure</i>
2-1	Current DOT practice for wire mesh/cable net system components .....	36
3-1	Description of tested specimens.....	46
3-2	Results from tension testing by WMEL.....	50
3-3	Anchors and test type.....	64
3-4	Theoretical ultimate vertical load of anchors.....	70
3-5	Test results for horizontal anchor load.....	74
6-1	Test results for various loading configurations.....	127
6-2	Summary of reactions obtained from FE analysis of field tests .....	129
6-3	Stress and strain for six scenario arrangements of anchors .....	133
6-4	Shear stress on three anchor diameters for six arrangements .....	133
6-5	Moduli and yield strengths of mesh types .....	136
6-6	Summary of von-Mises stresses for support rope arrangements .....	141
6-7	FE analysis results for interface friction .....	143
6-8	Mesh yield states as function of height for a vertical slope with no inter- face friction .....	144
6-9	Mesh yield states as a function of debris load .....	145
6-10A	Maximum length for top horizontal support rope v. slope height for double-twisted hexagonal and TECCO <sup>®</sup> mesh (no interface friction).....	146
6-10B	Maximum length for top horizontal support rope v. slope height for cable net backed with double-twisted hexagonal mesh (no interface friction) ...	147
7-1	Recommended fabric usage as a function of block size .....	164
7-2	Recommended maximum anchor spacing as a function of slope height...	166
7-3A	Recommended maximum length for top horizontal support rope v. slope height for double-twisted hexagonal and TECCO <sup>®</sup> mesh .....	173
7-3B	Recommended maximum length for top horizontal support rope v. slope height for cable net backed with double-twisted hexagonal mesh .....	173

# CHAPTER 1 INTRODUCTION

## 1.1 PROBLEM STATEMENT

Since the 1950s, heavy gage wire mesh has been used along North American highways to control rockfall on actively eroding slopes. Within the last 15 years, small diameter wire rope (cable) nets have been employed as a more robust alternative to wire mesh. To date, these systems have been designed primarily by empirical methods, engineering judgment, and experience. With the exception of the anchors and support cables, the basic design of these systems is comparatively similar throughout the U.S. It consists of a top horizontal cable suspended by regularly spaced anchors, typically a perimeter or widely spaced grid of support cables, and chainlink or double-twisted hexagonal wire mesh fabric laced to the support ropes (Figure 1-1). This basic design has been used by the Washington State Department of Transportation (WSDOT) since the late 1950s, where its use was originally limited to slopes less than 75 feet (23 m) high. However, even some of the earliest installations were successfully installed on slopes over 150 feet (45 m) high. Now, both wire mesh and cable net slope protection systems are routinely being installed on slopes far in excess of 75 feet. The basic design has been modified to address a variety of slope and loading conditions, so that numerous design variations now exist.

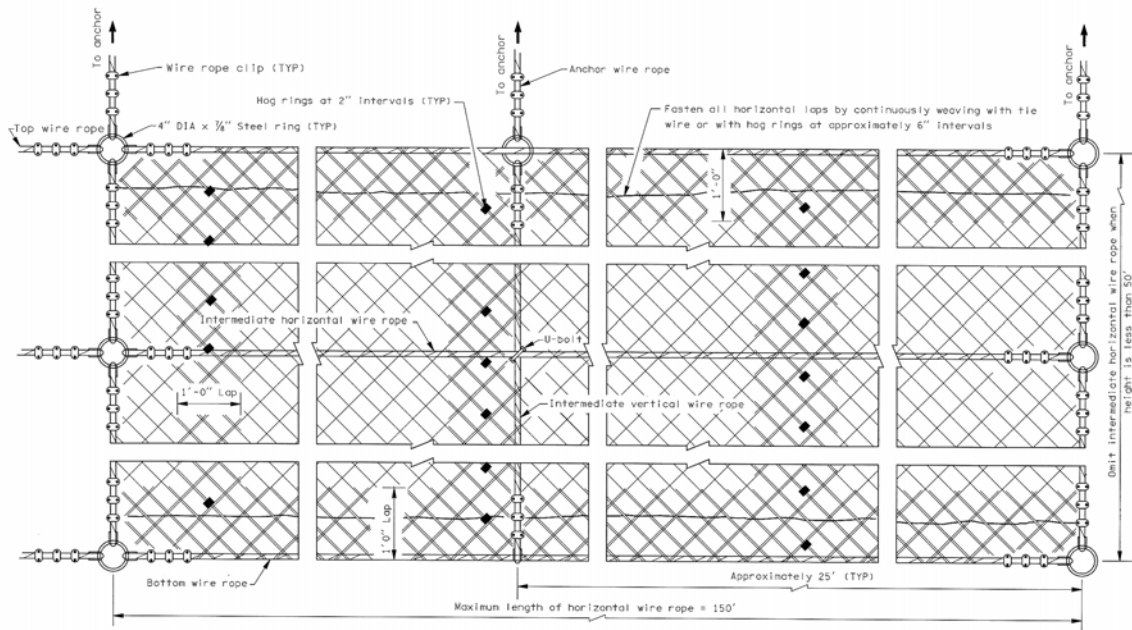


**Figure 1-1. Schematic drawing shows basic elements of a drape mesh system.**

While these basic designs have not been supported by quantitative design methodology, with one noted exception (Sandwell, 1995), overall, these systems have functioned very well. Recently, some consensus has developed among geotechnical specialists and contractors that certain system elements may be over-designed or even unnecessary. In addition, system failures under a variety of loading conditions have occurred within the last several decades, indicating that certain design elements may in fact be under-designed for their desired application. Although incomplete site characterization and inappropriate applications have been factors for some system failures, a general lack of understanding regarding load and energy transfer, as well as system capacity, remains a fundamental design obstacle. Furthermore, little quantified knowledge exists about two primary causes of system failures, debris accumulation and snow loading, and practical design guidance is needed for these loading conditions.

Given the design unknowns and observed performance of wire mesh and cable net slope protection systems, there is a substantial need to improve upon existing design methodology. The larger goals of this research are to

- develop a rational and broadly applicable design methodology
- make appropriate design revisions
- ensure optimal system performance
- where possible, construct more economical systems.

## **1.2 BACKGROUND**

The origin of and first transportation-related application of draped wire mesh for mitigating rockfall hazards is uncertain. Within the last 50 years, it has achieved widespread use in the transportation industry in the United States and Canada, due in large part to its effectiveness in controlling raveling type rockfall and its relatively low cost per unit area of treatment. Fortuitously, considerable benefit has accrued to the current research because of the large number installations and wide variety of applications that now exist in North America.

### **1.2.1 General Applications**

A number of factors influence the effectiveness, and thus appropriateness, of draped mesh systems to mitigate rockfall. These include

- orientation, length, irregularity/roughness of slope
- source, size, and frequency of rockfall
- trajectory of rockfall
- external loads such as debris and snow
- intrinsic design elements.

Draped mesh systems are commonly installed on slopes ranging from as flat as 35° to overhanging; however, most systems have probably been installed on steep rock slopes in the range of 60° to 80°. For North American highway applications, the maximum slope heights where these systems have been installed and function with minimal damage reach about 400 feet (120 m); more commonly, slope heights range from 50 to 150 feet (15 to 45 m). Mesh systems have been successfully applied to very uniform slopes and highly irregular slopes. The degree to which mesh contacts the slope is infinitely variable, since slope orientation and roughness, fabric type, and installation procedures influence it.

Draped mesh systems are most typically used to mitigate raveling type rockfall that involves small volume slope failures (< 10 cubic yards) comprising small block sizes [< 2 feet (0.6 m) in diameter for lighter weight wire mesh and < 4-5 feet (1.2 –1.5 m) for heavier weight cable nets], where other containment measures (e.g., ditches, rockfall barriers) are not available or provided. Failures of much larger volume and block size have also occurred without resultant damage to these systems. Slope raveling is a common occurrence; hence, systems are often installed on oversteepened, coarse surficial deposits (e.g., colluvium, alluvium, residual soils) and highly fractured rock masses. Many systems that are now several decades old have been installed on slopes with a high frequency of rockfall, and they exhibit little to no damage from rockfall.

Two generalized design approaches of draped mesh systems have evolved: secured and unsecured systems. The design philosophy of an unsecured system entails only anchoring the system along the top, allowing rockfall to occur between the rock face and the mesh, and controlling the trajectory into a containment area at the base of the

slope/installation. In effect, it seeks to minimize the external loading caused by accumulating debris. This design approach has further evolved in the last decade to elevated/suspended systems that contain rockfall originating upslope of the installation. Use of unsecured systems is predicated on having a suitable containment area at the base of the installation and accounting for the transient but possibly large impact load. To date, there is not a widely used methodology for designing for these transient loads, and current practice is dictated by experience. The North American transportation industry most commonly employs this unsecured design approach. Such an approach results in lower installation costs and simplified maintenance than secured systems.

Secured mesh systems incorporate anchors within the field of the mesh, often on a patterned spacing, and attempt to either stabilize the slope face (e.g., TECCO<sup>®</sup> system) or hold the debris between the mesh and the ground. This design approach is widely used in underground workings and is commonly seen along highway and rail slopes in Central Europe and Japan, where there is little tolerance for minor instability or containment area for debris accumulation. These systems are typically more costly, and those not appropriately designed may require frequent maintenance to minimize damaging debris loading.

Because many installations are located in mountainous regions in North America, many systems are exposed to snow loading. Recently, snow loading has caused several partial and entire system failures in Washington and Nevada. It is evident that, to date, the transfer of snow loads onto draped mesh systems has been poorly understood.

## 1.2.2 System Elements

Draped mesh systems consist of three primary elements: anchors, support cables, and mesh. While these common elements are shared, system components and installation details vary considerably.

Anchors can be grouped into those for intact rock or soil conditions. Rock anchors most commonly consist of a solid core, deformed steel, continuously threaded bar (Figure 1-2A) or, more recently, a wire rope tendon (Figure 1-2B) placed in a fully grouted hole. Some of the more common soil anchors include deadman-type, wire rope tendons, driven and/or grouted steel bars, hollow core drillable-groutable bars (Figure 1-3A), and MANTA RAY<sup>®</sup> (Figure 1-3B) anchors.

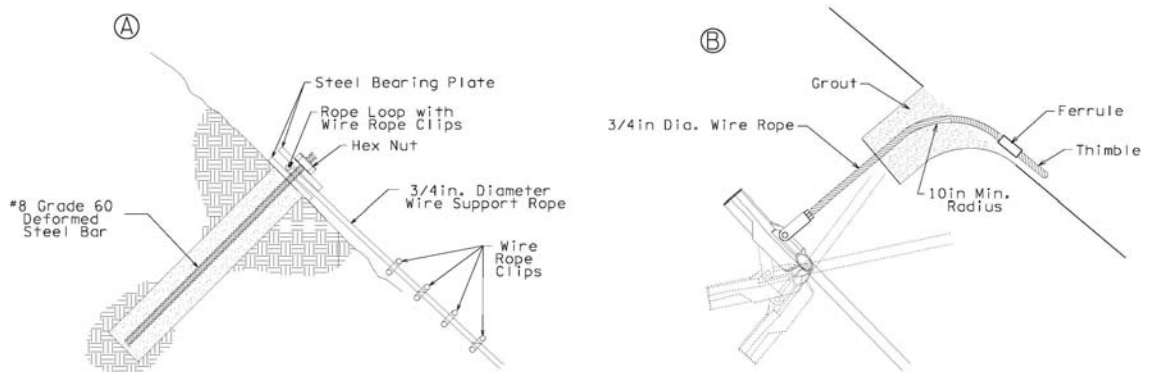


Figure 1-2. Typical rock anchors include (A) deformed steel threaded bar, and (B) a wire rope tendon.

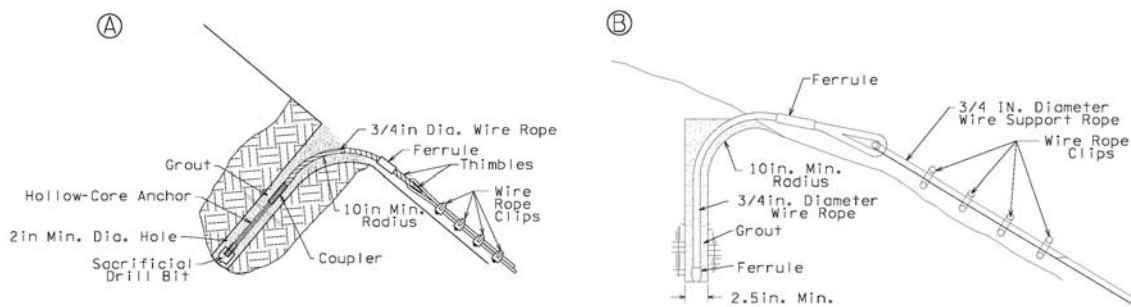


Figure 1-3. Typical soil anchors include (A) hollow core drillable-groutable bars and (B) MANTA RAY<sup>®</sup>.

A variety of support cable configurations are currently employed, varying from no support cables, to only a top horizontal cable, to an interior grid of horizontal and vertical cables.

Originally, chain link mesh was most commonly used for North American installations. In the 1980s, double-twisted hexagonal wire mesh started replacing the use of chain link mesh for slope protection systems, due in part to its higher strength (Agostini et al., 1988). In the late 1980s, cable nets were first used in North America on a 250-foot (75-m) high rock cut in the North Cascades of Washington State, after two previously installed, hexagonal wire mesh systems failed because of frequent, high-energy rockfall and severe ice loading. Around 2000, high tensile steel wire mesh (TECCO<sup>®</sup>) was introduced in North America as another high-strength mesh alternative.

### **1.2.3 Loading Conditions**

Load sources on draped mesh systems include the following:

- self-weight
- rockfall impact
- debris accumulation beneath the mesh
- snow/ice accumulation on top of the mesh.

Self-weight is the summation of system component weights, which includes the fabric, support ropes, lacing wire, and related appurtenances. Load transfer occurs in a complex manner through the mesh into the anchors. Support of the system is achieved through interface friction where the mesh is in contact with the slope and the anchors.

For unsecured systems, the primary design objective is debris containment rather than slope stabilization. It is, therefore, anticipated that most unsecured systems will be

repeatedly exposed to transient impact loads. The orientation and degree of loading is defined by the rockfall trajectory between the mesh and the slope. For typical installations installed against a steep slope, this impact loading is directed obliquely or near parallel to the mesh. The resultant load is then transferred in a complex manner through the mesh to the anchors.

Debris accumulation between the mesh and the slope can occur on unsecured systems and is a common cause of observed local and global system failures. Accumulation most commonly occurs where horizontal seams or support ropes inadvertently trap debris, or when the bottom of the mesh is pinned or buried, often by snow. Less commonly, protrusions on detached rock and abrupt slope convexities/irregularities can cause debris accumulation. Because of the sizable weight of earthen debris, its accumulation can rapidly impart damaging, unintended loads onto the system. Vegetation that grows through the mesh could also be considered as a debris load, particularly if the substrate is creeping or otherwise unstable.

Snow and ice accumulation is another source of loading in some geographic areas and has been a source of several recent system failures in Washington and Nevada. It is notable that the weight of a relatively thin snowpack of 1 to 2 feet on even a short length of slope is very great. Both the system and the ground potentially carry this load. Yet the degree to and manner in which load is transferred to the system have been largely unknown.

### **1.3 LITERATURE REVIEW**

While experience with these various designs has grown considerably, especially in the last decade, only one known study (available for citation) has attempted to

quantitatively evaluate the system components and overall performance of a mesh slope protection system (Sandwell, 1995). The Sandwell study, which was commissioned by the British Columbia Ministry of Transportation (BCMOT), used finite element modeling to evaluate the structural strength of their double-twisted, hexagonal wire mesh system to resist specified impact energies at several scenario locations. The modeling was used as a basis to make structural refinements to BCMOT's designs. Officine Maccaferri S.P.A. published a technical manual in 1988 (Agostini and others) for use in the design of rockfall protection systems. The publication includes some information on mesh properties, as well as general details and design guidelines for its products.

#### **1.4 RESEARCH OBJECTIVES**

The overall objective of this research was to develop design guidelines and generalized plans and specifications for unsecured wire mesh and cable net slope protection systems that can be applied by a geotechnical specialist to a broad range of field conditions. Toward this end, the research

- summarized the experiences of numerous designers, contractors and suppliers specializing in rockfall control
- evaluated contributing factors of numerous system failures
- instrumented a large cable net system to evaluate snow loading
- performed strength testing on various fabrics and seaming configurations for hexagonal mesh
- performed extensive structural and finite element analyses of these systems to better understand the performance of these systems
- compared the vertical and horizontal capacities of various anchors.

The specific goals of the project were as follows:

- (1) Develop methods to evaluate design loads from debris accumulation and snow, and study the global stability of the slope protection system.
- (2) Develop methods to analyze the structural capacity of system components.
- (3) Develop methods to describe load transfer characteristics.
- (4) Establish the resistance contributions from interface friction and anchors.
- (5) Refine the available methods of snow loading analysis with instrumentation and back-analysis of failed systems.
- (6) Develop methods to evaluate the local stability of mesh.
- (7) Develop an analytical method to assess the anticipated energies from impact loads

The results of the above objectives were used to develop design guidelines for slope protection systems for a variety of field conditions.

## **CHAPTER 2**

### **FIELD PERFORMANCE**

Rockfall initiation and trajectory are difficult to predict and quantify. Geology and climate are the principal causal mechanisms of rockfall, factors that include intact condition of the rockmass, discontinuities within the rockmass, weathering susceptibility, ground and surface water, freeze-thaw, root-wedging, and external stresses (Smith and Duffy, 1990; Hearn and Akkaraju, 1995; Hearn et al., 1995). Trajectory is a function of slope and rock geometry, as well as the slope and rock material properties (Ritchie, 1963; Pfeiffer, 1989). All of these factors that affect initiation and trajectory can be variable within and between slopes. The performance of rockfall control measures such as wire mesh/cable net systems is largely dictated by proper characterization of these factors and understanding of the function and limitations of the applied mitigation.

By examining the field performance of a select number of existing systems, this chapter seeks to summarize experience gained from more than five decades of application. This review had three principal objectives. The first was to characterize the limitations of these systems. Hence, the examples represent the more extreme range of loading conditions with regard to frequency, block/event size, impact energy, and external (snow) loads. Second, the review sought to identify the salient features of the design guidelines, installation, and performance. Last, these data were used to verify and calibrate analytical methods and support design recommendations that are presented in subsequent chapters.

The examples were selected from a number of sites visited by the investigators with input from the Technical Advisory Committee (TAC). For each site, the

presentation has been organized to provide a description of the rockfall hazard, installation, and performance.

## **2.1 GAVIOTA PASS, CALIFORNIA (HEXAGONAL WIRE MESH)**

### **2.1.1 Problem Description**

The Gaviota Pass site is located on California State Highway 101 between mileposts (MP) 46.80 and 47.90 in Santa Barbara County. Situated within the Santa Ynez Mountains, the Gaviota Pass is a steeply incised canyon of the Gaviota Creek drainage. The northbound and southbound lanes of Highway 101 are on opposite sides of the Gaviota Creek at an approximate elevation 200 feet. Steep slopes bound the roadway corridor, with the highest elevations above 3000 feet. Short duration, high intensity rains are common during the winter months, sometimes resulting in 3 to 5 inches per event, and high winds with gusts of up to 50 mph are common during the summer months. The rockfall that affects the highway primarily develops in the lower portion of the canyon, predominantly within the cut slopes (Figure 2-1). The cut slopes comprise Gaviota Sandstone, Holocene colluvium, and Quaternary landslide deposits. The cut slopes were designed with midslope benches and slope ratios from near vertical to 0.5H:1V. Rockfalls develop in the landslide and colluvial deposits as the result of differential erosion. Within the sandstone, rockfalls develop as planar and wedge rock block failures. In addition, the midslope benches gradually fail and fill with debris, creating rock-launching ramps. Small-scale rockslides, debris flows, and debris avalanches occur occasionally. Although some rockfall catchment area is available at the base of the slope, rockfalls 1 to 2 feet in dimension have reached the roadway.



**Figure 2-1. Slope condition before mesh installation; yellow line delineates coverage area**

### **2.1.2 Installation Description**

A hexagonal wire mesh system was constructed in 1992 to mitigate the rockfall hazard at two locations. One installation was approximately 200 feet wide and covered about 130 feet of slope length. The other site was approximately 260 feet wide and covered about 150 feet of slope length. The Gaviota drapery system was typical of California drapery design at the time. Along the top of the slope, 6-foot-long rock anchors were installed, set back from the top of the slope 6 to 9 feet. Anchor spacing was 20 feet or at significant changes in topography. The anchors consisted of 1-inch-diameter, threaded steel bar placed in a 2 ½-inch-diameter hole in bedrock and/or colluvium. A ½-inch cable (support cable) was laced through rings at each anchor secured by a nut and two washers. The wire mesh was attached to the support cable by folding the wire mesh

over the cable and securing the fold with hog rings spaced every 12 inches. Once attached, the mesh was draped down slope to road level. As the mesh was unrolled down the slope, workers pressed down on the mesh to conform it to the slope face. Vertical cables were used in an attempt to pull the wire mesh closer to the slope. The mesh was connected to the cables with a ¼-inch-diameter lacing cable. The wire panels overlapped a minimum of 12 inches and were connected with hog rings at 12-inch spacing. A horizontal cable was placed along the bottom of the mesh to dampen the curling effect of the wire mesh. Before installation, vegetation was pruned to ground level. Approximately 29,063 square feet of wire mesh were installed at both locations.

An estimated 70 percent of the wire mesh is in contact with the slope. The system was designed to allow for rocks to pass down slope in a controlled manner to a catchment area at grade. No anchors were installed in the field area of the net. The net terminates approximately 3 feet above the base of the roadway. The basis for the 20-foot maximum anchor spacing was the performance of similar systems and engineering judgment.

### **2.1.3 System Performance**

The overall performance of the wire mesh has been excellent and much better than expected. There have been no reported incidents of rockfall reaching the roadway, and vegetation is growing beneath the system. In some areas, vegetation cover has doubled from the pre-installation condition. After 12 years, the system is in good condition, with only minor damage requiring minor maintenance approximately every 5 years. The hexagonal wire mesh drapery systems, normally designed for controlling rocks smaller than 2 feet, exceeded expected levels by successfully controlling 4- to 7-cubic-yard rock slides. Although the drapery design controlled the small rockslides,

when individual block sizes within the slide mass exceeded 2 feet, the wire mesh was damaged and/or stressed. Once the drapery was installed, the interaction between the wire mesh and the rock surface increased to the extent that there is no visible load on the anchors. The horizontal cable placed along the bottom of the drapery, to prevent the bottom of the mesh from curling at the bottom, traps the rock from moving behind the mesh into the collection ditch. Trapping of rock was evident in other locations. Unfortunately, this led to increased stresses on the wire mesh and caused the mesh to tear. It was also observed that this increased stresses on the seams, causing some seams to split open. The vertical cables have not improved the ground contact of the mesh.

Ripped sections have been patched with new pieces of hexagonal wire mesh, and split seams have been re-fastened. In one section, a landslide undermined the anchor foundations, causing failure of the drapery system. The mesh and anchors were replaced, but the anchors were placed an additional 50 feet upslope to prevent further undermining.

## **2.2 MALIBU HIGHWAY, CALIFORNIA (CABLE NETS)**

### **2.2.1 Problem Description**

The Big Rock Mesa Bluff site is located on California State Route 1 between MP 42.7 and 42.9 in Los Angeles County. The highway is situated along the coastal bluffs at the base of the Santa Monica Mountains at an approximate elevation of 40 feet. The roadway passes between the coastal bluffs and the Pacific Ocean. The bluffs are part of the “Big Rock Mesa Landslide.” Short duration, high intensity rains are common during the winter months, sometimes resulting in 5 to 8 inches per event. Rockfall activity is most prevalent during heavy rainfall periods as the slide advances down slope, causing

small-scale slope instabilities such as rockslides, debris flows, and debris avalanches (Figure 2-2). The material consists of fractured sandstone overlain by Quaternary landslide deposits (angular fragments of sandstone, gravel, and silt). The slide is active and creeps during wet periods. The cut slopes have slope ratios of from near vertical to 1H:1V. Although some catchment area is available, rockfalls 3 to 6 feet in dimension, and small debris flows and rockslides 25 cubic yards in size have reached the roadway.



**Figure 2-2. Slope condition after the slope was covered with a cable net.**

### **2.2.2 Installation Description**

A cable net system was constructed in 1998 to mitigate the rockfall hazard at this site. In addition, a soldier pile wall with concrete lagging was installed to stop debris flows. The drapery installation is 400 feet wide and covers about 230 feet of slope length. The cable net was installed over portions of the slope that contained large boulders and outcrops of fractured bedrock. The cable net was constructed of 5/16-inch

cable woven into an 8-inch grid pattern with pressed steel clips. Along the top of the slope, 10-foot long rock anchors were installed, set back from the top of the slope 100 feet beyond the actively eroding brow of the cut. Anchor spacing was every 23 feet or at significant changes in topography. The anchor design called for a 1-inch-diameter, threaded steel bar, founded in a 3-inch-diameter hole in bedrock and/or colluvium. A 7/8-inch cable (support cable) was then connected to rings at 23-foot spacing. A cable tag line connected each ring to each ground anchor. The cable tag lines were secured at each anchor by a nut and two washers. Cable nets were attached to the support cable by lacing a 1/2-inch-diameter cable through the cable net and around the support cable. Once attached, the nets were draped downslope to road level. As the nets were unrolled down the slope, workers pressed down on the nets to conform it to the slope face. The cable net panels were connected to each other with a 1/2-inch cable laced through each mesh opening. Overlap was minimized as much as possible. No horizontal cables, vertical cables, or wire mesh backing were included in the design. Before installation, vegetation was pruned to ground level. Approximately 100,000 square feet of cable nets were installed.

An estimated 65 percent of the wire mesh is in contact with the slope. The system was designed to allow for rocks to pass down slope in a controlled manner to a catchment area at grade. No anchors were installed in the field area of the net. The net terminates approximately 6 feet above the base of the roadway. The basis for the 25-foot maximum anchor spacing was the performance of similar systems and engineering judgment.

### **2.2.3 System Performance**

The performance of the cable net system in controlling rockfalls has been good. There have been no reported incidents of rockfall reaching the traveled way. Because of the irregular surface profile, segments of the cable nets are not in contact with the rock surface. As mentioned previously, the interaction between the cable nets and the rock surface is in most cases sufficient to ensure stability of the system. Still, as observed in the field, the tag lines are slack, indicating no load on the anchors. Several other observations were made that are notable. The contractor built the nets and did not use standard manufactured nets. In addition, not all the cable was uniformly galvanized, and in many cases the cable started to corrode within months of the installation. The contractor also used different fasteners, some coated with zinc, some with no coating, and some were stainless steel. This resulted in two problems: corrosion and fastener tightness. In the coastal environment of salt fog and salt spray, many of the zinc-coated and non-coated fasteners corroded within months of installation. Furthermore, many of the fasteners were improperly connected or not connected. It is remarkable that in spite of very poor workmanship, this system has performed satisfactorily. The cable net, as expected, has retained rocks up to 5 ft. in dimension. In fact, these rocks have moved only minimally and have essentially been contained in place.

## **2.3 RAIN ROCKS, CALIFORNIA (HEXAGONAL WIRE MESH AND CABLE NETS)**

### **2.3.1 Problem Description**

The Rain Rocks/Pitkins Curve site is located on California State Route 1 between MP 21.1 and 21.4 in Monterey County. Known as the Big Sur Coast Road, Highway 1 winds along the base of the Santa Lucia Mountains hundreds of feet above the Pacific

Ocean. Short duration high intensity rains are common during the winter months, sometimes resulting in 4 to 6 inches per event. High winds with gusts of up to 40 mph are common during the spring. Rockfall activity is most prevalent during heavy rainfall periods, when the slopes are heated by the sun, and, to a lesser degree, during windy periods. Rockfall that affects the highway originates from the steep (0.25H:1V to 0.75H:1V) northwest-facing cut and natural slopes (Figure 2-3). Slopes in this area consist of meta-basalts (greenstone), sheared schist and phyllite with hard blocks of greenstone embedded in the matrix. Rockfalls develop as the result of differential erosion and as planar and wedge failures. Very little catchment is available, and prior to the placement of the drapery system, rockfalls and small rockslides frequently reached the roadway.



**Figure 2-3. Slope condition after the mesh installation (yellow line) at Rain Rocks site.**

### **2.3.2 Installation Description**

In 1998, a hexagonal wire mesh system was installed along the Rain Rocks section. This installation was 900 feet wide and covered about 400 feet of slope length. Along the top of the slope, 6-foot long rock anchors were installed, set back from the top of the slope 20 to 30 feet. Anchor spacing was every 40 feet or at significant changes in topography. The anchor design called for 3/4-inch-diameter cable anchors located in a 2 1/2-inch-diameter hole founded in colluvium. Manta Ray<sup>®</sup> anchors with a cable attachment were used on this project. The ends of the anchors had cable loops to which the tag line was connected with a cable loop. Cable tag lines connected the anchors to the top horizontal support cable, which was located 6 feet behind the top of slope. The support cable passed through cable loops in the ends of the tag line. The wire mesh was attached to the support cable by folding the wire mesh over the cable and securing the fold with high tensile steel (Spenax) hog rings spaced every 6 inches. Once attached, the mesh was draped down slope to road level. As the mesh was unrolled, workers pressed down on the mesh to conform it to the slope face. The mesh panels were overlapped a minimum of 12 inches and connected with Spenax rings at 12-inch spacing. Before installation, vegetation was pruned to ground level. Approximately 313,000 square feet of wire mesh were installed.

### **2.3.3 System Performance**

The overall performance of the Rain Rocks hexagonal wire mesh has been excellent. There have been no reported incidents of rockfall reaching the roadway, and vegetation is growing beneath the system. After 6 years, the system is in good condition, requiring minimal maintenance. In one case, a hole in the mesh was patched. This was

in an area where the mesh did not touch the ground, and a rock free fell into the mesh. Damage was not significant. Other maintenance has entailed clearing debris from the bottom of the mesh. The double twisted wire mesh, as expected, retains rocks up to 2 feet in dimension. In fact, these rocks have barely moved and have been essentially contained in place by the mesh weight and strength. Once the drapery was installed, the interaction between the wire mesh and the rock surface increased to the extent that there is currently no load on the anchors, evidenced by the slack in the tag lines.

In 2000, following severe winter rains, the Rain Rocks project limits were extended northward, by 150,000 square feet of slope area, in an area referred to as the Pitkins Curve Landslide. Expected rockfall sizes and rock avalanche volumes exceeded 2 feet and 20 cubic yards, respectively; however, because of cost constraints and emergency conditions, hexagonal wire mesh was installed. The installation was identical to the adjacent system except that half the ground anchors were 1-inch steel bar and half were ¾-inch cable anchors. This system worked effectively through the first year in controlling rockfalls (<2 feet in diameter) and small rockslides (<10 cubic yards). One-year later, however, increased rockfall and rockslide activity developed throughout the Pitkins Curve slide area. Relentlessly over a 3-month period, slope instability progressed upslope to the ridgeline. Every day, rockfalls 1 to 10 feet in dimension and rockslides 50 to 100 cubic yards in volume occurred. Initially, small rockslides accumulated at the toe, stressing the entire system. As debris accumulated, the load increased on the mesh, causing elongation of the wire. The Spenax rings held the mesh together, but in time the mesh began to tear apart. Under loading, the steel bar anchors bent and were compromised. The cable anchors, however, were not affected until they became

undermined. In three months, more than 20,000 cubic yards of slide debris were generated at this site. Eventually, this active instability destroyed the hexagonal wire mesh system. The drapery has not been replaced; instead, the roadway has been shifted away from the hillside, and a large rockfall catchment ditch has been constructed.

A small portion of the Pitkins Curve section extended into the original Rain Rocks installation. A small (500-cubic-yard) rockslide tore down the hexagonal wire mesh at the northern end, ripping the mesh from the infrastructure while the infrastructure stayed intact (Figure 2-4). Subsequent instabilities eventually undermined the infrastructure to failure. Again, the anchors and infrastructure were not damaged until the anchors were undermined. Within the slide scarp, a rock chute developed from which 3-foot-diameter rockfalls were regularly affecting the roadway. To mitigate this problem, the chute was covered with 7200 square feet of cable nets.



**Figure 2-4. Slope condition after slope instabilities destroyed the hexagonal wire mesh installation at Pitkins Curve adjacent to Rain Rocks chute.**

The cable net installation was 260 feet wide and covered 450 feet of slope length. The cable net was constructed of 5/16-inch cable woven into an 8-inch grid pattern with pressed steel clips. The cable was pvc coated, and the fasteners were stainless steel for corrosion protection in the harsh coastal zone. Along the top of the slope, 6-foot long rock anchors were installed, set back 100 to 200 feet beyond the actively eroding brow of the cut. Anchors were spaced at 25 feet or at significant changes in topography. Backup anchors were installed an additional 50 feet beyond the primary anchors and were used as directionals for cable tag lines. A 3/4-inch horizontal support cable was then connected to the anchors via cable tag lines of similar size. The anchor design and tag line connections were identical to those at the Rain Rocks installation. The cable net was underlain with pvc-coated, hexagonal wire mesh with 12-inch overlap and fastened with Spenax rings on 12-inch spacing. The wire mesh was first placed on the slope in one operation, and the cable nets were placed on the slope in a second operation. The drapery system was attached to the support cable by lacing a 1/2-inch-diameter cable through the cable net and around the support cable. Vertical cables were placed from top to bottom at each anchor location. The cable net and wire mesh panels were connected to each other and the vertical cables with a 1/2-inch cable laced through each mesh opening, and the wire was connected with Spenax rings at 12-inch spacing. Overlap was minimized as much as possible.

An estimated 75 percent of the wire mesh is in contact with the slope. The system was designed to allow rocks to pass down slope in a controlled manner to a catchment area at grade. No anchors were installed in the field area of the net. The net terminates approximately 50 feet above the base of the roadway.

To date, the system is functioning well, but maintenance has been necessary. Small rockslides, 5 cubic yards with rocks as large as 3 feet in dimension, have been caught in the mesh where the wire mesh and cable net were not secured tightly together. Once caught, the creeping load of the rock mass has caused local cable net fasteners to slide apart and the wire to tear in tension, resulting in an opening in the mesh panel. Repairs have consisted of patching the wire mesh with new wire mesh fastened in place with hog rings and re-establishing the cable net grid with cable clips. Other areas of concern have been at the boundaries of the cable net panels, overlapped sections of cable nets and wire mesh, and gaps in the connection between the hexagonal wire mesh and the cable nets. These are areas where rock debris is accumulating. This accumulation is imparting a load on the system, causing damage to the wire, cables, and fasteners. In contrast, rocks 1 to 4 feet in dimension and small rockslides 5 cubic yards in size creeping down slope away from the seams are causing little damage. To reduce this problem, areas likely to entrap rock debris should be eliminated. This could be improved by eliminating overlaps of the wire mesh and the cable mesh. Furthermore, the wire mesh and the cable nets should be tightly secured together. This was not successfully accomplished on the slope with this method of placement. The two fabrics should be connected together on the ground with fasteners on each side of the square of the cable net and then placed on the slope. The vertical cables also could have been eliminated. Interestingly, even with the rock accumulating in pockets in the mesh, no load is being transferred to the anchors, evidenced by slack tag lines.

## **2.4 FRANKLIN FALLS, WASHINGTON (CHAINLINK, HEXAGONAL MESH, CABLE NETS)**

### **2.4.1 Problem Description**

The Franklin Falls site is located in the central Washington Cascades adjacent to the eastbound lanes of Interstate 90 at MP 51.3 just west of the summit at Snoqualmie Pass. At elevation 3000 feet, the average maximum snowpack at the pass is 8 feet. The site consists of a 0.25H:1V (76°) cut slope in volcanic bedrock with heights to about 70 feet. Bedrock is overlain by about 20 feet of well-graded bouldery glacial till, which is mantled on the surface with 5 to 10 feet of cobble-boulder talus (Figure 2-5). Boulders 1 to 2 feet are typical, but the overburden deposits include boulders to 4 feet in dimension.

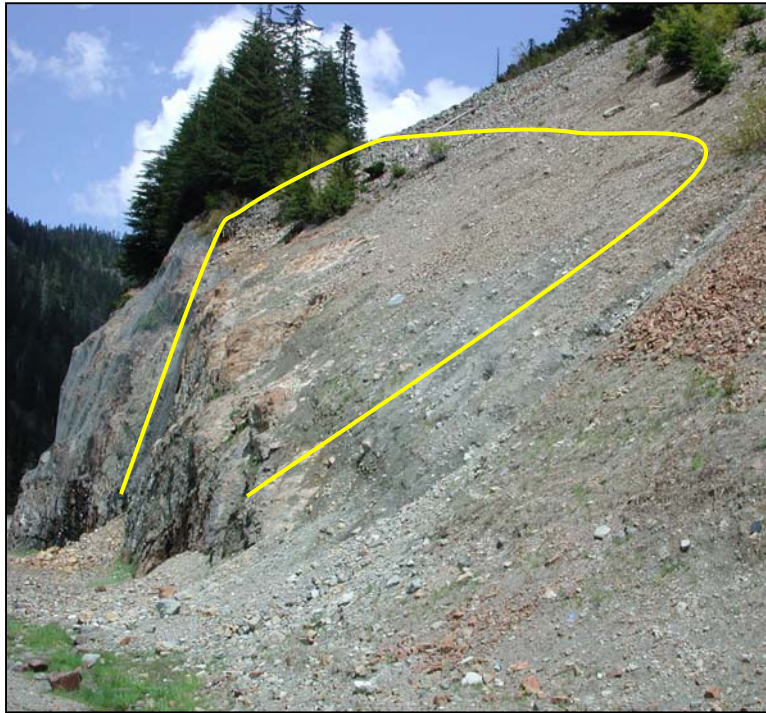


**Figure 2-5. Slope configuration for the western portion of the 1998 cable net installation (yellow line). Extreme snow loads during the winter of 1998/99 caused most of the cable net anchors located along the top of the installation to fail.**

The overburden deposits along the top of the cut are oversteepened between 1.25H:1V to 1H:1V (38° to 45°). These deposits are an active source for both raveling type rockfall

and small-scale (10 to 20 cubic yards) rotational failures. The talus slope above, which extends more than 200 feet upslope, is oriented around 38° to 40°. Snow avalanches originate above the cut, and regular avalanche control is required during the winter to mitigate for unstable snowpack.

#### **2.4.2 Installation Description**

The original installation was installed in 1982 and covered a slope area of about 800 feet in length. This early installation consisted of chainlink mesh fastened to a diagonal grid of ¾-inch-diameter wire rope cable. The support ropes had a roughly 50-foot spacing and were anchored to the slope face, where they intersected with No. 8 deformed, continuously threaded bars. Chainlink fabric was overlapped about 12 inches and seamed intermittently with light gauge steel hog rings.

Because of poor system performance and local instability of the eastern portion of the cut, the system was replaced in 1998 with sections of both hexagonal wire mesh and cable nets backed with chainlink fabric, and portions of the cut were regraded to increase the ditch width. Drillable-groutable anchors (Ischebeck Titan 30/11) were installed at a 25-foot spacing in the talus about 30 feet behind the cut slope; anchor lengths were about 6 to 8 feet.

During the winter of 1998-1999, snow accumulation was nearly twice the annual average. On the east end of the site, plowed snow covered the lower portion of the cable nets, which inhibited passage of debris behind the system. Snow accumulation on the system and localized debris accumulation behind the cable nets resulted in the failure of a several-hundred-foot section. On the west end, heavy snow accumulation had a similar effect, although the cable nets remained on the slope. In 1999, where the cable nets

remained on the slope, anchors were reinforced with a second Titan anchor placed approximately 10 feet upslope of the first anchor. The remainder of the failed nets was not replaced.

### **2.4.3 System Performance**

By the mid-1990s, the eastern portion of the initial chainlink installation was in very poor condition (figures 2-6A and 2-6B). Erosion had exposed many midslope and top anchors. Debris accumulation behind the support ropes and large boulders had caused extensive punctures and ruptures of the system.

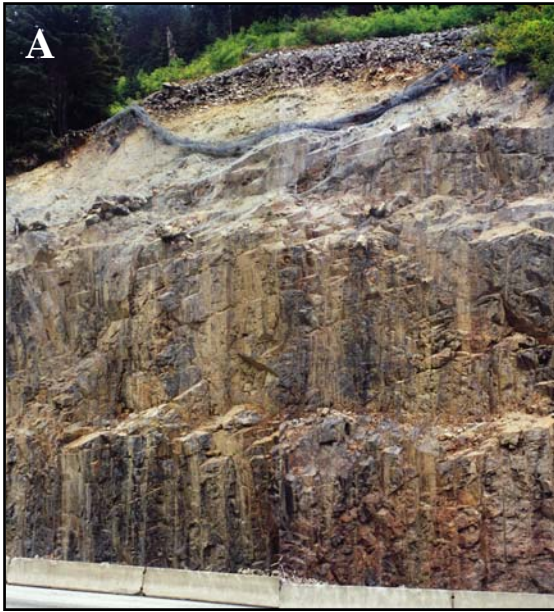


**Figure 2-6A. Failure in the eastern portion of the 1982 chainlink installation. Active erosion undermined the top row of anchors. Pockets of debris accumulated along intermediate support ropes. Figure 2-6B shows localized rupture by a 3- to 4-foot-diameter boulder that initiated from the bouldery talus shown at the top of photograph.**

Despite the replacement of the chainlink system with the more robust hexagonal wire mesh and cable net systems in 1998, heavy snows during the winter of 1998-99 caused extensive damage to the eastern and western portions of the system. Nearly all the anchors either failed in shear or pullout, or loads exceeded the passive pressure on the

anchors, causing severe ground deformation (figures 2-7A and 2-7B). The ultimate capacity of the anchors in shear was around 35,000 lbs. Slightly lower-than-design grout strengths and difficulties with grouting in the cobbles and boulders often void of matrix may have contributed to the anchors failing in pullout. Some of the anchors where passive earth pressures were exceeded had been installed vertically, rather than normal to slope, resulting in diminished capacity.

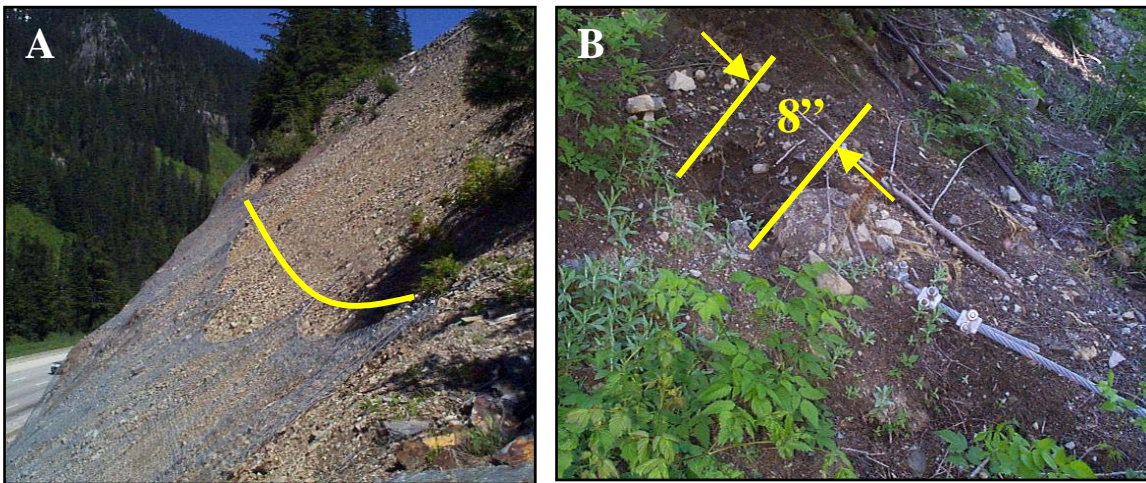


**Figure 2-7A.** Failure of the cable net system in the western portion of the site in July 1999. The yellow line is the approximate location of the top of the cable nets as installed in 1998. **Figure 2-7B** shows deformation of the ground where loads exceeded passive earth pressure, causing 8 inches of anchor deflection.

## **2.5 WEST SNOWSHED, WASHINGTON (HEXAGONAL WIRE MESH)**

### **2.5.1 Problem Description**

The West Snowshed site is located in the central Washington Cascades adjacent to the westbound lanes of Interstate 90 at MP 58.0 just east of the summit of Snoqualmie Pass. At elevation 2600 feet, the average maximum snowpack exceeds 4 feet. The oversteepened, south-facing cut slope is 100 feet high; the lower portion of the slope is oriented between 40° to 42° and steepens to around 50° in the upper portion (Figure 2-8).

The cut exposes very coarse colluvial and glacial deposits with boulders 1 to 4 feet in dimension comprising 30 to 50 percent of the deposits, and heavy seepage is prevalent in the cut slope. The upper, oversteepened portion of the cut is the source of both raveling-type rockfall and small scale (<10 yds<sup>3</sup>), surficial slumping.



**Figure 2-8. Looking west of the West Snowshed slope, active raveling near the crest of the cut slope and a large percentage of boulders within the debris.**

### **2.5.2 Installation Description**

The original installation was probably installed in the early 1980s and covered a slope area of about 600 feet in length. This early installation consisted of chainlink mesh fastened to a diagonal grid of ¾-inch-diameter wire rope cable. The support ropes had a roughly 50-foot spacing and were anchored to the slope face, where they intersected with No. 8 deformed, continuously threaded bars. Chainlink fabric was overlapped about 12 inches and seamed intermittently with light gauge steel hog rings.

Because of excessive damage primarily from debris accumulation beneath the mesh, the eastern half of the original system was replaced in 1998. The new system utilized hexagonal wire mesh fastened to a 50-foot square grid of ¾-inch-diameter support ropes placed on top of the mesh, which was attached to anchors installed on a 50-foot spacing along the top of the installation. The bottom of the mesh was folded outward to minimize debris accumulation. The mesh was overlapped 12 to 24 inches and fastened with high tensile steel hog rings at about a 12- to 24-inch spacing.

### **2.5.3 System Performance**

After several decades of severe slope erosion and heavy snow loads, the eastern half of the first installation was badly damaged. Many seams in the chainlink had split, and localized rupture and puncture had occurred in numerous locations near the base of the installation. Support ropes also trapped large quantities of rock debris, imparting significant debris loading on the system (Figure 2-9).

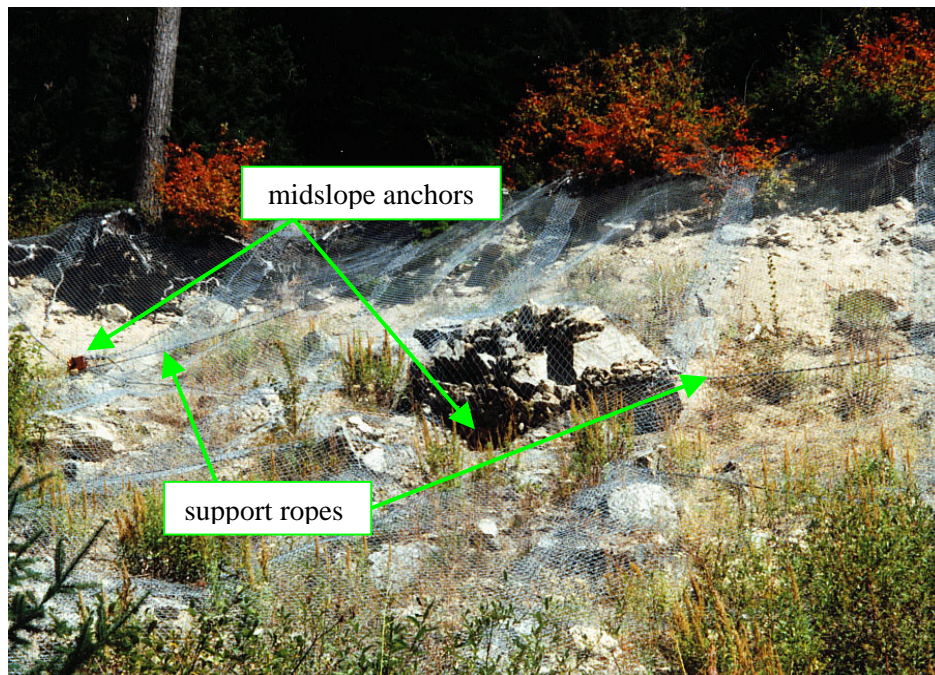


**Figure 2-9. Note the large accumulation of debris at the juncture of the underlying support ropes and the midslope anchor.**

Significant damage has occurred to the section that was replaced in 1998 with hexagonal wire mesh. While a different configuration of support ropes was placed on top of the mesh to better pass debris, a large quantity of debris has still accumulated beneath the lower half of the mesh (Figure 2-10).



**Figure 2-10. Rupture of the vertical seam and fabric; the midslope horizontal support cable was also damaged. The volume of debris associated with mesh failure is estimated to be 10 cubic yards, with block sizes of up to 3.5 feet in dimension.**

The reasons for the continued debris accumulation are believed to include the concavity and flattening of the slope; the ongoing erosion and voluminous quantity and large size of the debris generated; and the extended duration of a snowpack on the lower portion of the mesh, inhibiting the passage of debris. Elsewhere, numerous seams have

ruptured because of opening of the hog rings, most of which are located in the upper portion of the installation.

## **2.6 TUMWATER CANYON, WASHINGTON (CABLE NETS)**

### **2.6.1 Problem Description**

The Tumwater Canyon site is located on highway U.S. 2 between MP 97.0 and 97.1 on the eastern slope of the Washington Cascades. The highway is situated on the east side and at the base of the 3000-foot deep, steep-walled canyon around elevation 1500 feet. During winters with higher than average snowfall, a 24- to 30-inch snowpack develops in the lower portion of the canyon (Rick Woods, WSDOT Maintenance Supervisor; personal communication). The rockfall that affects the highway primarily originates from a 200-foot-high, 1H:1V, west-facing cut slope adjacent to the westbound lane. The cut exposes coarse-grained colluvial (and glacial?) deposits with boulders of up to 6 to 8 feet in size, discontinuously mantling intermediate to mafic intrusive bedrock that exhibits an adversely dipping planar structure (Figure 2-11). Ongoing erosion of the exposed colluvial deposits, and small planar failures to a lesser extent, produce regular rockfall that is evidenced by the damaged concrete barrier.

### **2.6.2 Installation Description**

A cable net system was constructed in 1997 to mitigate the rockfall hazard at this site. The installation was 180 feet wide and covered about 300 feet of slope length. The original anchor design called for a 5/8-inch-diameter steel rod with a welded eyelet, located in bedrock and a minimum of 50 feet beyond the actively eroding brow of the cut with a maximum spacing of 20 feet. During initial placement of the cable net, a number

of the anchors sheared and/or failed in tension. All the anchors were replaced with either ¾-inch wire rope or 1-inch deformed steel bar anchors. The nets were laced with 5/16-inch wire rope to the top horizontal wire rope and the ¾-inch vertical ropes that were spaced at 20-foot intervals; there are no intermediate or bottom horizontal support ropes. The net panels consisted of a 12-inch square grid of 5/16-inch wire rope joined at intersections with pressed steel clips. The cable net was overlain with 9-gage chainlink fabric with no overlap and fastened with hog rings on a roughly 24-inch square spacing.

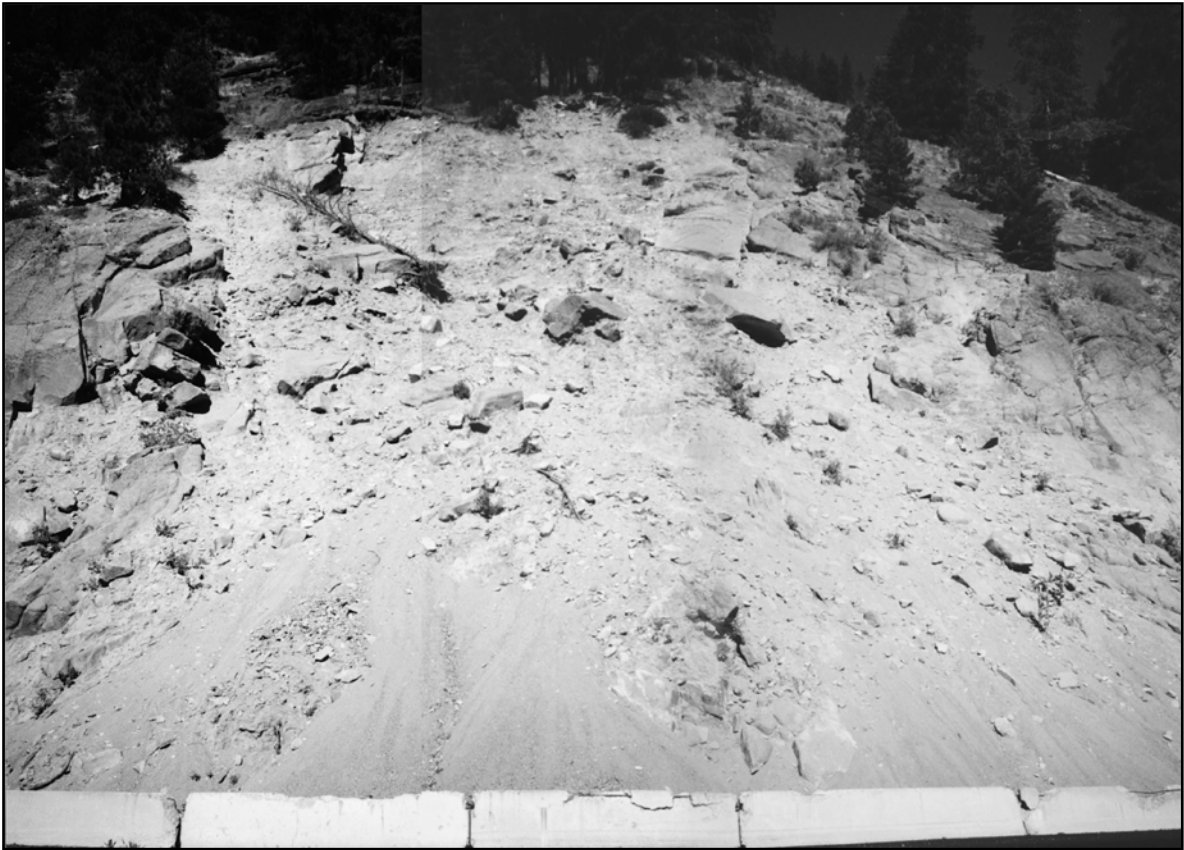


**Figure 2-11. Slope condition before cable net installation; note the rockfall-related damage to the concrete barrier.**

Given the moderate slope inclination and overall surface uniformity, an estimated 75 percent of the cable net is in contact with the slope. While the weight of the net

arrests much rockfall on this flatter slope orientation, the cable net system was designed to pass debris, and therefore, no anchors were installed in the field area of the net. The net terminates about 6 feet above the base of the ditch to facilitate ditch cleanout and minimize damage to the cable net system. The design also considered snow loads, but the calculated load that assumed full transfer to the anchors (no interface friction) was judged to be unrealistic and over-conservative. The basis of the 25-foot maximum anchor spacing was the performance of existing systems exposed to similar loads and engineering judgment.

### **2.6.3 System Performance**

The overall performance of the cable net system has been excellent. There have been no reported incidents of rockfall reaching the highway, and some low-growing vegetation is growing beneath the system. After six years, the system is in good condition, with only minor damage within the bottom 20 feet of the nets. On the south end, recent failures originating about 20 feet upslope, involving about six 5-foot-diameter, angular, discoid-shaped blocks and totaling about 10 to 15 cubic yards, deformed the cable net, broke one wire rope, and punctured a 12-inch-diameter hole in the chainlink. Some hog ring fasteners also burst, and the chainlink separated from the cable nets. On the north end of the installation, about 50 cubic yards of debris have accumulated behind the system 20 to 50 feet upslope of the ditch. Several large angular blocks have been caught, resulting in minor damage to the nets. The damage has consisted of slippage of the pressed clips over an area of about 10 square feet. One 1-foot-long x 6-foot-wide x 4-foot-thick block and one 7-foot-long x 3-foot-wide x 3-foot-

thick block originating from 40 to 50 feet upslope slid out beneath the cable nets without damaging the system.

Buildup of debris behind the cable nets and angular rocks with some rotational component of motion appear to have caused the only damage to the system. Overall, this damage is minor, and the nets are functioning as designed. During winter, snow regularly accumulates and slides off, failing within the snowpack or along the snow-chainlink/cable net interface with no apparent damage to the system.

## **2.7 STATE-OF-PRACTICE**

In North America, state/province departments of transportation (DOTs) probably represent the largest users of wire mesh/cable net slope protection for rockfall control. While there are some variations to design approach and detailing of these systems, a state-of-practice has evolved, mostly within the last 10 years, among DOTs. Table 2-1 summarizes the system components and detailing specified by DOTs, as well as general performance. A synopsis of experience and performance from a variety of transportation agencies is provided in Appendix A. Overall, the performance of systems that have been installed in North America has been good to excellent.

**Table 2-1. Current DOT practice for wire mesh/cable net system components**

<b>AGENCY</b>	<b>Rock Anchor Diameter (in)</b>	<b>Rock Anchor Spacing (ft)</b>	<b>Rock Anchor Depth (ft)</b>	<b>Soil Anchor Diameter (in)</b>	<b>Soil Anchor Spacing (ft)</b>	<b>Soil Anchor Depth (ft)</b>	<b>Soil Anchors Drilled (DR) Driven (DN) Deadman (DM) Hand Dug (HD)</b>	<b>Auxiliary Anchor Diameter (IN)</b>	<b>Support Cables Suspension (S) Horizontal (H) Vertical (V) Lacing Rope (LR)</b>	<b>Seam Fasteners Hog Rings (HR) Spenax (S) Tiger-Tite (TT) Lacing Wire (LW)</b>	<b>Performance Excellent (E) Good (G) Fair (F) Poor (P)</b>
Alaska DOT & PF	¾" to 1"		5'	¾" to 1"		5'		NA	3/8-¾" around panels; some mesh anchored on 10'x10' pattern	HR, LW	F – chain link E/G – double twist and cable net
British Columbia Ministry of Transportation	1¾" #14-75ksi threadbar <sup>1</sup>	12'	6'	1¾" #14-75ksi threadbar	12'	5'	HD - typically 12 to 24" diameter	7/8" #7-75ksi and 5/8" cable	S = ¾" H (Bottom) = ¾" LR = 1/4" no internal cables	S, TT	E - infrequent tears to mesh; easily repaired
California DOT	1" bar ¾" cable	WM: 50' <sup>2</sup> CN: 25' <sup>B</sup>	WM: 6' CN: 6'	1" bar ¾" cable	WM: 50' <sup>B</sup> CN: 25' <sup>B</sup>	WM: 6' CN: 6'	DR, DN, HD	same	WM: ½" (S) CN: ¾" (S) no internal cables	S, TT, LW or equal to stronger than the wire	E – wire mesh G/E – cable net seams/overlaps cause problems
Idaho Transportation Department	¾"	6'	5'	¾"	6	5	DR, DN	5/8"	5/8" (H) no internal cables	HR	G
North Carolina DOT	1" to 1-1/4"	5'	up to 15' for cable nets	?	?	?	?	variable for cable nets	1-1/4" to 1-5/8" for cable nets	HR, LW	?
New Hampshire DOT	1"	25'	5'	1"	12'	5'	DN, DR	NA	S/H/V = ¾" LR=9 gauge wire	HT, TT or LW	G-infrequent tears to mesh; problems w/ debris collecting on bottom cable
Nevada DOT	¾"	40'	6.5'	¾"	40'	6.5'	DR, DN	NA	all 3/8"	HR	G
New York State DOT	¾"	50'	6'	NA	NA	NA	NA	1"	S/H = ¾" no internal cables	HR or LW	E
Oregon DOT	¾" loop eye rock bolt	40' (h<75') 20' (h>75')	3'	Same as for rock	Same as for rock	Same as for rock	Typically, hand dug. Minimum hole size – 3'X12"	NA	S/H/V = 3/8" 6X19 wire rope LR not used	HR, S or TT	E - infrequent tears to mesh; easily repaired
Washington State DOT	¾" cable; #8-60ksi def. bar	50' for h<75' 25' for h>75' <sup>3</sup>	6'				DM or Contractor design	NA	for h<75', S/H/V=5/8" for h>75', S/H/V = ¾" LR = 9 gage wire	S, TT, or LW	G –problems w/ debris on horiz. cables and snow loads on anchors
Wyoming DOT	1" epoxy coated, thread bar	5.5'	5' (min)	1" epoxy coated, threaded bar	5.5'	5' (min)	Predominately DR (DM, DN allowed)	NA	Top Support Cable=1/2" no internal cables	S, LW	G – few problems w/ failures along slope crest and snow on bottom of mesh

<sup>1</sup> Anchors are raised 3 feet above ground surface.

<sup>2</sup> Anchors added at topographic changes.

<sup>3</sup> Spacings do not consider snow loads.

Currently, double twist hexagonal mesh (WM) and cable nets (CN) are being used by all surveyed DOTs.

### **2.7.1 Anchors**

In North America, anchors are usually located only along the top of the system, and debris is allowed to pass beneath the mesh. Midslope anchors are employed on occasion by DOTs to achieve greater mesh contact with the slope. Generally, this has been done to visually blend the mesh with the slope or to reduce slope erosion. Numerous documented failures associated with debris accumulation around midslope anchors have limited this practice to date. Ruvolum, a new design methodology for pattern-anchored systems developed in Switzerland, is seeing some implementation in North America.

DOTs are using two general anchoring designs for top-anchored systems, a close spacing and a wide spacing. The close spacing design specifies a range of 5 to 12 feet (1.5 to 3.5 m). The wide spacing uses 40 to 50 feet (12 to 15 m) for slope heights of less than 75 to 100 feet (20 to 30 m) and/or for wire mesh systems, and a spacing of 20 to 25 (6 to 7.5 m) feet for higher slopes and/or cable net systems. Typical anchors in rock include either a ¾-inch (19-mm) steel cable loop or a 1-inch, deformed steel threaded bar; anchor depths generally range from 3 to 6 feet (1 to 2 m). There are more variations in soil anchors. Anchors are typically driven, dug, or drilled and often consist of either a cable loop or a threaded bar.

In nearly all cases, documented anchor failures have resulted from external loads associated with snow and debris accumulation and high-energy impacts. A rare case of anchor failure due to static load (mesh weight) occurred at the Tumwater Canyon site in Washington. During the placement of the 300-foot (90-m) (slope length) cable net system, numerous anchors failed in shear. The anchors consisted of ½-inch- (12-mm)

diameter steel bars (utility-type anchor) with a capacity of around 10,000 to 15,000 lbf (44 to 67 kN).

Minimum anchor setbacks of 10 to 15 feet (3 to 4.5 m) from the slope brow are typically specified. However, numerous system deficiencies have been documented where the anchor setback from the brow of the slope was insufficient, and erosion undermined the anchors. This condition is most often observed in oversteepened bouldery deposits near the top of a cut slope.

### **2.7.2 Support Cables**

The use and dimensioning of support cables is varied among DOTs. Cable diameters range from  $\frac{3}{8}$  to  $1\frac{5}{8}$  inch (10 to 41 mm), with galvanized  $\frac{3}{4}$ -inch (19-mm), 6x19 wire rope being most typically specified. The lengths of top horizontal support cables are generally limited to between 50 and 150 feet (15 and 45 m). Internal support cables, when used, are commonly observed to be slack and not carrying load, suggesting that these cables are not adding to the system capacity. Additionally, recurring problems with debris accumulation along internal and bottom horizontal support ropes are well documented, particularly if the cable is located between the slope and fabric. For these reasons, a number of DOT's no longer use an internal grid of support cables but specify only a top horizontal and sometimes a bottom cable to facilitate cleanout behind the system.

### **2.7.3 Fabric**

In the last 10 years, double-twisted, hexagonal wire mesh has mostly replaced the use of chain link fabric for rockfall control, primarily because of its greater strength and perceived resistance to unraveling if a wire is cut. The hexagonal wire mesh most

typically used in North America consists of a 3-inch (8-cm) by 4-inch (10-cm) sized opening (referred to as 8x10 type); 0.12-inch- (3-mm) diameter galvanized wire; or a 0.11-inch- (2.7-mm) diameter wire for pvc-coated fabric. Hexagonal mesh is most often limited to slopes producing rockfall with block sizes of less than 2 feet in diameter, although on near-vertical slopes, double twist fabric has performed well for block sizes of 3 to 4 feet in dimension. On flatter slopes ( $\approx 45^\circ$  to  $50^\circ$ ) that produce large quantities of rockfall, 2-foot-diameter blocks have caused considerable damage, which has been evidenced at the West Snowshed site in Washington.

Most DOTs specify a 12-inch (300-mm) overlap of the hexagonal wire mesh but have switched from light gage steel hog rings for seaming to using high tensile steel fasteners (i.e., King Hughes and Spenax™) or interlocking fasteners (i.e., Tiger-Tite™). The specifications for the spacing of fasteners are varied, but they commonly range from 6 to 12 inches (150 to 300 mm). Most DOTs also allow for the use of lacing wire of equal or greater gage thickness for seaming. Rupture of seams is a recurring problem, particularly when light steel hog rings are used or the spacing of high tensile steel rings exceeds 12 inches (300 mm). Debris accumulation has even proven problematic with spacings of 6 inches (150 mm). Because of recurring problems with debris accumulation along overlaps, California DOT now prohibits overlapped seams.

Cable nets are typically constructed of either  $\frac{1}{4}$ - or  $\frac{5}{16}$ -inch (6- to 8-mm) wire rope woven in a 6-, 8-, or 12-inch (150-, 200-, and 300-mm) square grid. Pressed cross-clips have been used exclusively to bind cable intersections, although new connections are forthcoming in the North American market. Net panels are butted and laced with similar-sized cable. Because of the larger opening sizes, cable nets are normally backed

with either a chain link or hexagonal wire mesh to prevent smaller-sized rockfall from passing through the cable nets. The backing fabric is typically placed between the slope and the cable net. Where optimized slope contact is desired, chain link has proved to be somewhat better than hexagonal wire mesh because of its greater flexibility. The greater strength of 0.12-inch- (3-mm) diameter hexagonal wire mesh than the 0.11-inch- (2.7-mm) diameter chain link, however, suggests somewhat better puncture resistance with the hexagonal mesh when restrained by an outer cable net. A 24-inch (0.6-m) spacing of fasteners to connect the backing fabric to the cable nets is typically specified. California DOT has experienced problems with the backing fabric creeping beneath the cable nets and now requires fasteners on each side of the cable net cell. It also requires that the backing fabric be attached to the cable nets before placement. Properly fabricated cable nets have proved effective with block sizes of up to 4 to 5 feet (1.2 to 1.5 m) in diameter.

Recently, high tensile steel wire mesh (TECCO<sup>®</sup>) has been introduced in North America by Geobrugg as an alternative to cable nets. Maccaferri, one of the primary suppliers of hexagonal wire mesh, has also recently introduced a cable-reinforced, double twist mesh. To date, there is little documented experience or performance history with the first product and none with the second in North America.

#### **2.7.4 Load-Influencing Factors**

External loads on wire mesh/cable net systems are dominantly influenced by the slope configuration. External loads include debris and snow accumulation, as well as impacts from falling rock. Important elements of slope configuration include orientation, uniformity, and roughness; these elements in turn control the degree of contact that the system has with the slope.

Slopes steeper than about 70° typically do not accumulate debris because the majority of the mesh usually hangs free of the slope, and therefore, only a minor component of mesh weight acts against the slope. Mesh systems on flatter slopes exert a greater weight component and, hence, have a greater tendency to accumulate debris. In addition, slopes flatter than about 60° may also be at risk for accumulating snow, which can exert large loads on installations. Increased mesh weight and the degree of slope contact can also have the positive effect of arresting or reducing erosion and the movement of debris behind the mesh.

Slope uniformity is also an important factor affecting mesh contact and the accumulation of debris. More uniform slopes are more efficient at passing debris than slopes with inflections. A common location where debris accumulates is at abrupt convexities, for example, where a flatter slope of overburden materials lies above a steep rock cut. The slope-normal force acting at such an inflection can be quite large, inhibiting the passage of debris. Abrupt convexities may also be subjected to concentrated impact loads; puncturing of mesh fabric has been observed in these locations. In contrast, concavities are common locations where the mesh is not in contact with the slope. In this configuration, sagging in the mesh may actually impart an upslope force component along the bottom of the installation, acting to entrap debris.

Slope roughness similarly influences system load, but to a lesser degree than slope orientation and uniformity. In areas where the mesh is only in limited contact with the slope, roughness may also influence rockfall trajectory. Impact forces normal to the mesh are more likely on rough slopes than on smooth slopes.

## **CHAPTER 3 TESTING AND MONITORING DATA**

The analytical models and finite element simulations that are presented in subsequent chapters needed to be verified before they could be used to develop design guidelines. Therefore, selected laboratory testing, as well as field instrumentation and full-scale testing, were carried out as part of the research study. These included fabric testing, seam testing, instrumentation of a cable net installation to evaluate load distribution under snow loads, and full-scale testing of anchors. This chapter summarizes these testing and monitoring efforts used in the verification of the analytical and numerical models and in the development of design guidelines. Testing and monitoring data are included in the appendices of this report.

### **3.1 FABRIC TESTING**

#### **3.1.1 Objectives**

Current practice in North America utilizes two types of fabric for draped rockfall protection systems; these include double-twisted hexagonal wire mesh and woven cable nets with pressed cross clips. Within the last several years, high tensile steel wire mesh (TECCO<sup>®</sup>) has been introduced in North America. Each of these fabric types has distinctly different weight, strength, and elongation properties. Unfortunately, very little published data exist on such properties, and some of the published results have varied significantly. Furthermore, while some manufacturers have independently tested their products, hexagonal wire mesh is the only fabric type for which there is a widely accepted, standardized test method in North America to evaluate these properties (ASTM

A 975). Additionally, there is no widely accepted test method for comparing the engineering properties of a variety of fabric types.

To complete the analytical and finite element modeling necessary for this research, the elasticity modulus and strength of the fabric types commonly used in mesh systems needed to be determined. Solely for this reason, this research undertook a testing program to determine these properties. Known North American suppliers were contacted and solicited to supply their products. Of those contacted, Geobrigg provided cable nets and high tensile steel wire mesh (TECCO<sup>®</sup>), and Maccaferri provided hexagonal wire mesh and cable nets. As expected, the strength and modulus values that were obtained from this testing varied from the values reported by the manufacturers in some cases. This may have been due to differences in the types of tests, specimen size, and the boundary and loading conditions. Because the actual distribution of stresses that act on the overall mesh system determined from the finite element analysis were much less than the ultimate strength values of most of the fabrics, the effects of such variation would have minimal impact on the design estimates of overall systems. It must be emphasized that the testing performed for this research was not intended to compare similar fabric types from different manufacturers. However, testing the different types of fabric in the same manner did allow for some rough comparisons of their engineering properties and an opportunity to understand their observed range of field performance.

The testing was performed at the Wood Materials and Engineering Laboratory (WMEL) at Washington State University in Pullman, Washington. Sixteen tension tests were conducted. Eight were performed on five configurations/types of wire mesh fabrics, and eight were conducted on three types of cable nets. The summary test report by

Carradine (2004) is included in Appendix B. Subsequent to this testing by WMEL, independent test results were provided by Maccaferri for the hexagonal mesh and by Geobrugg for the TECCO<sup>®</sup> mesh. These test results are referenced in section 3.1.4 and are available from the manufacturers.

### **3.1.2. Methodology**

The test fixture shown in Figure 3.1 was designed, fabricated, and bolted to the reaction floor inside the WMEL's structural testing facility. The test fixture was fabricated to handle fabric specimens of up to about 3.5 ft (1 m) square. The intent of the test fixture was to load the meshes in tension at the two edges perpendicular to the direction of loading while restraining the edges parallel to the direction of loading from constricting as loads were applied. While it is recognized that it is not possible to entirely replicate the exact conditions in the field in a laboratory test program, the test fixture was designed to best represent the boundary and loading conditions in the field. The test fixture was also guided by similar fabric tests on TECCO<sup>®</sup> mesh performed by Geobrugg (LGA, 2003).

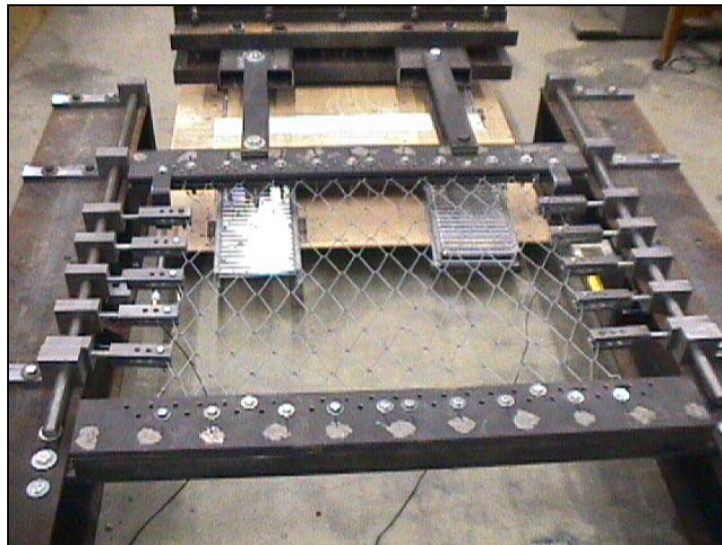


**Figure 3.1. Testing apparatus with TECCO<sup>®</sup> mesh.**

Testing was conducted by following ASTM A 975 Standard Specification for Double-Twisted Hexagonal Mesh Gabions and Revet Mattresses (Metallic-Coated Steel Wire or Metallic-Coated Steel Wire with Poly (Vinyl Chloride) (PVC) Coating) as a general guideline. Loads were applied by utilizing a 100,000-lbf (445-kN) capacity hydraulic actuator with a stroke of 10 inches (250 mm). It was controlled with an MTS 407 Controller, which received actuator displacement feedback from a string potentiometer. Load data were obtained by placing a 100,000-lbf (44-kN) capacity load cell in line with the loading apparatus. Linear variable differential transformers (LVDTs) and string potentiometers were used to monitor displacement of the loading head with respect to the base of the test apparatus in order to accurately record the distance that the meshes moved through the first 2 inches (50 mm) of displacement. These data were used in determining the elastic modulus of the meshes. Load data and displacement data from the string potentiometer and the two LVDTs were recorded by using LabVIEW version 6.1 software.

### **3.1.3 Test Specimens**

Table 3-1 provides information on the different types of specimens that were tested. All specimens were tested as delivered, although it was necessary to bend the untested portions of the *Mac Double Galv1* and the *Mac Double Coat* so that they would fit into the testing apparatus (Figure 3-2). Inadvertently, the meshes described as double consisted of two layers of hexagonal mesh (only one layer was intended to be tested), both of which were fixed to the testing apparatus and contributed to the load carrying capacity. Meshes described as having a coating were made from wires that were pvc-coated in either gray or brown. Meshes described as Narrow consisted of 6 x 8- type

(cm) hexagonal mesh and were approximately 34.5 inches wide (perpendicular to the direction of loading), while the remaining hexagonal mesh specimens were 8 x 10- type (cm) and ranged from 40.0 inches to 71.0 inches wide. Fabric specifications were provided by the manufacturers and are included in the appendix of the test report.

Differences in the dimensions of the meshes made it necessary to attach the specimens to the test apparatus slightly differently. As shown in Figure 3-1, the TECCO<sup>®</sup> mesh specimens were pinned to the loading plates and side restraints through holes machined in the steel components. All of the hexagonal mesh specimens were pinned through holes in the side restraints but were attached to the loading plates with bolts that were placed in the holes in the plates and that extended far enough above the plates to capture the mesh, as shown in Figure 3-2.

**Table 3-1. Description of tested specimens**

<b>Specimen</b>	<b>Description</b>
Geobruigg Twist 1	TECCO <sup>®</sup> G65 mesh (Geobruigg)
Geobruigg Twist 2	TECCO <sup>®</sup> G65 mesh (Geobruigg)
Geobruigg Twist 3	TECCO <sup>®</sup> G65 mesh (Geobruigg)
Mac Double Galv1	8x10 hexagonal wire mesh, galvanized (Maccaferri)
Mac Double Coat	8x10 hexagonal wire mesh, gray pvc coating (Maccaferri)
Mac Double Narrow	6x8 hexagonal wire mesh, galvanized (Maccaferri)
Mac Coat1	8x10 hexagonal wire mesh, brown pvc coating (Maccaferri)
Mac Coat2	8x10 hexagonal wire mesh, brown pvc coating (Maccaferri)
Geobruigg Square 1	5/16", 12" square grid, cable net (Geobruigg)
Geobruigg Square 2	5/16", 12" square grid, cable net (Geobruigg)
Geobruigg Diagonal 1	5/16", 12" diagonal grid, cable net (Geobruigg)
Geobruigg Diagonal 2	5/16", 12" diagonal grid, cable net (Geobruigg)
Mac Cable 1	3/8", 12" diagonal grid, cable net (Maccaferri)
Mac Cable 2	3/8", 12" diagonal grid, cable net (Maccaferri)
Mac Cable 3	3/8", 12" diagonal grid, cable net (Maccaferri)
Mac Cable 4	3/8", 12" diagonal grid, cable net (Maccaferri)

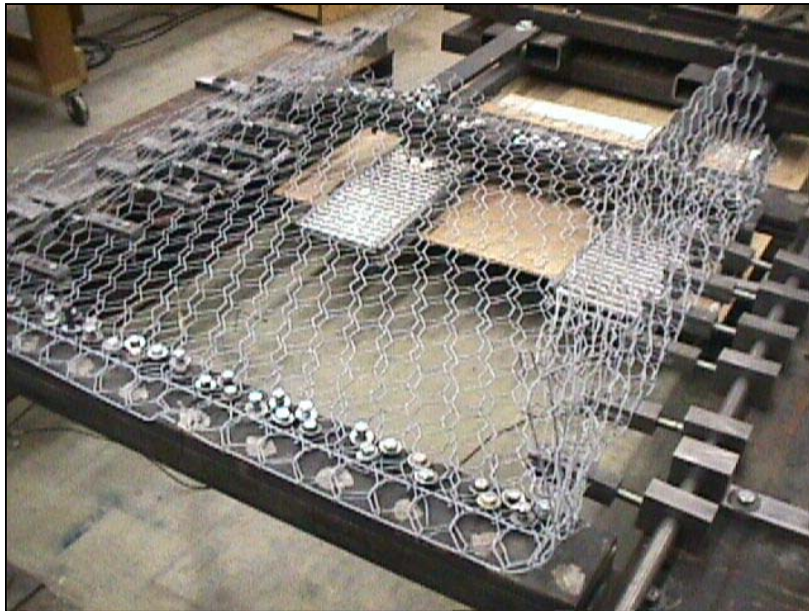


**Figure 3-2. Setup for *Mac Double Galv1* mesh with bolts extended above the loading plates.**

Attachment of the loading plates was done far enough in from the ends of the meshes that the wires would not unravel before failure. Longer segments of threaded rod were required to attach the lateral restraints to the meshes described as *Narrow*. The Geobruigg square grid cable nets were attached to the end plates and lateral restraints in the same manner as the TECCO<sup>®</sup> mesh specimens, except that segments of steel plate were attached to the lateral restraints to maintain the distance between parallel cables, as shown in Figure 3-3A. The diagonally woven cable net manufactured by Geobruigg was attached to each end plate with two bolts, and long threaded rod segments were utilized on the lateral restraints to maintain the shape of the nets, as shown in Figure 3-3 B.

All specimens were placed in the fixture so that slack could be taken out of the specimens to ensure that they would undergo enough deformation to cause failure. In general, very little load was applied to these specimens as they were installed in the test fixture. Cable net specimens manufactured by Maccaferri were approximately 75 inches long, parallel to the direction of loading, which made it necessary to remove the loading

plate closest to the actuator and some of the steel linkages so that the mesh could be directly attached to the loading apparatus connected to the load cable, as shown in Figure 3-4. Four lateral restraints were used on each side because of the shape of the Maccaferri cable nets.

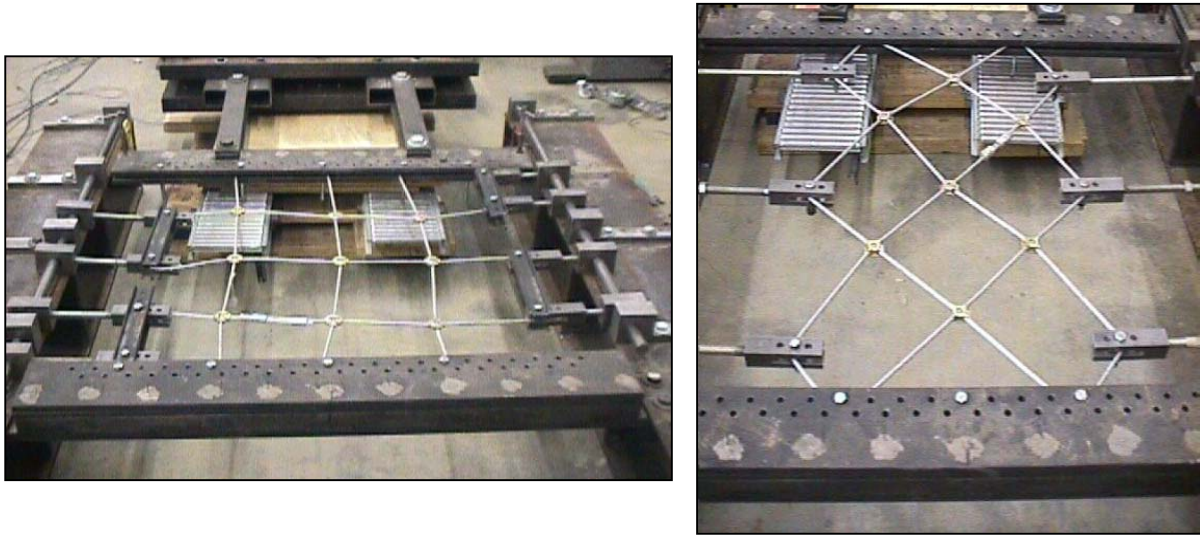


**Figure 3-3. Setup for (A) Geobrug square grid cable net and (B) Geobrug diagonal grid cable net.**

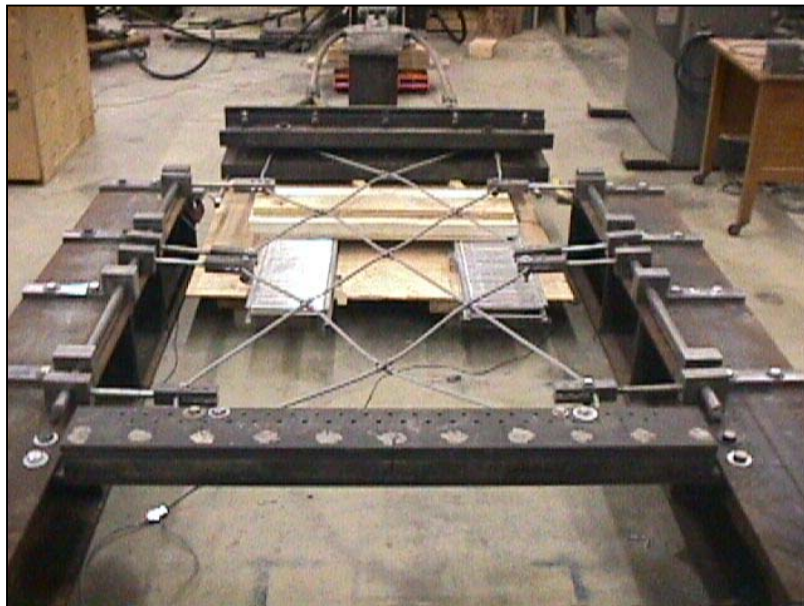


**Figure 3-4. Setup for Maccaferri diagonal grid cable net utilizing modified test apparatus.**

The specimens were secured in the test frame, and then the LVDTs or string potentiometers were installed so that the maximum amount of displacement data could be recorded before the instruments ran out of stroke on the plunger or extension of the string. After installation of the displacement measuring devices, the data acquisition program and the hydraulic actuator were started. Load was induced by the hydraulic actuator, which ran at 0.25 inches (6 mm) per minute under displacement control. All specimens were loaded to the full stroke of the actuator, with the exception of the cable net, which failed before reaching the available stroke distance on the jack. Testing results and descriptions of failure for the various specimens are presented in the following section. Following each test, specimens were removed from the test apparatus, and the regions of failure were documented.

#### **3.1.4 Results**

Figure 3-5 shows an example of a typical load versus displacement curve from which elastic modulus values were obtained. Note that the data from the initial portions of the load versus displacement curves were neglected when elastic modulus values were determined; this is because the initial data were erratic for most specimens because of settling within the test fixture as loads were applied. Table 3-2 summarizes the tension testing results, which include the dimensions, ultimate load, yield strength, and elastic modulus for each specimen. Note that the different specimen types failed in different manners; the descriptions of the failures are provided in Carradine (2004). Subsequent test reports have been provided by the manufacturers for two fabrics and are included in Table 3-2.

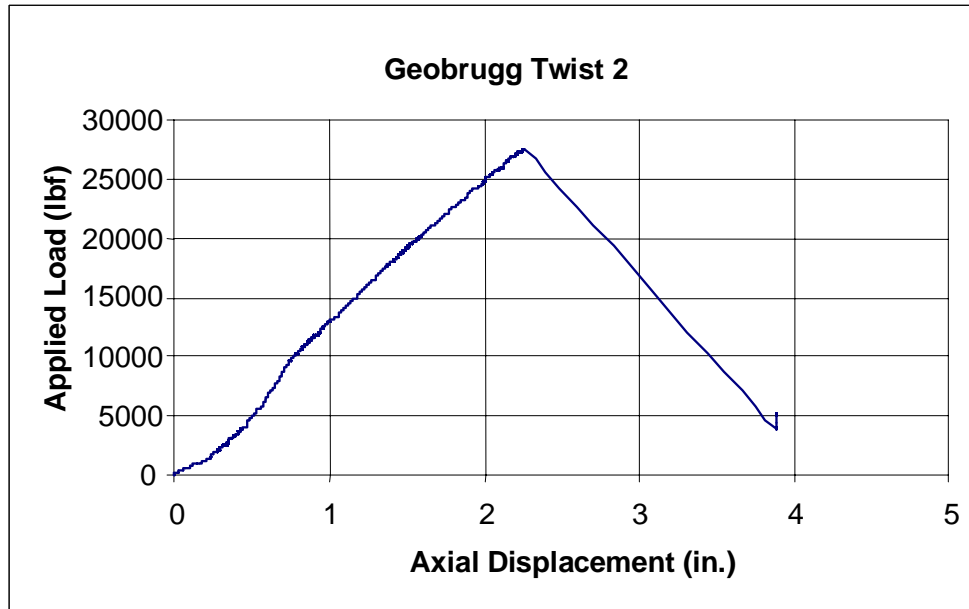


Figure 3-5. A load versus displacement graph for determining elastic modulus is shown for the TECCO® mesh.

Table 3-2. Results from tension testing by WMEL

Specimen	Initial Mesh Width/Length <i>in (cm)</i>	Ultimate Load <i>lbf (kN)</i>	Tensile Strength <i>lbf/ft (kN/m)</i>	Elastic Modulus <i>lbf/in (kN/m)</i>
Geobruigg Twist 1	40.0/40.0 (101/101)	25,500 (113)	7,650 (111)	9,880 (1730)
Geobruigg Twist 2	40.0/40.0 (101/101)	28,200 (125)	8,460 (123)	12,400 (2170)
Geobruigg Twist 3	40.0/40.0(101/101)	27,800 (124)	8,340 (122)	11,600 (2030)
TECCO® G65 3mm <sup>1</sup>	39.4/42.5 (100/108)		11,000 (160)	14,300 (2500)
Mac Double Galv1	45.0/42.0 (114/107)	13,000 (57.8)	3,470 (50.6)	3,820 (669)
Mac Double Coat	45.0/42.0 (114/107)	14,800 (65.8)	3,950 (57.5)	2,970 (520)
Mac Double Narrow	35.0/43.5 (89/108)	14,100 (62.7)	4,830 (70.5)	6,010 (1050)
Mac Coat1	35.0/42.5 (89/108)	8,700 (38.7)	2,980 (43.3)	3,070 (538)
Mac Coat2	35.0/42.5 (89/108)	7,040 (31.3)	2,410 (35.1)	1,670 (293)
8x10, pvc coated 2.7mm <sup>2</sup>	29.5/48.0 (75/122)		3,530 (51.5)	2,060 (360)
Geobruigg Square 1	40.0/40.0(101/101)	21,400 (95.2)	6,110 (93.7)	15,900 (2780)
Geobruigg Square 2	40.0/40.0(101/101)	22,300 (99.2)	6,370 (97.6)	19,900 (3490)
Geobruigg Diagonal 1	24.0/39.0 (61/ 99)	19,200 (85.4)	9,600 (140)	11,200 (1960)
Geobruigg Diagonal 2	24.0/39.0 (61/99)	18,800 (83.6)	9,400 (137)	12,000 (2100)
Mac Cable 1	31.0/75.5 (79/192)	33,800 (150)	13,100 (203)	11,800 (2070)
Mac Cable 2	31.0/75.5 (79/192)	32,300 (144)	12,500 (183)	12,600 (2210)
Mac Cable 3	31.0/75.5 (79/192)	35,200 (157)	13,600 (199)	14,900 (2610)
Mac Cable 4	31.0/75.5 (79/192)	33,000 (147)	12,800 (186)	9,540 (1670)

<sup>1</sup> Subsequent test report for TECCO® provided by Geobruigg from LGA Nuremburg (dated 4/17/2003); the modulus was not reported but calculated from the test data.

<sup>2</sup> Subsequent test report for hexagonal mesh provided by Maccaferri from CTC-Geotek, Inc. of Denver, CO (dated 5/16/2001) following ASTM A 975 test method.

## **3.2 SEAM TESTING FOR DOUBLE-TWISTED HEXAGONAL MESH**

One of the more commonly observed failures of hexagonal mesh installations is seam rupture. Mesh panels are probably most often seamed by rapidly fastening hog rings with a pneumatic tool. Hog rings currently in use generally consist of two types: a medium tensile strength, 9-gage ring, and a high tensile steel, 9-gage ring (i.e., Spenax™ or King Hughes). Other available seaming alternatives include a hooked fastening ring (Tiger-Tite™) and lacing wire/cable. Current practice of a number of DOTs has prohibited the use of the medium gage hog rings because of their known poor seaming performance for the high loading conditions associated with these systems. Furthermore, lacing wire is generally not used when other alternatives are allowable because of the time-consuming fabrication of such seams.

Because of the observed frequency of seam failures and the unknown capacity of the various seaming details, limited tensile strength testing was performed in support of this research.

### **3.2.1 Objectives**

A simple testing program was undertaken by WSDOT to determine the performance limitations of the high tensile steel hog rings for seaming double-twisted hexagonal mesh. Three seaming details using high tensile steel hog rings were also tested (Fig. 3-6).

The primary objectives of the testing were to determine the tensile strength differential between typical seaming details and intact hexagonal mesh, and to develop an optimized design for high tensile steel fasteners.

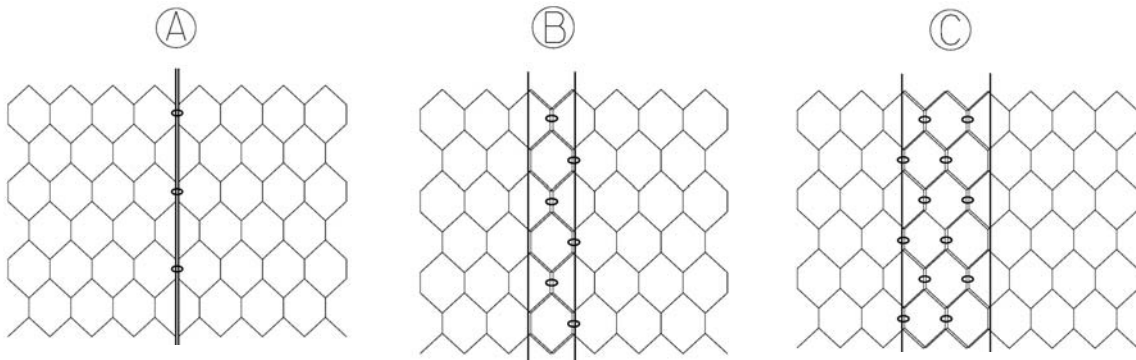


**Figure 3-6. Tested seams included (A) butted seam with 6-inch fastener spacing, (B) single-cell overlap with 3-inch fastener spacing, and (C) two-cell overlap with doubled fasteners on 3-inch spacing. The dark vertical lines represent the finished longitudinal edge of the fabric, and the ellipses represent fasteners.**

### **3.2.2 Methodology**

The fabric specifications consisted of an 8 x 10-type, galvanized, hexagonal mesh with an approximate mesh opening (cell size) of 3.25 inches (83 mm) by 4.5 inches (114 mm). The wire diameter was approximately 0.12 inches (3 mm) with a minimum tensile strength of 2985 lbs/in<sup>2</sup> (20.6 MPa).

To replicate field-loading conditions, tensile testing was oriented perpendicular to the twist. The tensile tests were performed on a 600,000-lbf (2670-kN) steel tensile testing machine. Given the constraints of the machine, fabric sample dimensions were restricted to about 30 inches square, and the maximum extension during testing was limited to 8 inches. A clamping apparatus was fabricated to test approximately a six-cell width and to tension the cells oriented in the direction of the wires (Figure 3-7), which is somewhat less than what is required in the ASTM A975 test procedure for gabions and revet mattresses. To reduce edge effects and unraveling of the mesh during tensioning, the fabric was cut and clamped to maintain a two-cell perimeter around the clamping apparatus. Unlike the ASTM A975 test method for double-twisted hexagonal mesh, the

sides were not restrained. Consequently, some necking of the sample occurred during tensioning.

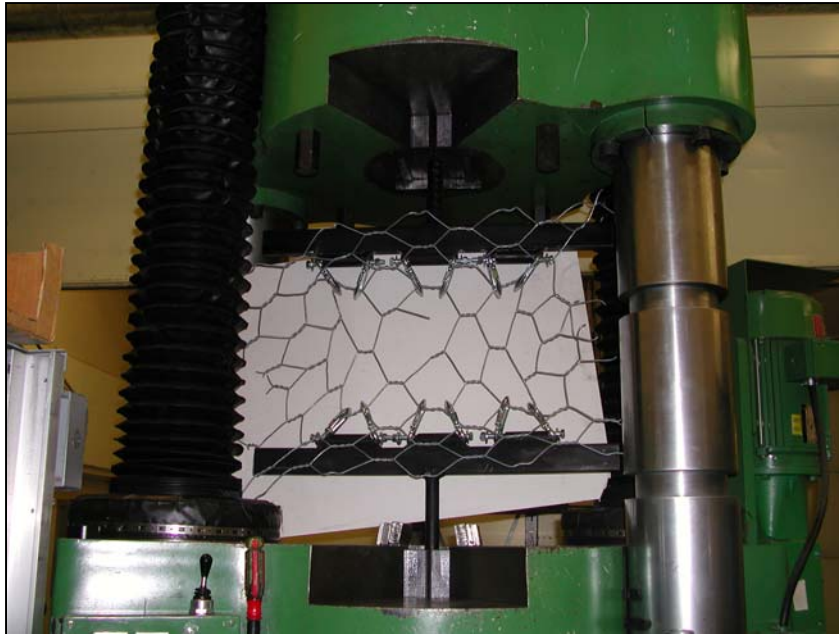


**Figure 3-7. Testing/clamping apparatus and failed specimen of bulk material (no seam).**

A series of bulk material (no seam) samples were tested first to verify the testing apparatus and methodology and to determine the tensile strength of the fabric for this test setup. Tensioning was terminated when one wire broke. Samples of the three seam types were then run. Tensioning was continued for either the full 8 inches (200 mm) of machine travel or until no increase in load could be achieved.

### **3.2.3 Results**

Four samples of the bulk material (no seams) were tested. The spacing between the clamping apparatus varied between three and four cells (9.75 to 13 inches / 250 to 330 mm). All wire breakage occurred at least one cell inside the connections points. Yield strengths ranged from 1830 to 2070 lbf/ft (26.6 and 40.0 kN/m), resulting in an average yield strength of 1990 lbf/ft (29.0 kN/m). These strengths exceeded the

minimum strength requirements perpendicular to twist of 1800 lbf/ft (26.3 kN/m) specified in ASTM A975 test method.

Four seam tests were run on the three seams shown in Figure 3-6. One test was run on seam A, which effectively tested two high tensile steel hog rings spaced around 6 inches (150 mm). The seam failed at 850 lbf/ft (12.4 kN/m) by consecutively popping each hog ring. Two tests were run on seam B, which effectively tested five hog rings spaced around 3 inches (75 mm). The seams failed at between 930 and 1110 lbf/ft (13.5 and 16.1 kN/m) by either consecutively popping each hog ring or breaking wires individually. One test was run on seam C, which effectively tested ten hog rings doubled and spaced around 3 inches (75 mm). The seam failed at 950 lbf/ft (13.8kN/m) by consecutively popping each hog ring.

Load transfer during tensioning occurs through individual wires of the mesh resulting in point stress concentrations at the fasteners. Consequently, the testing was more a demonstration of the strength of the fasteners than of a continuous seam. In this sense, scale limited the effectiveness of the testing in determining seam strengths. However, in field conditions, the load transfer would likely be similar, in that point stress concentrations would occur at the fasteners. On the basis of this limited testing, it appears that high tensile steel fasteners spaced between 3 and 6 inches (75 and 150 mm) provide a seam that is only half as strong as the mesh. This result is in rough agreement with the reported requirements of test method ASTM A975, which requires a seam strength that is only 40 percent of the required longitudinal mesh strength. Furthermore, lacing wire is reported to provide seam strength that is only 60 to 70 percent of the longitudinal mesh strength (G. Brunet, personal communication 2004). These results

demonstrate that seams are inherently the weakest areas of the mesh. Specifications requiring seams to be as strong as the longitudinal mesh strength are not being achieved with currently known seaming details, nor may they be practically achieved in construction.

### **3.3 TUMWATER CANYON INSTRUMENTATION**

#### **3.3.1 Objectives**

As detailed in Chapter 2, most of the anchor failures at Washington installations were associated with snow loading. Snow load applied to a mesh system is a function of depth and density of snowpack, but many factors influence its magnitude, such as temperature and slope surface conditions. Unfortunately, very little information exists about the mechanisms and magnitude of loads that are transmitted to the system. Therefore, to understand the mechanism of snow load on mesh systems, a cable net system was instrumented at the Tumwater Canyon site in Washington, which annually develops snowpack. The specific objectives of the instrumentation were to determine how snow load varied with snow depth, snowfall, and temperature and how load was accommodated within the support cables and anchors.

#### **3.3.2 Methodology**

In early November 2001, strain gauges were installed by the WSDOT and were continuously monitored from November 2001 through April 2002. The details of the system and the location of strain gauges are as shown in Figure 3-8. Twenty Phoenix Geometrix vibrating wire strain gauges were installed at ten locations on the upper portion of the installation. Strain gauges were installed in couples welded onto cable

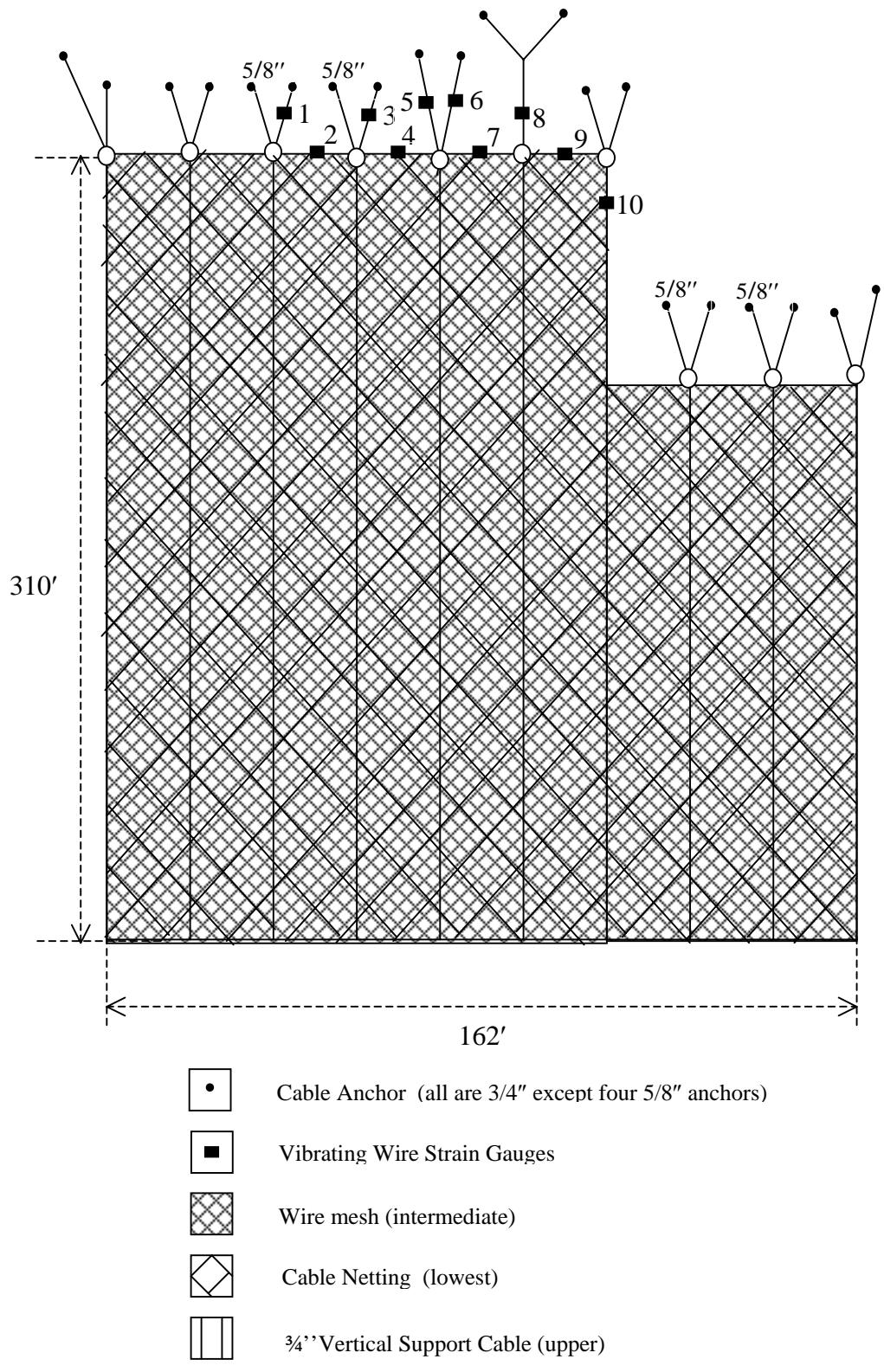


Figure 3-8. Dimensions and configuration of the cable net system and layout of the instrumentation.

clamps on the wire ropes, with one gauge on the top of the cable and another on the bottom. The values from the two gauges were averaged to decrease error due to differential strain on the cable. The strain gauges were continuously monitored with a multiplexer and a Campbell Scientific CR10x data logger. The instrumentation was sampled twice daily, at noon, and at midnight.

The ¾-inch (19-mm) cables had an elasticity modulus of  $15 \times 10^6$  lb/in<sup>2</sup> ( $10^6$  MPa), with a metallic cross-sectional area of 0.272 in<sup>2</sup> (1.75 cm<sup>2</sup>).

The strain gauges were installed several years after the system was installed. The cables were not slacked to install the strain gauges but were installed on cables that already were sustaining the static load of the system. Consequently, the measured loads reflected a change in load relative to the initial reading.

### **3.3.3 Results**

Because of the variation of the topographic and ground conditions, the measured loads and their trends at each location were not consistent. Furthermore, the times at which the maximum loads were recorded by the different strain gauges were also different. Therefore, appropriate averages of the readings were calculated to obtain an overall trend of the load variation with temperature, snowfall, and snow depth. Accordingly, the readings at locations 1, 3, 5, 6, and 8 were averaged to check the variation of the loads on the vertical ropes (Figure 3-8). Similarly, the readings at locations 2, 4, 7, and 9 were averaged to check the loads on the top horizontal ropes.

Figures 3-9 and 3-10 show the variation of the loads, temperature, snowfall, and snow depth during the period of November 2001 to April 2002. The snowfall and snow depth data were collected from the records at the Leavenworth 3S weather station,

located about 2 miles (3 km) east of the site. To compare the data, the loads, temperature, and snowfall were normalized with respect to their individual maximum values. Note that snowfall data were not available after February 2002. The maximum and minimum temperatures recorded during this period were 51.3°F (10.7°C) and 18.8°F (-7.34°C), respectively, and the largest 24-hour snowfall and maximum accumulated snow depth were 11 inches (279 mm) and 25 inches (635 mm), respectively.

It can be seen that the first snowfall occurred on November 28, 2001, and almost all strain gauges recorded its accumulation on the mesh by an increase in load (figures 3-9 and 3-10). The snow depth soon reached about 18 inches (457 mm) and fluctuated around this value until early January 2002. Notice that during this period, there were at least ten snowfall events, and the temperature was below 32°F (0°C) for most of the time. However, also during this period, the snow load continued to increase because of the snowfall, despite the approximately constant measured snow depth around 20 inches (508 mm). Therefore, it can be concluded that new snow increased the density of, and possibly deformed, the snowpack during this period. On January 12th, the temperature increased to 35.9°F (2.14°C), and the snow depth subsequently decreased a little (figures 3-9 and 3-10). However, the loads recorded by both the longitudinal and horizontal strain gauges increased from January 13th to January 18th without any additional snowfall. We suspect that because of above-freezing temperatures, the cable net and snowpack decoupled from the slope, possibly caused by melting along this boundary. Therefore, perhaps the load initially supported by the snow cohesion (Equation 4-16) was transferred to the anchors, increasing the recorded loads on the strain gauges.

A similar phenomenon appears to have occurred on February 10th and February 21st. On February 10th, the temperature sharply increased. The load recorded on the longitudinal rope increased a day after, and a similar load increase on the horizontal rope followed several days later (on February 13th and 14th). The same phenomenon repeated on February 21st. The temperature reached its maximum of 51.3°F (10.7°C) on February 21st. The snowpack on that day was about 8.25 inches (210 mm). Notice, however, that the loads on the vertical and horizontal strain gauges experienced an abrupt increase delayed by two to three days (figures 3-9 and 3-10).

The above discussion of the field data shows that the load on the cable net system increased shortly following above-freezing temperatures. These results were used to confirm some aspects of the snow model equations (4-17 and 4-18) proposed later in the report.

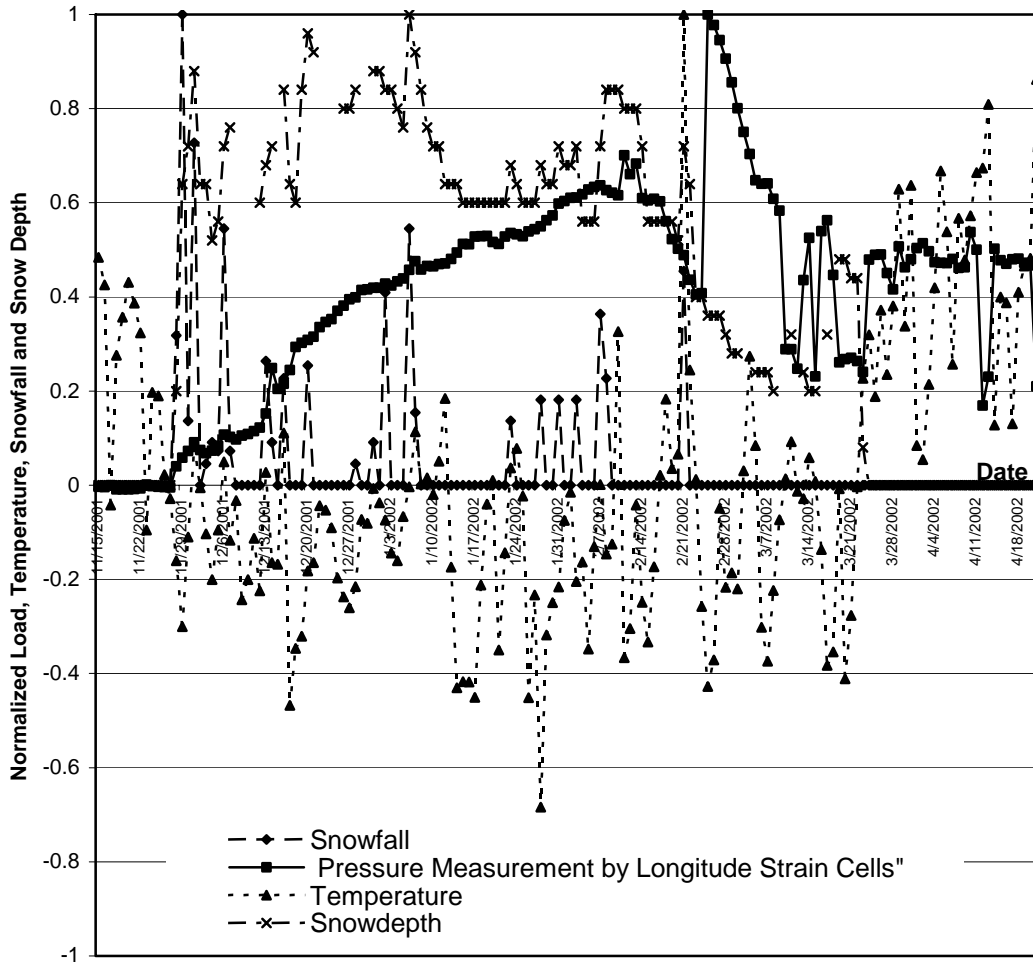


Figure 3-9. Normalized values of load for vertical (longitudinal) strain gauges, temperature, and snow depth.

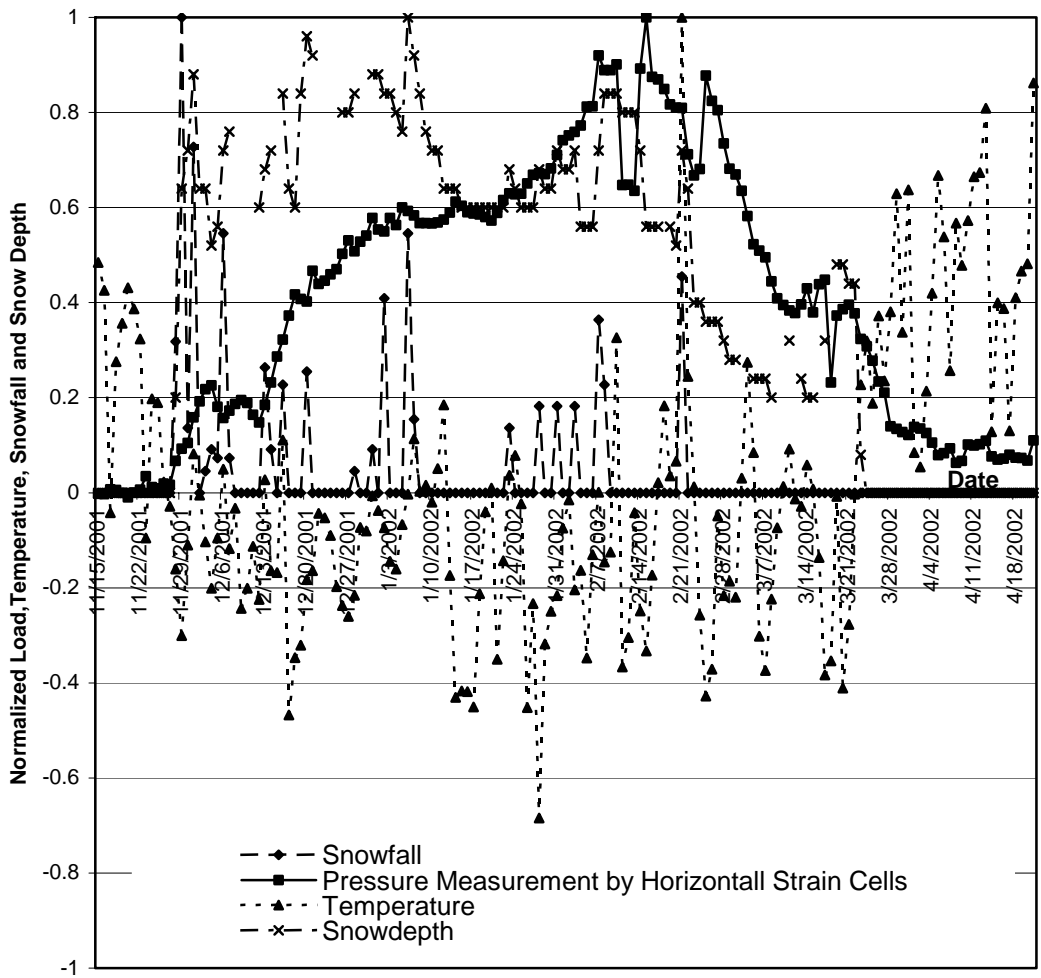


Figure 3-10. Normalized values of load for horizontal (transverse) strain gauges, temperature, and snow depth.

### 3.4 ANCHOR TESTING

#### 3.4.1 Objectives

For wire mesh and cable net rockfall protection systems, anchors are used to carry the transmitted loads. The type of anchor, grout quality, and the direction of loading may result in different failure modes, such as pullout, exceeded passive earth pressure, tensile yielding of cables/tendons, and shear. The present knowledge of anchors is mostly

limited to pullout failure (anchors loaded parallel to the tendon) and guided only by experience in the geotechnical field. However, anchors for wire mesh/cable net systems are typically loaded perpendicular to the bonded tendon/cable. For this manner of loading, there is a relatively high level of confidence in the capacity of anchors founded in various bedrock conditions, but much less confidence in the capacity of anchors founded in soil conditions. The primary objective of this testing program was to investigate the field performance of anchors founded in soil that are currently used in rockfall protection systems.

### **3.4.2 Methodology**

The anchors were installed by WSDOT and HI-TECH Construction Company of Forest Grove, Oregon, at a material borrow source located on State Route 14 near milepost 26 east of Camas, Washington. The anchors were sited in unconsolidated slope deposits (colluvium) consisting of moist, medium dense, silty gravel with sands, cobbles, and small boulders. Standard Penetration Test (ASTM D1586-99) uncorrected N values ranged from 9 to 22 within this material (Figure 3-11).

Twenty anchors were installed for the test program at the locations shown in Figure 3-12. Five types of anchors were used for the testing; four of the anchors were installed in a 4.5-inch- (115-mm) diameter, HW-size drill hole and fully grouted; only the upper 2-foot portion of the Manta Ray anchors were drilled and grouted. The five anchors were (Figure 3-13) as follows:

- driven Manta Ray<sup>®</sup> MR-2 anchor
- 1-inch (25 mm) deformed steel threaded bar
- drillable-groutable, hollow core, 1-inch (25 mm) deformed steel bar
- single-strand, ¾-inch (19-mm) wire rope anchor
- Geobrug double-strand, ¾-inch (19-mm) wire rope anchor.

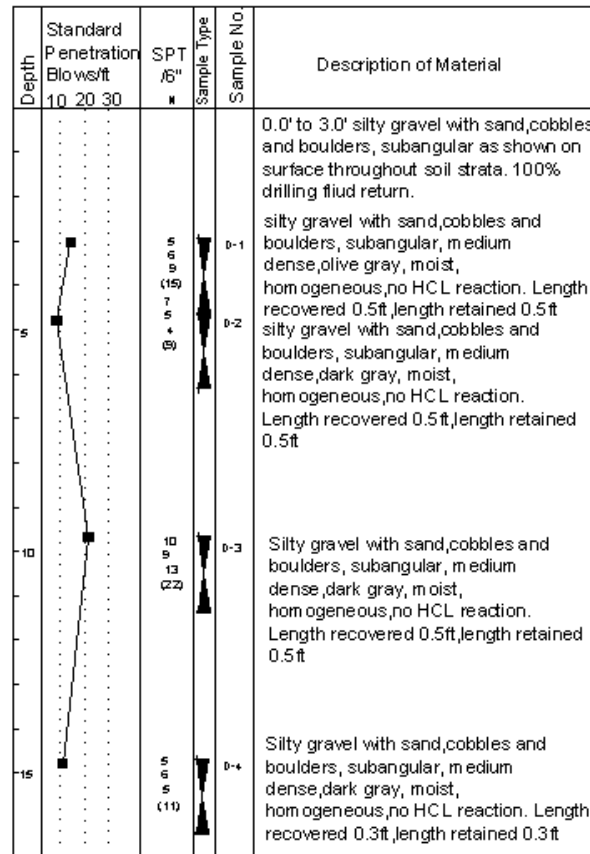


Figure 3-11. A boring log depicts the subsurface conditions in which the anchors were founded. The depths are recorded in feet.

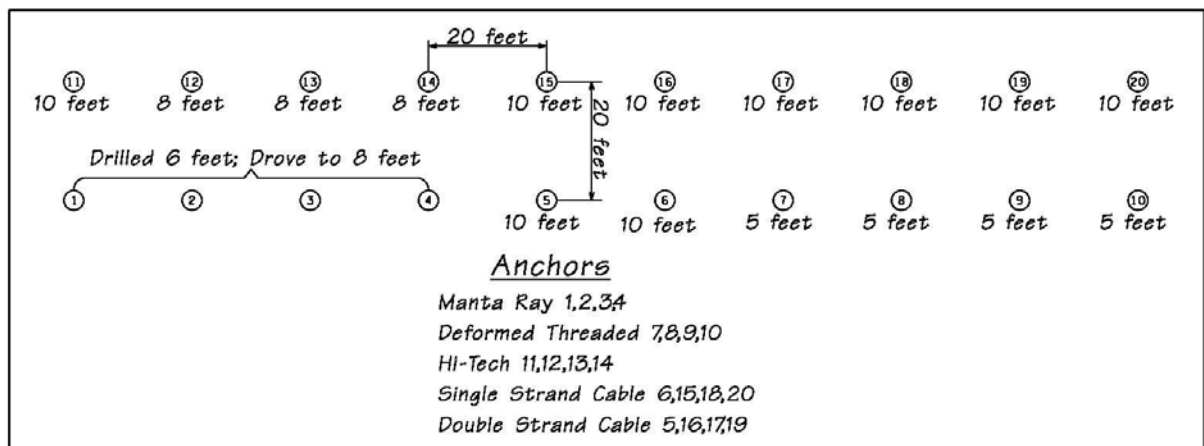
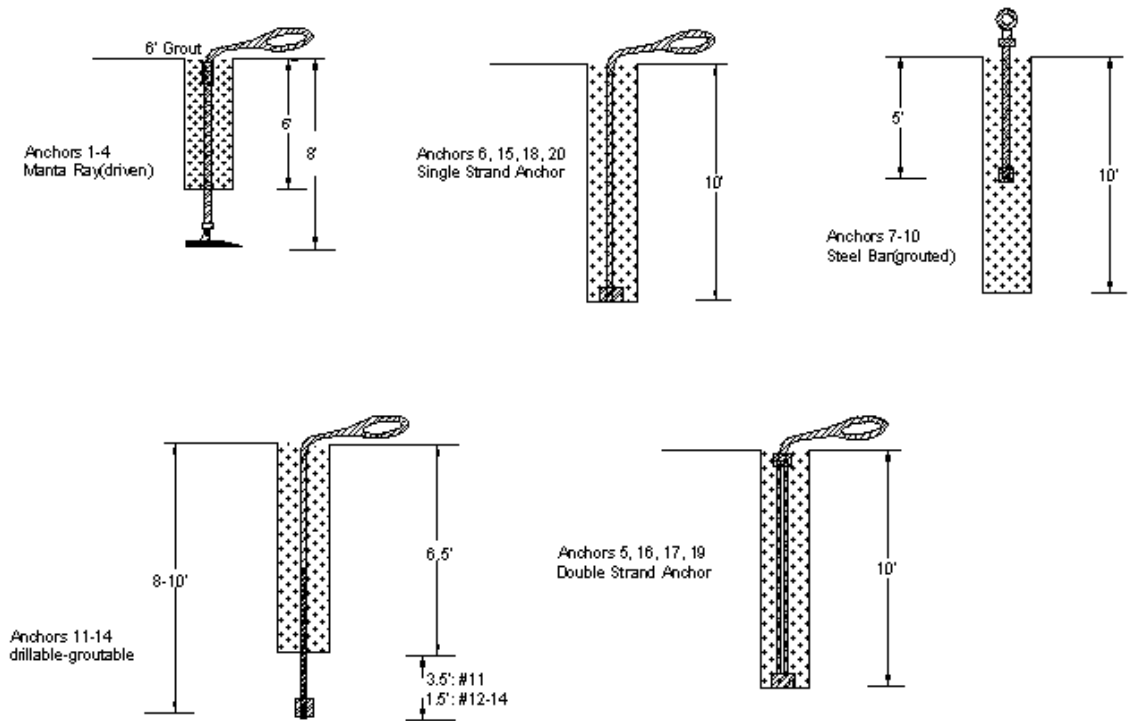


Figure 3-12. Layout of anchors and the depths to which they were installed.



**Figure 3-13.** The tested anchors included (A) Manta Ray<sup>®</sup>; (B) single-strand cable; (C) deformed steel threaded bar; (D) HI-TECH (drillable-groutable); and (E) Geobrug double-strand cable.

Ten anchors were loaded vertically, and ten were loaded within 15° of horizontal.

The type of anchors and the corresponding loading direction are summarized in Table 3-

3.

**Table 3-3. Anchors and test type**

Anchor Number	Anchor Type	Test Type	Anchor Number	Anchor type	Test Type
1	Manta Ray <sup>®</sup>	Vertical	11	HI-TECH	Vertical
2	Manta Ray <sup>®</sup>	Horizontal	12	HI-TECH	Vertical
3	Manta Ray <sup>®</sup>	Vertical	13	HI-TECH	Horizontal
4	Manta Ray <sup>®</sup>	Horizontal	14	HI-TECH	Horizontal
5	Double Cable	Horizontal	15	Single Cable	Vertical
6	Single Cable	Vertical	16	Double Cable	Horizontal
7	Steel Bar	Vertical	17	Double Cable	Vertical
8	Steel Bar	Horizontal <sup>1</sup>	18	Single Cable	Horizontal
9	Steel Bar	Horizontal	19	Double Cable	Vertical
10	Steel Bar	Horizontal	20	Single Cable	Horizontal

<sup>1</sup> The test was terminated because of a wood beam breaking in the initial setup at a 22-kip load.

The test apparatus for the vertical load test is shown in Figure 3-14. It consisted mainly of a hydraulic jack, load cell, motor, displacement dial gauge, and a load frame supported on two 8,000-lb (3600-kg) concrete blocks. To minimize the influence of the load frame on the soil reaction, the load frame was designed to span 10 ft (3 m) with minimal deflection for the anticipated range of loads

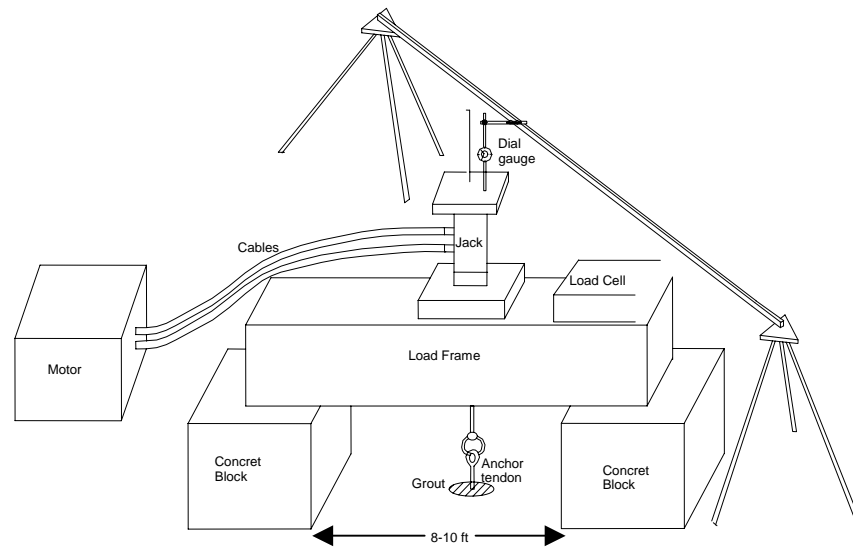


**Figure 3-14. Setup for vertical loading.**

The test setup for the horizontal series of tests is shown in Figure 3-15. The arrangements used in the vertical test were adopted. In addition, a 35,000-lb (15,900-kg) Caterpillar D5 bulldozer with rippers was used to provide counter-resistance in the horizontal tests. The setup used was a load frame with a load cell and hydraulic jack attached to the anchor cable. Offset distances similar to those of the vertical tests were maintained to minimize the influence of stresses within the soil.

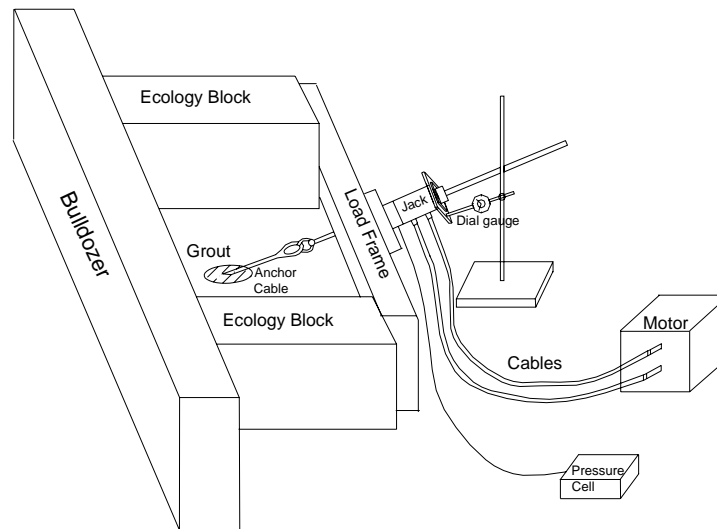


**Figure 3-15. Setup for horizontal loading.**

### **3.4.3 Results**

#### **3.4.3.1 Vertical Test Series**

The results of the vertical load testing are plotted and shown in Figure 3-16; graphs of each test are also included in Appendix C. All but one of the anchors achieved a load of 20,000 lbf (89 kN) and did so within about 1 inch (25 mm) of deflection. All the anchors that used a wire rope for the tendon (all but Anchor #7) required more displacement than the deformed steel bar (Anchor #7). Presumably, the greater displacements to mobilize anchor capacity were due to the stretch of the cable.

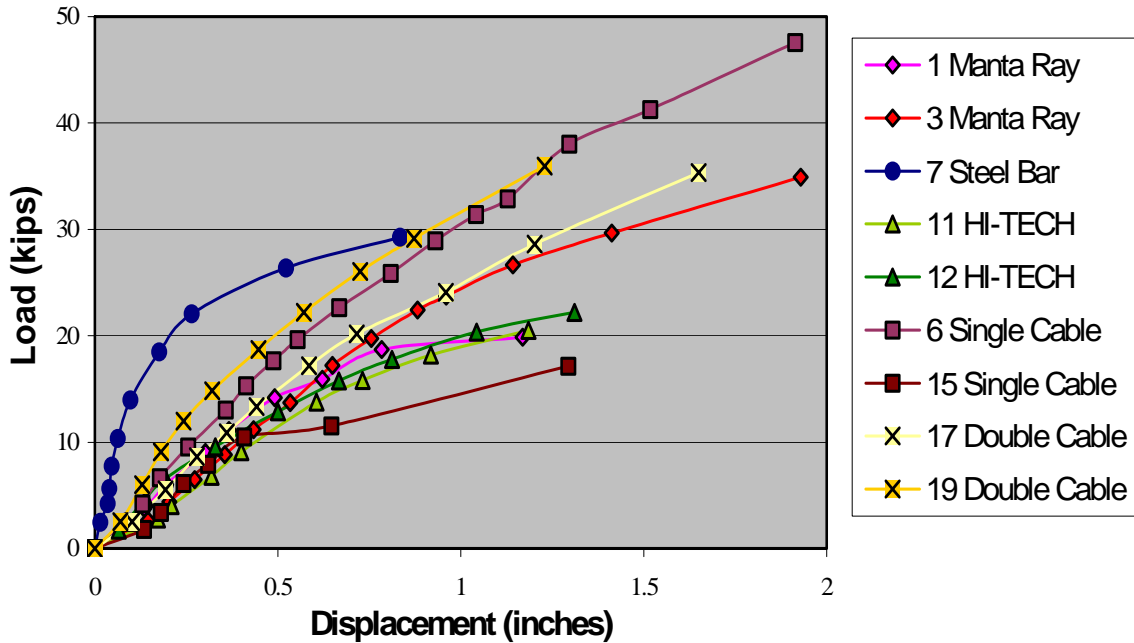


Figure 3-16. Load versus displacement plot for all vertical anchor tests.

It can be seen that the displacement curves were nonlinear. A displacement curve can be approximated by a hyperbolic relation give by:

$$P = \frac{e}{Me + C} \quad (3-1)$$

where  $M$  and  $C$  are material constants,  $P$  is the applied load, and  $e$  is the displacement. Rearrangement of Equation 3-1 as  $e/p$  against  $e$  results in a linear relation with a slope  $M$  and intercept  $C$ :

$$\frac{e}{P} = Me + C \quad (3-2)$$

Further rearrangement of Equation 3-2 results in:

$$M = \frac{1}{P} - \frac{C}{e} \quad (3-3)$$

It can be seen that when the displacement,  $e$ , becomes very large (i.e.,  $e \rightarrow \infty$ ) and  $P$  reaches the ultimate capacity of the anchor,  $P_{ult}$ , Equation 3-3 reduces to:

$$M = \frac{I}{P_{ult}} \quad (3-4)$$

Therefore, the ultimate load that can be carried by the anchors, assuming the soil is the limiting condition, can be determined as the inverse of  $M$ . Differentiation of the force  $P$  with respect to the displacement  $e$  in Eq (1) leads to:

$$\frac{dP}{de} = \frac{(Me + C) - Me}{(Me + C)^2} = \frac{C}{(Me + C)^2} \quad (3-5)$$

When  $e$  is equal to zero, then

$$\frac{dP}{de} = \frac{1}{C} \quad (3-6)$$

Or:

$$C = \frac{de}{dP} \quad (3-7)$$

Thus, the inverse of the slope of the load-displacement curve  $\frac{de}{dP}$  at the origin is given by the intercept value  $C$ .

In many of the vertical tests, because of the limitation of the test setup, the ultimate load of high capacity anchors could not be determined. Because the ultimate capacity is given as the inverse of  $M$ , the hyperbolic formulation can be used to determine its value with available test data. Again, the ultimate capacity is controlled by not only the soil-anchor interaction but also the capacity of the individual elements of the anchor.

The load displacement curve for Anchor #7 plotted in Figure 3-16 is represented on the  $e/p$  versus  $e$  plot shown in Figure 3-17. It can be seen that the data plotted as a straight line (Equation 3-2), confirming the hyperbolic variation. On the basis of this

plot, the ultimate load for this test was determined to be 34 kips (151 kN). Nine full-scale vertical pull tests were carried out to investigate the load capacity of different anchors. The theoretical ultimate vertical loads of the nine anchors were determined by using the hyperbolic approximation of the load-displacement curves, and the results are as shown in Table 3-4. The testing revealed that the double-strand cable anchors should have had the highest capacity of the five types tested. Another finding from the vertical testing was the large area of visible ground deformation that occurred for the given soil conditions (Figure 3-18). In a number of cases, the cracking extended beyond the concrete blocks, indicating that the load frame somewhat influenced the soil reaction. The extent of ground deformation for loose to medium dense soil conditions for this range of loads would suggest that vertical pullout testing of anchors as a conformance test may not be practical under many field conditions.

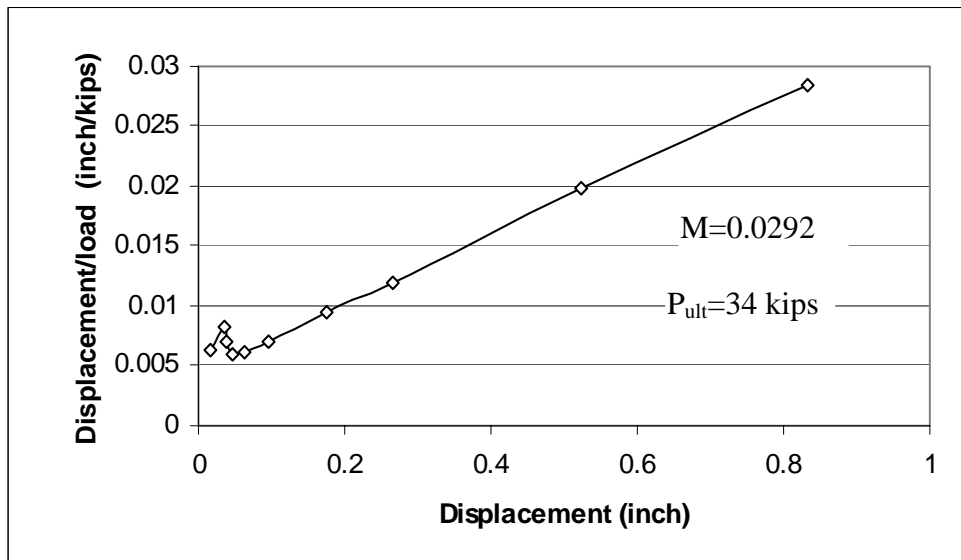


Figure 3-17. The data from Anchor 7 in Figure 3-16 are plotted as a hyperbolic relation.

**Table 3-4. Theoretical ultimate vertical load of anchors**

<b>Anchor Number</b>	<b>Anchor type</b>	<b>Theoretical Ultimate Load <i>lbf (kN)</i></b>	<b>Average Theoretical Ultimate Load<sup>1</sup> <i>lbf (kN)</i></b>
1	Manta Ray	33,000 (147)	49,000 (218)
3	Manta Ray	65,000 (289)	
7	Deformed Steel Bar	34,000 (151)	34,000 (151)
11	HI-TECH	53,500 (238)	46,200 (206)
12	HI-TECH	39,000 (173)	
6	Single Cable	119,000 (529)	73,000 (325)
15	Single Cable	27,000 (120)	
17	Double Cable	88,500 (380)	79,700 (348)
19	Double Cable	70,900 (315)	

<sup>1</sup> The average ultimate load is a theoretical value for the maximum capacity for the given soil conditions. The actual ultimate load is also a function of the capacity of structural elements that compose the anchor.



**Figure 3-18. Ground cracking (white painted lines) that developed around Anchor 17 (double cable anchor) during vertical loading.**

With the exception of a single-strand cable anchor (#15), which sustained just over 17,000 lbf (75 kN), all of the anchors sustained loads above 20,000 lbf (89 kN). However, the highest load of 47,000 lbf (209 kN) was also obtained with a single-strand cable anchor (#6). All these loads were achieved with less than 2 inches (50 mm) of

displacement. The deformed steel threaded bar (Anchor #7) behaved much stiffer than those anchors that utilized a cable and achieved a near-yielding condition within 1 inch (25 mm) of displacement.

#### **3.4.3.2 Horizontal Test Series**

Because for most mesh systems the load is applied to the anchor in a direction sub-parallel to the ground surface, the second series of tests was conducted in a near horizontal load direction. Unlike the vertical series of tests, the load in the horizontal direction could not be increased monotonically until failure without reaching the limit of the hydraulic jack. As the horizontal load was increased, the surrounding soil deformed, and the anchor grout started to crack, leading to larger displacement. When the accumulated displacement reached around 3 inches (75 mm), which was the throw limit of the hydraulic jack, the load was removed to recover the jack, and the dial readings were zeroed. Subsequently, the load was increased until the next limit, and the process repeated until the maximum load was reached.

The typical results of the horizontal series of tests are presented in figures 3-19, 3-20, and 3-21. The load-displacement relation followed a linear stress path before the reapplied load exceeded the maximum load of the previous cycle. Once past the previous maximum value, the anchor started to yield, as evidenced by the nonlinear stress path. Three to six loading cycles were completed to find the ultimate horizontal capacity or until the load limit of the jack and load cell were reached. For some anchors, the ultimate load may not have been determined. In all tests, for each cycle, the yielding load was higher than that in the previous cycle. This may have been due to the anticipated progressive cracking of the grout from the top down. In all cases, even though the cumulative displacements reached values as high as 18 inches (46 cm), the testing was

unable to completely fail the anchors, and they continued to sustain load despite large deflections. The highest load achieved in the tests reached 55,000 lbf (245 kN). Table 3-5 summarizes the test results for all of the anchors; in addition, plots of each of the tests are included in Appendix C. The testing revealed, however, that the horizontal displacements would be very high (in excess of 8 inches (200 mm)) before the ultimate capacity of the anchor was reached. The Manta Ray<sup>®</sup> anchors demonstrated some of the best performance in terms of consistency and capacity, with a moderate degree of deflection. The steel bars required the highest amount of deflection to develop the lowest range of capacity. Note, however, that the steel bars were only 5 ft (1.5 m) long; all the other anchor types ranged from 8 to 10 ft (2.4 to 3.0 m) long.

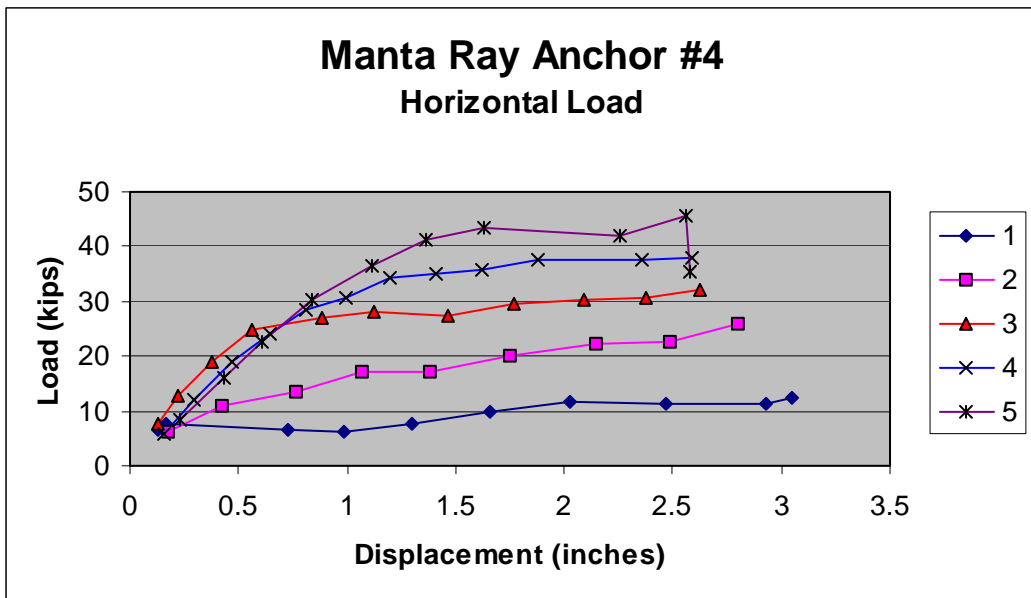


Figure 3-19. Load-displacement plot for horizontal test of a Manta Ray<sup>®</sup> anchor (#4).

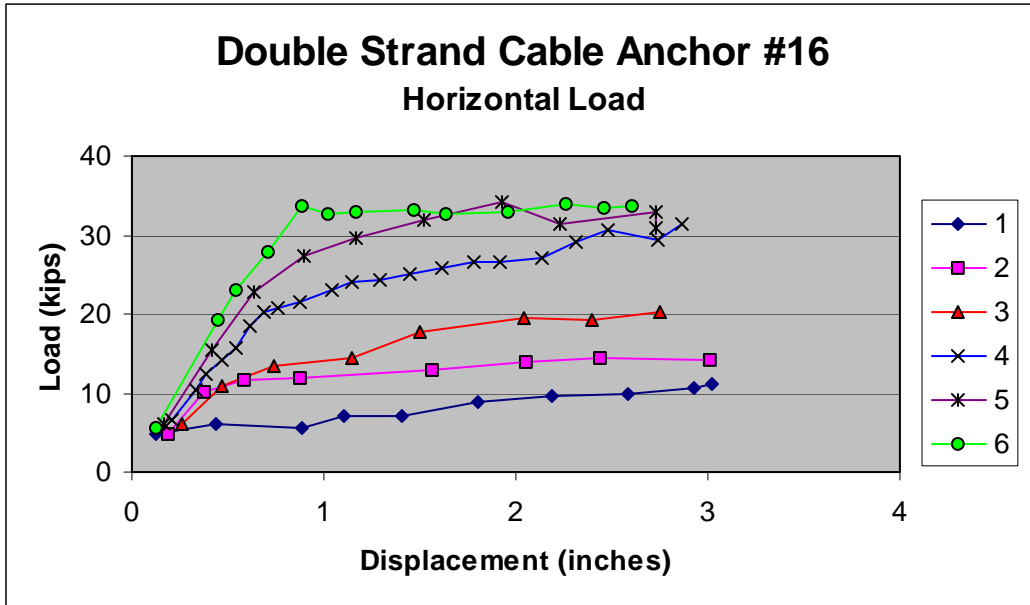


Figure 3-20. Load-displacement plot for horizontal test of a double-strand cable anchor (#16).

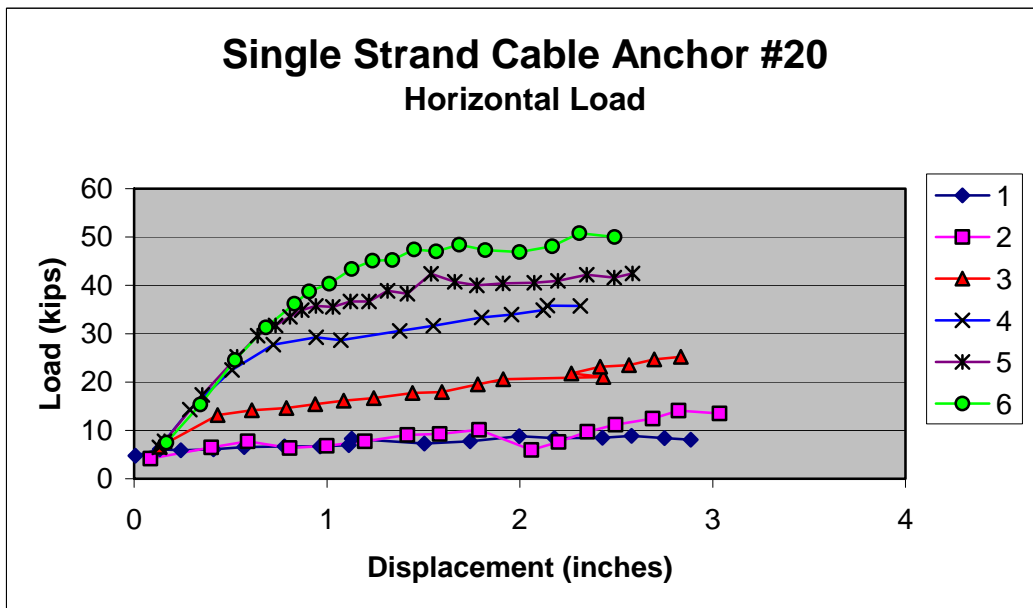


Figure 3-21. Load-displacement plot for horizontal test of a single-strand cable anchor (#20).

**Table 3-5. Test results for horizontal anchor load**

<b>Anchor #</b>	<b>Anchor Type</b>	<b># of Load Cycles</b>	<b>Maximum Load <i>lbf (kN)</i></b>
2	Manta Ray®	4	55,000 (245)
4	Manta Ray®	5	45,700 (203)
9	Steel Bar	6	19,600 (87.2)
10	Steel Bar	6	32,400 (144)
13	HI-TECH	6	39,900 (178)
14	HI-TECH	3	29,600 (132)
18	Single Cable	4	21,400 (95.2)
20	Single Cable	6	50,800 (226)
5	Double Cable	5	43,800 (195)
16	Double Cable	6	34,200 (152)

It appears that large displacement is mainly associated with progressive grout cracking from the top to the bottom of the anchor. Consolidation on the passive side of the anchor also contributes to the observed displacement. Hence, a larger anchor grout diameter on the top could reduce deflection and increase capacity. Furthermore, the depth of the grout column may not be a critical parameter in limiting deflection, so it may not be necessary to grout an anchor to its full depth.

## **CHAPTER 4 SNOW LOADS**

Snow has unique physical and mechanical properties, such as a wide range of densities, stages of metamorphism, and free water content, that distinguish it from other natural materials. Consequently, the properties of snow are not well established for use with a high degree of confidence (Brown, 1989). Most of the current knowledge about snow load on structures has been obtained by researchers in the field of snow avalanche defense (Haefeli, 1948 and McClung, 1982). However, this information cannot be directly used to calculate snow load because avalanche load estimates are for structures oriented normally to the slope, whereas the snow load on mesh systems acts parallel to the slope.

However, the basic concepts of snow mechanics derived from avalanche defense offer some guidance toward the development of models suitable for snow load calculations on mesh systems. Therefore, this chapter presents snow mechanics relevant to the present study. The state of stress and deformation of snowpack on a slope were first analyzed to gain an understanding of the mechanics of snow load on mesh. Subsequently, a snow load model appropriate for mesh systems was developed. The model was then used to evaluate the performance of some existing mesh systems exposed to snow loads.

### **4.1 SNOW LOAD ON AVALANCHE STRUCTURES**

A one-dimensional element along the neutral section of a snowpack, which is the central section where no slope-parallel gradients (e.g., density, deformation, and stress) exist, is shown in Figure 4-1. The one-dimensional equilibrium equation for the

snowpack element can be developed by averaging the relevant parameters with respect to the depth (McClung 1982).

The depth-averaged stress is defined as:

$$\overline{\sigma_x} = \frac{1}{H} \int_0^H \sigma_{xx} dz \quad (4-1)$$

where  $\sigma_{xx}$  is the normal stress in the x-direction at a point within the snow pack. Similarly, the stress in the z-direction and the density can also be depth averaged to give  $\sigma_z$  and  $\rho$ , defined as the depth-averaged density of snow. By using the average parameters, the equation of equilibrium can be written as:

$$H \frac{d\overline{\sigma_x}}{dx} = \overline{\rho}gH \sin \theta - \tau(x) \quad (4-2)$$

where  $g$  is acceleration due to gravity, and  $\tau(x)$  is snowpack drag at the interface (due to creep and glide), which is expressed as:

$$\tau(x) = \frac{\mu u(x)}{D} \quad (4-3)$$

where  $\mu$  is the shear viscosity,  $D$  is the stagnation depth, and  $u$  is creep velocity.

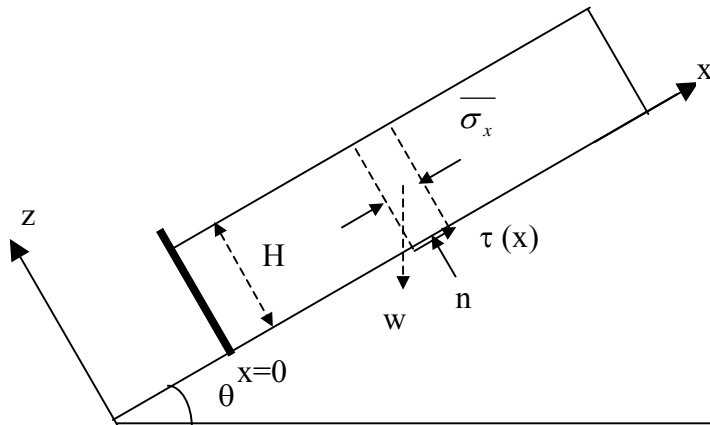


Figure 4-1. Stress components of snowpack upslope of an avalanche structure.

Because of the interruption of creep and glide movement by the avalanche structure, the variation of the drag force and the velocities along the slope assume the pattern shown in Figure 4-2. Accordingly, the following boundary conditions are assumed:

$$\begin{aligned} \bar{u} &= 0 & \text{at } x = 0 & \text{( the location of the structure)} \\ \bar{\dot{e}} &= \bar{\dot{e}}_{max} & \text{at } x = 0 \\ \bar{u} &= U_0 & \text{for } x \rightarrow \infty & \text{( neutral zone)} \\ \bar{\dot{e}} &= 0 & \text{for } x \rightarrow \infty \end{aligned}$$

where  $\bar{\dot{e}} \approx \frac{du}{dx}$  is the compressional strain rate,  $u$  is the slope parallel creep velocity component, and  $U_0$  is the slope parallel creep velocity component in the neutral zone.  $\nu$  is the viscous Poisson's ratio, and  $\rho$  is the density of snowpack. The superscript bar indicates that the quantity is averaged within the snowpack depth.

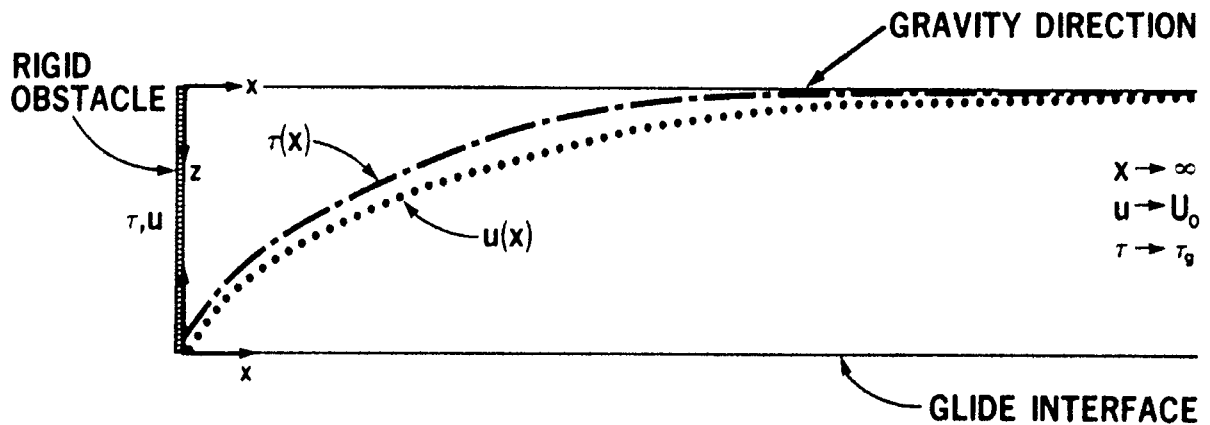


Figure 4-2. A cross-section of snowpack upslope of an avalanche structure illustrates the distribution of drag force and velocity along the slope (McClung, 1982).

With  $D$  and  $\nu$  taken constant throughout the zone of influence of the structure, the solution at  $x = 0$  is of the form:

$$\bar{\sigma} \Big|_{x=0} = \left[ \frac{2}{1-\nu} \left( \frac{D}{H} \right) \right]^{\frac{1}{2}} \tau_g + \frac{\nu}{1-\nu} \bar{\rho} g (\cos \theta) \frac{H}{2} \quad (4-4)$$

The term,  $\sigma \Big|_{x=0}$ , therefore, depends on  $v$ ,  $\theta$ , and the boundary conditions on the structure.

Equation 4-4 is often used to calculate the pressure applied by the snowpack acting perpendicularly to the structure. Note that some avalanche researchers have preferred to use the original snow load model proposed by Haefeli (1948). However, the basic principles of both models are almost identical.

#### **4.2 SNOW LOAD ON MESH SYSTEMS**

In the case of draped mesh systems, there is no structure oriented normally in relation to the slope to interrupt the movement of snowpack, as there is in avalanche defense. Because on slopes that accumulate snow the mesh generally lays in contact with the slope, the drag force between the mesh and the ground surface can be assumed to be uniform along the slope, as shown in Figure 4-3. Therefore,  $\tau(x)$  in Equation (4-2) becomes constant and is independent of  $x$ . Furthermore, the velocity  $u(x)$  will also be independent of  $x$ . As a result, the snow load model for a structure oriented parallel to the slope, such as the mesh system, is much simpler than that for a structure oriented normally in relation to the slope, such as a snow fence. However, as a complicating factor, the temperature changes and metamorphism within the snowpack affect the load transfer, as was observed at the Tumwater Canyon site discussed in Chapter 3. Two cases are thus considered: snow loads associated with below- and above-freezing temperatures.

### 4.2.1 Snow Load below Freezing

In the case of temperature below freezing, the snowpack, mesh, and slope surface are frozen together and can be assumed to behave as a continuous body. The forces acting on the snowpack and the mesh for this condition are as shown in Figure 4-3. Haefeli investigated the dependence of the magnitude of shear and normal stress of a snow sample as a function of the gliding velocity. Using his experimental data, Salm (1977) proposed the following relation for shear strength:

$$\tau = a_0(\sigma_z, t) + a_1(\sigma_z, t) \cdot v_g \quad (4-5)$$

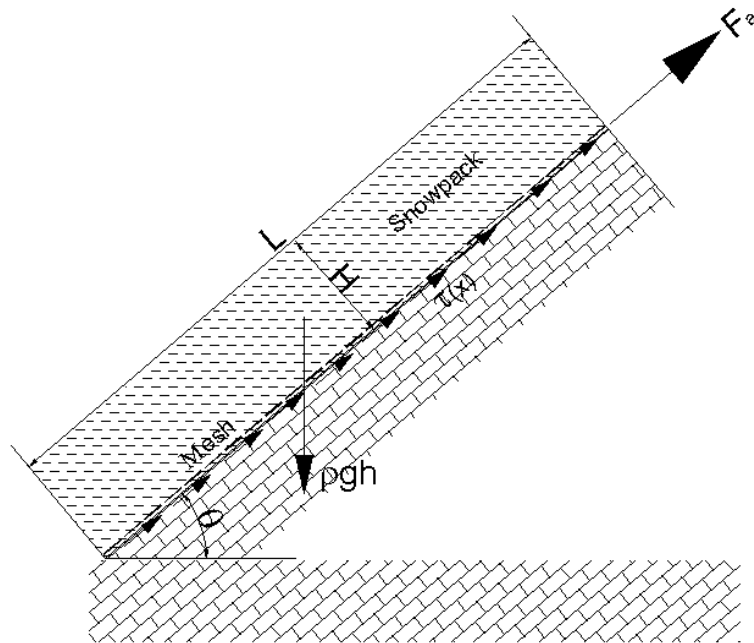


**Figure 4-3: The force components of the mesh and snowpack when the snow is bonded to both to the mesh and ground.  $F_a$  is the drag force on the anchors for a section of mesh  $L$  in length.**

where  $a_0$  and  $a_1$  are functions of the normal stress  $\sigma_z$ ,  $t$  is the temperature, and  $v_g$  is the glide velocity. On the basis of a series of tests with a constant temperature  $t = 0^\circ \text{C}$ , Salm found that:

$$a_0 = c \quad (4-6a)$$

where  $c$  is a constant termed snow cohesion and:

$$a_1 = \frac{\mu_w}{\delta} \quad (4-6b)$$

where  $\mu_w$  is the viscosity of the water (at  $t = 0^\circ \text{C}$ ), and  $\delta$  is the thickness of the shear boundary layer that increases linearly with the magnitude of the normal stress. Therefore, it can be concluded that the strength of snow is composed of a stress independent cohesion and a Newtonian viscosity.

If the snowpack is held along the ground surface in this case, the glide velocity of the snowpack along the ground can be assumed to be 0. Therefore, the strength is dominated by the cohesion:  $\tau = c$ . Then, the force carried by an anchor for per unit width of the mesh,  $F_a$  is as follows:

$$F_a = \rho g H L \sin \theta - Lc \quad (4-7)$$

The magnitude of  $c$  is dependent on the density of the snowpack and the temperature. For loose snow, it may be close to zero.

#### **4.2.2 Snow Load above Freezing**

When the temperature rises above freezing, the mesh may uncouple from the ground surface and the snow load is transferred to the mesh system. This phenomenon was evident from the load cell data obtained from the instrumented cable net system at Tumwater Canyon. The measured snow load always increased significantly just after a rise in temperature above  $32^\circ\text{F}$  ( $0^\circ\text{C}$ ) even without any snowfall (figures 3-9 and 3-10).

Considering the somewhat theoretical case in which there is no interface friction, the resistance between the frozen snowpack/mesh and the ground would be negligible.

The force components acting on the snowpack and mesh system would then be as shown in Figure 4-4.

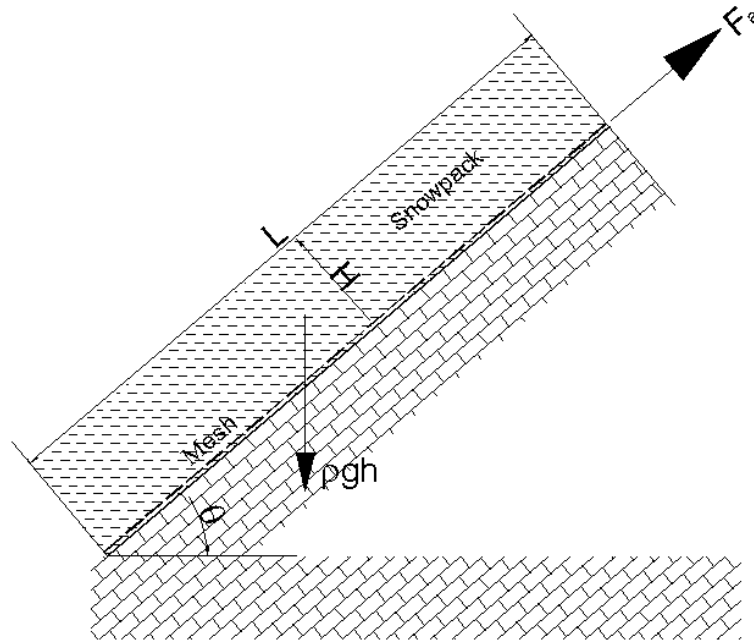


**Figure 4-4. The force components of the mesh and snowpack when the snow is bonded to the mesh but uncoupled from the ground. In this theoretical case, the mesh system is entirely supported by the anchors.**

For this case, the force  $F_a$  applied to an anchor per unit width of mesh would be:

$$F_a = \rho g H L \sin \theta \quad (4-8)$$

In actuality, if a slope were shallow enough to accumulate snow, the mesh would have some ground contact, and thus some interface friction would exist. As a result, the mesh would be subjected to a drag force from the upper snow and resistance from the ground. The forces applied to the mesh are shown in Figure 4-5. For this case, the force  $F_a$  applied to an anchor by per unit width of mesh is:

$$F_a = \rho g H L \sin \theta - \rho g H L \cos \theta \cdot \tan \phi \quad (4-9)$$

where  $\tan \phi$  is the interface friction coefficient between the mesh and the ground.

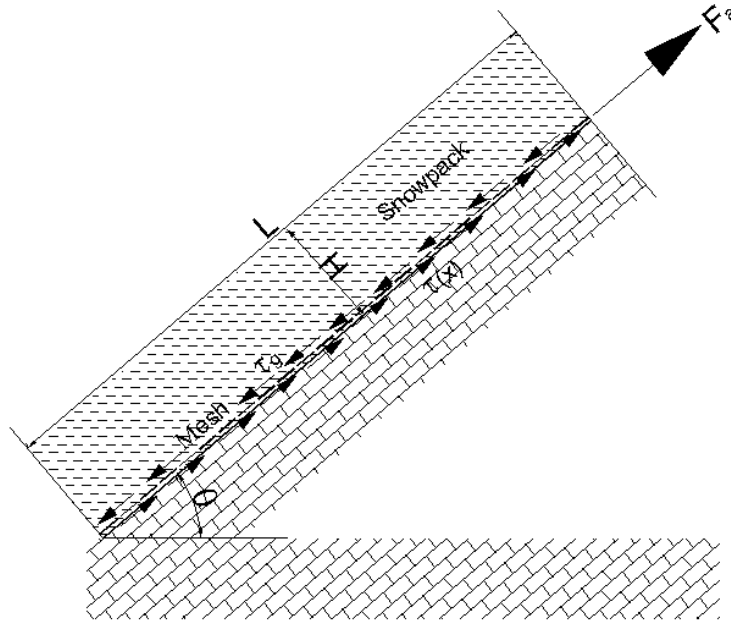


**Figure 4-5 The force components of the mesh and snowpack snow, including the contribution of interface friction.**

The first case is more critical, as the interface friction is assumed to be near zero. Consequently, Equation 4-8 could be considered to give a conservative maximum load on the anchors. Note that in the case of an undulating or rough slope surface, mesh protrusions increase the effective interface resistance to the mesh system. Such effects can be accounted for by assuming an equivalent interface friction angle in Equation 4-9.

### **4.3 PERFORMANCE OF MESH SYSTEMS**

The interface friction between the mesh and the slope surface can be a major contributor to resistance under normal conditions. The presence of snow will reduce this resistance. The above snow models were used to study the performance of six mesh systems in snowy regions in order to evaluate the reduced resistance and the contribution/limitation of interface friction. This was done by rewriting Equation 4-9 as:

$$\tan \phi = \frac{\rho g H L \sin \theta - F_a}{\rho g H L \cos \theta} \quad (4-10)$$

The above equation was used to back calculate the interface friction angle at five sites (three hexagonal wire mesh and two cable net installations) in Washington State and one hexagonal mesh installation in Nevada. Four of the systems failed because of snow loads, and the remaining two had sustained repeated seasonal loading with no visible damage to the systems. Regrettably, determination of the loads at failure was not possible. The failures were only evident after spring melt, so the load at failure could only be surmised on the basis of the snowpack conditions observed by DOT maintenance personnel or reported by nearby snow observation stations. Furthermore, the following assumptions were made in the analyses:

- Slope segments with angles of greater than 60° were assumed to be too steep to retain snow. If steep segments occurred at the base of the slope, they did not contribute to the snow load on the mesh on such sections. However, if a steep segment was above a shallow segment, the snow load for the steep segment was included, since it was assumed that snow from a steep segment would slide down and accumulate on the shallower slope segment.
- Snow density can vary widely, from about 2 to 40 lbs/ft<sup>3</sup> (30 to 600 kg/m<sup>3</sup>). Snow densities were assumed to be in the range of 19 to 25 lbs/ft<sup>3</sup> (300 to 400 kg/m<sup>3</sup>), given typical late winter snowpack densities for the respective regions.

The back-calculated interface friction angles from these six sites were used later to calibrate the interface friction modeling results in Chapter 6 and the field characterization guidelines in Chapter 7.

#### **4.3.1 Upper Tumwater Canyon Site #1 (hexagonal wire mesh, 53° slope)**

This system was installed along the westbound lane of highway US 2 around MP 90.9 in Tumwater Canyon, located on the eastern slope of the Washington Cascades about 5 miles (8 km) northwest of Leavenworth at around elevation 1600 ft (500 m). The system was installed in 1997 and failed as a result of snow loading during the winter of 2001-2002. The installation was approximately 90 to 100 feet (30 m) wide and about 50 feet (15 m) high (Figure 4-6). The slope is compound, with a steep lower portion adjacent to the roadway and an upper, moderately inclined (53°) portion (Figure 4-7).

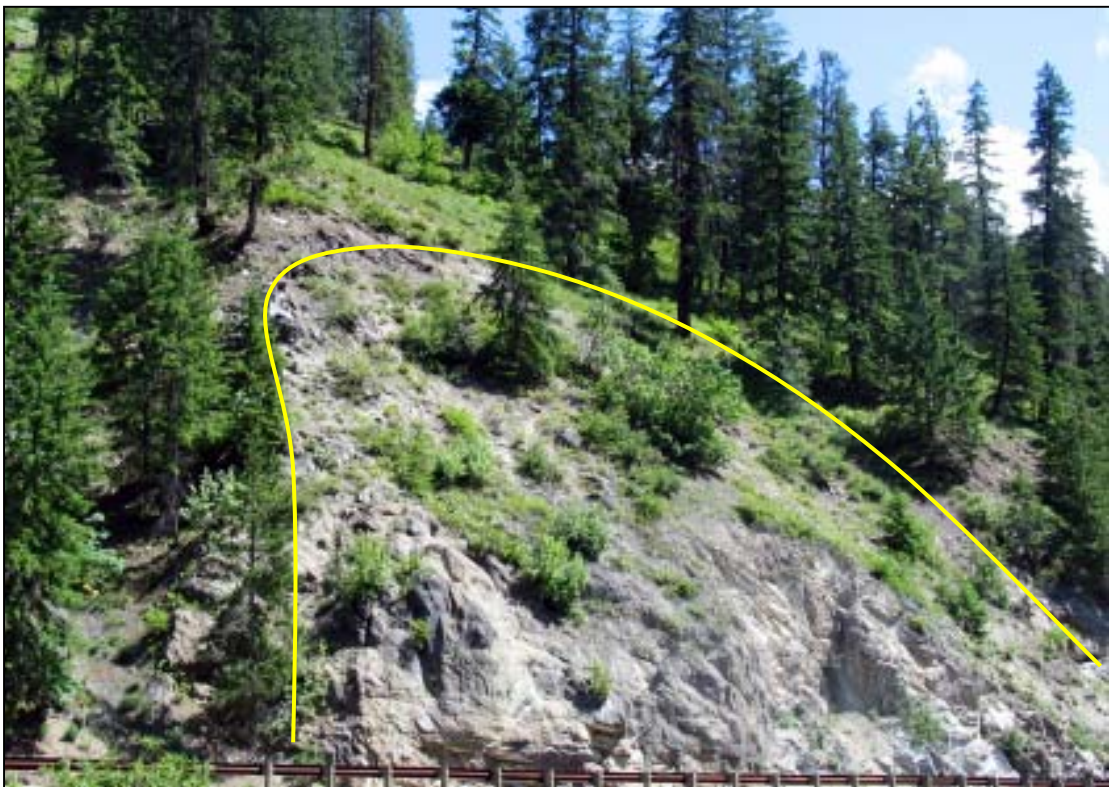


**Figure 4-6: Mesh installation (yellow line) on a planar and relatively smooth slope segment upslope of the steep bedrock exposures at roadway level. Snow accumulates only on the upper slope segment.**

The double-twisted hexagonal mesh was initially suspended with five ½-inch- (13-mm) diameter, mild steel anchors that were founded in rock, with an anchor spacing

of 16 to 25 feet (5 to 8 m). The estimated yield strength of the bar in shear was around 13,000 lbf (60 kN). Four of the five anchors failed in shear in this section, but the system remained on the slope supported only by the center anchor and the interface friction.

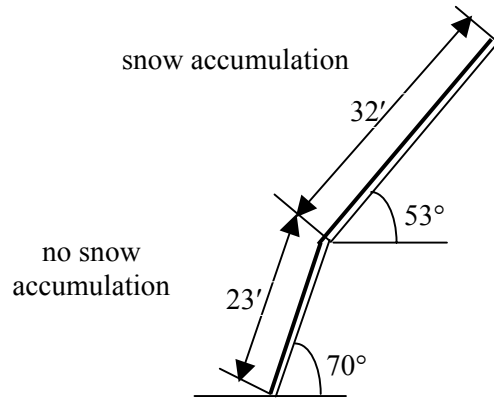


**Figure 4-7: Cross-section of installation with slope configuration and area of snow accumulation.**

Instrumentation data from the cable net system (presented in Chapter 3) that was located in the canyon about 5 miles (8 km) to the south showed that the maximum snow depth for the season was 25 inches (635 mm). Although snow accumulation occurs annually at this site, DOT Maintenance personnel reported that snow slides do not initiate on the upper slope area. The 2001-2002 winter did not receive the most snowfall of the five winters that the system had been in place, nor was it the coldest. The reason for failure during this winter rather than a wetter, colder winter can only be surmised. For back-analyzing the failure, the accumulation of snow was assumed to occur entirely on the upper portion of the slope, since the lower portion is too steep to retain snow. For an anchor spacing of 25 feet (7.6 m) this translated into  $F_a = 13000/25$  per unit width. The result of applying Equation 4-10 was that the corresponding interface friction angle for failure would be less than 39°:

$$\tan(\phi) = \frac{400 \text{ kg} / \text{m}^3 \times 0.0624 \times 25' \times 0.083 \times 32' \times \sin 53^\circ - \frac{13000}{25}}{400 \text{ kg} / \text{m}^3 \times 0.0624 \times 25' \times 0.083 \times 32' \times \cos 53^\circ} = 0.81$$

The upper slope segment, which accumulates snow, is planar and has few protrusions (Figure 4-8).

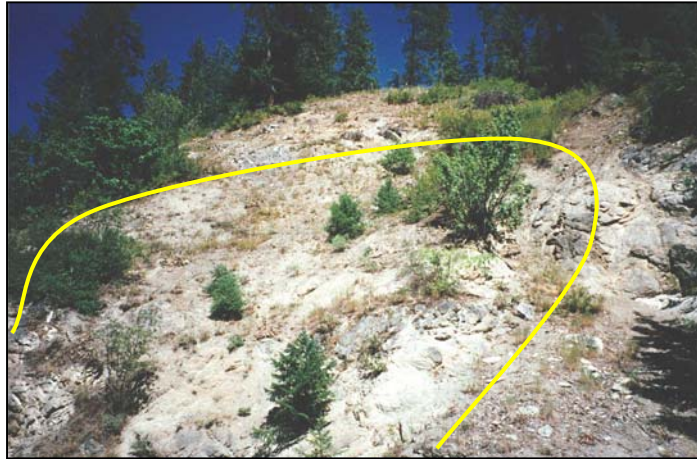


**Figure 4-8. Upper slope area before 1997 installation and the area where snow accumulates. Yellow line delineates approximate coverage area of mesh. Note planar condition and absence of irregularities over much of the upper slope.**

In 2002, the anchors were replaced with higher capacity wire rope anchors (>25,000 lbf/110 kN) on the same spacing. The following two winters resulted in similar depths of snowpack, and no signs of system instability were observed.

#### **4.3.2 Upper Tumwater Canyon Site #2 (hexagonal wire mesh, 45° slope)**

This installation was located about 250 feet (75 m) south of Site #1 around MP 91.0 and was installed the same year and similarly failed during the 2001-2002 winter. It was approximately 80 to 90 feet (25 m) wide and about 100 feet (30 m) high, covering about 127 feet (39 m) of slope length (Figure 4-9). The slope is roughly oriented around 45° and consists of a shallow salient/chute on an otherwise uniform upper slope (Figure

4-10). The double-twisted hexagonal mesh was also initially suspended with five ½-inch (13-mm) mild steel anchors founded in rock, with an anchor spacing of 16 to 18 feet (5 m). All five anchors failed in shear, but the mesh remained on the slope after being caught by a tree in the upper northwest corner of the mesh section and through interface friction.



**Figure 4-9. Slope area in (A) 1997 before and (B) 2002 five years after mesh installation and just after repair of the system.**

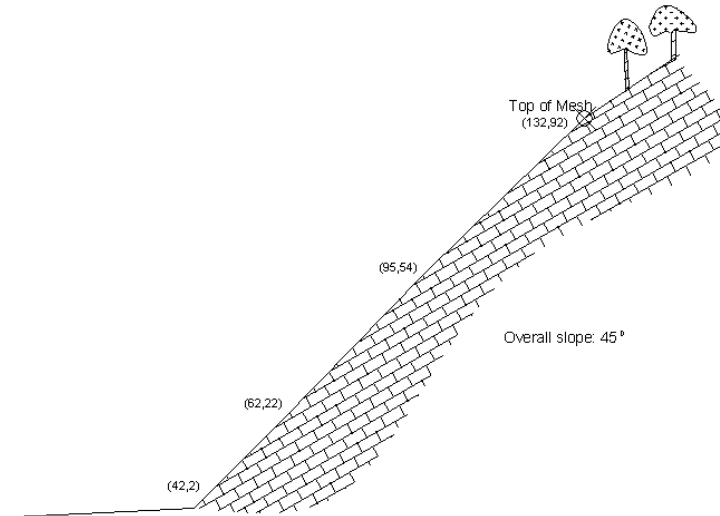


**Figure 4-10. Cross-section of installation shows approximate slope configuration. Snow accumulates on the entire area of the installation.**

Given similar parameters as in the previous case but an anchor spacing of 17 feet, the corresponding interface friction angle for failure would be less than 40°:

$$\tan \phi = \frac{(400 \text{ kg} / \text{m}^3 \times 0.0624 \times 25'' \times 0.083 \times 127' \times \sin(45^\circ) - \frac{13000}{17})}{400 \text{ kg} / \text{m}^3 \times 0.0624 \times 25'' \times 0.083 \times 127' \times \cos(45^\circ)} = 0.84$$

The 1997 photo (Figure 4-9A) shows the overall planar condition with few irregularities/protrusions.

In 2002, the anchors were replaced with higher capacity wire rope anchors (>25,000 lbf/110 kN) at the same spacing. The following two winters resulted in similar depths of snowpack, and no signs of system instability were observed.

### **4.3.3 Instrumented Tumwater Canyon Site (cable nets, 45° slope)**

The instrumented cable net system was described in both chapters 2 and 3, and a photo of the slope before the installation of the system in 1997 is shown in Figure 2-11. The overall slope angle of the installation is 45°, and the total width is about 160 ft (50

m). Three longitudinal sectional profiles of the installation were measured and their lengths were found to be 317 ft, 308 ft, and 330 ft; an average length of 320 ft (98 m) was used in the analysis. Twenty anchors suspended the mesh system at an average anchor spacing of 9 ft (2.7 m). The anchors consisted of 3/4-inch- and 5/8-inch-type cable with corresponding breaking strengths of 53,000lbs (235 kN) and 37,000lbs (165 kN), respectively. This mesh system has performed well with this anchor configuration.

Utilizing the 2001-2002 snowpack depth of 25 inches (635 mm) in Equation 4-10:

$$\tan \phi = \frac{(400 \text{ kg} / \text{m}^3 \times 0.0624 \times 25'' \times 0.083 \times 320' \times \sin(45^\circ) - \frac{37000}{9})}{400 \text{ kg} / \text{m}^3 \times 0.0624 \times 25'' \times 0.083 \times 320' \times \cos(45^\circ)} = 0.65$$

the corresponding interface friction angle to maintain limiting equilibrium for the given anchor capacity would be at least 33°. As shown in Figure 2-11, the slope surface is planar to undulating, but it contains numerous large protrusions/asperities in the upper half of the slope and is mostly planar and smooth in the lower portion.

#### **4.3.4 Daggett Pass, Nevada (hexagonal wire mesh, 39° slope)**

The installation is located in the eastern Sierras, east of Lake Tahoe, adjacent to highway 207 around milepost 3.8, just below Daggett Pass around elevation 7000 ft (2130 m). It was installed in 1999 and failed during the following winter because of snow loads. The mesh covered a planar and relatively smooth cut slope that was oriented around 40° (Figure 4-11). At the time of the site review, the vast majority of the mesh was in contact with slope. The slope length was about 150 feet (45 m), and the cut exposed highly to completely weathered granite at full height. According to reports by DOT Maintenance personnel, the maximum average snow depth at the site was 3 to 4 ft (1 m).



**Figure 4-11. Eastern half of the damaged installation still partially suspended on the slope, held in place mostly through interface friction and the few remaining intact anchors.**

The mesh installation consisted of double-twisted hexagonal mesh fastened to a 50-ft (15-m) square grid of horizontal and vertical,  $\frac{3}{4}$ -inch (19-mm) wire support ropes. The anchoring system consisted of two #8 (25-mm) rebar anchors in tandem at roughly 50-ft (15-m) spacing for an assumed effective spacing of 25 ft (8 m). The estimated yield strength in shear was about 45,000 lbf (200 kN). The anchors consisted of #8 rebar, threaded on one end. The anchor lengths were between 3 to 4 feet (1 to 1.3 m), set in a 1-ft- (0.- m) diameter grouted hole. The anchors were loaded primarily perpendicularly to the bar, and they failed in both shear and pullout.

Assuming a snow density of 20 lbs/ft<sup>3</sup> (300 kg/m<sup>3</sup>) and using Equation 4-10:

$$\tan \phi = \frac{300 \text{ kg} / \text{m}^3 \times 0.0624 \times 4' \times 25' \times 150' \times \sin 40^\circ - 45000 \text{ lbs}}{300 \text{ kg} / \text{m}^3 \times 0.0624 \times 4' \times 25' \times 150' \times \cos 40^\circ} = 0.63$$

the maximum interface friction angle would be no more than 32°. Figure 4-11 shows the very planar, smooth condition of this slope.

#### **4.3.5 Franklin Falls Site (cable nets, compound slope: 39° upper/46° lower)**

The Franklin Falls site, system elements, and the conditions at failure are described in Chapter 2; a photograph of the western portion of cable nets that failed because of snow loading, and that is the subject of this evaluation is shown in Figure 2-5. The width of this failed section of the cable net was around 230 feet (70 m). The slope profile through this failed section is as shown in Figure 4-12. The snow accumulation zone of the profile consisted of two slope segments: one composed of talus, and the other composed of glacial till. The talus slope was inclined at around 39° and consisted of uniform, mostly cobble-sized material. The glacial till was moderately rough, undulating with boulder protrusions and was inclined at around 46°. Anchors were spaced at 25 ft (7.5 m) apart and consisted of Ischebeck Titan 30/11 hollow core anchors with a yield strength in shear of about 35,000 lbf (155 kN). Anchor failures consisted of shearing of the bar, pullout, and passive pressure failure.

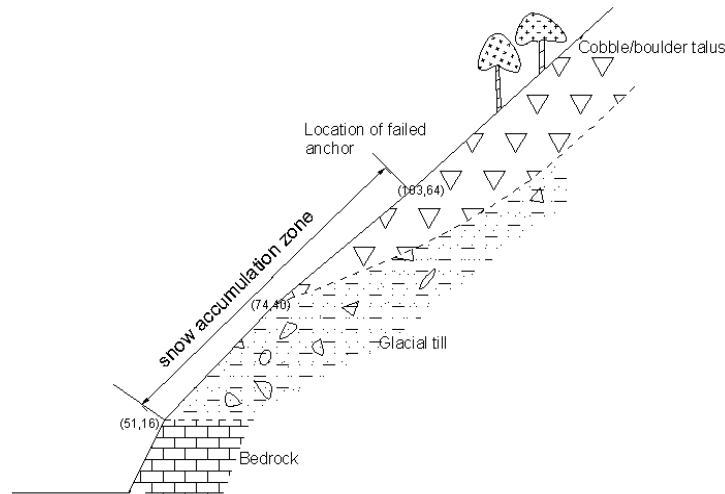


**Figure 4-12. Cross-section through failed cable net shows the portion of the installation that accumulated snow. Snowpack also extended upslope of the installation. The entire slope above the bedrock portion is highly susceptible to snow avalanches.**

The maximum snowpack depth for the 1998-1999 winter when the system failed was among the highest on record, estimated to be around 85 inches (2.2 m) (C. Wilbour, personal communication). Typical late winter snow densities for the area are around 25 lbs/ft<sup>3</sup> (400 kg/m<sup>3</sup>). Using Equation 4-10:

$$\tan \phi = \frac{(400 \text{ kg/m}^3 \times 0.0624 \times 85'' \times 0.083 \times [33' \times \sin(46^\circ) + 38' \times \sin(39^\circ)] - \frac{35000}{25})}{400 \text{ kg/m}^3 \times 0.0624 \times 85'' \times 0.083 \times [33' \times \cos(46^\circ) + 38' \times \cos(39^\circ)]} = 0.76$$

the corresponding interface friction angle at the limiting state would be 37°. Because the mesh system failed as a result of the snow load, the actual friction angle must have been less than this value. Figure 2-5 shows the planar condition of the slope with few irregularities. As alternative and/or contributory causes of failure, creep and/or glide forces within the snowpack upslope of the installation may have imparted additional slope-parallel stresses to the cable nets. WSDOT Maintenance personnel also mentioned additional snow loading from plowing activities along the bottom of the installation.

#### **4.3.6 US 20 Rainy Pass Site (hexagonal wire mesh, 38° slope)**

This site is located in the North Cascades of Washington west of Rainy Pass around MP 146.2 (Figure 4-13). With an elevation of around 3000 ft (900 m), the site develops a maximum snowpack depth of around 5.5 ft (1.6 m) (A. Warner, personal communication), with a late winter snow density of around 20 lbs/ft<sup>3</sup> (300 kg/m<sup>3</sup>) (C. Wilbour, personal communication). The slope consists of a steep bedrock portion adjacent to the highway, capped with coarse alluvium and glacial deposits.



**Figure 4-13. The slope conditions; snow accumulation occurs on the upper portion of the slope.**

The slope profile is shown in Figure 4-14. It includes two segments: the top segment is inclined at  $38^\circ$  and is planar to undulating but contains numerous boulders that protrude from the slope (Figure 4-15). Snow accumulates on this upper slope segment. The lower segment consists of a roughly  $72^\circ$  cut slope in bedrock and does not accumulate a significant quantity of snow. The installation was about 200 ft (60 m) wide and consisted of double-twisted hexagonal mesh suspended with  $\frac{3}{4}$ -inch (19-mm) cables in buried concrete deadman at a 50-ft (15-m) spacing. The system was installed in the late 1980s; since that time, the system has performed well.

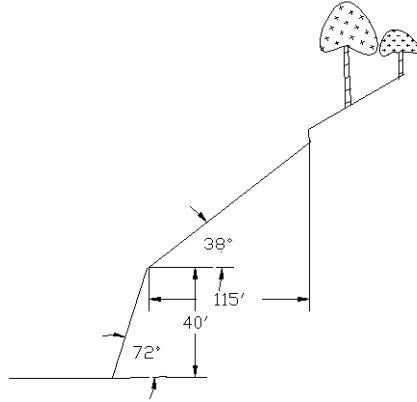


**Figure 4-14. Cross-section shows upper and lower slope segments. The upper segment comprises the zone of snow accumulation on the installation.**



**Figure 4-15. View looking downslope; note numerous boulders protruding into the mesh. With the exception of the top, where erosion has partially undermined the installation, the mesh is largely in contact with the slope.**

Using an assumed capacity of the deadman anchors based on the wire rope breaking strength of 53,000 lbf (155 kN) and Equation 4-10:

$$\tan \phi = \frac{(300 \text{ kg} / \text{m}^3 \times 0.0624 \times 5.5' \times 121' \times \sin(38^\circ) - \frac{53000}{50})}{300 \text{ kg} / \text{m}^3 \times 0.0624 \times 5.5' \times 121' \times \cos(38^\circ)} = 0.67$$

the interface friction angle required to maintain limiting equilibrium must at least be 34°.

#### **4.4 SUMMARY OF PERFORMANCE ANALYSIS**

Despite the relatively crude data on snowpack and the corresponding depths at which failures occurred, the back-analyzed values of interface friction for the six systems provide some insight into the ranges of interface friction for various slope conditions. For planar slopes, the back-calculated interface friction was less than  $32^\circ$  for no substantive irregularities and less than  $37^\circ$  to  $40^\circ$  for minor, infrequent irregularities. For planar to undulating slopes with significant protrusions, the back-calculated interface friction angles were at least  $33^\circ$  to  $34^\circ$ .

Intuitively, an increase in slope roughness should correspond with reduced slope contact. It might then seem to follow in some cases that the effective interface friction for an installation would be less with decreasing slope contact. Thus, an important distinction about slope contact, thus, arises. If slope contact is limited by slope configuration (i.e., a concavity or reentrant), no interface friction is realized. However, if slope contact is limited by roughness, significant gain in interface friction should be expected.

Overall, the back-calculated values of interface friction correspond favorably with the range of values determined quantitatively through finite element modeling, presented in Chapter 6. Furthermore, these back-calculated values seem appropriate given observational assessments of surface roughness.

As stated earlier and shown in the previous examples, if interface friction is not considered for systems subjected to snow loads, unrealistically high anchor loads would be calculated. Interface friction is an important contributory resistance factor for the global stability of the system and, therefore, should be included in the anchor design.

Once interface friction has been estimated, Equation 4-9 provides for rapid evaluation of expected anchor load due to snow for a given slope and depth of snowpack. While it may be simplistic in that it assumes full load transfer of the snowpack to the system, it is appropriately conservative given the uncertain mechanics of load transfer from snowpack. The application of an appropriate safety factor would account for uncertainties of interface friction, snowpack depth and density, and degree of slope contact.

## **CHAPTER 5**

### **LOCAL STABILITY OF MESH SYSTEMS**

Mesh rupture has been observed at many installations and has been attributed to static load from the accumulation of debris. Puncture is another type of localized mesh failure that results from impact forces from falling rocks. These failures occur when the local stress exceeds the yield strength of the mesh or the mesh seams. Such localized failures diminish or nullify system performance. It is, therefore, necessary to examine the conditions that result in localized mesh failure.

The complex nature of the interaction among the external forces on the mesh, coupled with variations in surface geometry and boundary conditions, makes the accurate analytical determination of local stresses a prohibitively difficult task. Assumptions have been made to simplify the problem and to allow for the development of analytical models to evaluate conditions that would result in local failures.

#### **5.1 DEFORMATION AND STRENGTH ANALYSIS**

Because the mesh fabric consists of open-grid structures, the mechanics of its deformation from imposed loads can be modeled in a manner similar to modeling done for geogrid reinforcement. The following analysis for mesh fabrics was based on a study by Bergardo et al. (2001) of geogrid deformation within soils. In North America, mesh systems used for draped rockfall protection consist of two basic types of cells: hexagonal and quadrilateral. The analysis presented here focused on the hexagonal cell, but the methodology could easily be adapted for quadrilateral cells.

### 5.1.1 Free Sides

The grid structure of the mesh consists of cells along the perimeter of the mesh and those in the central region. Because of symmetry, when a tensile stress is applied to the mesh, the centerline cells move only in the pull direction, whereas the cells along the two sides that are not fixed are assumed to move toward the center. Continued deformation would lead to transverse constriction (necking) of the fabric. Figure 5-1 illustrates the case in which both sides of the mesh are free, and external force results in the deformation of a single cell in the middle or the center portion of a hexagonal mesh.

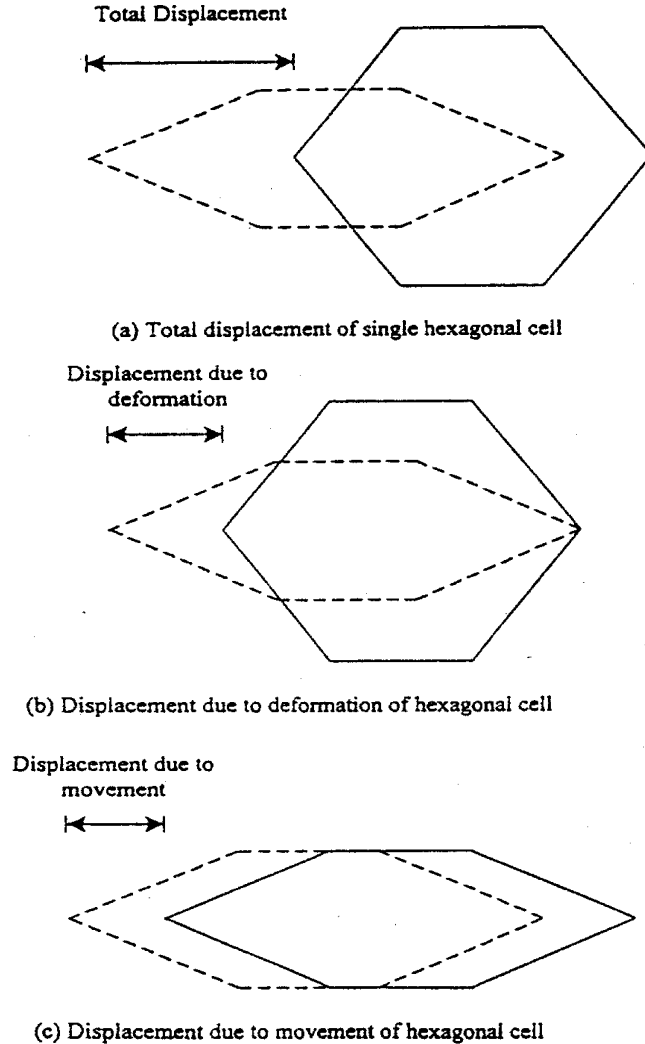


Figure 5-1. Displacement of single hexagonal cell at centerline of an impact cone (from Bergado et al., 2001).

The total displacement of the cell consists of its deformation (Figure 5-1b) plus displacement due to translational movement along the centerline (Figure 5-1c). The geometry of a deformed hexagonal element with original and deformed angles of configuration is as shown in Figure 5-2a. Similarly, the geometry of the translational movement of the hexagonal element is as shown in Figure 5-2b.

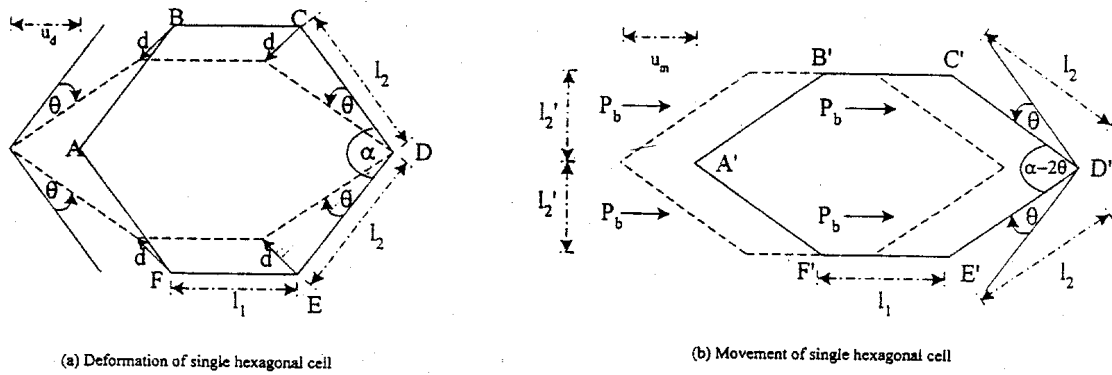


Figure 5-2. Deformation and movement of a single hexagonal cell (from Bergado et al. 2001).

Point D is assumed to be fixed (Figure 5-2a). The displacement  $d$  of the point B in the hexagonal cell can be related to the angle of the deformation,  $\theta$ , by:

$$d = 2 \cdot l_2 \cdot \sin(\theta / 2) \quad (5-1)$$

where  $l_2$  is the undeformed length of the side, and  $\theta$  is measured from the original position of the side to its deformed position. The component of  $d$  in the direction of pull (Figure 5-2b) can be expressed by:

$$d' = l_2 \left( \cos\left(\frac{\alpha}{2} - \theta\right) - \cos\left(\frac{\alpha}{2}\right) \right) \quad (5-2)$$

where  $d'$  is the displacement component of point B in the pull direction, and  $\alpha$  is the undeformed angle of the single cell.

Similarly, the displacement  $u_d$  of point A in the hexagonal cell can be related to the angle of deformation,  $\theta$ , by:

$$u_d = 2 \cdot l_2 \left( \cos\left(\frac{\alpha}{2} - \theta\right) - \cos\left(\frac{\alpha}{2}\right) \right) \quad (5-3)$$

The displacement of point A is twice that of point B in the pull direction, and it is accommodated by the rotation of transverse wires AB and CD. Note that the displacements of points C, E, and F in Figure 5-2a are the same as the displacement of point B. Point D is assumed to be fixed.

If the relationship between the applied tensile force on a cell material and its resultant displacement is assumed to be hyperbolic, then the pullout force on a hexagonal cell element AB (Figure 5-2a) and its displacement can be related by:

$$P_{bx} = \frac{(l_2)^2 \cdot \sin\left(\frac{\theta}{2}\right) \cdot \sin\left(\frac{\alpha}{2} - \theta\right) \cdot \sin\left(\frac{\alpha}{2} - \frac{\theta}{2}\right)}{\frac{1}{E_i} + \frac{l_2 \cdot \sin\left(\frac{\theta}{2}\right) \cdot \sin\left(\frac{\alpha}{2} - \frac{\theta}{2}\right)}{d \cdot \sigma_{ult}}} \quad (5-4)$$

where  $d$  is the diameter of the transverse element,  $E_i$  is the initial slope of bearing resistance/normalized displacement,  $\sigma_{ult}$  is the ultimate value of the pullout bearing resistance, and  $P_{bx}$  is the pullout resistance force.

The point D in element CD is assumed to be fixed. Therefore, the bearing resistance distribution will be triangular (Figure 5-2b) and can be determined as follows:

$$P_{bx}^{CD} = \frac{(l_2)^2 \cdot \sin\left(\frac{\theta}{2}\right) \cdot \sin\left(\frac{\alpha}{2} - \theta\right)}{\frac{1}{E_i} + \frac{2 \cdot l_2 \cdot \sin\left(\frac{\theta}{2}\right)}{d \cdot \sigma_{ult}}} \quad (5-5)$$

The transitional movement of the hexagonal cell is as shown in Figure 5-2b. The bearing resistance acting on a transverse element can be described by:

$$P_b = \frac{l_2' \cdot \sin\left(\frac{\alpha}{2} - \theta\right) \cdot u_m}{\frac{1}{E_i} + \frac{u_m}{d \cdot \sigma_{ult}}} \quad (5-6)$$

where  $u_m$  is displacement due to movement of the hexagonal cell,  $l_2'$  is the equivalent length of the transverse element (Figure 5-2), and  $P_b$  is the bearing resistance due to movement. If only one cell is considered and point D is fixed, then the displacement can be plotted against pullout resistance, as shown in Figure 5-3. It can be seen that the cell resistance exhibits “softening” after reaching a peak value. This is due to the necking of the cell as it becomes progressively slimmer with increasing pull force.

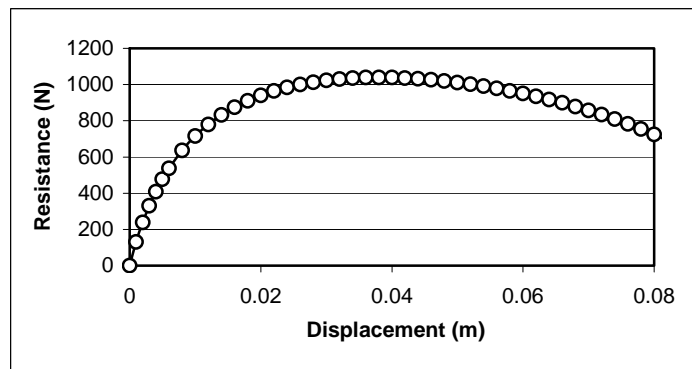


**Figure 5-3. Pullout displacements versus pullout resistance assuming free sides.**

### 5.1.2 Fixed Sides

When the two lateral sides of the cells are fixed, only movement in the pull direction can occur. The deformation of one cell is shown in Figure 5-4. If the resistance between the wires and the ground is ignored, then the loads applied to the transverse sides and lateral sides are shown in equations (5-7) and (5-8). These equations imply that (1) the loads applied to the transverse sides are always larger than those applied to the lateral sides, and (2) yield will first occur in the transverse sides.

$$P_1 = \frac{P}{2 \cos(\alpha/2)} \quad (5-7)$$

$$P_3 = \frac{P}{2} \quad (5-8)$$

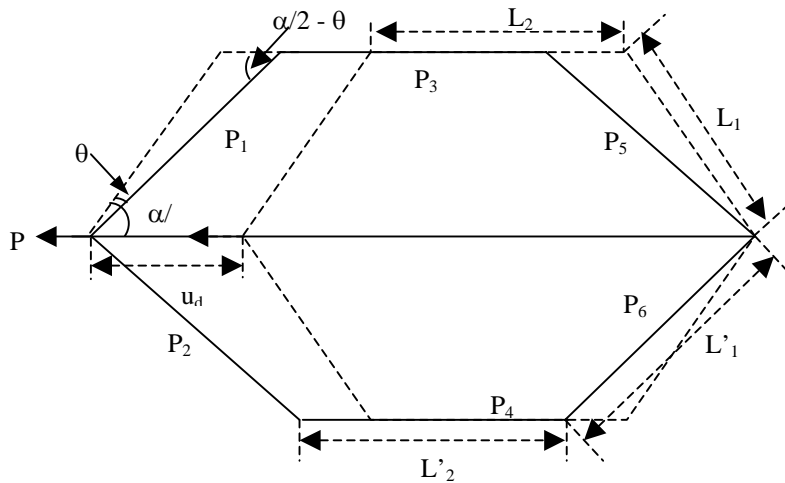


Figure 5-4. Deformation of single hexagonal cell with two sides fixed.

The displacement of the cell,  $u_d$ , under load  $P$  can be expressed as follows:

$$u_d = \frac{\sqrt{P^2 + 4SEP \cos(\alpha/2) + 4S^2 E^2 \cos^4(\alpha/2) - 2SE \cos^2(\alpha/2)}}{SE \cos(\alpha/2)} l_1 + \frac{P}{2SE} l_2 \quad (5-9)$$

where  $S$  is the cross-sectional area of wires, and  $E$  is the elastic modulus of the wire material. The plot of the displacement of the cell against the applied load (Figure 5-5) shows that the rigidity of the cell almost keeps constant with increasing load, assuming that the elastic limit is not exceeded.

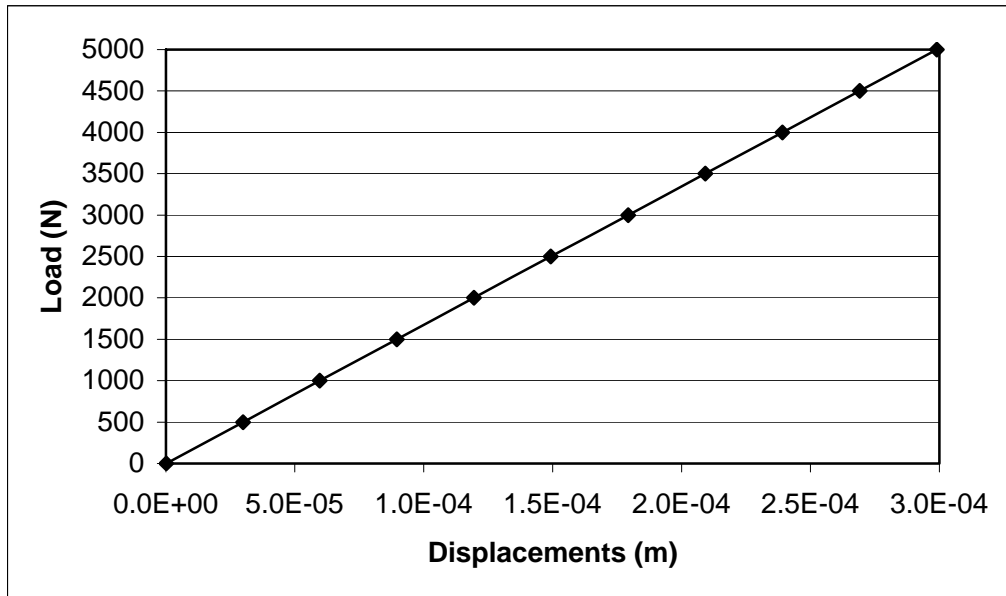


Figure 5-5. Applied load versus displacement of a cell assuming fixed sides.

## **5.2 LOCAL FAILURE ANALYSIS**

Two forms of mesh rupture failure can be caused by debris accumulation: (1) transverse failure and (2) seam failure. The methods for evaluating the conditions for initiation of such failures are as follows.

### **5.2.1 Transverse Failure**

Entrapment of debris commonly occurs along the base of the mesh, around the midslope anchors, and at slope constrictions or inflections. Such entrapment has led to numerous localized failures through increased tensile stress on the mesh wires. The

pressure applied by the accumulated debris on the mesh results in deflection of the mesh wires. Assuming that the shape of the deflection is circular, a relationship between the debris pressure and the yield strength of the mesh wires can be developed. A schematic of a circular membrane under a constant pressure  $p$  is shown in Figure 5-6. For vertical equilibrium:

$$T = p \times r \quad (5-10)$$

where  $T$  is the tensile force and  $r$  is the radius of the circle.

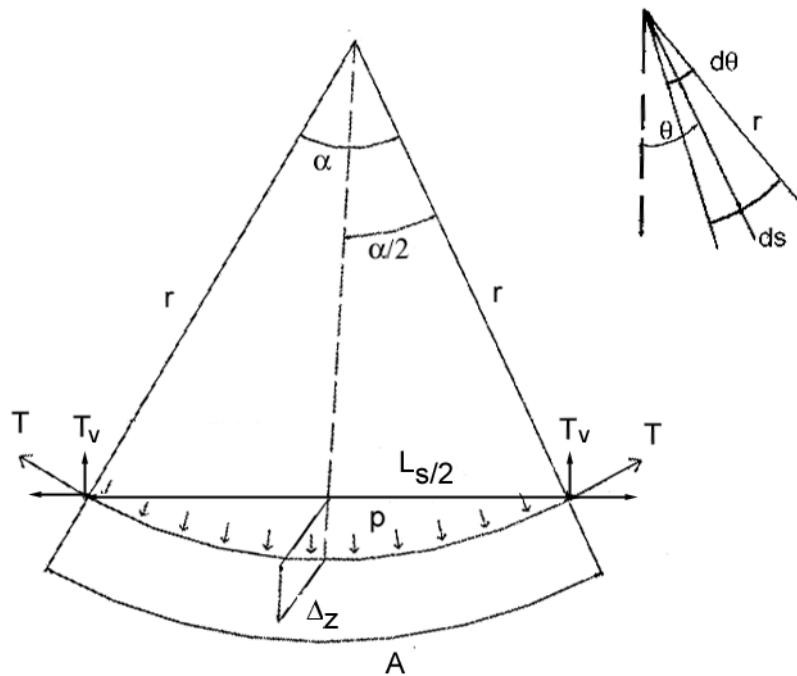


**Figure 5-6: Forces on a circular membrane.**

Let us assume that the length of the mesh segment before the accumulation of debris is  $L_s$ . If the strain  $\epsilon_y$  at yielding within this segment is assumed to be uniform, the deformed arc length,  $A$ , can be given by:

$$A = L_s (1 + \epsilon_y) \quad (5-11)$$

The radius of the circle and the subtended angle  $\alpha$  are related by:

$$r = \frac{L_s}{\sin \frac{\alpha}{2}} \quad (5-12)$$

By using the Taylor series expansion and approximating an explicit expression,  $\alpha$  can be obtained as:

$$\frac{\alpha}{2} = \sqrt{6 \left( 1 - \frac{L_s}{A} \right)} \quad (5-13)$$

Combining equations 5-10 through 5-13, the pressure  $p$  can be determined as:

$$p = \frac{T \sin \left( \sqrt{\frac{6T}{SE + T}} \right)}{L_s} \quad (5-14)$$

where  $S$  is the total cross-sectional area and  $E$  is the elastic modulus of the stressed mesh wires.  $T$  is the total limit force that can be carried by the stressed wires, defined as the product of the yield strength and the total cross-sectional area of the stressed wires. Equation (5-14) is useful for calculating the allowable debris pressure that can be carried before a transverse failure occurs.

### **5.2.2 Seam Failure**

Current practice in North America is to allow the passage of debris and to avoid retention of debris. However, if two lateral sides of the mesh are fixed (either physically by anchors or effectively by significant lateral extent and weight of the adjacent mesh), the mesh may rupture along the seams (Figure 5-7). Where high tensile steel hog rings are used for seaming double-twisted hexagonal wire mesh, the testing presented in Chapter 3 discovered that the seams are only half as strong as the mesh. Hence, the seams of hexagonal mesh that are fastened with hog rings are a common area of localized failure. When the volume of entrapped debris increases, the tensile pressure produced

within the mesh wires increases. The limit of the tensile stress in the mesh wires corresponds to a critical volume of debris. If the cross-sectional shape of a pocket of debris is also assumed to be circular and a similar approach to the debris pocket case is adopted, the critical depth (which can be equated to volume) of debris accumulation,  $\Delta Z$ , can be determined as follows:

$$\Delta Z = r(1 - \cos(\frac{\alpha}{2})) \quad (5-15)$$

Substituting equations 5-11, 5-12 and 5-13 into Equation 5-15 yields:

$$\Delta Z = L_s [\cos ec(\sqrt{\frac{6T}{T + SE}}) - \cot(\sqrt{\frac{6T}{T + SE}})] \quad (5-16)$$

where  $L_s$  is the initial width of the drapery,  $S$  is the cross-sectional area, and  $E$  is the elastic modulus of the mesh wires.  $T$  is the yielding force of the mesh wires.

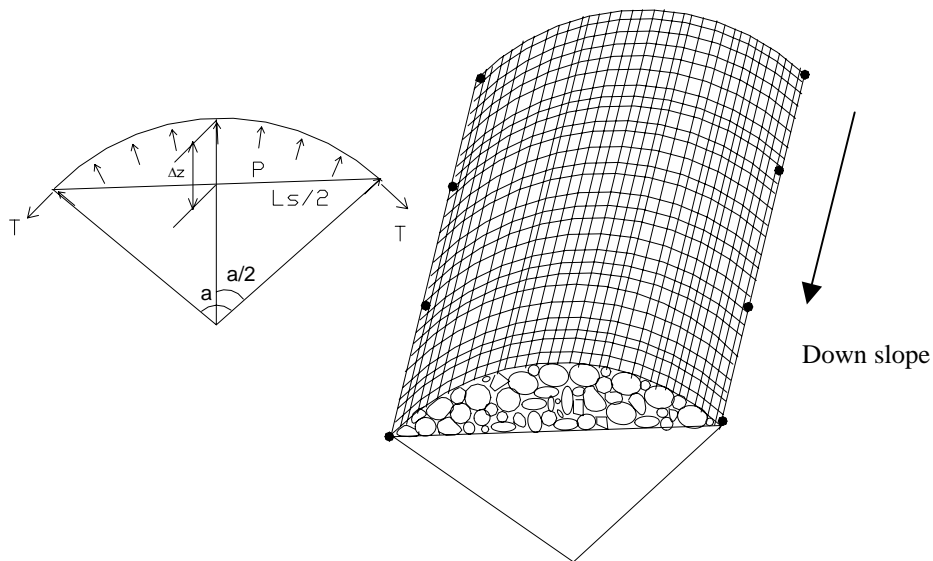


**Figure 5-7. Assumed circular cross-sectional shape of the mesh and the conditions that would result in seam failure.**

### **5.3 PUNCTURE FAILURE**

In the absence of full-scale testing to confirm the theoretical models of puncture failure, effort was undertaken to compile available, referential data on the performance of mesh fabric and systems exposed to impact loads. Sources of data included limited field test data, finite element analyses, and back-analyses of the performance of several mesh systems. Given the very limited available data and analyses on the effect of impact loads on mesh systems, only rudimentary conclusions could be drawn about the expected performance of hexagonal mesh and cable net systems. More robust numerical analysis corroborated by full-scale testing is needed to characterize the limitations of mesh systems exposed to impact loads.

#### **5.3.1 Field Test Data**

Regrettably, only two citable sources of field testing were acquirable for use in this research.

The first was work performed by Duffy (1992) that examined the performance of a restrained panel of double-twisted hexagonal wire mesh suspended on a rockfall barrier subjected to a range of kinetic energy. While the purpose of this testing was to determine the capacity of this fabric to act as a rockfall fence/barrier, the testing was also useful to demonstrate the low-bound capacity for this fabric. It was assumed for this study that a mesh panel partially restrained between two posts would be somewhat more limited in its deflection, and thus its energy absorption capacity, than would a draped mesh system. Duffy (1992) tested a 8-ft-high (2.5-m) by 16-ft-wide (5-m) panel of galvanized, 0.12-inch (3-mm), 8x10-type, hexagonal wire mesh suspended on posts spaced 16 to 20 ft (5 to 6 m) apart. In addition to the mesh, ½-inch (12-mm) wire ropes were longitudinally

placed at 20-inch (50-mm) intervals between the posts. The mesh was fastened to the cables with tie wire at 1.6-ft (0.5-m) intervals and laced to the top and bottom cables with 0.16-inch (4-mm) wire. Of the nine rocks rolled at the fence, only four struck the fence. The velocity and kinetic energy of the rocks ranged from 56 to 82 ft/s (17 to 25 m/s) and 4 to 16.7 ft-tons (10 to 45 kJ). The fence stopped only one rock at 4.0 ft-tons (10 kJ); the other three pierced the mesh between 7.5 and 16.7 ft-tons (20 to 45 kJ). The report did not mention the contributory effect of or damage to the longitudinal cables.

While numerous data have been published regarding impact tests on fences utilizing cable net fabric, the fence systems have employed energy absorption devices. One test by Kane and Duffy (1993) examined the performance of a 5/16-inch (8-mm) wire rope woven into an 8-inch (200-mm) square grid, typical of a drapery panel, suspended on a rockfall barrier subjected to a range of energy. Although energy-absorbing devices were used in these tests, some insight can be gained into the dynamic capacity of the cable net panel by observing the maximum energy the cable net absorbed before activation of the energy-absorbing device. Kane and Duffy (1993) tested an 8-ft- (2.5-m) high by 20-ft- (6-m) wide panel of galvanized, 5/16-inch (8-mm) wire rope suspended on posts spaced 20 feet (6 m) apart. Of the twelve rocks rolled at the fence, all struck the fence. The velocity and kinetic energy ranged from 26 to 40 ft/s (8 to 12 m/s) and 2 to 17 foot-tons (5.4 to 46 kJ), respectively, before activation of the energy-absorbing device. The velocity and kinetic energy that initiated the energy-absorbing device were 43 ft/s (13 m/s) and 33 foot-tons (89 kJ), respectively. The researchers concluded that 25 foot-tons (68 kJ) was the maximum impact that would cause activation

of the energy-absorbing device, inferring a similar impact (puncture) resistance for a restrained cable net panel.

### **5.3.2 Finite Element Analyses for BCMoT**

The British Columbia Ministry of Transportation (BCMoT) commissioned a structural evaluation of its slope mesh system by Sandwell Engineering and Construction Services Group of Vancouver, B.C. (Sandwell, 1995). The study examined, in part, two scenario rockfalls involving a 2-ft- (600-mm) diameter rock striking a BCMoT-designed hexagonal mesh system. The scenarios included a low velocity (4 m/s), sub-perpendicular impact of 0.9 ft-tons (2.4 kJ) at the top of the mesh (Mode 1), and a rock falling 100 ft (30 m), striking a bench, and hitting the mesh sub-perpendicular at 46 ft/s (14 m/s), resulting in an 11-ft-ton (30-kJ) impact (Mode 2).

The study included fabric testing, which entailed incrementally loading a fixed panel and monitoring the deflection of the mesh. Energy absorption was then calculated by integrating the area under the load-displacement plot. A finite element model was developed to simulate the observed deflection, and then the model was used to calculate energy absorption for mesh areas of 8.7 ft<sup>2</sup> (0.81 m<sup>2</sup>) and 147 ft<sup>2</sup> (13.7 m<sup>2</sup>). Next, a log-log plot of energy absorption as a function of area was prepared. This model was then used to extrapolate energy absorption for much larger areas that more closely represented field conditions. The modeling determined that a circular area of 1830 ft<sup>2</sup> (170 m<sup>2</sup>), corresponding to a radius of about 24 ft (7.3 m), had an energy absorption capacity of 11 ft-tons (30 kJ). This model suggested that the energy absorption capacity theoretically decreases with decreasing area.

The modeling concluded that a system exposed to Mode 2 rockfall would require at least 23 ft (7 m) of length below the bench to dissipate the energy. While the actual required length may be disputable, the modeling confirmed the extensive experience in North America that hexagonal mesh systems are highly effective with block sizes of up to 2 ft (600 mm) for slope heights far in excess of 100 ft (30 m), producing a similar or even larger range of kinetic energy.

### **5.3.3 Back-Analyses of Impacts to Mesh Systems**

Three sites in Washington State were selected for back-analyses to quantify ranges of kinetic energy and better understand observed performance. Two of the three sites were hexagonal mesh installations, and the other was a cable net installation. Because the rockfall events of interest were not directly observed, the back-analyses could only estimate the block size, source area, and trajectory from the field conditions. Rockfall energy was estimated by using version 4.0 of the Colorado Rockfall Simulation Program (Jones et al., 2000).

#### **5.3.3.1 US 20 Rainy Pass Site**

Conditions at the Rainy Pass site are summarized in section 4.3.6 of the report. This hexagonal mesh installation had experienced several puncture failures just above the convex inflection in the lower third of the slope (figures 4-13 and 4-14). The typical size of the punctures was around 12 inches (300 mm). It was assumed that the block sizes associated with the punctures were at least this dimension. Numerous blocks of up to 4 ft (1.2 m) in size are present on the upper slope.

The analyses assumed an initiation point near the top of the installation, a slope distance above the punctures of about 120 ft (35 m), with an overall slope orientation of

38°. The analyses considered a range of spherical blocks 1 to 2 ft (0.3 to 0.6 m) in diameter. Assuming a trajectory path unencumbered by the mesh, kinetic energy ranged from 2.6 to 5.2 ft-tons (7.2 to 14.0 kJ). On the basis of the observed conditions, this range appeared to represent a minimum kinetic energy to cause puncture failure for hexagonal mesh.

### **5.3.3.2 US 12 White Pass Site #1**

This site is located in the Central Washington Cascades on highway US 12 at MP 154.6 just east of White Pass. The installation consists of a post-supported cable net system located just above an abrupt slope convexity (Figure 5-8). The fabric has an 8-inch (200-mm) square grid weave with 5/16-inch (8-mm) wire rope and is backed with galvanized hexagonal mesh. Tabular to orthogonal blocks 18 to 30 inches (450 to 750 mm) in size ravel from loose colluvial deposits that extend 150 ft (45 m) upslope of the installation.



**Figure 5-8. Modified cable net installation, upslope source of rockfall, and typical range of block sizes that impact the installation in a sub-perpendicular orientation.**

The calculated kinetic energy ranged from a low of about 3 ft-tons (8 kJ) for the smaller sized rocks to upwards of 20 ft-tons (54 kJ). The installation has been in place for about 5 years, and there is no observable damage to the cable nets and only minor damage to the hexagonal mesh backing. Several similar installations nearby exposed to similar rockfall conditions have also performed satisfactorily.

#### **5.3.3.3 US 12 White Pass Site #2**

A second site on White Pass located at MP 155.7 consists of a post-supported hexagonal mesh installation sited below a steep, bedrock chute (Figure 5-9A). The suspended portion of the mesh had several punctures that ranged in size from 12 to 18 inches (300 to 450 mm) (Figure 5-9B). It was assumed that the block sizes associated with the punctures were at least this dimension. Numerous discoidal blocks 18 to 30 inches (450 to 750 mm) in size were entrapped beneath the mesh about 50 ft (15 m) downslope from the top of the installation. An estimated 10 to 15 yds<sup>3</sup> (7 to 11 m<sup>3</sup>) of debris had accumulated in this area and resulted in a rupture failure of the mesh. Because of access difficulties, detailed characterization of the chute was not possible. An overall slope orientation of 40° was measured from the highway with a clinometer, and a slope distance for the chute of 150 ft (45 m) was measured with a laser rangefinder. Roughness was visually estimated to be about 1.5 to 2.0 ft (450 to 600 mm) as adjusted for typical block sizes.

Calculations using conservative estimates for smaller boulder sizes yielded a low bound kinetic energy of about 3 ft-tons (8 kJ).

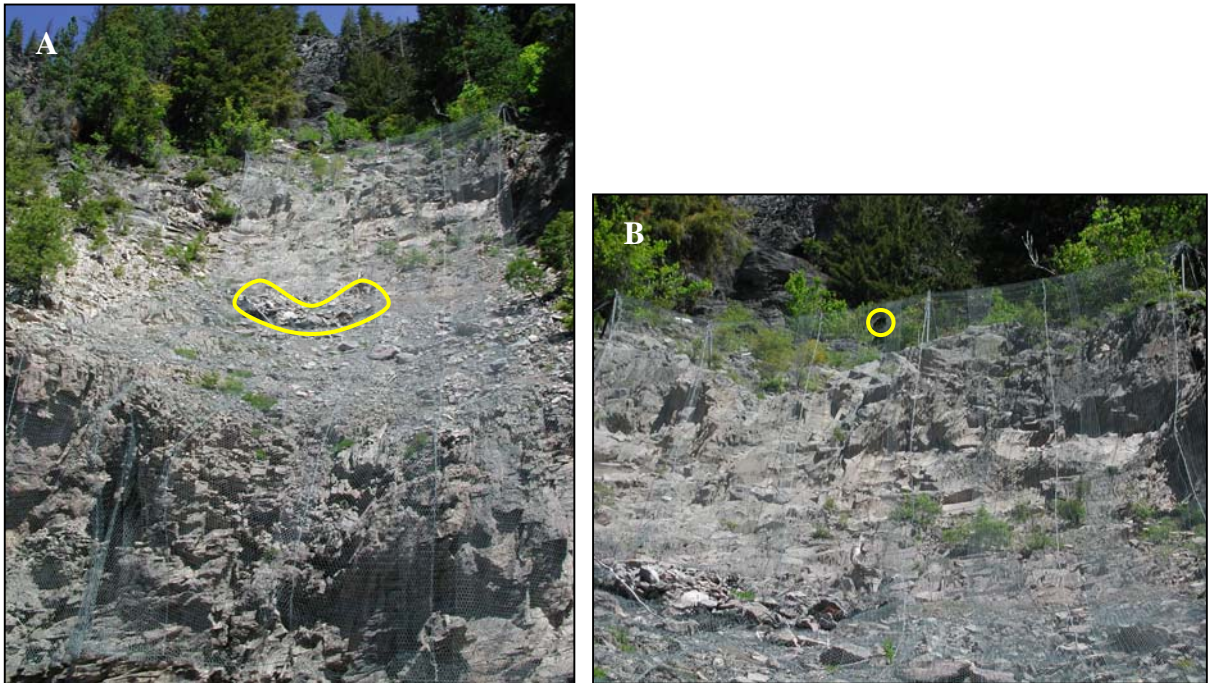


**Figure 5-9. (A) Configuration of slope and installation. Yellow line outlines area of debris accumulation and rupture failure. (B) Enlarged view of top of mesh, downslope of chute. Yellow circle highlights 18-inch (450-mm) puncture of the mesh.**

### **5.3.4 Anticipated Performance from Impact Loads**

The very limited amount of citable performance data, field testing, and analysis allowed for only crude generalization of anticipated performance for hexagonal mesh and cable net systems subjected to sub-perpendicular impacted loads. For hexagonal mesh installations, the data suggested that impact loads in the range of 3 to 4 ft-tons (8 to 10 kJ) near the perimeter (top) of a system are sustainable with minimal to no damage. In the field of the mesh within 25 ft (7 m) of a perimeter, the BCMoT study found that kinetic energies of up to 11 ft-tons (30 kJ) are sustainable with minimal to no damage. Extensive performance history supports this finding. With regard to cable net installations, the very limited available data suggested an upper bound of puncture resistance for a restrained panel in the range of 20 to 25 ft-tons (54 to 68 kJ).

## CHAPTER 6 GLOBAL STABILITY OF MESH SYSTEMS

### 6.1 LIMIT EQUILIBRIUM MODEL

Failures of mesh systems can occur within the anchors, support ropes, mesh, and/or connections. Anchor failures can occur when the overall capacity of the mesh system is compromised. The rupturing or puncturing of the mesh and the failure of connections constitute local failure. This chapter describes the development of a simple model, based on limit equilibrium analysis, for overall stability of the system.

Consider the case of a mesh installation on an inclined surface of a slope with an angle  $\beta$  with respect to horizontal ground (Figure 6-1). The mesh is secured at the top by a row of anchors. A grid of horizontal and vertical cables may be used to reinforce the system. Rock debris becomes trapped behind the mesh and accumulates, often at the bottom of the mesh, contributing to the external load on the system. Depending on the site geology and geometric conditions of the slope, falling rock may contribute some impact force onto the system. In cold regions, snow load may develop on the system and can greatly decrease the stability of the system. (Snow loads are addressed separately in Chapter 4.) For debris loads, the free body diagram of the force components on the system is shown in Figure 6-1.

At the limiting state of equilibrium, the factor of safety, FS, for the system can be defined by:

$$FS = \frac{\textit{Shear resistance of the system}}{\textit{Mobilized force on the system}} \quad (6-1)$$

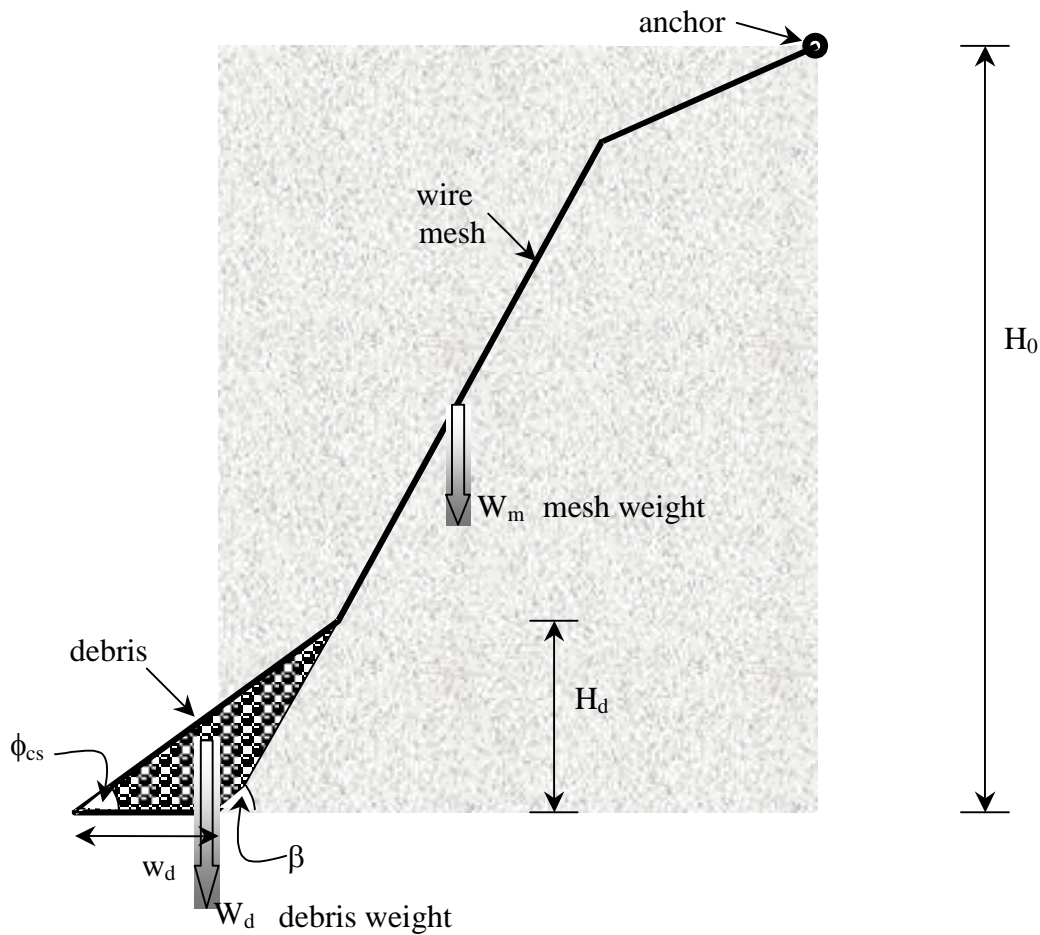


Figure 6-1. Mesh installation and loads that act on the system.

The shear resistance of the system is composed of the anchors ( $f_a$ ), the normal components of the weight of the rock debris ( $f_d$ ) and mesh system ( $f_w$ ), and the interface friction between the mesh and the ground. The rock debris is assumed to provide resistance only when it accumulates outside the mesh, which is an uncommon occurrence. The mobilized force on the system is composed of the mesh weight ( $f_{wm}$ ) and rock debris ( $f_{dm}$ ). Accounting for these forces, Equation 6-1 can be written as:

$$FS = \frac{f_a + f_w + f_d}{f_{dm} + f_{wm}} \quad (6-2)$$

The distribution and mode of snow load on the drapery system is different from those due to the weight of the mesh or rock debris accumulation. Similarly, the impact of falling rocks is different in that it is a very short-term, transient load, which commonly results in localized rather than global system failure. Consequently, the analysis here is restricted to the effects of the weight of the mesh and debris accumulation.

### **6.1.1 Anchor Capacity**

The anchor capacity is dependent on the tensile and/or shear strength of the anchor element, the grout quality, the interface friction between the ground and the grout, and the strength/passive resistance of the ground. The resistance contribution,  $f_a$ , from the anchors can be expressed by:

$$f_a = PJ \quad (6-3a)$$

where  $J$  is the number of anchors and  $P$  is the capacity of an anchor. Here, the weakest of anchor tensile strength, shear strength of a tendon, and ultimate pullout resistance of an anchor is taken as the anchor capacity.

### **6.1.2 Interface Friction**

The contribution of the weight of the mesh to the shear resistance of the system is dependent on the interface friction developed between the mesh and the ground surface. This shear strength contribution from the normal component,  $f_w$ , can be calculated as:

$$f_w = \gamma_w S_w \cos \beta \tan \delta \quad (6-3b)$$

where  $S_w$  is the area of the mesh in contact with the ground surface,  $\delta$  is the mesh-ground interface friction angle, and  $\gamma_w$  is the “density of the mesh” per unit area. The interface friction is controlled by the macro and micro roughness of the surface. Macro

roughness is the degree of large-scale irregularities of the slope, and micro roughness is defined as the texture of the surface. Where the slope is planar and the surface is smooth or when the slope is steep, minimal interface friction may be present. In these cases, the mobilized force on the system is carried largely by the anchors. Where slopes are highly irregular and the surfaces are rough or have abrupt protrusions, very high interface friction may be present. In these cases, very little to no mobilized force may be imparted to the anchors. Unfortunately, interface friction is a difficult parameter to quantify in practice. In the absence of either back-calculated or field measurements, the interface friction angle can be estimated for the observed slope irregularity and surface roughness by using the guidelines below.

- i. *Rough:* The slope surface is very irregular and undulating and has many and/or prominent protrusions on the surface. As a result, both micro and macro roughness contribute to a large effective increase in the interface friction on the slope. For such cases, the interface friction angle is assumed to be above  $60^\circ$ . For a moderate to high degree of mesh contact with the slope, the possibility of global instability of a system on such a slope is very low under normal conditions. As a point of caution, as slope irregularity and surface roughness increase, mesh contact often decreases.
- ii. *Undulating:* The slope is undulating but there are few and/or small abrupt protrusions on the surface. As a result, both micro and macro roughness contribute to an effective increase in the interface friction of the slope. Accordingly, the interface friction angle is assumed to be between  $36^\circ$  and  $59^\circ$ .

- iii. *Planar*: The slope is planar, and the surface is fairly smooth and has few small undulations. In this case, only micro roughness is assumed to contribute to the frictional resistance. Accordingly, the interface friction angle is assumed to be between 25° and 35°.

### **6.1.3 Mesh Weight**

Mesh weight is resolved into two components that are normal and shear components. The normal component is beneficial to stability through interface friction with the slope surface, and its value can be calculated by using Equation 6-3b. The shear component,  $f_{wm}$ , however, reduces the overall stability of the system and can be calculated with Equation 6-3c,

$$f_{wm} = \gamma_w S_w \sin \beta \quad (6-3c)$$

where  $\gamma_w$  is the density of the mesh per unit area,  $S_w$  is the area of contact, and  $\beta$  is the slope angle.

### **6.1.4 Debris Load**

The magnitude of the force applied by debris accumulation to the mesh installation is a difficult parameter to predict. The distribution of the accumulated debris, its angle of repose, and conditions at the base of the installation influence it. Debris accumulates as a result of either the base of the mesh system being fixed or entrapment of the rock debris by the mesh and/or support cables. The calculation of the force due to debris accumulation on the mesh system is simplified by assuming that only its weight is contributing (see Figure 6-1) and that no momentum force has been applied. For this

case, the contribution of the accumulated debris to the available shear resistance,  $f_d$ , can be expressed by:

$$f_d = 0.5H_d^2\gamma_d w_d \cos \beta(\cot \phi_{cs} - \cot \beta) \tan \delta \quad (6-3d)$$

where  $H_d$  is the accumulated debris height,  $\gamma_d$  is the unit weight of rock debris,  $\phi_{cs}$  is the estimated slope angle of accumulated debris; and  $w_d$  is the width of the accumulated debris.

The mobilized force on the system due to accumulated debris can be obtained by resolving them parallel to the slope.

$$f_{dm} = 0.5H_d^2\gamma_d w_d \sin \beta(\cot \phi_{cs} - \cot \beta) \quad (6-3e)$$

For given slope conditions of the mesh-anchor system, the number of anchors required to maintain static equilibrium of the system can be calculated by substituting the components (Equations (6-3a, b, c, d, e)) into Equation (6-2) and equating FS to unity.

### **6.1.5 Parametric Study of Overall System Performance**

The overall stability of the system is dependent on the slope conditions and mesh parameters, the number of anchors used, and the external (debris) loads applied to the system. A parametric study was performed to characterize the influence of key parameters on the overall stability of the system. For a given installation, the overall stability increases with the number of anchors, up to the yield strength of other system components (i.e., mesh, fasteners, support ropes, and others). This discussion focuses on the minimum number of anchors required to maintain equilibrium. This can be calculated by equating the factor of safety to unity (Equation 6-2).

For this parametric study, the unit weights of the rock debris and wire mesh were assumed to be 130 lbf/ft<sup>3</sup> (20.8 kN/m<sup>3</sup>) and 0.82 lbf/ft<sup>3</sup> (0.13 kN/m<sup>3</sup>/m), respectively. In

addition, the effect of the interface friction angle as a function of the internal angle of friction of the rock surface was also considered. For simplicity, the interface friction was uniformly applied over the entire area of the mesh, meaning that the irregularities of the slope were assumed to be uniform. A typical slope height of 100 ft (30 m) was examined. For illustrative purposes, the analysis determined the number of anchors to carry an assumed load of 22,500 lbf (100 kN).

#### **6.1.5.1 Effect of Debris Accumulation**

Figure 6-2 illustrates the anchor load applied when debris accumulates (as a function of debris height and slope angle; see Figure 6-1) in the mesh system. The graph shows the expected relationship of increasing anchor load with slope angle as interface friction decreases. For example, for a debris height of 10 ft (3 m), the anchor load increases from 2880 lbf (12.8 kN) at a slope angle of 40° to 39,200 lbf (174.2 kN) at slope angle of 90°. Note that for this graph, a constant debris accumulation angle of 35° and a constant interface friction angle of 36° are assumed. These calculated increases in load as a function of debris accumulation corroborate numerous observed system failures caused by excess debris accumulation. Design details such as horizontal support cables and horizontal seams/folds in the drapery located on the slope-side of the mesh have been observed to entrap debris and cause failures (Badger, 1998).

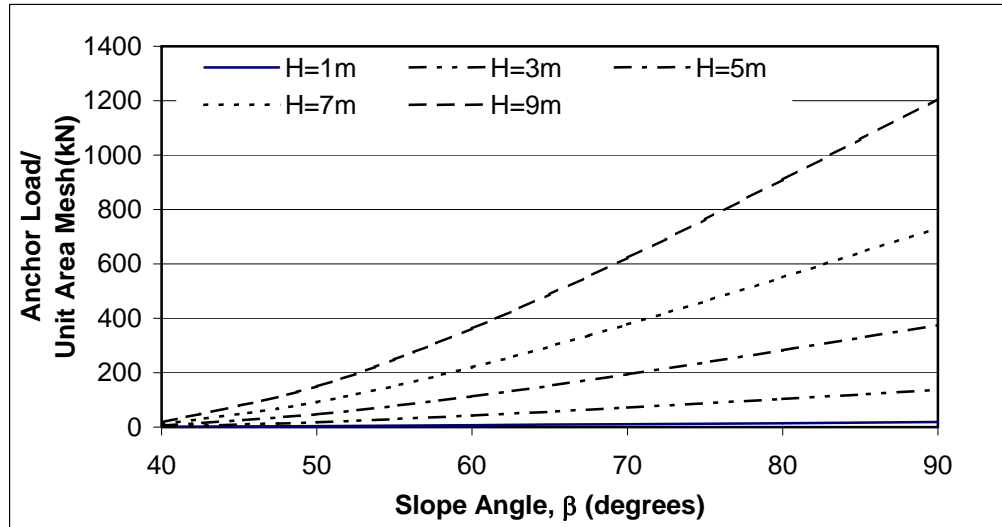


Figure 6-2. Effects of debris accumulation ( $H$  = height of debris) on anchor load as a function of slope angle with an assumed interface friction angle ( $\delta$ ) of  $36^\circ$  and debris accumulation angle ( $\phi_{cs}$ ) of  $35^\circ$ .

### 6.1.5.2 Effect of Interface Friction

As mentioned previously, the mesh contact with the soil and/or bedrock was treated as a continuous surface. The interface friction angle is determined by the surface properties of the slope. Figures 6-3 and 6-4 show the effects of interface friction angle for different loading conditions. Figure 6-3 shows the effect of interface friction angle for the case of a slope of  $50^\circ$  for a range of accumulated debris heights located at the bottom of the mesh/slope. As expected, the anchors loads increase with debris height, but the rates of increase vary with the interface friction angle. It can be seen that with higher interface friction angles the mesh can be carried with minimal requirement for anchors (e.g.,  $\delta = 60^\circ$ ).

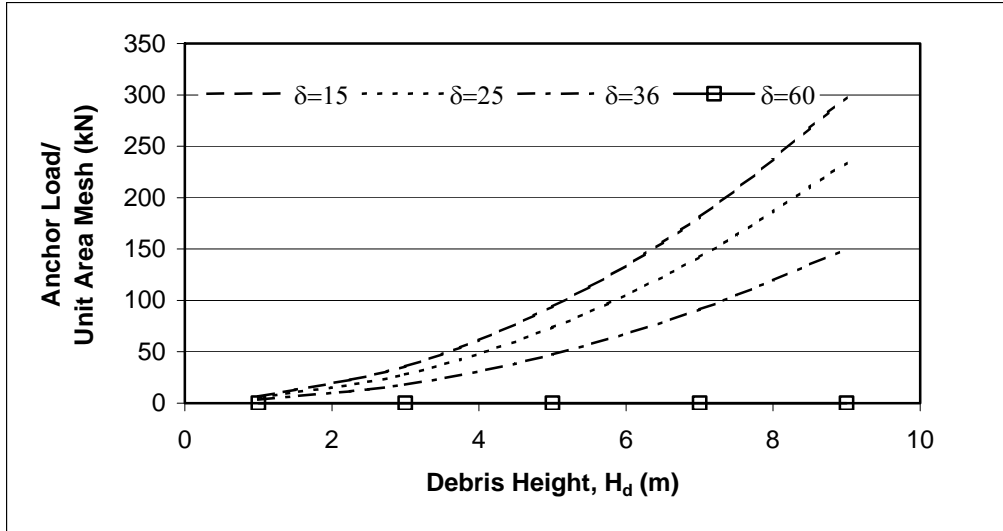


Figure 6-3. The effects of interface friction angle ( $\delta$ ) on anchor load for 30-m (100-ft) slope heights for a range of debris heights on a 50° slope.

Figure 6-4 shows the effects of interface friction angle for a range of slope inclinations without the presence of accumulated debris. It is evident from this figure that interface friction affects the anchor load. Without external load, theoretically, the mesh system can adhere to the slope without anchors when the slope angle is less than the interface friction angle.

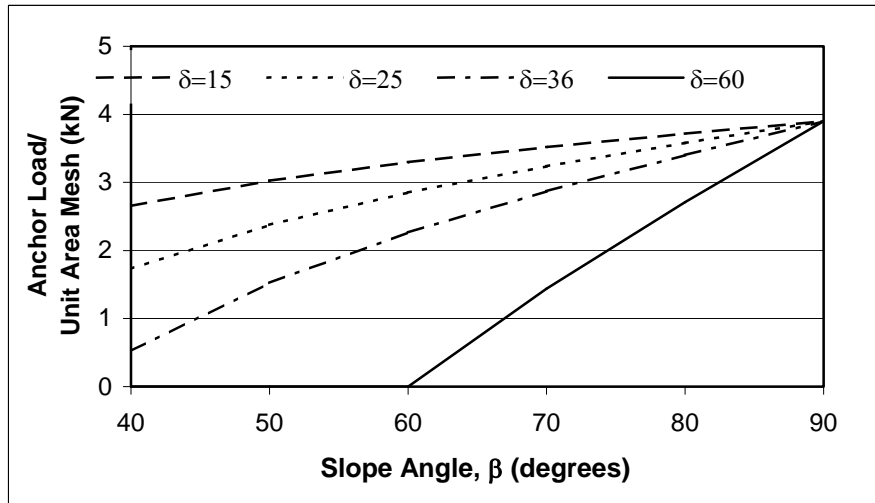


Figure 6-4. The effects of interface friction angle on anchor load for a 30-m (100-ft) high slope with no external load on the system.

## **6.2 FINITE ELEMENT ANALYSIS**

### **6.2.1 Overview**

Finite element analysis is a numerical method for solving a system of governing equations over the domain of a continuous system. The method applies to many fields of science and engineering. It is used here to analyze the mesh system under different loads. The basis of the finite element method for analysis of a solid structure is summarized in the following steps (Knight, 1997). Small parts called *elements* subdivide the domain of the solid structure (Figure 6-5). These elements assemble through interconnection at a finite number of points on each element called *nodes*. This assembly provides a model of the solid structure. Within the domain of each element, a simple general solution to the governing equations is assumed. The specific solution for each element becomes a function of unknown solution values at the nodes. Application of the general solution to all the elements results in a finite set of algebraic equations to be solved for the unknown nodal values. By subdividing a structure in this manner, one can formulate equations for each separate finite element, and those are then combined to obtain the solution for the whole system. The solution is performed by appropriate numerical procedures.

Because the continuum domain is divided into finite elements with nodal values as solution unknowns, the structure loads and displacement boundary conditions must translate to nodal quantities. Single forces such as  $F$  (Figure 6-5) apply to nodes directly, whereas distributed loads such as  $P$  are converted to equivalent nodal values. External supports resolve into specified displacements for the supported nodes.

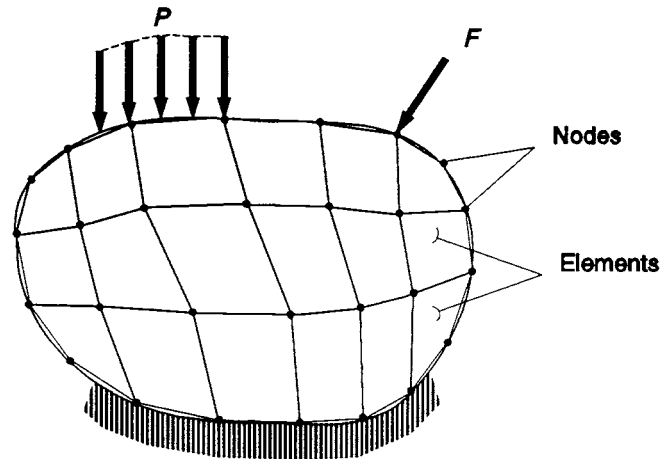


**Figure 6-5. Finite element discretization shows loads (P) and forces (F) acting on mesh (Knight, 1997).**

Different types of elements have been formulated in the literature to address each class of structures. Elements are broadly grouped into two categories: structural elements and continuum elements. Structural elements are trusses, beams, plates, and shells. Continuum elements are two- and three-dimensional solid elements.

The finite element method has advanced extensively in recent years. Many finite element codes are being used to analyze geotechnical and structural problems. Each code has its advantages and limitations. On the basis of extensive experience with the use of FE codes, the investigators decided to use the FE program ABAQUS for the current work. ABAQUS is a general-purpose, 3-D FE code. It has a suite of structural elements and continuum elements in its library. ABAQUS was used here to examine the mesh system under static loading. The FE model performance was first verified with full-scale laboratory test results conducted by Ruegger Systems based in St. Gallen, Switzerland (Flum, 2002). It was then used to conduct a number of studies to identify conditions of failure initiation in the mesh system for a variety of external load conditions. The results were used later to develop design templates.

### **6.2.2 FE Model**

Wire mesh and cable net systems consist of three main elements: anchors, support cables, and fabric (mesh). Because the mesh carries the load with its end restraints in a “membrane type” action, the mesh was modeled with a three-dimensional membrane element from the ABAQUS library. The cable was modeled by using a three-dimensional hybrid beam element. The hybrid beam element was a special purpose element capable of simulating a cable-type structural element. Boundary conditions were input according to the problem being analyzed. The FE model was validated with results from three recently conducted field tests conducted on a TECCO<sup>®</sup> mesh.

Because the mesh generally lays on a rigid surface, its deformation is restricted on a plane and in only one direction of pull. Therefore, the FE analysis was approximated to be plane strain, and deformation was allowed in the direction of pull by imposing appropriate boundary conditions. The mesh weight was input as a body force of the membrane element.

The frictional effect between the mesh and rock can also be incorporated in the FE analysis. The ground surface was assumed to be rigid, and full contact between the mesh and ground surface was also assumed. Determining an appropriate coefficient of friction for mesh-rock contact is a difficult and often subjective task. Therefore, it was evaluated in qualitative manner, as discussed in section 6.1.2.

### **6.2.3 Description of Field Tests**

Ruegger Systems conducted a series of tests to investigate the behavior of TECCO<sup>®</sup> mesh and to determine the relevant strength characteristics (Flum, 2002). The test setup was designed to replicate the loading conditions that exist in the field. The

mesh was placed into a square steel frame 4.35 m (14.3 ft) in dimension and clamped at the edges, as shown in figures 6-6 and 6-7.

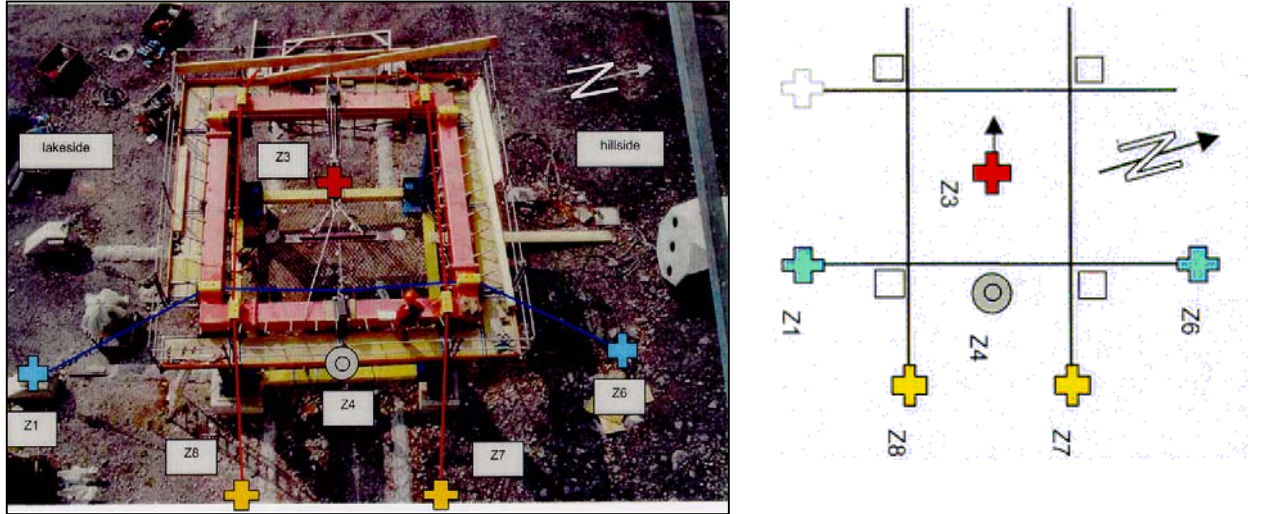


**Figure 6-6. Test setup and locations of load cells. Z4 is the load cell used to measure the force at the stabilizing anchor. Z3 is the load cell used to measure the applied load. Load cells Z1, Z6, Z7, and Z8 measure force at the other supports.**

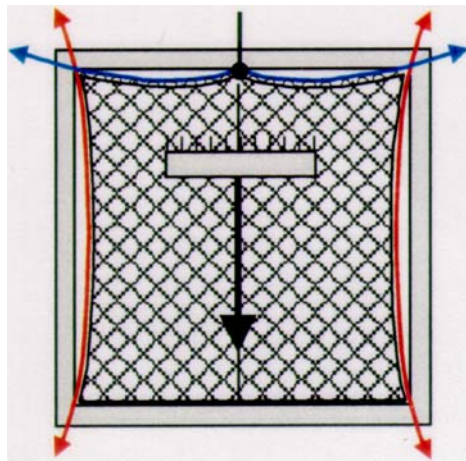


**Figure 6-7. The direction of loading of the TECCO® mesh by the steel beam and the load transfer to perimeters (support ropes and anchors) of the mesh panel. The beam is fixed to a variable number of mesh cells referred to in Table 6-1. The unit of measure for the distance of the beam to the anchor is in the number of mesh cells.**

Load was applied through a steel beam connected at certain locations on the mesh (Figure 6-7). The load was increased gradually until the mesh ruptured (failed). The applied load and the loads transmitted to the stabilizing anchor at the center of the cable and other supports were measured with load cells. Figure 6-6 shows the layout of the load cells.

The mesh type tested was TECCO<sup>®</sup> G65 manufactured by Geobrugg. The diameter of the high tensile steel wire and wire seaming ropes were 0.12 and 0.24 inches (3 and 6 mm), respectively. The mesh density was 0.34 lbf/ft<sup>2</sup> (1.65kg/m<sup>2</sup>); the converted equivalent mesh density for the FE analysis was 43.4 lbs/ft<sup>3</sup> (6812.5 N/m<sup>3</sup>). The details of the three tests are given in Table 6-1.

**Table 6-1. Test results for various loading configurations.**

Test No	Number of mesh cells fixed to steel beam	Number of mesh cells between steel beam and anchor
1	7	8
2	24	8.5
3	24	8

#### **6.2.4 Verification of FE Analysis**

The three field tests were used to verify the FE analysis. The stress-strain relationship of the TECCO<sup>®</sup> mesh in the laboratory is as shown in Figure 6-8. The mesh deformation characteristics can be approximated as linear elastic and were assumed to remain linear elastic until failure. Young's modulus was found to be 39,700 lbf/ft<sup>2</sup> (1898 kN/m<sup>2</sup>). The corresponding Poisson's ratio for plane strain condition was found to be 0.217.

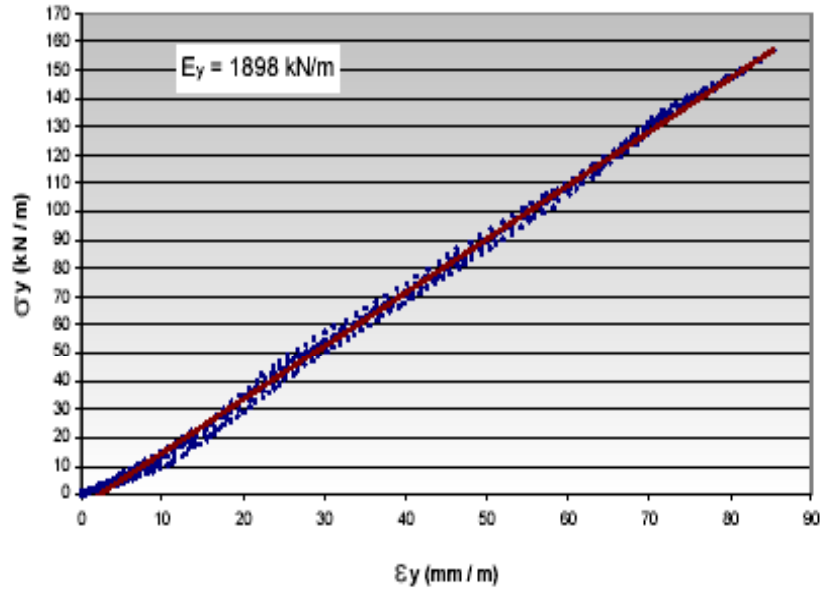
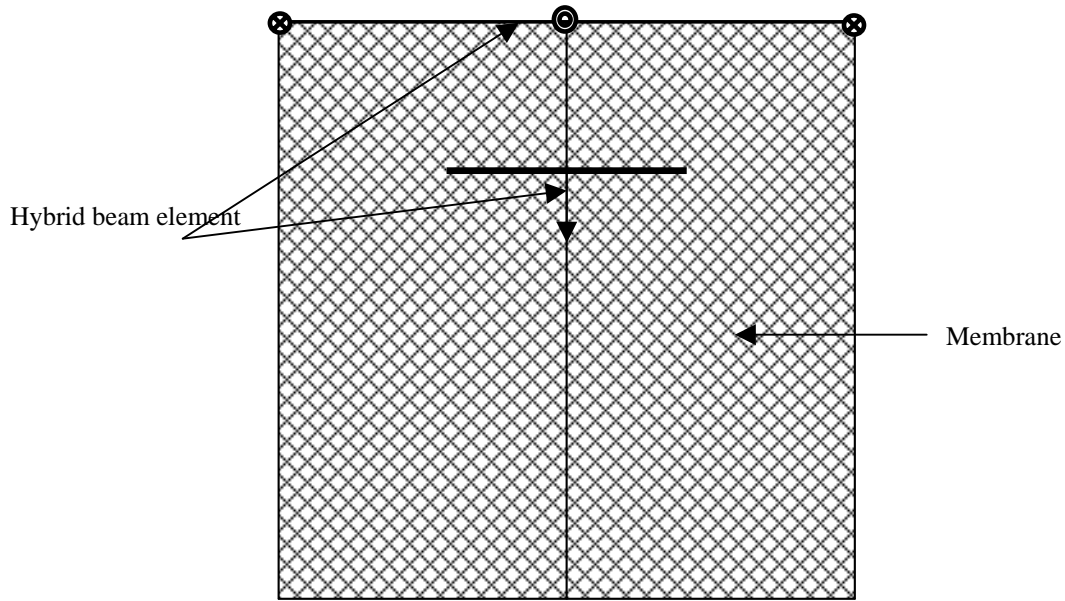


**Figure 6-8. Stress- strain relationship for TECCO® G65 mesh.**

The FE discretization of the mesh system is as shown in Figure 6-9. The mesh was assumed to be pinned along the top nodes shown at the top. The translation of the left and right edges of the mesh in the X-axis direction was fixed to ensure plain strain conditions. The force measured at Z3 (Figure 6-6), was taken as the applied external force. It was applied in the FE analysis as a concentrated nodal force. The results were verified by comparing the reaction measured at location Z4 (Figure 6-6) to that obtained from the FE analysis as shown in Table 6-2. It can be seen that the results matched very well.



- ⊙ -Indicates pin support at which the reaction is measured
- ⊗ -Indicates pin support

**Figure 6-9. FE model setup shows locations of anchors and beam.**

**Table 6-2. Summary of reactions obtained from FE analysis of field tests.**

Test #	Reaction measured in field <i>lbf (kN)</i>	Reaction obtained from FE analysis <i>lbf (kN)</i>
1	10,200 (45.5)	10,100 (44.9)
2	24,300 (108)	24,600 (110)
3	14,300 (63.8)	14,200 (63.4)

One of the features of the FE analysis is that in addition to the reaction forces, many other engineering parameters such as the stress and strain contours within the mesh for the loading can be easily obtained by post-processing of the results. For example, the stress and strain contours for Test #1 are as shown in figures 6-10 and 6-11, respectively. These diagrams clearly show the localized regions of stress and strain within the mesh. In fact, the failure of the mesh in the field tests initiated at the high stress region around the mid anchor.

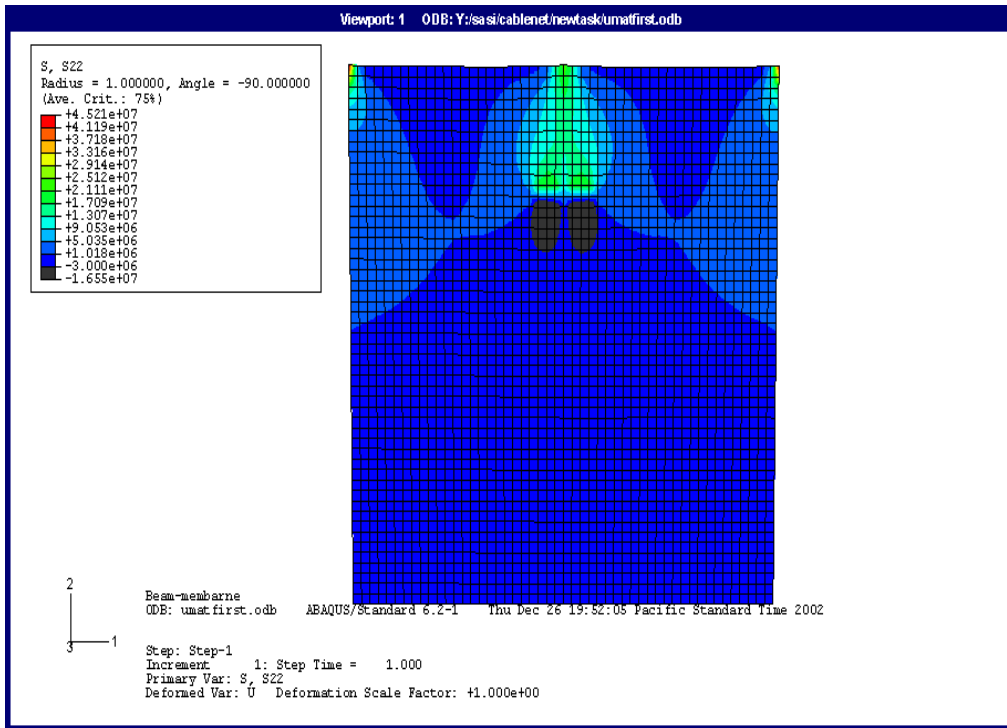


Figure 6-10. Stress contours for Test 1.

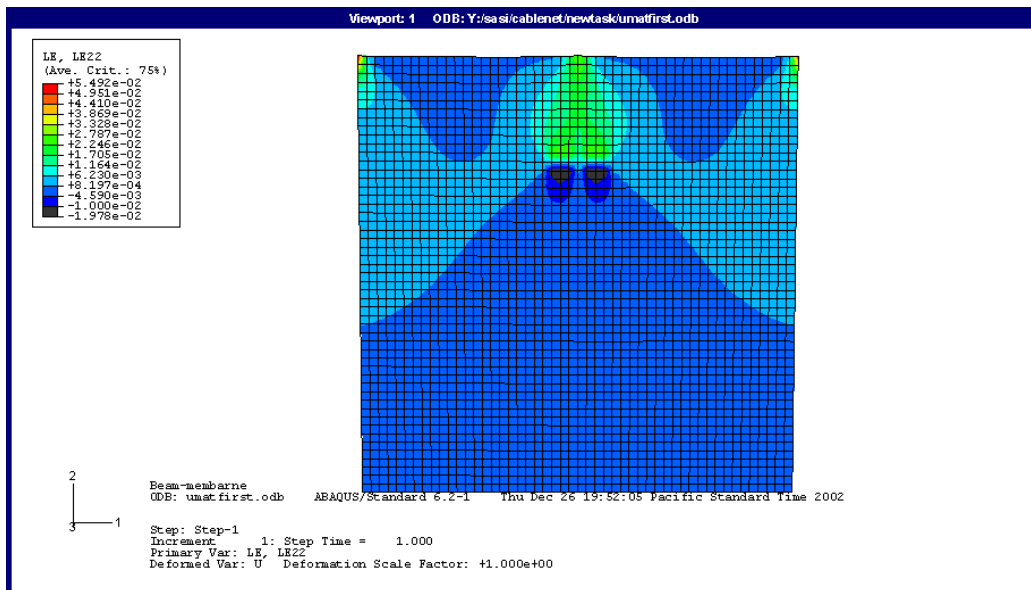


Figure 6-11. Logarithmic strain contours for Test 1.

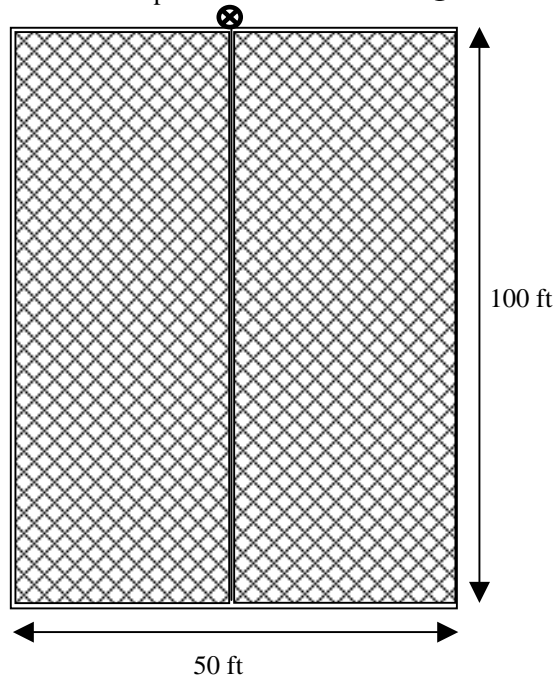
### **6.2.5 Parametric Studies**

The verified FE model was used to study the effects of a number of loading conditions to which a drapery system is subjected. For instance, it has been noted that a critical loading condition for a system can occur during installation, when localized stress can be very high on portions of the system. The FE analysis is a useful means of identifying the locations of localized high stresses and strains during various installation scenarios.

For purposes of illustration, a system 50 ft (18 m) wide by 100 ft (30 m) long made of TECCO<sup>®</sup> G65 mesh was used. The mesh weight of the TECCO<sup>®</sup> was estimated to be 43.4 lbf/ft<sup>3</sup> (6812.5 N/m<sup>3</sup>), and its yield strength was estimated to be 5440 lbf/in<sup>2</sup> (37.5 MPa) (LGA, 2003). To study the installation conditions, six anchor arrangements were evaluated, as shown in Figure 6-12.

The maximum values of the reaction of the anchors and the maximum stresses and strains on the mesh obtained from the FE analysis for the various arrangements are summarized in Table 6-3. The maximum reaction was converted to the shear force on the anchor for three anchor diameters, as shown in Table 6-4.

Arrangement 1: Fixed at mid point      ⊗ - Indicates anchors



Arrangement 2 - Fixed at edges



Arrangement 3 - Fixed at two locations



Arrangement 4 - Fixed at three locations



Arrangement 5 - Fixed at four locations



Arrangement 6 - Fixed at five locations



**Figure 6-12. Anchor arrangements that were investigated for a mesh system of 50 ft (18 m) wide by 100 ft (30 m) long.**

**Table 6-3: Stress and strain for six scenario arrangements of anchors.**

Arrangement	Maximum anchor reaction <i>lbf (kN)</i>	Maximum von Mises stress in mesh <i>lbf/in<sup>2</sup> (MPa)</i>	Maximum (logarithmic) strain x 10 <sup>3</sup>
1	1980 (8.83)	300 (2.07)	2.40
2	994 (4.42)	331 (2.28)	2.25
3	994 (4.42)	152 (1.05)	1.20
4	971 (4.32)	170 (1.17)	1.17
5	638 (2.84)	117 (0.81)	0.80
6	486 (2.16)	94 (0.65)	0.64

**Table 6-4: Shear stress on three anchor diameters for six arrangements.**

Arrangement	Shear stress in anchor <i>lbf/in<sup>2</sup> (MPa)</i>		
	1 in (25 mm)	2 in (50 mm)	3 in (75 mm)
1	2530 (17.42)	632 (4.36)	281 (1.94)
2	1260 (8.71)	316 (2.18)	141 (0.97)
3	1260 (8.71)	316 (2.18)	141 (0.97)
4	1210 (8.37)	303 (2.09)	135 (0.93)
5	806 (5.56)	202 (1.39)	90 (0.62)
6	628 (4.33)	157 (1.08)	70 (0.48)

From the results, it can be seen that the stresses and strains on the mesh were much lower than the yield strength of the TECCO mesh. Therefore, the possibility of the mesh failing under its own weight did not exist for this mesh configuration. It is, however, possible for anchors to shear, depending on the type of arrangements, especially when the mesh is supported by only few anchors (Table 6-4).

In addition to determining maximum stresses and strains, their distributions can also be obtained from FE analysis. For example, the stress and strain contours for Arrangement 1 (only one anchor) and Arrangement 6 are shown in figures 6-13 through 6-16. These diagrams show the locations of localized stresses and strains.

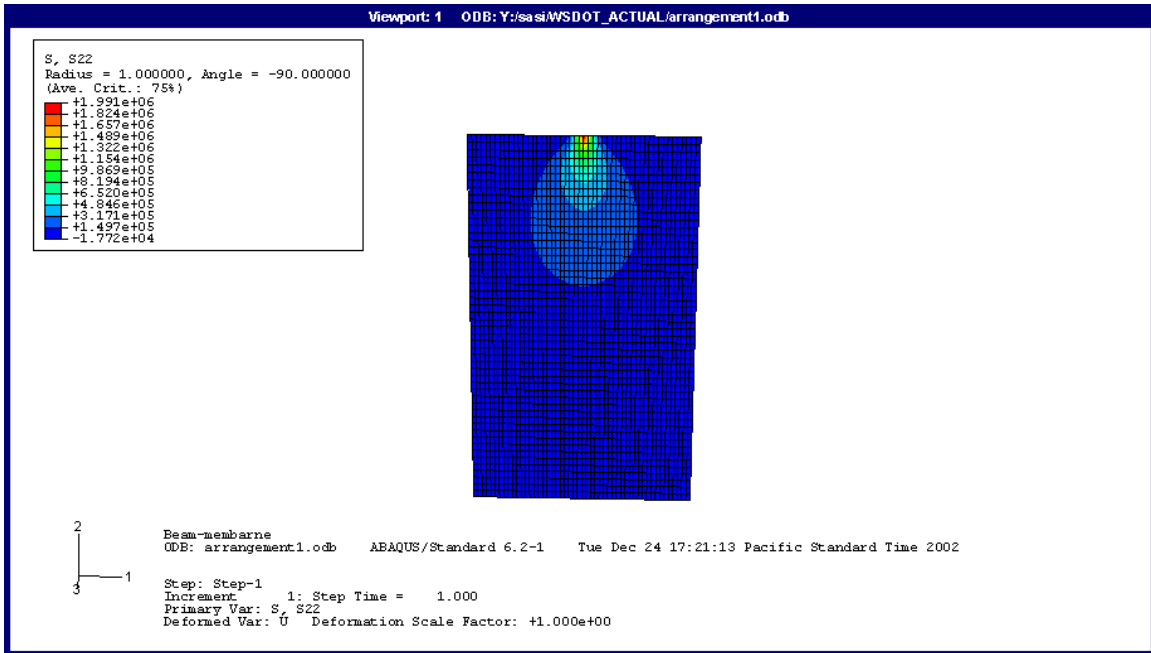


Figure 6-13. Stress contours for arrangement 1.

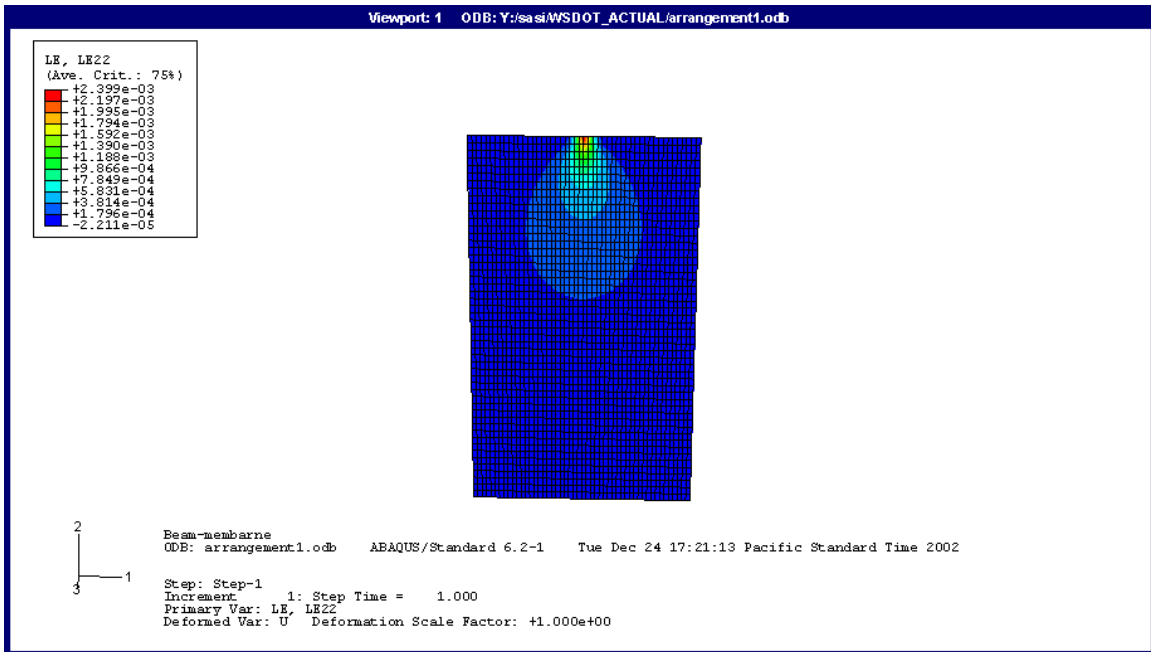


Figure 6-14. Strain contours for arrangement 1.

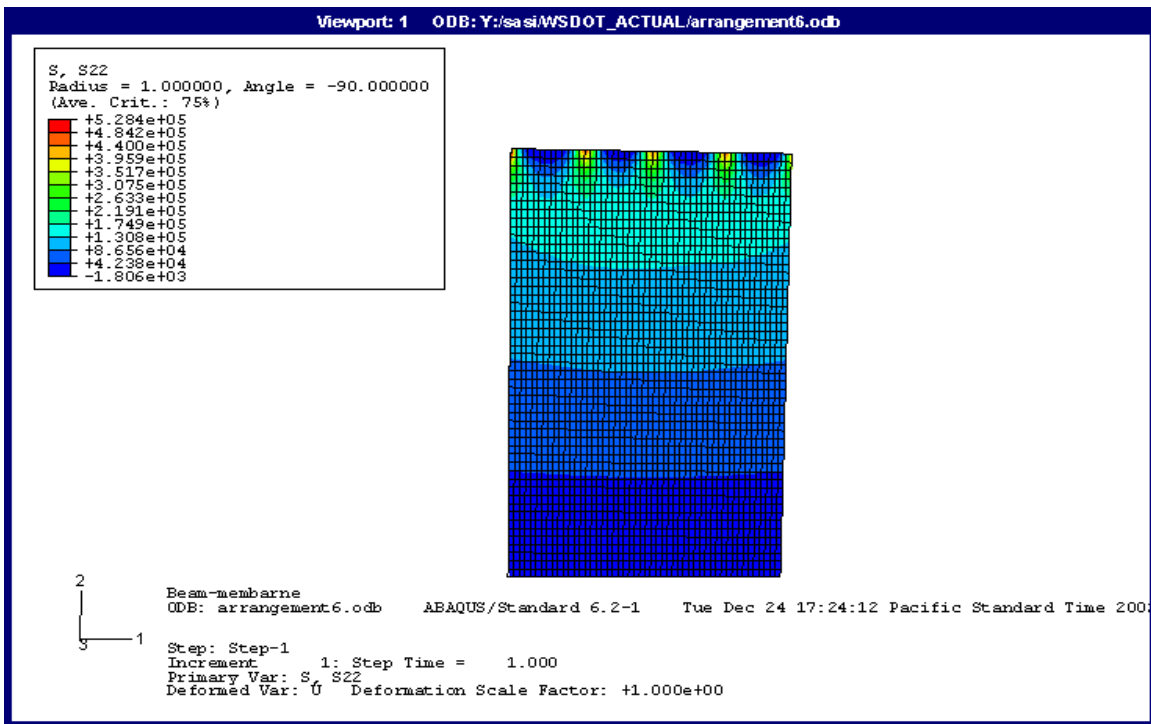


Figure 6-15. Stress contours for arrangement 6.

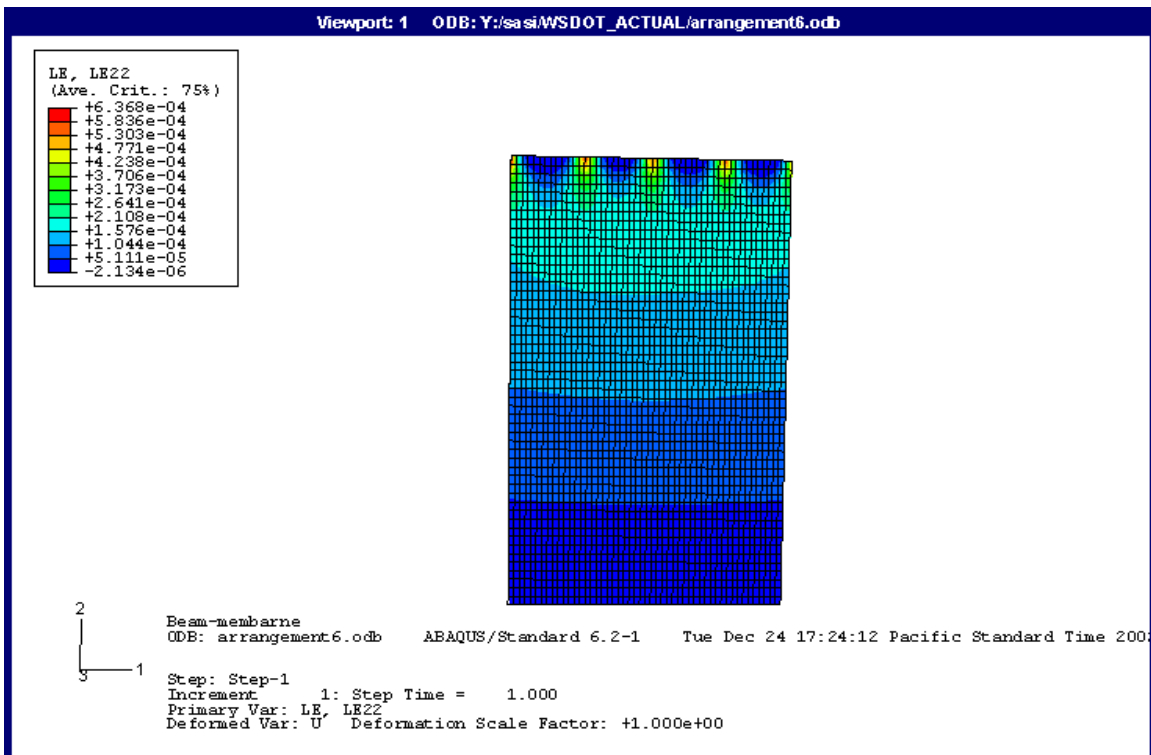


Figure 6-16. Strain contours for arrangement 6.

### **6.3 MODELING RESULTS**

The finite element analysis was subsequently used to estimate the loads transferred to the anchors for the different mesh types that are commonly used in current practice. They included

- an 8x10-type, double-twisted hexagonal mesh of galvanized 0.12-inch- (3-mm) diameter wire (supplied in this study by Maccaferri)
- a high tensile steel, TECCO<sup>®</sup> G65 mesh of corrosion protected 0.12-inch- (3-mm) diameter wire (supplied by Geobrugg)
- a 12-inch (600-mm) square grid, cable net of 5/16-inch- (8-mm) diameter wire rope (supplied by Geobrugg).

The necessary FE model parameters, such as modulus and strength, were derived from independent testing (Appendix B) or from data provided by the manufacturers and are summarized in Table 6-5.

**Table 6-5. Moduli and yield strengths of mesh types.**

<b>Fabric</b>	<b>Young's modulus <i>lbf/in<sup>2</sup> (MPa)</i></b>	<b>Yield strength <i>lbf/in<sup>2</sup> (MPa)</i></b>
double-twisted hexagonal mesh	1.23 x 10 <sup>5</sup> (850)	2180 (15)
TECCO <sup>®</sup> G65 mesh	2.46 x 10 <sup>4</sup> (170)	4350 (30)
cable net	2.03 x 10 <sup>6</sup> (14000)	2.54 x 10 <sup>4</sup> (175)

#### **6.3.1 Anchorage and Top Connection**

The calculated loads from solely the mesh weight transferred to the system anchorage are provided for double-twisted hexagonal wire mesh, TECCO<sup>®</sup> G65 mesh, and cable nets in figures 6-17, 6-18, and 6-19, respectively. The graphs plot anchor load

as a function of anchor spacing for slope lengths of 50, 100, 200 and 300 ft (15, 30, 60, and 90 m). For design conservatism, the plots are for a vertical slope, which would neglect the contribution of interface friction, and represent the highest load condition on the anchors (neglecting other external loads). Similar charts were developed for slope orientations of 45° and 60° for the three categories of slope roughness (interface friction); these are included in Appendix D.

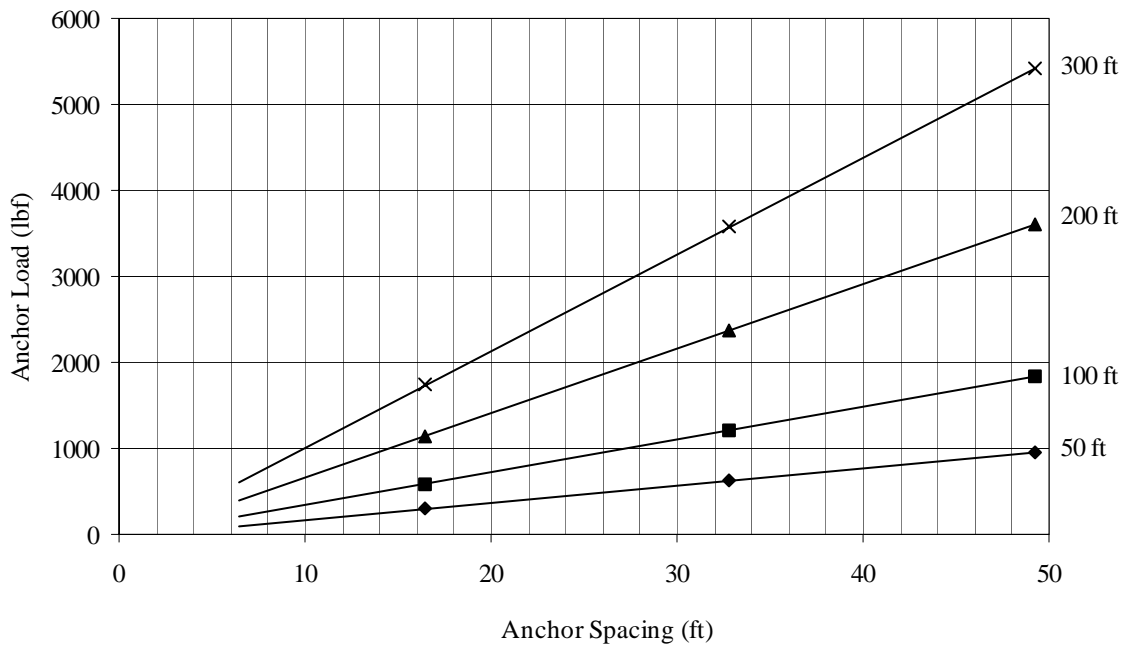


**Figure 6-17. Anchor load v. spacing for double-twisted hexagonal wire mesh for a vertical slope (no interface friction) ranging in height from 50 to 300 ft (15 to 90 m).**

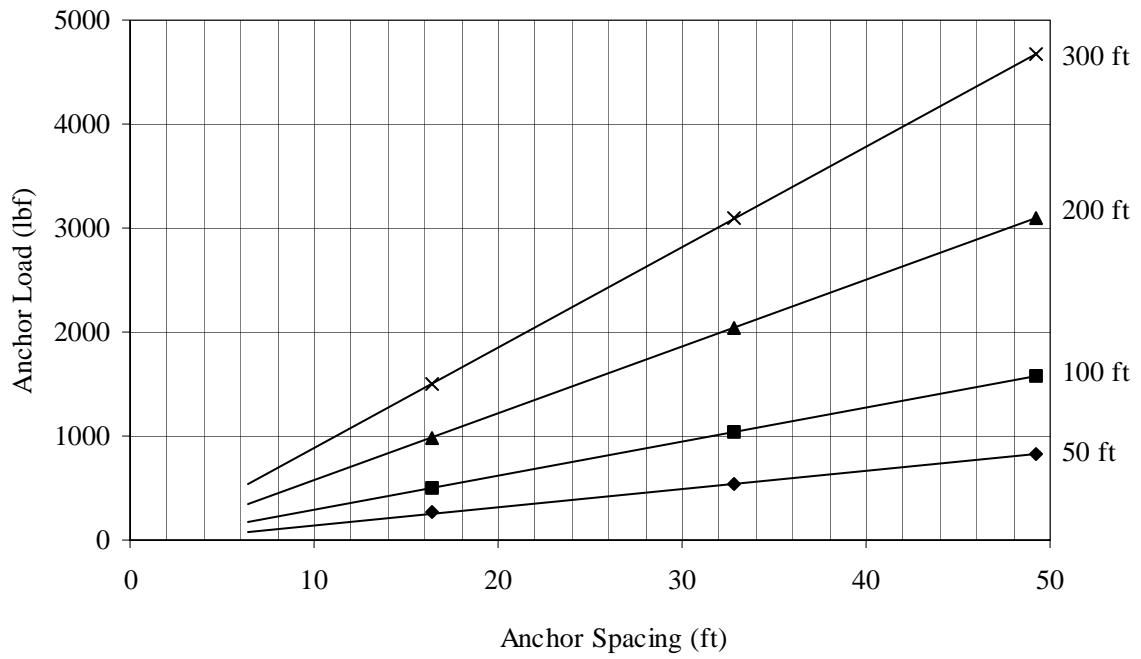


**Figure 6-18. Anchor load v. spacing for TECCO® G65 mesh for a vertical slope (no interface friction) ranging in height from 50 to 300 ft (15 to 90 m).**

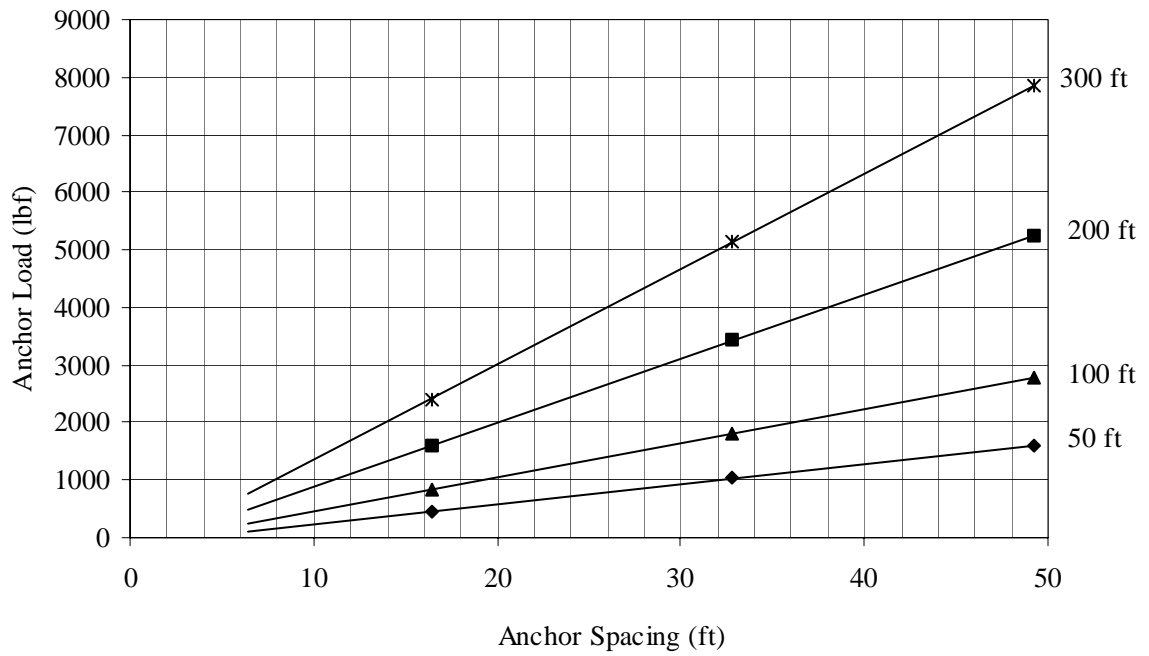


**Figure 6-19. Anchor load v. spacing for cable nets for a vertical slope (no interface friction) ranging in height from 50 to 300 ft (15 to 90 m).**

### **6.3.2 Support Cables**

The current application of wire mesh/cable net protection systems often includes a widely spaced grid of interior horizontal support ropes, as well as vertical support ropes, throughout the field of the mesh. However, it is known through field observation that this practice does not have a strong mechanical basis. Therefore, the need for a grid of interior support ropes was evaluated with finite element analysis for a typical installation (Figure 6-20) on a vertical slope (no interface friction). The length and the width of example installation were 125 ft (38 m) and 50 ft (15 m), respectively. The installation system was analyzed with only mesh weight, and no external forces were applied. First, the installation was analyzed without any horizontal and vertical support ropes (Figure 6-20), and von-Mises stress and stress/strain contours were obtained.

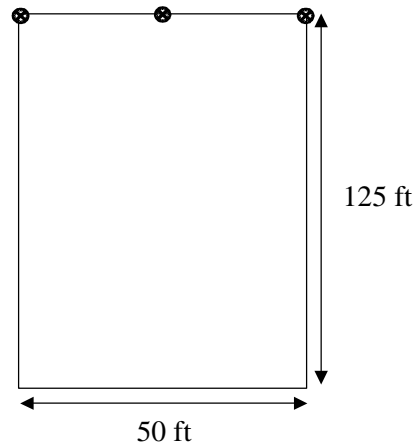
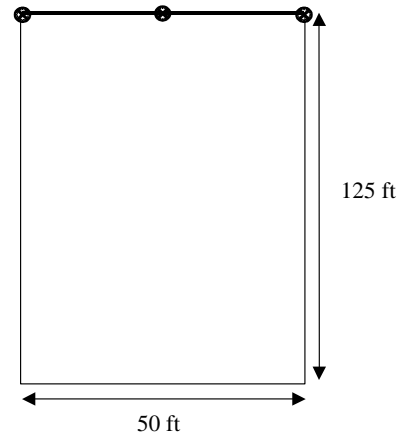


**Figure 6-20. Mesh without support ropes.**

Subsequently, the system with a top horizontal support rope (Figure 6-21) was analyzed and the stress and strain contours obtained.

**Figure 6-21. Mesh with top horizontal support rope.**



Vertical support ropes were then introduced to the installation system (Figure 6-22), and a similar analysis was carried out. Finally, the benefits of interior horizontal support ropes on the mesh were evaluated with the arrangements shown in figures 6-23 and 6-24.

**Figure 6-22. Mesh with top horizontal and vertical support ropes.**

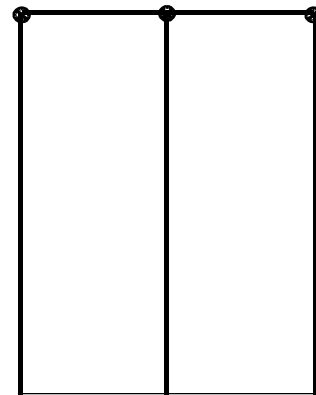


**Figure 6-23. Mesh with top and interior horizontal support ropes.**

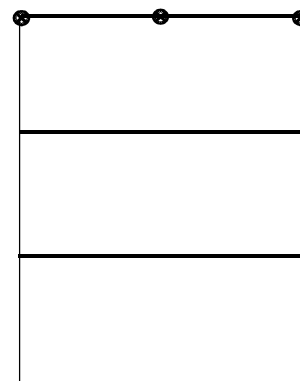
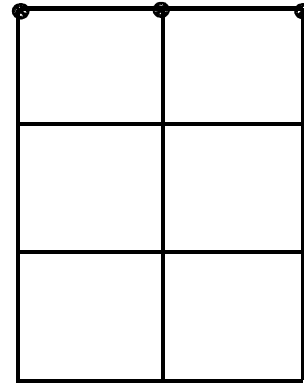


**Figure 6-24. Mesh with both vertical and horizontal support ropes.**



The summary of the maximum von Mises stress within the mesh, as well as the top horizontal rope and vertical rope in each of the cases, is presented in Table 6-6. Comparison of the results for the arrangements in figures 6-20 and 6-21 show that use of a top horizontal rope significantly reduces the stress level within the mesh (Table 6-6) by distributing it along the entire length of the support rope. However, the stress values obtained for figures 6-21 and 6-23 are identical to those for figures 6-22 and 6-24. Note that the stresses in the mesh are significantly less than the yield strength of the mesh. Thus, it is apparent that the inclusion of interior horizontal support ropes in addition to the top horizontal rope does not reduce the stress within the mesh and, therefore, provides no mechanical benefit.

**Table 6-6. Summary of von-Mises stresses for support rope arrangements.**

Arrangement	von-Mises stress <i>lb/in<sup>2</sup> (MPa)</i>		
	mesh	horizontal rope	vertical rope
Figure 6-20	812 (5.60)	-	-
Figure 6-21	464 (3.20)	10,300 (71.2)	-
Figure 6-22	213 (1.47)	6230 (43.0)	160 (1.10)
Figure 6-23	464 (3.20)	10,300 (71.0)	-
Figure 6-24	213 (1.46)	6230 (43.0)	160 (1.10)

The modeling shows that the inclusion of vertical ropes in addition to a top horizontal rope (figures 6-22 and 6-24) reduces the stress concentration on the mesh, as well as along the top horizontal rope (Table 6-6). Furthermore, the stresses on the vertical support rope are much smaller than those on the top horizontal support rope, so the vertical ropes do not need to be as strong. In current practice, where vertical support ropes are included, the mesh is fastened to vertical ropes with lacing wire and does not grip the rope. Thus, there is no vertical load transfer by the mesh to the vertical support ropes; hence, with current practice, there is no effective mechanical benefit. If the mesh were clamped at close spacing to the vertical ropes, the mechanical benefit would potentially be realized up to the localized yield stress of the mesh/connection detail.

### **6.3.3 Verification of Interface Friction**

Extensive finite element analyses were conducted to verify the friction angles assigned in section 6.1.2 to rough and undulating slopes. In rough and undulating slopes, the contribution of interface friction to the shear resistance of the system should be enhanced because of slope irregularities and surface roughness, assuming that the mesh-slope contact is maintained. Analyses were carried out for interface friction with selected internal supports along a typical slope oriented at 45°, as shown in Figure 6-25. Numerous iterations were run varying the location of the internal support to determine the most critical configuration. For an undulating slope, the location of the internal support was varied, whereas for a rough slope two to three internal supports were varied inside the mesh. The reaction loads on anchors with the internal supports were obtained first (Table 6-7). Then, the interface friction angle on an equivalent slope with no internal support was varied until the results matched. It can be seen that the equivalent

interface friction values produced results that were close to the anchor loads where internal support was included. Clearly, field conditions are highly variable. While the analysis is an obvious simplification of the expected variability, it does illustrate the potential effect of slope irregularity and surface roughness for two generalized slope conditions and the resultant influence on anchor load.

**Figure 6-25. The arrangement for verification of assigned friction includes a top horizontal cable and the inclusion of an internal point of support to simulate a protrusion on the slope.**

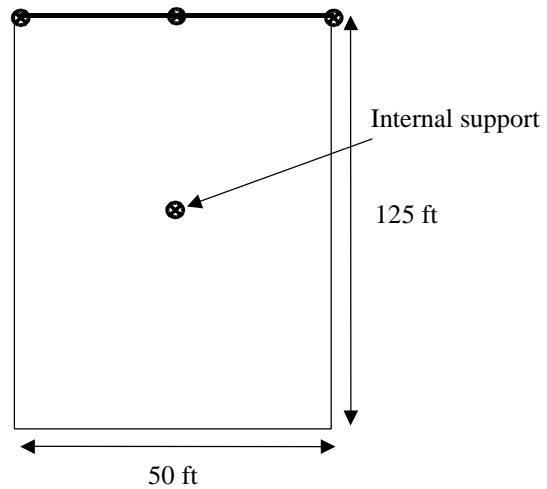


**Table 6-7. FE analysis results for interface friction.**

Slope	Anchor load with internal support <i>lbf (kN)</i>	Anchor load with friction angle <i>lbf (kN)</i>	Assigned friction angle
Undulating	1239-1378 (5.5-6.1)	1291-1360 (5.7-6.0)	36°-59°
Rough	774-998 (3.4-4.4)	788-1098 (3.5-4.9)	Above 60°

### **6.3.4 Limiting Conditions on Global Stability**

FE analysis was also used to determine the following three limiting conditions for the different mesh systems:

- the maximum height of the installation for each fabric
- the maximum debris load for each fabric

- the maximum fabric area to exceed the breaking strength of the top horizontal rope.

#### 6.3.4.1 Maximum Installation Height

To determine the maximum height of installation for a specific type of mesh/cable net, the analyses assumed a 90° slope (no interface friction) for both a 20-ft (6-m) and 50-ft (15-m) anchor spacing. The three fabrics that were evaluated were as before:

- an 8x10-type, double-twisted hexagonal mesh of galvanized 0.12-inch- (3-mm) diameter wire (supplied in this study by Maccaferri)
- a high tensile steel, TECCO® G65 mesh of corrosion protected 0.12-inch- (3-mm) diameter wire (supplied by Geobrugg)
- a 12-inch (600-mm) square grid, cable net of 5/16-inch- (8-mm) diameter wire rope (supplied by Geobrugg).

The result for each mesh type is shown in Table 6-8. Note that these yield states are considerably larger than the highest installations currently used in North America.

**Table 6-8. Mesh yield states as function of height for a vertical slope with no interface friction.**

Mesh	Maximum height of installation for 50 ft (15 m) anchor spacing <i>ft (m)</i>	Maximum height of installation for 20 ft (6 m) anchor spacing <i>ft (m)</i>
Double-twisted, hexagonal mesh	350-375 ft (105-115 m)	>550 ft (>170 m)
TECCO® G65 mesh	450-500 ft (135-150 m)	>700 ft (215 m)
Cable net	600-750 ft (180-230 m)	>825 ft (250 m)

#### 6.3.4.2 Maximum Debris Load

FE analyses were carried out to determine the maximum debris load for a planar (interface friction = 25°), 45° slope, with 100-ft (30-m) slope length and both 20-ft (6-m)

and 50-ft (15-m) anchor spacing. It was assumed that a debris load with a unit weight of 130 lbf/ft<sup>3</sup> (2100 kg/m<sup>3</sup>) would be distributed uniformly over the entire width. Note that the maximum debris load for double-twisted hexagonal mesh and TECCO<sup>®</sup> G65 mesh was determined by limiting the yield strength of the meshes. With an assumed anchor capacity of 20,000 lbf (90 kN), a cable net installation for the given configuration would yield first at the anchor for the calculated debris load (Table 6-9). Assuming that the anchor is not the limiting factor but that the cable net is first to yield, then much higher debris loads can be carried by the cable nets, as shown in the bracketed values in Table 6-9. The corresponding anchor loads for this yield state for a 50-ft (15-m) and 20-ft (6-m) anchor spacing are 61,750 lbf (275 kN) and 52,500 lbf (230kN), respectively.

**Table 6-9. Mesh yield states as a function of debris load.**

<b>Mesh</b>	<b>Maximum debris volume for 50 ft (15 m) anchor spacing <i>yds<sup>3</sup> (m<sup>3</sup>)</i></b>	<b>Maximum debris volume for 20 ft (6 m) anchor spacing <i>yds<sup>3</sup> (m<sup>3</sup>)</i></b>
Double-twisted hexagonal mesh	2.5 yds <sup>3</sup> (1.9 m <sup>3</sup> )	2.1 yds <sup>3</sup> (1.6 m <sup>3</sup> )
TECCO <sup>®</sup> G65	4.8 yds <sup>3</sup> (3.7 m <sup>3</sup> )	3.8 yds <sup>3</sup> (2.9 m <sup>3</sup> )
Cable net	6.5 yds <sup>3</sup> [25 yds <sup>3</sup> ] (5.0 m <sup>3</sup> )	7.5 yds <sup>3</sup> [20 yds <sup>3</sup> ] (5.7 m <sup>3</sup> )

### **6.3.4.3 Maximum Length of Top Horizontal Rope**

The top horizontal support rope is a critical structural element in any installation. Figure 6-26 shows the typical loading arrangement of a top horizontal support rope. Maximizing the uninterrupted length of the top horizontal rope and, thus, minimizing connections reduce the installed cost of a system. This length, however, is limited by both the rope's tensile capacity and the amount of deflection between the anchor points. As a most conservative estimation, this length can be determined by using the set of

equations developed in section 6.3.1 for a vertical slope (no interface friction). Assuming the capacity of typical horizontal ropes of ½-inch (13-mm) and ¾-inch (19-mm) diameter to be approximately 25,000 (110 kN) and 50,000 lbf (220 kN), respectively, the maximum length for an unsupported section of a rope (no interface friction) was found for double-twisted hexagonal and TECCO® mesh (Table 6-10A) and cable net backed with double-twisted hexagonal mesh (Table 6-10B). Note that these values are for mesh weight only. If other external loads such as snow or debris contribute, then the lengths will become shorter.

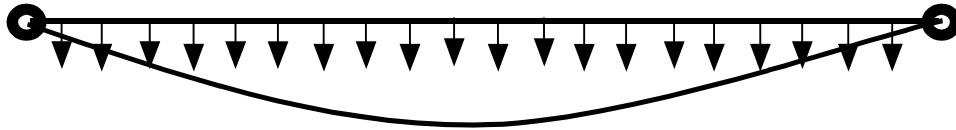


Figure 6-26. Load distribution in the top horizontal support rope.

Table 6-10A. Maximum length for top horizontal support rope v. slope height for double-twisted hexagonal and TECCO® mesh (no interface friction).

Slope Height <i>ft (m)</i>	Max. length for ½” (13 mm) cable fabric weight only <i>ft (m)</i>	Max. length for ¾” (19 mm) cable fabric weight only <i>ft (m)</i>
50 ft (15 m)	460 ft (140m)	830 ft (250 m)
100 ft (30 m)	240 ft (75 m)	430 ft (130 m)
200 ft (60 m)	120 ft (35 m)	220 ft (65 m)
300 ft (90 m)	80 ft (25 m)	150 ft (45 m)

**Table 6-10B. Maximum length for top horizontal support rope v. slope height for cable net backed with double-twisted hexagonal mesh (no interface friction).**

<b>Slope Height <i>ft (m)</i></b>	<b>Max. length for ½" (13 mm) cable fabric weight only <i>ft (m)</i></b>	<b>Max. length for ¾" (19 mm) cable fabric weight only <i>ft (m)</i></b>
50 ft (15 m)	160 ft (50m)	300 ft (90 m)
100 ft (30 m)	80 ft (25 m)	150 ft (45 m)
200 ft (60 m)	40 ft (12 m)	80 ft (25 m)
300 ft (90 m)	30 ft (8 m)	50 ft (15 m)

## **CHAPTER 7 DESIGN GUIDELINES**

The primary objective of this research was to develop a rational and broadly applicable methodology for designing wire mesh and cable net systems to control rockfall on steep slopes. The research sought to pragmatically combine several decades of field performance, recent testing of system elements, and quantitative analyses of system function when exposed to various external loads. A large component of the research focused on the back-analysis of observed system failures and the characterization of factors contributing to them, as well as systems that have performed satisfactorily. This proved to be a difficult task because loading conditions were often not directly observable/measurable and, therefore, did not allow for direct quantitative analyses. Fortunately, most systems have performed satisfactorily, and as a result, the guidelines below in many respects confirm the best of existing practice and can more widely disseminate these successes.

Nevertheless, examination of system failures confirmed that in some cases there was a fundamental lack of understanding of loading conditions and load transfer. This is particularly true for snow and impact loads. As a result of this research, some advancement was made in the evaluation of and design for snow loads. On the other hand, determining and analyzing the impact loads and load transfer resulting from rockfall trajectories, both sub-parallel and perpendicular to the mesh/slope, proved less productive, predominantly because full-scale testing was needed to confirm the analyses but was not achievable within the scope of the research. This remains an important research topic, as systems are now frequently being located on slopes that require the

containment of more horizontally directed, high-energy rockfall. Last, the examination of both global and localized failures of these systems and their components revealed that, in part, “the devil is in the [fabrication and construction] details.”

In recent years, designers have utilized wire mesh and cable net systems for increasingly demanding conditions, and as expected, failures have resulted. A goal of this research was to identify and quantify the limiting states of the system components and external loads.

The guidelines that follow provide a generalized approach, recommendations, and limitations for

- evaluating site suitability
- characterizing potential external loads
- fabric selection
- anchorage requirements
- system details and specifications
- addressing aesthetic concerns
- construction and maintenance.

A flow chart summarizes the overall design approach presented in these guidelines (Figure 7-1). The approach first entails an assessment of site conditions: characterization of the mode(s), size, volume and frequency of slope instability, and evaluation of the potential external loads that the system must withstand. Following this assessment and a favorable determination of site suitability, the fabric is selected that is best suited for the anticipated conditions. A juncture is then reached at which the potential for snow load must be considered. Anchor loads for either mesh weight or

snow load are then determined. A recommended range for the factor of safety is then applied to the mesh weight to account for debris and impact loads and to the snow load to account for variability in the maximum potential loading state. Anchor capacity and spacing are then determined, followed by the specific detailing of the system.

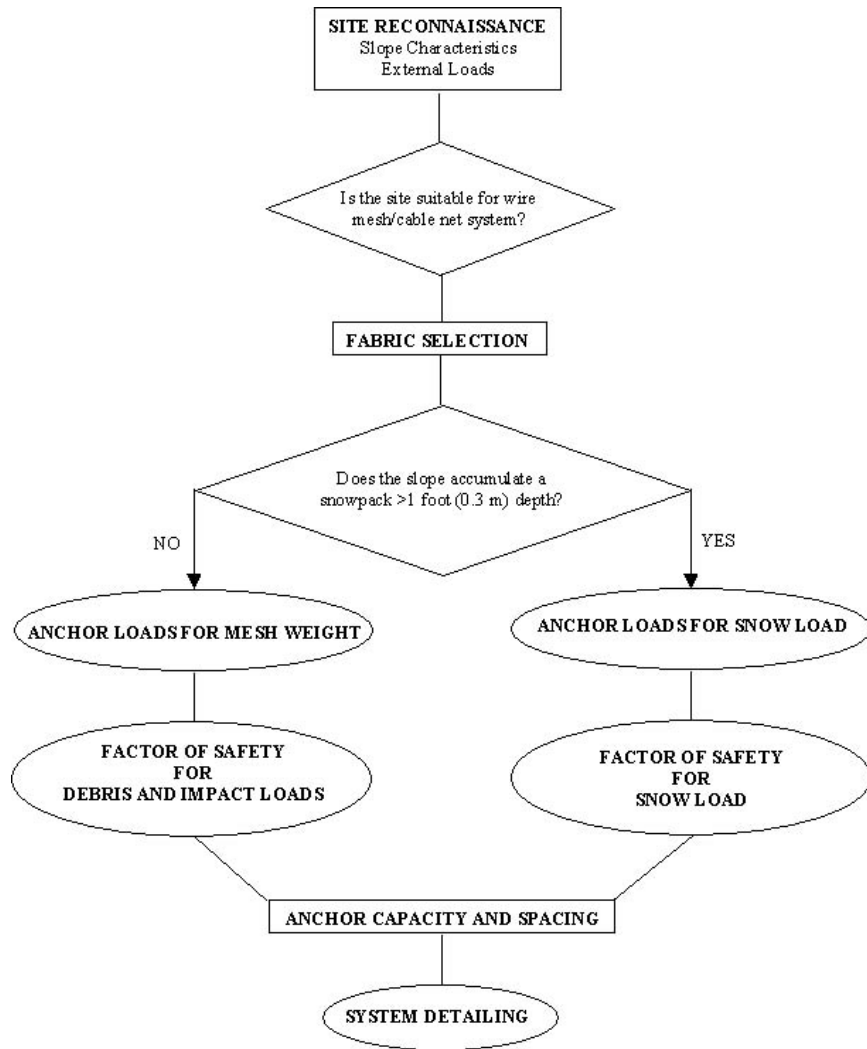


**Figure 7-1. Recommended design approach for wire mesh/cable net systems.**

The greatest challenge in preparing guidelines is anticipating the range of site conditions and external loads that could be experienced, yet avoiding an excessively cumbersome or complex design process. Where feasible, the guidelines provide specific

design recommendations for certain system elements. However, for a number of conditions, such specificity is not practical or the mechanical behavior of the system is not sufficiently understood to provide detailed recommendations. In these instances, the guidelines attempt to highlight dominant concerns or limitations, and designers must then exercise their best judgment.

These guidelines and recommendations are based on the collective geologic and engineering experience and judgment of this project's Technical Advisory Committee (TAC), as well as the findings of the study's Principal Investigator, Professor Muhunthan, and his graduate students. The guidelines address generalized site and loading conditions, and, where appropriate, recommend a range of safety factors for these anticipated conditions. Undoubtedly, site conditions exist that exceed and/or are different from those anticipated in the guidelines or that have been presented in this research report. It is the expectation of the authors and the TAC that due care and sound geologic and engineering judgment be exercised by designers when they apply these guidelines, and that caution is warranted in utilizing these systems for conditions that lie outside the bounds provided in this research report.

## **7.1 SITE SUITABILITY AND CHARACTERIZATION**

Wire mesh/cable net systems have been installed on slopes of all shapes and sizes for mitigating rockfall hazards. However, numerous examples exist of systems that have been installed on slopes that are poorly suited for this mitigation, or that are over- or under-designed for the site/loading conditions. Characterization of the site and loading conditions is the first and most important step in determining site suitability and in designing an appropriate system for the expected conditions.

### **7.1.1 Block/Event Size**

As with any structural system, there are limitations on repeated sustainable loads for mesh systems. The size of individual blocks or small-scale instabilities is the most important factor in determining site suitability. While there are many examples of installations that have sustained apparent extreme debris or impact loads, in practice, wire mesh/cable net systems have well demonstrated limitations in terms of block size. That threshold is roughly block sizes of 5 ft (1.5 m). If potentially unstable block sizes exceed this threshold, other mitigation measures should be considered or added, such as removal or reinforcement with anchors/shotcrete. Rockfall consisting of single or several blocks is the mode of slope instability that draped mesh systems are intended to address. Again, there are many examples of systems that have sustained little or no damage when subjected to slope instabilities tens to hundreds of cubic yards (meters) in volume. However, forensic assessment of such cases has generally shown that little load was actually transferred to the system, and the debris simply slid beneath the system. Analyses and case histories presented previously in this report bear out that systems secured only at the top, as is the general practice in North America, cannot sustain loads much in excess of 10 cubic yards (meters) of debris (assuming full load transfer of the debris). If anticipated modes of slope instability would result in single events larger than roughly 5 to 10 cubic yards (meters) in volume, additional or alternative mitigation measures should be considered.

Evaluation of block sizes or potential debris volumes per event should entail not only direct observation but also anecdotal information from past events.

### **7.1.2 Slope Conditions**

Slope configuration largely controls rockfall trajectory. Rockfall on near-vertical slopes is dominantly governed by a trajectory of freefall, whereas flatter slope orientations result in a bouncing or rolling trajectory path. It is also well known that slope asperities, sometimes referred to as launching features, can impart a significant horizontal component to a free falling trajectory. Mesh systems on near-vertical slopes function somewhat differently than those on flatter slopes. Given the orientation and often limited contact on near-vertical slopes, the mesh imparts little stabilization effect through its weight, and rocks can generally pass unimpeded between the mesh and the slope. On flatter slopes, mesh contact is often greater, and its weight can impart a significant resistance force on individual blocks. As a result, in many cases, rockfall frequency is reduced, and the trajectories of dislodged blocks are generally slowed considerably. Entrapment of loose blocks and debris is commonly observed with mesh systems installed on flatter slopes.

For a variety of reasons, it is important to anticipate, as well as to design and construct, how the mesh will lay on the slope. To this end, slope uniformity needs to be assessed. Mesh contact is typically greatest on uniform slopes and least on concave slopes. Slope uniformity also influences where and how rockfall impacts the system and debris accumulates or passes beneath the system. As examples, figures 7-2A and 7-2B illustrate typical concave and convex slopes, respectively, and the influence that slope configuration has on debris accumulation and impact loading.

Slope height and length, as well as area of coverage, need to be defined. In North America, mesh systems have been successfully installed on slopes approaching 450 feet in slope length and 300 feet in height. When coverage area and slope length are

considered, the bottom elevation of the mesh is largely a function of the available catchment area at the base of the slope and its effectiveness at containing debris as it clears the installation. Aesthetic concerns or snow accumulation at the base of the installation may also influence the lower terminus. Unless the top of the mesh is raised or suspended (modified systems), the mesh should cover all the observed/anticipated source areas of rockfall. It is also important to consider ongoing slope degradation, so the mesh should extend upslope a sufficient distance to cover the expected long-term configuration of the slope. Although mesh may often slow erosion, there are numerous examples of installations where the top of mesh and the anchors have been undermined because of retrogression of an actively eroding slope crest (Figure 7-3). With respect to slope width, salients and reentrants increase surface area and, generally, result in an increase in the required mesh quantity. While mesh systems are often a highly economical and effective measure for mitigating rockfall, other containment or avoidance alternatives may be more cost effective if the coverage area becomes excessive.

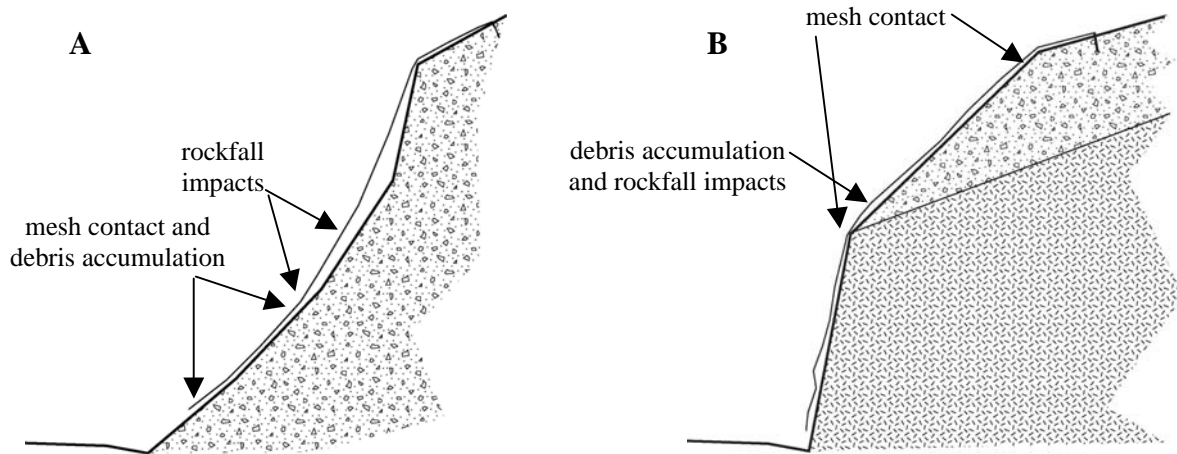


**Figure 7-2. Cross-sections show typical (A) concave and (B) convex slopes and the areas of mesh contact, debris accumulation, and rockfall impacts.**



**Figure 7-3. Ongoing erosion threatens a wire mesh system installed in the late 1980s in the North Cascades of Washington.**

An evaluation of slope characteristics should also include an assessment of anchoring conditions. Difficult access generally necessitates small portable drills for anchor installation. This is not usually a problem for installations in bedrock, but loose, cobble/boulder deposits can pose challenging installations for small, hand-operated equipment.

### **7.1.3 Interface Friction**

Where the mesh is in contact with the slope, interface friction provides a resistance component to the stability of the system. The interface friction is controlled by macro and micro roughness of the surface. Macro roughness is defined by large-scale

irregularities of the slope, and micro roughness is defined as the texture of the surface. Where the slope is planar and the surface is smooth, minimal interface friction may occur, and the mobilized force on the system is carried largely by the anchors. Where slopes are highly irregular and the surfaces are rough or have abrupt protrusions, very high interface friction may occur. In these cases, very little to no mobilized force may be imparted to the anchors.

Unfortunately, interface friction is a difficult parameter to quantify in practice. Furthermore, to include this contribution with the necessary resistance force for a system, a designer must estimate the amount of mesh contact. This task is also difficult, since mesh contact is influenced by slope configuration, fabric flexibility, and installation methods. Because of weathering, interface friction can also be a transient condition. For these reasons, the guidelines do not include the resistance contribution of interface friction to determine anchor requirements for mesh weight, debris load, and impact load. Instead, the guidelines apply a factor of safety to a range of system configurations for a vertical slope (no interface friction) to determine the anchor requirements for these loading conditions.

The one exception is that where snow load is anticipated, interface friction should be assessed. In the absence of either back-calculated or field measurements, the interface friction angle can be estimated for the observed slope irregularity and surface roughness by using the guidelines below.

- i. *Rough*: The slope surface is very irregular and undulating and/or has many prominent protrusions on the surface (Figure 7-4). For such cases, the interface friction angle is assumed to be above 60°.

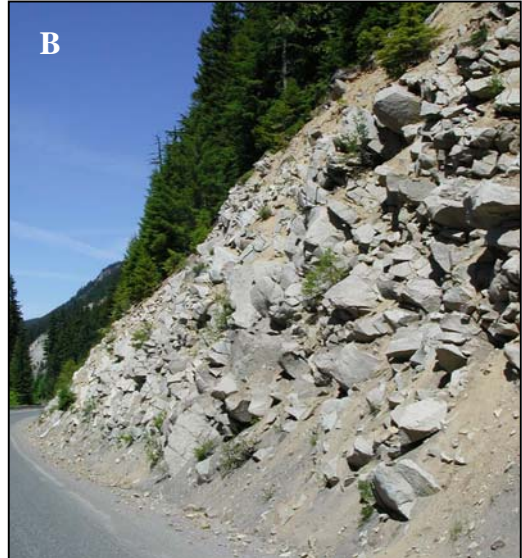


**Figure 7-4. Rough slopes exhibit a high degree of surface roughness with planar, uniform profiles.**

- ii. *Undulating*: The slope is undulating, and the surface contains some minor protrusions (Figure 7-5). The interface friction angle is assumed to be between  $36^{\circ}$ - $59^{\circ}$ .

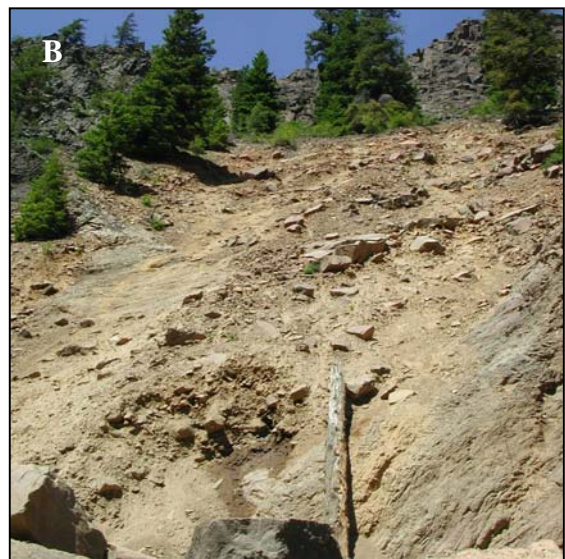


**Figure 7-5. Undulating slopes exhibit profiles with (A) somewhat uniform particle distribution with limited overall roughness, and (B) numerous localized protrusions.**

- iii. *Planar*: The slope is planar, and the surface is relatively smooth and has few small undulations (Figure 7-6). The interface friction angle is assumed to be between 25°-35°.

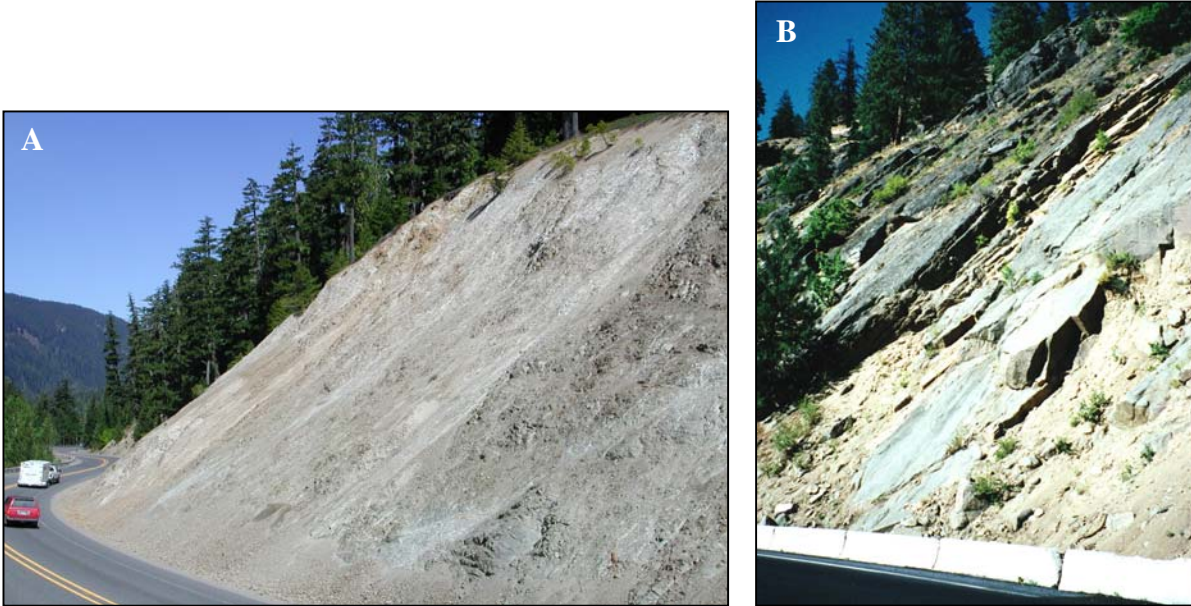


**Figure 7-6. These planar slopes exhibit little surface roughness or slope irregularity. In the case of (A), the slope profile is controlled by the very highly fractured condition of the rockmass. The slope profile in (B) is the result of a highly persistent set of discontinuities that dips coincident with the slope.**

#### **7.1.4 Debris Loads**

Debris loading is a common source of both local and global system failures. As discussed previously, wire mesh/cable net systems begin to yield with debris accumulations as low as 5 to 10 cubic yards (meters). Therefore, it is critical that an assessment be made of the expected type, size, volume, and frequency of slope instabilities. This assessment should be coupled with an evaluation of how and where debris might accumulate once the mesh has been installed. Common accumulation locations include slope convexities and salients, along the base of the mesh, and above any restraints/anchors along the perimeter or interior field of the mesh. One often

unanticipated restraint is snow and debris covering the base of the mesh that either accumulates as snow slides off the mesh or from snow plowing. It is important to note that debris simply caught beneath the mesh that is otherwise stable may impart little load on the system. Where the mesh impedes movement of unstable debris, significant load can be transferred to the system.

### **7.1.5 Impact Loads**

Rockfall impacts apply transient, short-term loads on the system. The actual load imparted is a function of the mass and velocity of the block and the manner in and orientation at which the block impacts the system. On near-vertical slopes where the mesh is sub-parallel to the slope and in limited contact, the rockfall trajectory is generally also sub-parallel to the slope. Unless the falling rock snags the mesh or deflects horizontally upon striking some asperity, there is little opportunity to transfer a large portion of the kinetic energy to the system. On moderately steep slopes, the velocities of rolling/bouncing blocks are significantly reduced by the greater mesh contact. Thus, kinetic energy should be (significantly) less for a rolling/bouncing rock beneath the mesh than what would be expected on an undraped slope.

Significant impact loads can be imparted to the system when blocks impact sub-normal to the mesh. Such is the case where systems are suspended across chutes or raised on posts to contain rockfall that originates upslope of the installation. Increasingly in recent years, systems have been installed for these applications. Another common configuration exposed to sub-normal impact loading occurs on slopes with abrupt convexities, such as a moderately steep slope in surficial deposits overlying a near vertical cutslope in rock (Figure 7-2B), midslope benches, and transitions between

excavated lifts. Rockfall initiating near the top of the installation impacts the mesh just above the slope inflection; this is a frequent location of puncture failures.

The kinetic energy of scenario rockfalls can be estimated by using widely available rockfall modeling software, such as the public domain Colorado Rockfall Simulation Program (Jones et al., 2000). What remains poorly understood, however, is how kinetic energy is transferred as a load to the system. Regrettably, this research was unable to fully quantify the mechanism of impact load transfer to the system through full-scale testing. As a result, only limited design guidance is provided to account for impact loads, the basis of which is summarized in section 5.4 of this report. This includes mesh systems that are raised above ground level and subjected to sub-perpendicular impacts. For double-twisted hexagonal wire mesh, impacts near the top of the installation should not exceed 4 ft-tons (10 kJ), and impacts should not exceed 11 ft-tons (30 kJ) within 25 feet (7 m) of the mesh perimeter. For 5/16-inch wire rope, 8-inch square grid cable nets, the very limited available data suggest that an upper bound of puncture resistance for a restrained panel would be in the range of 20 to 25 ft-tons (54 to 68 kJ). Guidance for the puncture resistance of a 5/16-inch wire rope, 12-inch square grid panel, which was the basis for the testing and analysis performed in this report, is not presently available.

#### **7.1.6 Snow Loads**

For installations in regions that develop winter snowpack, the respective loads potentially transferred to the system must be evaluated. However, only slopes that accumulate snow need to be considered; this would only include slopes of moderate inclination, that is less than 55° to 60°. Slopes flatter than 30° to 35° generally do not produce rockfall. A minimum threshold of 1-foot (300 mm) depth is specified in the

design flow chart (Figure 7-1) for design consideration. The design methodology presented later in this chapter is only intended to consider the static load of the snowpack on the installation. If the slopes above the installation are prone to unstable snowpack and these outside forces could be transferred to the installation, the site is probably not suitable for a draped mesh system.

Both climatological and anecdotal data sources should be consulted in determining a design snowpack. In the western U.S., the Western Regional Climate Center collects climatological data from a large number of sites and maintains a database of historical observations that includes temperature, precipitation, snowfall, and snow depth. Data can be accessed at its website (<http://www.wrcc.dri.edu/summary/>). The database does not include data on snow density or moisture, so direct measurement or estimation must be made to determine snow load. The U.S. Department of Agriculture Natural Resource Conservation Service collects snow data (SNOTEL) that include daily historical records of snow water equivalent, which can be used directly to estimate snow load. SNOTEL data can be accessed via the USDA website (<http://www.wcc.nrcs.usda.gov/snotel/>). In addition, anecdotal data sources, such as area maintenance personnel, often provide valuable site-specific information. This might include localized weather and/or slope conditions that influence snow depth and density, and the retention (stability) of snow on and above the planned installation.

When the site suitability for anticipated snow loads is evaluated, caution is warranted on

- all smooth planar slopes (low interface friction)
- slopes oriented between 45° and 60°

- concave slopes where ground contact would be limited.

## **7.2 DESIGN METHODOLOGY**

Once the site has been determined to be suitable for a wire mesh/cable net system, the recommended design process is to first select the appropriate fabric and then determine the needed anchor capacity and spacing for design load conditions.

### **7.2.1 Fabric Selection**

Selection of the appropriate fabric should be primarily based on the expected block/event size that the system will retain. Other fabric properties besides strength, such as puncture resistance and flexibility/rigidity, may also be relevant, depending on site conditions. The guidelines for fabric selection are based mostly on observed performance and are augmented with limited strength testing of relatively small-sized samples. The scale-dependence of the test data must be emphasized when overall system performance is considered. While fabric strength is important for static loading, flexibility, especially within the entire system, is an attribute that has been well demonstrated to be necessary for sustaining dynamic loads.

Fabric types currently available in North America for rockfall protection systems include chain link (diagonal) wire mesh, double-twisted hexagonal wire mesh, high tensile steel wire mesh (TECCO<sup>®</sup>), cable nets, ring nets, and a hybrid fabric that combines both wire mesh and cable nets.. For each of these fabrics, variations are available in wire/cable size and grid/opening size; square and diagonal weaves are also available for the cable net fabric. In North America, current performance experience is with three basic fabrics: chain link (diagonal) mesh, double-twisted hexagonal mesh, and

cable nets. Within the last decade, hexagonal mesh has replaced chain link mesh in current practice among DOTs. This change has been implemented because of its greater strength, better performance after the fabric has been damaged, and comparable unit cost (Agostini et al., 1988). The hexagonal mesh most typically used is an 8x10 type mesh with either 0.12-inch- (3-mm) diameter galvanized wire or 0.11-inch (2.7-mm) pvc-coated wire. Presumably, the best performance should be realized with the galvanized hexagonal wire mesh because of the slightly larger wire diameter, although no documented field performance has been acquired to verify this assumption. Cable nets are typically specified to use 5/16-inch (8-mm) wire rope and a square weave with 6-, 8-, or 12-inch (150-, 200-, or 300-mm) opening size. As shown by fabric testing, a diagonal weave has superior strength to a square weave. The performance of a 6-inch (150-mm) grid should be superior to that of larger grid openings; however, no documented field performance has been acquired to verify this assumption. Unless otherwise stated, a 12-inch (300-mm) square grid with a 5/16-inch (8-mm) wire rope was used in preparing these guidelines.

On the basis of the limited fabric testing performed for this study, high tensile steel wire mesh (TECCO<sup>®</sup>) has a strength comparable to that of cable nets. A fundamental difference between the fabrics, however, is the weight; TECCO<sup>®</sup>'s weight is about half that of a 12-inch (300-mm) grid cable net and very near that of hexagonal wire mesh. Because of the recent introduction of this fabric in North America, performance experience is limited.

In summary, two primary fabric types have been used in North America for roughly the last decade: hexagonal wire mesh and cable nets. The current North

American practice for their use is presented in Table 7-1. It should be emphasized that, at the present time, there is no widely accepted test method for evaluating cable net, ring net, or hybrid fabrics and, hence, no quantifiable means for comparing fabrics from different manufacturers.

**Table 7-1. Recommended fabric usage as a function of block size.**

Fabric	Block Size
double-twisted hexagonal mesh	≤ 2 ft (0.6 m)
cable net	≤ 4 – 5 ft (1.2 – 1.5 m)

The intended application of wire mesh/cable net systems is to retain rockfall that would involve a single block up to several blocks. That said, both fabrics have repeatedly withstood localized slope failures with volumes of 5 to 10 cubic yards (meters) with minimal damage, if individual block sizes have not exceeded the respective size limit for each fabric. Typically, fabric damage increases with decreasing slope angle, since debris is more likely to accumulate on slopes of flatter orientation. Thus, a designer might consider using hexagonal mesh for a near vertical slope where block sizes approached 3 ft (0.9 m) and rockfall frequency was low. Conversely, localized damage to hexagonal mesh has been observed on moderately inclined slopes (~ 40° to 50°) that actively produce 2-foot (0.6-m) boulders; cable net fabric might be better suited for such conditions.

Fabric flexibility and optimal slope contact may also be important factors for certain sites. These may be important if snow loads or aesthetics are a concern. On near vertical slopes, however, it is more difficult, and perhaps less important from a structural perspective, to achieve a high degree of slope contact. Of the fabrics in current use,

double-twisted hexagonal wire mesh is the most inflexible. Comparatively, chain link and cable nets are more flexible. TECCO<sup>®</sup> mesh is flexible in the longitudinal direction but quite stiff in the transverse direction. To maximize flexibility of cable nets, chain link fabric is recommended over hexagonal wire mesh for backing. Hexagonal mesh, however, has greater strength than chain link, and thus probably provides somewhat better puncture resistance for small-sized rocks.

### **7.2.2 Anchor Capacity and Spacing**

While interface friction alone can provide, in some cases, sufficient resistance to hold a mesh system on a moderately inclined slope, anchors should provide the primary support for mesh systems. Unlike interface friction, the resistance contribution from anchors is easily quantifiable and unchanging over the life of the system. For these reasons, it is recommended that the design of system support for debris and impact loads relies solely on the anchors. Snow loads, however, require the consideration of interface friction to develop a cost-effective anchor design. These two approaches to anchor design are treated separately in the sections that follow.

Current practice in North America generally utilizes anchor elements that exceed a 20,000-lbf (90-kN) minimum yield strength in both tension and shear. Common tendons include a 1-inch (25-mm), continuously threaded deformed steel bar and ¾-inch (19-mm) wire rope. Consequently, a minimum capacity of 20,000 lbf (90 kN) has been assumed in the design charts presented below. The charts presented in figures 6-18, 6-19, and 6-20 can be used for anchors of different capacity for common fabric types with an appropriate safety factor. Additional charts for common fabric types (provided in Appendix D, figures D-1 through D-18) account for interface friction for slopes oriented

at 45° and 60° with planar, undulating, and rough slope surfaces. An appropriate factor of safety should also be applied to these anchor loads and spacings.

### 7.2.2.1 Debris and Impact Loads

The recommended design methodology attempts to account for potential variability in debris and impact loads for a given site, as well as the current lack of understanding of how impact loads are transferred to the system. This is done by applying a large factor of safety (5 to 10) to the anchor requirements for the system weight alone, with no resistance contribution from interface friction (figures 6-18, 6-19 and 6-20). The maximum recommended anchor spacings presented in Table 7-2 also coincide with repeated successful application of the wider range of anchor spacings discussed in section 2.7.1. For simplification, the recommended maximum spacings are suitable for hexagonal mesh, TECCO® G65 mesh, and 12-inch (300-mm) square grid cable nets backed with either hexagonal or chain link mesh. Narrower spacings should be considered if different fabrics are used that are significantly heavier than the specified cable net. Other factors, such as topography, may also warrant closer spacings.

**Table 7-2. Recommended maximum anchor spacing as a function of slope height**

Slope Height <i>ft (m)</i>	Anchor Spacing <sup>1,2</sup> <i>ft (m)</i>
≤ 100 ft (30 m)	50 ft (15 m)
100 – 200 ft (30 – 60 m)	35 ft (10 m)
200 – 300 ft (60 – 90 m)	20 ft (5 m)

<sup>1</sup>Maximum spacings suitable for hexagonal mesh, TECCO® G65 mesh, and 12-inch (300-mm) square grid cable nets backed with either hexagonal or chain link mesh.

<sup>2</sup>Anchor spacing is based on a minimum anchor capacity of 20,000 lbf (90kN).

Anchor load charts for 45° and 60° slopes with planar, undulating, and rough configurations are included in Appendix D. As an alternative to the use of Table 7-2,

these charts can be used to determine the anchor loads from mesh weight alone for these flatter slope orientations. A similar factor of safety should then be applied to determine anchor capacity and spacing.

#### 7.2.2.2 Snow Loads

As documented in Chapter 4, snow loads have been responsible for numerous system failures. All known system failures have occurred as a result of anchor yielding, caused by either the strength or passive resistance of the ground being exceeded or the yield strength of the tendon being surpassed. No ancillary damage to the mesh, support ropes, or connections has been observed at any of these snow-related failures. The anchor capacities and spacings used at these sites were in general accordance with those presented in Table 7-2, supporting the conclusion that these spacings may be too wide for systems exposed to snow loads. However, if the anchors were assumed to carry the entire snowpack weight and interface friction was neglected, unrealistically large anchor loads would be calculated. The instrumented Tumwater Canyon and the U.S. 20 Rainy Pass sites summarized in Chapter 4 clearly demonstrate the important resistance contribution provided by interface friction. The anchor force due to snowpack per unit width of mesh,  $F_a$ , can be calculated with Equation 4-9:

$$F_a = \rho g H L \sin \theta - \rho g H L \cos \theta \tan \phi$$

where  $\rho$  is the overall density of the snowpack,  $g$  is the gravity constant (for metric units),  $H$  is the thickness of the snowpack oriented normally to the slope,  $L$  is the slope length of the installation,  $\theta$  is the slope angle, and  $\phi$  is the interface friction angle. The design challenge lies in characterizing the interface friction of the entire installation. The case histories presented in section 4.3 and the photos in section 7.1.3 can aid in this

characterization. A safety factor of 2 to 3 should be applied to account for larger than anticipated snowpack and overestimation of interface friction.

It is evident from the equation that for slopes that have an interface friction equal to or greater than the slope angle, a snowpack should cause no load increase on the anchors. Conversely, when interface friction is less than the slope angle, a portion of the snow load is transferred to the anchors, and load increases rapidly as the angles diverge. Two examples are provided to illustrate the effect of interface friction ( $\rho = 25 \text{ lbf/ft}^3$ ;  $H = 2 \text{ ft}$ ;  $L = 150 \text{ ft}$ ;  $\theta = 45^\circ$ ;  $\phi = 30^\circ, 40^\circ$ ) for an assumed anchor capacity of 20,000 lbf (90kN):

$F_{a30^\circ} = 2240 \text{ lbf/ft}$ ; a FS=2 results in a roughly 5 ft anchor spacing

$F_{a40^\circ} = 850 \text{ lbf/ft}$ ; a FS=2 results in a roughly 12 ft anchor spacing

### **7.3 DESIGN DETAILS AND SPECIFICATIONS**

The research results are compiled into specific design details in the following section and in a set of generic plan sheets included in Appendix E. The designer is referred to this chapter for specific detailing and dimensioning.

#### **7.3.1 Slope Coverage**

The area of coverage is determined from geologic/geotechnical assessment of the potential source areas of rockfall. The necessity of extending the mesh beyond the current slope brow should be considered and defined in the final design. A distance of 10 to 15 ft (3 to 4 m) beyond a potential source area is often considered a minimum. Additional upslope extent may be warranted if the crest of the slope is actively eroding, like the slope in Figure 7-3, to ensure slope coverage for the life of the system.

Generally, the bottom of the mesh should extend to within 3 to 5 ft (1 to 1.5 m) of the base of the slope. If it is located much higher, the catchment area becomes more critical in retaining debris that passes the mesh system. If the base of the slope serves as an area for snow storage, then consideration should be given to raising the bottom of the mesh to reduce the potential of accumulating debris during winter months excessively loading the system. If little catchment area is available, it may be advisable to lower the mesh to near the ditch line; however, these installations will require more frequent inspection and maintenance if debris accumulates and loads the system.

The coverage area is well depicted on photographs of the slope area taken in elevation view (Figure 7-7). Slope lengths at station intervals can be included to facilitate the estimation of material quantities. Salients and reentrants increase surface area. Quantity estimates should be increased if the slope is not uniform; a range of 10% to 15% is common. A more accurate method is to determine quantities by surveying the slope.

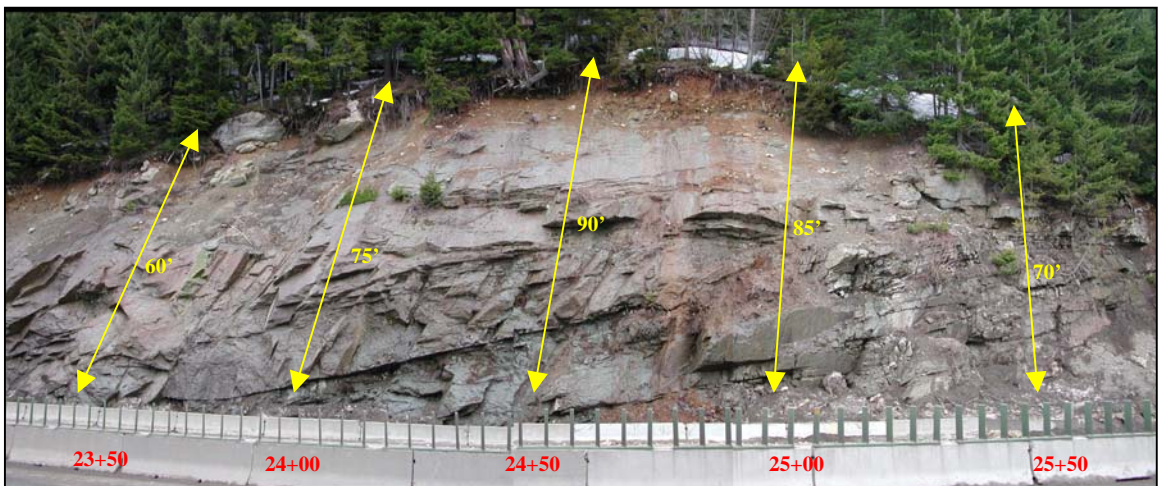


**Figure 7-7. Coverage area depicted by stationing and slope length.**

### **7.3.2 Anchors**

Anchors can be located either along or upslope of the top horizontal cable. Often there are benefits to allowing latitude in siting anchors, such as ease of installation or avoiding obstructions. Siting anchors upslope of the top horizontal cable optimizes anchoring opportunities and often results in a superior anchor. Siting the anchors upslope also reduces the risk of the anchors being undermined by ongoing erosion. On the downside, there is additional cost for the wire rope and connectors required to link the anchors and top the horizontal support rope.

Unlike most ground anchors, anchors for mesh systems are generally loaded perpendicular to the anchor. This is noteworthy for two reasons. First, rigid tendons, such as deformed steel bars that might be used to anchor in rock, are loaded more in shear than in tension. It is well known that the strength of steel in shear is about 75 percent of the ultimate tensile strength. In recent years, current practice has moved more toward the use of wire rope for anchor tendons for both soil and rock conditions. Because of its flexibility, wire rope accommodates load in tension by bending toward the direction of loading, thus optimizing the strength of the tendon. The second reason that the direction of loading is important involves the mobilization of passive resistance of the ground. Anchors oriented normally to the ground surface optimize passive resistance. Passive resistance, and thus capacity, is reduced when anchors are oriented toward vertical. While passive resistance is not a concern when anchors are set in rock, it can be a significant concern for systems anchored in soil that are exposed to severe loading conditions.

The anchor testing performed as part of this research (see section 3.4 and Appendix C) resulted in some valuable observations about the capacity and performance

testing of anchors founded in soil. All but one of the anchors loaded vertically held 20,000 lbf (90 kN) and did so within 1 inch (25 mm) of displacement. Continued loading resulted in visible ground deformation over a diameter of at least the length of the anchor. Anchors loaded horizontally typically required 6 to 10 inches (150 to 250 mm) of displacement to mobilize a similar load, and they were able to sustain increasing load with displacement often well beyond 20,000 lbf (90kN). These results have significant bearing on the field verification of anchors. For nearly every installation, a minimum number of every anchor type should be tested. Depending on the criticality of the installation, 25 percent is a recommended minimum. If possible, the verification testing should be oriented in the direction of actual loading (sub-horizontal). This can be accomplished by extending a cable from the anchor to the base of the slope and tensioning the cable in the manner shown in Figure 7-8. If vertical load testing is performed, it is important that the load frame be sufficiently wide to not influence stresses within the soil.

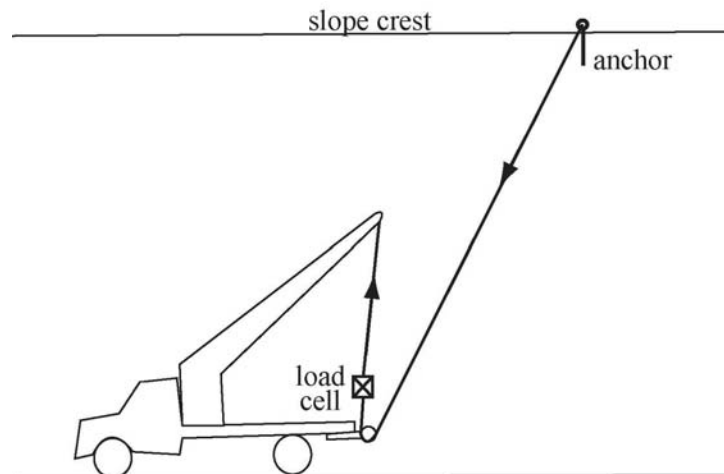


**Figure 7-8. Testing setup of anchors in a sub-horizontal direction.**

### **7.3.3 Support Ropes**

The finite element modeling proved useful in refining the design of support for mesh systems. The modeling confirmed observations that horizontal and vertical support ropes below the top horizontal support cable provide effectively no structural function. In addition, interior horizontal support ropes located between the mesh and the slope have repeatedly been the cause of debris accumulation leading to local and global system failures. Therefore, interior support ropes (both vertical and horizontal) are unnecessary and should be avoided. A possible exception would be the use of a horizontal rope along the bottom of the mesh to facilitate cleanout behind the mesh. If a bottom rope is included, it should be placed on the outside of the mesh and either it should be fastened to the mesh with lacing wire or the mesh should be folded outwardly over the cable and fastened with high tensile steel rings.

Another refinement of current practice addresses the maximum uninterrupted length of the top horizontal support. For the purposes of analysis and design uniformity, cable diameters of ½ inch (13 mm) and ¾ inch (19 mm) with breaking strengths of around 25,000 lbf (110 kN) and 50,000 lbf (220 kN), respectively, have been considered for top horizontal support ropes. Based on a factor of safety of approximately 2 for the top horizontal support rope, the recommended maximum lengths for double-twisted hexagonal and TECCO<sup>®</sup> G65 mesh are provided in Table 7-3A and for cable nets backed with hexagonal mesh in Table 7-3B.

**Table 7-3A. Recommended maximum length for top horizontal support rope v. slope height for double-twisted hexagonal and TECCO® mesh.**

<b>Slope Height <i>ft (m)</i></b>	<b>Max. length for ½” (13 mm) cable fabric weight only <i>ft (m)</i></b>	<b>Max. length for ¾” (19 mm) cable fabric weight only <i>ft (m)</i></b>
50 ft (15 m)	230 ft (70m)	400 ft (120 m)
100 ft (30 m)	120 ft (35 m)	200 ft (60 m)
200 ft (60 m)	60 ft (18 m)	100 ft (30 m)
300 ft (90 m)	40 ft (12 m)	75 ft (22 m)

**Table 7-3B. Recommended maximum length for top horizontal support rope v. slope height for cable net backed with double-twisted hexagonal mesh.**

<b>Slope Height <i>ft (m)</i></b>	<b>Max. length for ½” (13 mm) cable fabric weight only <i>ft (m)</i></b>	<b>Max. length for ¾” (19 mm) cable fabric weight only <i>ft (m)</i></b>
50 ft (15 m)	80 ft (25m)	150 ft (45 m)
100 ft (30 m)	40 ft (12 m)	75 ft (22 m)
200 ft (60 m)	20 ft (5 m)	40 ft (12 m)
300 ft (90 m)	15 ft (4 m)	25 ft (7 m)

These tables may be conservative for flatter slopes because they do not account for the resistive contribution of interface friction. Conversely, the maximum length of the top horizontal support rope should be reduced if extreme sustained loads (i.e., snow) are anticipated. As an example of an extreme loading condition, the instrumented Tumwater Canyon cable net installation employs two anchors spaced at about 20 ft (6 m) and breaks the horizontal support rope at each anchor group.

The use of thimbles and wire rope clips should follow the manufacturer’s recommendations for size, number, spacing and torque. Steel rings that join sections of the top horizontal rope should also be sized to have an ultimate breaking load that is

compatible with the ultimate yield strength of the wire rope. Note that the ultimate load for weldless steel rings is substantially higher than the published minimum working load. As an example, a 7/8-inch x 4-inch-diameter, galvanized, weldless steel ring with a minimum working load of 10,000 lbf would be suitable for use with a 3/4-inch-diameter, 6x19 IWRC wire rope with a minimum breaking strength of 45,000 lbf.

#### **7.3.4 Fabric Seaming and Fastening**

The fabric must be both fastened to the support ropes and seamed together. For hexagonal mesh, tests of different seaming configurations with high tensile steel fasteners (i.e., King Hughes, Spenax) revealed that all the seams were all about half as strong as the mesh. Lacing wire would be needed to achieve a seam that would approach the strength of the hexagonal mesh. A supporting argument could be made for incorporating weaker elements in a system so that when an unanticipated yielding condition occurs, only a portion of the system fails rather than the entire system. In other words, repairing a ruptured seam is considerably cheaper than reinstalling an entire system. If a “weak link” is desired, then vertical seams of hexagonal mesh should be fabricated with either a butted seam or a one-cell overlap of approximately 3 inches (8 cm) and fastened with a high tensile steel fastener at every cell, resulting in a 4-inch (10-cm) fastener spacing. There appears to be no benefit to using the often-specified overlap of 8 to 12 inches (200 to 300 mm). If used, lacing wire should be of similar gauge as the mesh or larger and should pass through each cell. Moderate tensile strength fasteners (i.e., standard hog rings) should not be used for seaming hexagonal mesh in draped rockfall protection systems. Horizontal seams should be discouraged; if needed, they should be closed with lacing wire, with the lower panel placed on the outside to prevent debris accumulation.

Current practice for attaching hexagonal mesh to the top horizontal rope typically utilizes a 12-inch (300-mm) fold over the rope and fastening the overlap with either lacing wire or high tensile steel rings at a spacing of 6 to 12 inches (150 to 300 mm). Although no failures attributed to steel ring fasteners were reported, lacing wire instead of rings is recommended for this application in conjunction with the fold.

The manufacturer, Geobrugg, provides recommendations for both the seaming and hanging of TECCO<sup>®</sup> mesh.

Cable nets should be similarly seamed and hung with lacing cable of similar gauge or larger, ensuring that the cable passes through each cell of the interior weave of the net panel. The cable nets backing can be of either chain link or hexagonal mesh. Chain link mesh is recommended if flexibility and conformance to the slope is of primary importance. Hexagonal mesh should be used if puncture resistance is of greater importance. The fabric should be fastened with high tensile steel rings to each side of the wire rope grid to inhibit differential movement of the fabrics. The backing mesh should be fastened to the nets on the ground; it is nearly impossible, as well as highly inefficient, to do it separately on the slope. The backing fabric should be placed on the inside of the cable net against the slope.

#### **7.4 AESTHETIC CONCERNS AND MITIGATION**

Increasingly, the selection of the preferred mitigation for rockfall is judged not only on the method's engineering and economic merits but on aesthetic concerns as well. This is particularly the case in areas of considerable scenic or recreational value, where a design objective to visually subordinate engineered facilities may be required or legislated. In some cases, managers and design professionals responsible for aesthetic

stewardship have found the use of wire mesh/cable nets objectionable. The principal concerns have stemmed from the typically large coverage area, the visual contrast between the wire mesh and the slope, and the potential for poor mesh contact with the slope. Design efforts to mitigate these aesthetic concerns may focus on

- reducing/limiting the coverage area
- achieving greater mesh contact with the slope
- colorizing system components or promoting vegetation to visually merge the system with the slope
- considering other slope stabilization alternatives.

#### **7.4.1 Limiting Coverage Area**

For some slopes, it may be possible to reduce or limit the coverage area of a mesh system and still provide adequate rockfall containment. Rather than draping the entire rockfall source area on a slope, the top of an installation can be lifted off the ground to effectively contain rockfall originating upslope. Such an approach is commonly used for chutes/swales and along abrupt convexities. If such a design approach is pursued, the prospective impact energy on the raised portion of the system must be considered. Conversely, opportunities may exist to limit the bottom elevation of the system to keep it above the immediate view of passing motorists. However, when the bottom of the mesh is raised more than a few feet above the ditch line, debris passing from beneath the mesh may not be contained in the available catchment area. In these cases, catchment should be evaluated. Provisions to increase or improve the catchment area may be required.

### **7.4.2 Increasing Mesh Contact**

For many moderately inclined slopes (40° to 60°) and some steeply inclined slopes (>60°), efforts to maximize mesh contact with the slope yield both functional and aesthetic benefit (Figure 7-9A). Functional benefits can include greater interface friction and overall system capacity, as well as decreased slope erosion and rockfall. A reduction of slope erosion commonly promotes re-vegetation of the underlying slope. Mesh contact also reduces/eliminates the gap between the mesh and the slope, which is often quite discernable when the installation is viewed from the side, as by a passing motorist (Figure 7-9B). On steep slopes, it is often more difficult to achieve mesh contact, and because of the reduced component of normal force, it is difficult to maintain contact as the system is loaded.

Mesh contact, particularly on moderately inclined slopes, commonly reduces slope erosion, which in turn can promote reestablishment of vegetation. Growth of vegetation into the mesh can significantly reduce visual contrast and aid in the visual blending of the mesh with the slope, as well as increase the stability of the surface materials. More proactive re-vegetation efforts have been undertaken, such as placing erosion-control fabrics beneath the wire mesh, hydro-seeding, and installing plantings. Although installing mesh around existing vegetation can increase installation costs, in some cases protecting existing vegetation may be either beneficial or even required.



**Figure 7-9. (A) The mesh was carefully installed to closely conform to this moderately inclined slope. (B) On a steep to overhanging slope where mesh conformance is generally more difficult to achieve, the mesh can become more visually apparent.**

While vegetation most often provides benefit, installation damage/failures have occurred because of trees growing through the mesh. The damage has occurred when trees have subsequently fallen (a common occurrence on steep slopes) or when the substrate in which they have grown has crept or experienced other shallow instability. If the slope is prone to such shallow instability, the growth of larger woody vegetation through the mesh should be discouraged, or another mitigation measure besides wire mesh/cable nets should be considered.

### **7.4.3 Colorizing System Components**

Wire mesh and cable net fabrics are generally supplied with a galvanized or other corrosion-protection coating. When installed, these coatings and some cross-clips of cable net fabrics have a metallic, often shiny or light colored appearance that may strongly contrast with the slope. Over time, the shininess of galvanizing typically fades to a dull gray color. Coloring of fabrics has become more common in recent years to reduce the visual contrast between the mesh and the slope.

Three methods of coloring are currently used: painting, polyvinylchloride (pvc) coating, and powder coating. While painting may be preferred for system components, painting a large area of fabric is typically not practical because of environmental and logistical constraints, as well as the laboriousness of the task. Coating the wire or cable with colored pvc has been used extensively for double-twisted hexagonal mesh, chainlink, and, more recently, cable net fabric. The coating is applied before the fabric is woven, which results in a very cost-effective colorizing method. Extreme exposure of pvc to ultraviolet radiation has been known to cause considerable lightening of the coating. Powder coating is a fused colorized coating that provides a durable coloring alternative to painting and pvc coating. Powder coating is typically applied after fabrication and is used predominantly for cable net fabric. Note that this treatment can be two to three times as expensive as standard galvanizing.

## **7.5 CONSTRUCTION CONSIDERATIONS**

Consideration for how a system will be installed and inspection of its construction best ensure that the design objectives of function, aesthetics, and cost effectiveness are met. Generally, other specified stabilization work (e.g., scaling and installing rock

anchors) should be performed before placement of a mesh installation; however, in some cases it may be safer to install rock anchors after mesh placement. Also note that slope scaling before mesh installation often provides only limited long-term benefit. Furthermore, slopes best suited for mesh/cable nets are often more hazardous to scalers than slopes that require other stabilization measures (e.g., rock anchors). Scaling before the mesh installation should focus on the slope preparation necessary for mesh installation and the removal of occasional, potentially damaging oversized blocks or other discrete zones.

Prior to construction, the contractor, construction inspector, and designer should field verify and measure the coverage area. The actual locations of the top, bottom, and lateral extent of the installation should be determined at this time, as well as the optimal location of each anchor. Depending on the criticality of the installation, a minimum number of anchor tests should be specified and successfully completed. Wire rope clips should be carefully inspected for proper clamping orientation, spacing, and torque. In some cases, wire rope clips have loosened over time. Re-tightening them several days or more after the initial installation may be necessary.

Unless individual panels will be rolled out from the top of the slope, a staging area near the base of the slope will be required for layout and seaming. For cable nets with a wire mesh backing, a staging area is essential to properly prepare the panels. The contract should require that the backing fabric be fastened to the net panels on the ground. The selection of the staging area will be influenced by the method of placement (boom truck, crane, or helicopter) and the size of the installation. For large installations, helicopter placement is usually the fastest and most cost-effective method. However,

helicopter work requires an emergency landing area as part of the staging operations; traffic control and proximity to aerial utilities also need to be considered.

Load is often concentrated on the anchors and the top support rope during the hanging of the mesh/net panels. In one known instance, this concentration led to anchor failures. Design guidelines provided for the maximum length of the top horizontal rope should be adhered to, and care should be exercised during hanging to minimize load concentrations on the anchors. If mesh conformance/contact with the slope is a design objective, the maximum width of fabric placement in any crane/helicopter pick should be limited to one panel width. After the top of the panel has been secured to the top support rope, workers should walk down each panel, pushing the fabric into slope irregularities. The next panel can then be placed and secured to the top support rope, seamed longitudinally to the adjacent panel, and then similarly walked-down.

## **7.6 MAINTENANCE**

For most slope conditions, the recommended design methodology presented above should result in an installation requiring minimal maintenance over the design life of the system. The dominant maintenance concern is averting damaging debris loads. Some debris accumulation should be expected. Often, this debris does not directly load the system. Deformation or bulging of the fabric is an indication that the system is being loaded, and maintenance to remove or pass the debris should be initiated. A horizontal bottom cable or cable at other constriction points laced to the outside of the mesh can be used to lift the mesh.

While the growth of vegetation on an actively eroding soil slope is generally desirable to reduce erosion, the growth of shrubs and trees through the mesh can create

problems. Toppling of trees that have grown through the mesh has caused localized and global failures. Additionally, creeping of underlying slope materials (common in some surficial deposits) can induce unanticipated load on the anchors if excessive intertwining of shrubby vegetation with the mesh has occurred. In these cases, some management of vegetation growth through the mesh may be required to ensure long-term performance of the system.

Where snow load is anticipated, it is prudent to periodically inspect the anchor and support ropes, particularly after a heavy snow year.

## **7.7 FUTURE WORK**

The research identified several topics requiring further study or evaluation. Very little performance data are currently available where systems are exposed to sub-horizontal impacts. Information is needed not only on the puncture resistance of partially restrained mesh, but also on how the impact energy is transferred to the support system. These data are very much needed to support the design of suspended (modified) systems for containing rockfall produced upslope of the installation.

Currently, reliance and acceptance of fabrics are largely based on past performance. With the development and introduction of new fabrics, a means of predicting performance is needed. Test methods must also be developed to determine minimum standards of performance and to compare similar fabrics from different manufacturers.

The estimation of interface friction and its contribution to system resistance remains a task with inherent uncertainty. Additional guidance in determining appropriate interface friction is needed.

## ACKNOWLEDGMENTS

A number of individuals and organizations have contributed in many ways to the successful completion of this project. The research was sponsored by the Washington State Department of Transportation through a pooled-fund study with contributions from the Alaska Department of Transportation and Public Facilities, Arizona Department of Transportation, British Columbia Ministry of Transportation, California Department of Transportation, Pennsylvania Department of Transportation, Idaho Transportation Department, Nevada Department of Transportation, New Hampshire Department of Transportation, New York State Department of Transportation, North Carolina Department of Transportation, Oregon Department of Transportation, and the Wyoming Department of Transportation.

A Technical Advisory Committee (TAC) was formed and met several times and provided invaluable technical input during the course of the research project. The participants included:

- Bob Lewis and Dave Stanley, Alaska Dept. of Transportation & Public Facilities
- David Gerraghty and Mike Dowdle, British Columbia Ministry of Transportation
- John Duffy, California Dept. of Transportation
- Tri Buu, Idaho Transportation Department
- Parviz Noori, Nevada Dept. of Transportation
- Dick Lane, New Hampshire Dept. of Transportation
- Alex Yatsevich and Priscilla Duskin, New York State Dept. of Transportation
- Nilesh Surti, North Carolina Dept. of Transportation
- Don Turner, Oregon Dept. of Transportation
- Steve Lowell, Tom Badger, and Keith Anderson, Washington State Dept. of Transportation
- Jim Coffin, Wyoming Dept. of Transportation
- Erik Rorem, Geobruigg Cable Products
- Howard Ingram, HI-TECH Rockfall Construction
- Larry Pierson, Landslide Technology

Special thanks are given to Erik Rorem (Geobrugg Cable Products) and Ghislain Brunet (Maccaferri) for supplying the fabric for independent testing and for sharing proprietary test results. Dr. David Carradine and his team at the Wood Materials and Engineering Laboratory at Washington State University fabricated the test apparatus and performed the independent testing of the different fabrics. The authors are very appreciative for their valuable effort with the fabric testing program and subsequent data interpretation.

Thanks are also due to Howard Ingram and his staff (HI-TECH Rockfall Construction) for installation support with the instrumentation at the Tumwater Canyon site and the anchor load testing program. The authors also recognize the significant contributions of Robert Grandorff and Vaughn Jackman (WSDOT) for installing and monitoring instrumentation at Tumwater Canyon and for assisting with the anchor testing.

## REFERENCES

- Agostini R., P. Mazzalai, and A. Papetti, 1988, Hexagonal wire mesh for rock-fall and slope protection, *Officine Maccaferri S.p.a.*, Bologna, Italy, 111 p.
- Badger, T.C., 1998, Draped rockfall protection systems: a WSDOT perspective, *Association of Engineering Geologists Program with Abstracts*, pp. 76.
- Bergado, D.T., P. Voottipruex, A. Srikongsri, and C. Teerawattanasuk, 2001, Analytical model of interaction between hexagonal wire mesh and silty sand backfill, *Canadian Geotechnical Journal*, 38, pp.782-795.
- Brown, R. L., 1989, Perspective on mechanical properties of snow, in *Proceedings of the 1<sup>st</sup> International Conference on Snow Engineering*, Santa Barbara, California, USA Cold Regions Research and Engineering Laboratory, Special Report 89-6, pp. 502-503.
- Carradine, D.M., 2004, Tensile capacity testing of twisted wire mesh and cable net mesh for use as rock fall protection, *Wood Materials and Engineering Laboratory, Washington State University*, WMEL Report No. 03-043, 16 p.
- Duffy, J.D., 1992, Field tests for flexible rockfall barriers, *report for Brugg Cable Products, Inc.*, 90 p.
- Flum, D., 2002, Preliminary tests part I, 10<sup>th</sup>-20<sup>th</sup> April, 2002 carried out in the quarry 'Lochezen' above Walenstadt, *Ruegger Systems Report 40 304 – 03*, St. Gallen, Switzerland.
- Haefeli, R., 1948, Schnee, Lawinen, Firn und Gletscher. in *Ingenieur-Geologie*, ed. L. Bendel, Springer-Verlag, Wien, pp. 663-735.
- Hearn, G., and L.Akkaraju, 1995, Analysis of cable nets for boulder impacts, *American Society of Civil Engineering 10<sup>th</sup> EMD*, Boulder, Colorado, pp. 289-292.
- Hearn, G., R.K. Barrett, and H.H. Henson, 1995, Testing and modeling of two rockfall barriers. *Transportation Research Record 1504*, National Research Council, Washington, D.C., pp. 1-11.
- Jones, C.L., J.D. Higgins, and R.D. Andrew, 2000, Colorado Rockfall Simulation Program Version 4.0, *Colorado Department of Transportation*, 127 p.
- Kane, W.F., and J.D. Duffy, 1993, Brugg Low Energy Wire Rope Rockfall Net Filed Tests, Technical Research Report 93-01, *Department of Civil Engineering, University of the Pacific*, Stockton, California.

- Knight, C.E., 1997, The finite element method in mechanical design, PWS-KENT.
- LGA, 2003, Test Report BGT-0230101 System TECCO® G65 for Geobrugg Protection Systems, Nuremberg, Germany, 60 p.
- McClung , D. M., 1982, A one-dimensional analytical model for snow creep pressures on rigid structures, *Canadian Geotechnical Journal*, 19, pp. 401-412.
- Pfieffer, T.J., 1989, Rockfall hazard analysis using computer simulation of rockfalls, *Colorado School of Mines* unpublished M.S. thesis, 103 p.
- Ritchie, A.M., 1963, The evaluation of rock fall and its control, *Transportation Research Record 13*, National Research Council, Washington, D.C., pp. 13-28.
- Salm B., 1977, Snow forces, *Journal of Glaciology*, 19, pp. 67-100.
- Sandwell Incorporated, 1995, Structural evaluation of slope mesh system, prepared for British Columbia Ministry of Transportation, *Sandwell Report 113576*.
- Smith, D. D, and J.D. Duffy, 1990, Field tests and evaluation of rockfall restraining nets, *California Department of Transportation Report CA/TA-90/05*, 1385.

**APPENDIX A**

**SURVEY OF STATE-OF-PRACTICE FOR DOT'S**

## CONTENTS

Alaska Department of Transportation & Public Facilities .....	A-3
British Columbia Ministry of Transportation .....	A-5
California Department of Transportation.....	A-10
Idaho Transportation Department .....	A-13
Nevada Department of Transportation.....	A-14
New Hampshire Department of Transportation.....	A-15
North Carolina Department of Transportation.....	A-17
Oregon Department of Transportation.....	A-18
Washington State Department of Transportation .....	A-19
Wyoming Department of Transportation.....	A-21

## **ALASKA DEPARTMENT OF TRANSPORTATION & PUBLIC FACILITIES**

David Stanley, C.P.G.

### **Usage of both WM and CN for rockfall protection:**

AKDOT/PF has only a few cable net installations, all of which were installed within the last 4 years. There are two short sections in the Anchorage area each less than 50 feet long. Both are performing to expectations with no failures. There is one other installation planned in the Ketchikan area. In response to a Department-wide questionnaire, Maintenance identified just seven wire mesh installations. The Geology Section identified eight other installations. The oldest known wire mesh installation is 20 years old; most are less than 10 years old. Wire mesh is predominantly used to control the trajectory of falling rock, talus slides and stones weathering out of soil slopes. About half of these installations are chain link fabric and the remainder consists of double-twisted hexagonal wire mesh.

### **Typical WM and CM design components and significant design modifications:**

#### Cable Net

The cable net installations are all typical Geobrugg installations. The energy rating for these installations are not known. One installation is at the base of a 75'-100' high slope adjacent to a tunnel portal. Another is located about 75' up a 100' high slope and was installed on a bench to catch rounded boulders weathering out of a sandy cut slope.

#### Wire Mesh

Typical chain link or hexagonal wire mesh installations slope drape uses 3/4" to 1" soil or rock anchors to depths of less than 5'. The chain link panels are joined by lacing wire and/or hogrings. Typical installations have wire rope ranging from 3/4" to 3/8" diameter around the margins of the panels. About one third of the draped installations have the mesh pattern anchored to the slope on about 10' square spacing. The remaining draped installations have the panels only supported at the top of the panels.

### **Typical WM and CN applications:**

Slope heights and angles vary from ¼H:1V or vertical rock slopes over 100 ft in height to soil slopes as flat as 1H:1V and up to about 75 ft in height. Rockfall source areas range broadly from bouldery glacial or colluvial deposits to a great variety bedrock conditions. Bedrock types range from fresh meta-sedimentary rock that produces cobble-sized raveling rockfall, to granitic rocks producing meter-size and larger angular blocks, to deeply weathered schists that produce everything from silt to boulders. Rockfall events peak in frequency in the spring as our slopes thaw and release water and rock particles, and in the fall with the rainy season.

Maintenance forces have been using mesh for about 20 years, and our engineering design teams are now adding mesh as a part of rock slope design for long-term mitigation and for short-term mitigation during construction. We are looking forward to gaining more design guidance, so we can continue to integrate mesh into our slope design work. We have difficulties with users and agencies about aesthetics of mesh installations vs. safety.

**Design problems or failures of installations:**

Draped chain link mesh installations have generally been successful, but there have been some failures. The typical failure is caused by rockfall exceeding the capacity of the fabric and separating panels or pulling out anchors. At a 20-year-old installation, cubical granite blocks in meter-plus-sizes pull down a mesh panel or two every year. In another location, the chain link mesh was installed many years ago to control talus. The panels have been pulled loose from anchors by repeated impacts of rock falling from well above the mesh installation area.

The hexagonal wire mesh installations have performed well. One installation has been damaged with one end of the installation losing anchor support when a portion of the slope partially slumped into the ditch. An installation in the Aleutian Islands was installed on a rock cut slope with the top of the mesh well below the top of the soil overburden and below the top of the rock slope. This has resulted in several instances of debris overtopping the mesh and causing some damage to the mesh. The mesh continues to function, and Maintenance remains satisfied with its performance.

**Installations exposed to significant horizontal impact energy:**

**Applications exposed to snow or avalanche loads:**

All our mesh installations are subject to snow loading. In some cases, there is significant ice loading potential. However, most of our mesh is installed on slopes of 3/4:1 or steeper. I am not aware of any mesh installed at an active avalanche site.

**Other related information/experience:**

## BRITISH COLUMBIA MINISTRY OF TRANSPORTATION

David Gerraghty, BCMoT<sup>1</sup>

Over the years, four main types of wiremesh/cable net systems have been used to control rockfall from soil and rock slopes on highways maintained by the British Columbia Ministry of Transportation (BCMoT). The different types of systems can be grouped based on the type of mesh and, to a degree, on the structural components used:

- Group 1: Hexagonal gabion mesh with and without horizontal and vertical cable reinforcement
- Group 2: Hexagonal gabion mesh with diagonal cable reinforcement
- Group 3: Wire rope cable net with and without chain-link or gabion backing
- Group 4: Chain link mesh

All systems are essentially empirically based, but system designs have evolved over time based on experience, system performance, availability of new products, and limited engineering analysis. Hexagonal gabion mesh systems (Group 1) comprise the largest number of installations in the province. The remaining types of systems combine to form a much lower percent of the total installations. The last upgrade of the Group 1 system occurred in 1995, when for the first time, a limited finite element analysis of the structural system was performed (Sandwell<sup>2</sup>) to try and bring a degree of engineering design to an empirical system.

BCMoT gave Sandwell three key design objectives. First, the suspension cable had to be raised 3 ft above the ground surface, which requires anchors extending 3 ft from the ground surface. Second, the diameter and spacing of the anchors supporting the suspension cable had to be selected to withstand low energy impacts of 1.1-1.4 ft-tons (3-4kJ). Third, the mesh system would also have to withstand low energy impacts of 1.1-1.4 ft-tons (3-4 kJ).

Raising the suspension cable attempts to provide a limited degree of containment against a potential low energy rockfall originating upslope of the installation. This is a concern since natural slopes along BC highways are generally moderately steep continuing upslope to higher elevations. Suspension cables are not raised when mesh systems are installed across known snow avalanche paths. In most cases, the suspension cable is placed against the ground surface to avoid the high dynamic loading associated with avalanche activity. In these situations, avalanches tend to pass over the mesh without causing damaged.

---

<sup>1</sup> Summarized from “Report to Ministry of Transportation on Performance of WireMesh/Cable Net Systems”, Fieber Rock Engineering Services, D. Fieber, January 2003.

<sup>2</sup> “Structural Evaluation of Slope Mesh System”, Sandwell Engineering., R.T. Reynolds, A.G. Martin, K.S. Chang, G. Neumann, April 12, 1995.

Recommendations from the Sandwell analysis and revisions made by BCMoT are summarized below.

- Suspension Cable:* Increase diameter from  $\frac{3}{4}$  in (19mm) to  $\frac{7}{8}$  in (22mm). BCMoT elected to stay with the  $\frac{3}{4}$  in diameter cable for ease of installation and suitability in all but the worst situations.
- Auxiliary Cables:* Reduce diameter from  $\frac{3}{4}$  in (19mm) to  $\frac{5}{8}$  in (16mm). BCMoT made this change.
- Lacing Cable:* Not assessed as part of analysis. BCMoT elected to reduce the size from  $\frac{1}{2}$  in (13mm) to  $\frac{1}{4}$  in (6mm) to simplify installation.
- Diagonal Cables:* Benefit uncertain. BCMoT eliminated from design.
- Anchors:* Maintain existing anchor diameter of  $1\frac{3}{4}$  in (44 mm) and spacing of 12 ft (4 m). Auxiliary/tie-back anchors use two  $\frac{7}{8}$  in (22 mm) diameter anchors at ends of system and one  $\frac{7}{8}$  in (22 mm) anchor for intermediate locations. Anchors in rock set 6 ft (2 m) deep with minimum diameter 2.5 in (66 mm); anchors in soil set 5 ft (1.5 m) deep with a minimum diameter of 1-2 ft (0.3-0.6 m).
- Mesh Seam:* Improve strength seam. Through independent analysis, BCMoT increased strength by reducing fastener spacing from 12 in (300 mm) to 2 in (50 mm) and secured with either Spenax™ or Tiger-Tite™ fasteners.

#### **Description of Rockfall Conditions:**

The greatest rockfall problem along the BCMoT highway system occurs from steep cuts developed in complex assemblages of hard granite and metamorphic rocks and to a lesser degree from steep cuts developed in shale or other sedimentary rock types prone to weathering. Many steep cuts were constructed in the late 1950's to early 1960's. This is a time before the benefits of controlled blasting were known and before the importance of good ditch catchment was realized. These steep cuts are generally standing at about  $\frac{1}{4}H:1V$  ( $76^\circ$ ) and range from 30ft (10m) to 130ft (40m) high, but at select locations rockfall originates from the valley side slopes many hundreds of feet above the crest of the constructed highway cut. Rockfall from cuts in the sedimentary rocks or other poor quality rocks can be different in terms of magnitude and frequency than rockfall from cuts in hard good quality rock. The sedimentary rock cuts tend to produce small magnitude events but at a high frequency.

Rockfall from gullies incised into these cuts is also a problem. Gullies are usually bedrock controlled and extend a minimum distance upslope of double the cut height but typically are longer. Rockfall from gullies is unique in that the rockfall is usually confined to the gully channel and may attain considerable energy near highway level.

Another sporadic rockfall problem occurs within soil slopes containing cobbles and small boulders or talus slopes composed of smaller size material. Along province highways, these slopes typically stand at about  $1\frac{1}{4}H:1V$  ( $38^\circ$ - $40^\circ$ ) and generally range in height from 30ft (10m) to 250ft (75m). Soil slopes also have generated unique problems. Slopes experiencing high erosion rates may redistribute or concentrate the load on the mesh system eventually leading to mesh damage. Also, rockfall from talus slopes may

originate from a rock face above the talus leaving mesh systems on talus prone to impact damage.

### **Hexagonal Mesh Systems Installed on Rock Cuts**

For BCMoT projects, hexagonal mesh is the most common type of installation regardless of rock type and slope angle. On steep rock cuts this type of installation commonly referred to as a drape or curtain application is designed to control the path of falling rock directing it into catchment at the toe of the slope. On steep cuts this mesh is installed as the final mitigating technique after stabilizing blocks on the cut face larger than about 2ft in diameter. The mesh hangs freely from the rock face and no intermediate anchoring to the rock face is done.

A different anchoring method is used if a layer of soil greater than 2m thick exists above the crest of a rock cut. In these situations anchors are placed in 5ft deep hand dug holes a minimum of 1ft in diameter. Holes are backfilled with lightly reinforced concrete. The diameter of the hole was selected to resist lateral loading based of the results of a simple passive failure analysis.

The standard mesh system on these steep rock cuts has performed well without any structural component failures. The only damage has been the occasional mesh tear. Tears are patched with the same 11-gauge mesh.

### **Mesh Systems Installed on Soil Cuts**

BCMoT has also installed standard hexagonal wire mesh systems on flatter boulder soil/talus slopes standing at about 1¼H:1V (38°-40°). These systems are intended to add surface stability to eroding soil slopes containing cobbles and boulders. Even though these slope conditions exist throughout the province, the steep high rock cuts generally present a greater hazard and have been the focus of mitigation over recent years. Mesh systems on these flatter slopes account for a small percent of the total systems installed.

Future systems placed on soil slopes would likely be anchored using the 1ft-diameter holes currently used for anchoring systems in soil above rock cuts. Talus slopes receive separate consideration because often there is difficulty in finding suitable stable anchor point across the width of a slope. Sometimes this can be overcome by attaching cables at intermediate points along the length of the suspension cable and extending these cables well upslope to anchors founded in bedrock.

Most mesh systems on flatter boulder/talus slopes pre-date the last major mesh system upgrade in 1995. An example of an older system, in this case over twenty years old, involves chain link mesh on a granular slope containing small boulders. At this site anchors consist of old ¾ in diameter jackhammer drill steel driven in the ground and not grouted. Depth of anchors are unknown but drill steel was available in 3 ft lengths therefore anchors depths are probably 6 ft. Drill steel anchors are spaced 5 ft to 10 ft but spacing did range as wide as 20 ft to 40 ft. This installation has performed well. There have been occasional tears along short lengths of one mesh seam, which were easily repaired. For this site, the low capacity anchorage has proved adequate.

For flatter slopes the mesh is often directly in contact with most of the slope surface, therefore the slope may be carrying a higher percentage of the system weight reducing the need for substantial anchoring along the crest. The above example certainly supports this observation.

Experience has shown care is needed when considering mesh for soil slopes with high erosion rates and talus slopes subject to impact energy from rockfall generated upslope of the installation. Slopes with high erosion rates tend to cause either a redistribution or concentration of load on the mesh system. These high erosion rates tend to develop if the angle of the slope exceeds  $38^{\circ}$  (1¼H:1V) and the matrix material surrounding the boulders is uniformly graded; other factors may also have a contributing effect on the erosion rate.

Performance of mesh systems on flatter soil/talus slopes has generally been good. For a few sites, where the unique conditions described above were not recognized at the time of installation, long term performance has not been as good as expected.

### **Mesh with Diagonal Cable Reinforcement**

BCMoT experimented a few years ago with a cable-reinforced hexagonal wire mesh developed in-house for use on steep rock slopes. The system employed ¾ in (19 mm) diameter wire rope on a diagonal pattern forming 9 ft (2.8 m) square openings. The diagonal pattern of cables was fabricated over the hexagonal mesh on-slope. The system was used where it was anticipated rockfall would involve blocks greater than 2 ft in diameter. This system was abandoned because of the difficulty maintaining uniform net openings, the high installation cost, and the suspected inability of the system to meet design objectives. At about the same time, pre-manufactured net products were gaining greater acceptance throughout the province. This experimental design was replaced with pre-manufactured nets, since the pre-manufactured nets are fully engineered products with proven design capacities.

### **Wire Rope Cable Nets**

The BCMoT also installs cable nets where bedrock controlled gullies incise the cut slope and at other areas where higher energy events are expected. Depending on site conditions, nine-gauge chain link is used as a backing to cable net systems.

For draped cable net installations, the structural support is the same as used for the gabion mesh even though the net systems are heavier. The decision to use the hexagonal mesh structural support system was an empirical decision based on the gabion mesh system's good performance and in anticipation that the slope rather than the structural support system would carry the weight of the net wherever the net contacted the slope. Modifications of the system support are made when some or all of the suspension cable is free spanning, which is a common situation for gully conditions. For these situations, the anchors systems at either end of the installation are designed with greater capacity. Occasionally, it has been possible to provide intermediate support along the suspension cable with guy cables extending well upslope to favorable anchor locations.

Performance of cable net systems has been good, and no net damage has been observed. BCMoT has experienced one entire system failure as a result of an impact from a rare, extremely high-energy event. The failure appeared to be isolated to the capacity of the cable clamps holding the suspension cable rather than to the net or other structural components. This system will be reinstalled pending a review of the cable clamping capacity. The performance of chain link backing to cables nets has been good.

### **Chain Link Mesh**

Nine-gauge chain link mesh has been used once as a stand-alone system to control rockfall. The application is a steep cut in sedimentary rock that produces a high frequency of small magnitude events. Even though chain link has lower tensile strength than hexagonal mesh, the chain link appears to be more flexible with greater energy absorbing characteristics than the hexagonal mesh. It has been well suited for the small magnitude, low energy events at this site. Given the somewhat unique site conditions, the decision to use the chain link was supported by the results of limited rolling rock testing.

The chain link installation is supported on a special raised post and suspension system that allows the chain link to hang freely without contacting the cut face. This anchoring system was selected due to anticipated difficult anchoring conditions in fine, loose talus material.

Overall, the performance has been good except for one short section that has been damaged by frequent, higher-than-expected energy rockfall originating upslope of the system. The damaged section has been replaced with a heavier six-gauge chain link, and its short-term performance has been good.

## CALIFORNIA DEPARTMENT OF TRANSPORTATION

John D. Duffy, Senior Engineering Geologist

### **Usage of both WM and CN for rockfall protection:**

California DOT has installed about 21 cable net installations the first of which was installed in 1995. About 53 wire mesh (both chain link and hexagonal fabric) installations have been constructed since around 1979, most of which were installed in the last 15 years

### **Typical WM and CN design components and significant design modifications:**

#### Anchors and anchor spacing/locations

- For wire mesh, grouted anchors are specified for both cable and steel bar, but cable is preferred. Minimum diameter is 1 inch, and minimum specified hole size is 2 times the anchor diameter. Dead man anchors like Manta Ray<sup>®</sup> are used but not specified due to sole-sourcing issues. Typically, proprietary anchors are implemented as a cost reduction incentive proposal from the contractor; this is a common occurrence. These dead man anchors work very well. Anchor spacing is 50 feet or at every change in topography.
- For cable nets, anchor spacing is 25 feet or at significant changes in topography. Anchor selection is at the discretion of the contractor. Our cable net fabric and anchor specifications are performance-based. The vendor specifies a load and it is the contractor's responsibility to achieve that load with a ground anchor.
- In both cases, we will specify an unbonded length. This is dependent on the soil/rock conditions. The intent is that anchor strength is not developed or relied on within the shallow surface materials that could erode and undermine the anchor.

#### Support cables

- For wire mesh, our support cables are ½ inch, which have worked well for all known loading conditions. This has never been a weak link in the system, and it may be possible to even use thinner cable.
- Cable mesh is performance spec and provided by the vendor. It varies but we have never had a failure in this area. Again, it is not a weak link.

#### Fabric

- We typically use hexagonal wire mesh, 9 gage and plastic coated mesh material. If hexagonal mesh is used for rocks less than 2 feet in dimension and small 5-yard small slides develop, the mesh functions well. As quantities increase, the mesh will rip, but it still provides protection although maintenance increases significantly. We have had the mesh completely fail due to large rockslides and landslides that were well beyond the capacity of the system.
- Cable nets have worked well. However, we have had the fasteners open and slide and, in some cases, pop off. This damage occurred under static load because of rockslides and rocks being caught in the mesh.

### Connection details

- Wire mesh is connected to wire mesh with “connections equal to or stronger than the mesh”. Spacing is every 4 inches. The type of fasteners is not specified, but Spenax rings are used almost exclusively; these fasteners have worked very well. We do not allow any overlap of the mesh. We also do not include any support cables (besides the top horizontal cable) with the wire mesh system. Nor do we include a bottom horizontal cable. Our experience has been that debris accumulates along bottom cables and causes failures.
- Cable nets are connected together per vendor’s specifications (they also do not overlap). We always back cable nets with wire mesh with the wire mesh being placed between the cable nets and the ground. The wire mesh is connected to the cable mesh with “connections equal to or stronger than the wire mesh”. Spacing is every 12 inches. The type of fasteners is not specified, but Spenax rings are used almost exclusively; these fasteners have worked very well. We specify that the cable net and wire mesh must be connected together prior to installation on the slope to ensure a good connection between the two.

### **Typical WM and CN applications:**

Both wire mesh and cable nets are used, and their selection is based on the results of the geotechnical investigation. Wire mesh is used where block sizes are less than or equal to 2 feet in dimension and where small shallow surficial slides do not exceed about 5 cubic yards in volume. Cable nets are used for block sizes between 3 to 5 feet in dimension and small rockslides 10 to 50 cubic yards in volume. We have found that these criteria work very well and result in minimal maintenance. In some instances, larger events (~20 % larger) have occurred and the systems still provided protection but required maintenance. Drapery systems are not used for landslide mitigation. If anchors are undermined by sliding or large slides occur, the mesh is not capable nor is designed for such events. Chain link has performed well. It does not unravel, but it is more difficult to install because of its flexibility. Many of our pre 1980 installations are chain link, and we have not had any problems. The largest and most notable is an installation at Malibu. This installation has been through two El Nino cycles and 25 years of weather. When properly used for rockfall problems within design guidelines, no systems have failed.

### **Design problems or failures of installations:**

- Seam overlap has been the biggest problem we have experienced and the one requiring the most maintenance. Where cable or wire mesh is overlapped, rocks will accumulate and slowly load the system causing tearing and stressing of the system. The drapery should be as smooth and even as possible.
- Additional horizontal cables in the system also have resulted in debris accumulation often causing tearing and excessive stresses on the system.
- For cable net systems, differential movement between the wire mesh and cable mesh has been problematic. Rock debris drags on the underlying mesh and gets caught in the subsequent fold and load the mesh. Repairing this is difficult.
- Older hogring fasteners have opened.

**Applications exposed to significant horizontal impact energy:**

We have several installations where we have a suspended drapery. The rock hits the upper portion of the mesh and dribbles down slope under the lower portion of the mesh. We have both cable and wire mesh installations. We have not had any problems from horizontal impacts. On hexagonal drapery systems, we attribute the holes to creep loading. There is one mysterious hole in the Gaviota mesh, possibly from a rock impact.

**Applications exposed to snow or avalanche loads:**

We have two wire mesh systems in snow country, and as of yet have not had any problems.

**Other related information/experience:**

Overall, systems have functioned well. There have been no widespread failures.

Less is more. Adding cables doesn't seem to do anything except increase costs. Increases in anchor spacing, a big cost in the system, is working.

Flexibility. Flexible anchors. Not restricting the mesh with internal intermittent anchor. Flexibility is very important.

The system designs are getting fine-tuned and the costs are coming down.

## IDAHO TRANSPORTATION DEPARTMENT

Tri Buu

### **Usage of both WM and CN for rockfall protection:**

- Approximately 3 installations which have been constructed in the last 5 years

### **Typical WM and CN design components and significant design modifications:**

- anchors spaced 5-6' along top of slope
- 5/8" diameter support cables
- double twisted hexagonal mesh

### **Typical WM and CN applications:**

- slope heights and angles range from 50 to 200 feet high and 1H:1V to 0.75H:1V
- applied to slopes with rock sizes 1 foot or less
- used to minimize or stop rocks from entering the roadways and thus reducing the need for constant rockfall patrol during spring/fall season and rain storms.

### **Design problems or failures of installations:**

None

### **Applications exposed to significant horizontal impact energy:**

N/A

### **Applications exposed to snow or avalanche loads:**

N/A

### **Other related information/experience:**

We have very limited experience with draped wire mesh or cable net for rockfall control.

## NEVADA DEPARTMENT OF TRANSPORTATION

Jeff Palmer

Use of wire mesh systems by NDOT has been done since the 1960's and most are still in place. Cable net systems have not previously been used but are being considered for future use. In the last ten years, about ten wire mesh systems have been placed on slopes and more are being considered in the near future. There are approximately 50 of the older wire mesh systems located in various places around Nevada.

Our current design uses rectangular sections of wire mesh 20' wide and 26' long. They are attached to 3/8" diameter horizontal and vertical steel cables (seaming rope) with hog ring fasteners at a spacing of 6". The cables are connected to each other with 4" diameter, 0.87" cross-sectional diameter steel rings and wire rope clips. The wire mesh is 0.12" thick galvanized gabion wire mesh. The wire mesh hangs down to about 4' above the bottom of slope.

The anchors for the wire mesh systems are placed every 40', at every other wire mesh section. The minimum length of cable between the mesh and the anchor is 5'. The anchors must be placed a minimum of 15' beyond the brow of the slope. Both soil and rock anchors are 3/4" diameter, 6.5' long threaded loop eye rock bolts. The rock bolts are installed using either Type III Portland Cement or rock bolt adhesive (ASTM E 1512).

At this time cable net systems are not used, but are being considered in the future for slopes with a height greater than 75' and a slope angle of 60° or more. In addition, cable net systems are considered for slopes with adverse conditions that are considered to have a higher risk of rockfall. The conditions may include water seepage from the slope, faults or joints at adverse orientations or slopes susceptible to higher rates of erosion.

There have been no failures with the recent wire mesh systems however; some of the older systems have come loose at the anchors. The wire mesh slides down the slope and then needs to be replaced. Other problems occur when rocks get caught in the mesh and are not able to reach the ditch.

Any significant horizontal impact or high snow or avalanche loads may cause the wire mesh systems to break or pull the anchors out. If this occurs, a cable net system or change in anchor design may be necessary.

## NEW HAMPSHIRE DEPARTMENT OF TRANSPORTATION

Dick Lane

### **Usage of both WM and CN for rockfall protection:**

The first installation of wire mesh rock fall netting in the state of New Hampshire was in 1978 on the Interstate 93 Northbound Off-Ramp at the Wellington Road Interchange in the city of Manchester. NHDOT has since installed one more wire mesh installation.

### **Typical WM and CN design components and significant design modifications:**

#### Anchors and anchor spacing/locations

Thread deformed, 1-inch diameter bars were used to anchor the wire mesh system. All the anchors were extended a minimum of 5 feet into bedrock and anchored with resin grout. Rock bolt anchors were installed at the intersection of vertical and horizontal wire ropes at 50-foot intervals along the upper edge of the mesh. At these locations, the steel rings were sandwiched between two steel bearing plates. Additional rock bolt anchors were installed with a maximum spacing of 25 feet. At these locations, the mesh was placed between the rock and a steel bearing plate.

#### Support cables

The support cables were  $\frac{3}{4}$  inch zinc-coated steel wire 6X19 strand wire rope with a fiber core for flexibility and resiliency. Horizontal wire ropes were run along the top, bottom and at two intermediate locations. Vertical wire ropes were hung at a maximum interval of 50 feet. Steel rings (4  $\frac{1}{2}$  inch diameter) were used to join the intersecting vertical and horizontal wire ropes at 50-foot intervals along the upper edge of the mesh, at 150-foot intervals along the bottom and at 150 foot intervals for intermediate horizontal wire ropes. The wire ropes were threaded through the rings, doubled over using a rope thimble and secured with u-bolts. All remaining intersections of wire ropes were secured with u-bolts.

#### Fabric

The wire mesh was 11 gauge, galvanized wire with a double twist, hexagonal weave. The mesh openings were 4  $\frac{1}{2}$  inch X 3 inch with all perimeter edges selvaged. The wire mesh was installed in 15-foot wide vertical strips, each lapped over the other by a minimum of 12 inches.

#### Connection details

Adjacent vertical strips of wire mesh were connected with galvanized steel hog rings. At the top and bottom, the mesh was folded underneath to form a minimum of 12-inch lap. Horizontal laps were threaded by continuous weaving of galvanized steel lacing wire. The mesh was secured to the underlying wire rope grid by continuous weaving of lacing wire.

### **Typical WM and CN applications:**

Wire mesh installations are on slopes 55 to 70 feet in height with slope angles ranging from 1H:1V to 1H:6V. Rock fall events generally consisted of rock fragments ranging in size from 2 to 10 inches in diameter with an occasional block, 2 to 3 feet in diameter.

Source areas are typically highly weathered and fractured zones of rock. The wire mesh system is freely draped down over the face of the rock slope to guide falling rocks safely into the ditch.

**Design problems or failures of installations:**

There have been some problems caused by deficiencies in the original design. The problems include the following:

- The wire mesh netting should not have been extended to the toe. This allowed rock and debris to be trapped behind the mesh, causing stress on the wire mesh netting. The bottom of the mesh has to be lifted periodically to clean out the accumulated material.
- The hog rings were too small and not the locking type, resulting in the separation of adjacent strips of mesh at the vertical overlap.
- The mesh was torn at several locations by falling rocks, greater than 3 feet in diameter. Occasionally rock fragments are caught by the horizontal wire ropes.
- Although there have been no failures of wire ropes, the cable loop detail was incorrect. The cable loop diagram should show four U-bolts installed in alternating and opposite directions.
- Several of the anchors have pulled out because they were placed in weathered rock. In addition, the resin grout did not completely fill some of the anchor holes.

**Applications exposed to significant horizontal impact energy:**

The nature of the rock fall has been a combination of falling, bouncing and rolling. The wire mesh system has handled rock fall up to 3 feet in diameter without failure.

**Applications exposed to snow or avalanche loads:**

The only external loads experienced by these wire mesh systems have been ice and snow build-up (estimated 1-2 feet thick) at a few locations.

**Other related information/experience:**

The deficiencies in the system have been corrected. The bottom of the wire mesh netting is now extended to within 4 to 6 feet above ditch elevation, allowing for falling rocks to exit from behind the mesh. The hog rings have been replaced with locking wire mesh fasteners to improve the holding strength at the vertical overlaps. The installation procedure for the clips (U-bolts) on the cable loop has been corrected. All the anchors are extended a minimum of 5 feet in competent rock and fully grouted with cement grout.

## NORTH CAROLINA DEPARTMENT OF TRANSPORTATION

Nilesh Surti and Jody Kuhne

### **Usage of both WM and CN for rockfall protection:**

NCDOT has 2 installations of cable net and approximately 10 wire mesh (½ pinned, ½ draped). Wire mesh has been in use for about 17 years; cable net installations have been installed within the past 6 years.

### **Typical WM and CN design components and significant design modifications:**

#### Anchors and anchor spacing/locations

Wire mesh draped: 1 ¼" every 5' across top,

Wire mesh pinned: 1" anchors, 10' O.C., approx. 200' x 300' area over tunnel portal  
2 anchors + 1 tensioning anchor, fabricated plate w/ 4 1 1/8" rock anchors each, 15' long (9/97 cable net installation); 4 anchors + 1 tensioning anchor, fabricated plate w/ 1 ¼" rock anchors each, 15' long (10/02 cable net installation)

#### Support cables

2 anchor points, nets suspended by 1 3/8" cable (9/97 cable net installation)

4 anchor points, suspended by 1 ¼" cable, 160 kips (10/02 cable net installation)

#### Fabric

10' x 20' Brugg (cable net) panels, 5/16" net w/ 8" openings, 5/8" outer cable;  
5/16" lacing rope

#### Connection details

Crosby clamps: 7 for each anchor assembly or suspension cable connection, w/ Flemish eyes for pulleys and anchors. Lashing fastened w/ hog rings

### **Typical WM and CN applications:**

Wire mesh: 50-100' slope heights placed on 1H:1V to vertical slopes

9/97 cable net installation: 500' slope length @ 1½H:1V; rockfall source area up to 300 feet upslope of suspended net; successfully stopped 20 yd<sup>3</sup> fall w/ large horiz. velocity, block size 1-2'

10/02 cable net installation: slope length 170' @ 1H:1V; 50 yd<sup>3</sup> slope failure occurred under nets almost fully contained w/ very little horizontal velocity, block sizes 1-4'

### **Design problems or failures of installations:**

Removing debris from under large drape cable net installation

### **Describe applications exposed to significant horizontal impact energy:**

See above.

### **Describe applications exposed to snow or avalanche loads:**

N/A

### **Other related information/experience:**

N/A

**OREGON DEPARTMENT OF TRANSPORTATION**  
Larry Pierson (Landslide Technology, Portland, OR)

**Usage of both WM and CN for rockfall protection:**

ODOT has about 50 wire mesh installations and no cable net installations. The oldest installation was constructed around 1970; most have been installed within the last 20 years.

**Typical WM and CN design components and significant design modifications:**

- Anchors and anchor spacing/locations – In rock, ¾” x 3’ loop eye rock bolt every 40 feet unless installation is over 75’ tall then every 20’. Same in soil except the anchor is set in concrete in a 3’ by 12” hand-dug or augured hole.
- Support cables: Cables are 6X19 wire rope with an IWRC.
- Fabric – Standard galvanized or PVC coated gabion mesh.
- Connection details – Cable connections use a wire rope thimble and three wire rope clips spaced 3¾” apart.

**Typical WM and CN applications:**

Installations placed on slopes up to 160 feet, oriented nearly vertical to 1H:1V. On flatter slopes a draped WM with fence extension is used at a mid-slope location to reduce the quantity of mesh. WM is used on both hard rock and soil/rock slopes, and typically where block sizes are less than 2 feet in diameter to minimize maintenance. Where maintenance is acceptable, alternative WM has been installed where rockfalls up to 5 feet in diameter may occur rarely.

**Design problems or failures of installations:**

WM has problems with environmental acceptance; color PVC coatings help alleviate this problem. Poorly installed anchors have led to rare anchor pull out or sloughing failures, especially where required depth is not attained. No cable failures have occurred even though a relatively small (3/8” diameter) cable is used. Mesh failures have occurred (primarily separation of adjacent mesh panels but rare mesh tearing) when rockfalls involve blocks larger than 2 feet in diameter.

**Applications exposed to significant horizontal impact energy:**

Typically not an issue for draped mesh applications. Where mesh is installed from a fence at some intermediate slope location, impact damage has occurred at only one site. In that case, the impact section was reinforced with Brugg cable nets.

**Applications exposed to snow or avalanche loads:**

Have not experienced any snow load or avalanche caused system failures even in Cascade Range locations. These installations have performed similarly to low snow load locations.

**Other related information/experience:**

Wire mesh is one of the most economical and effective techniques available. Slope should be scaled thoroughly before installation.

## WASHINGTON STATE DEPARTMENT OF TRANSPORTATION

Tom Badger/Steve Lowell

### **Usage of both WM and CN for rockfall protection:**

Wire mesh (chain link fabric) was first used along Washington highways for rockfall protection around 1960. Since the mid 1980's, WSDOT has used double twist fabric instead of chain link for protection from smaller-sized rockfall. To date, about 50 wire mesh systems have been installed by WSDOT. In the late 1980's, cable nets were first used in the U.S. by WSDOT for a steep, 250 ft. high rockslope in the North Cascades. Frequent, large-sized (3-5 feet) rockfall and extreme icing had severely damaged a previous double twist installation, resulting in its replacement with cable nets. Since then, WSDOT has installed about a dozen cable net systems at sites prone to more severe rockfall.

### **Typical WM and CN design components and significant design modifications:**

WSDOT designs for slope protection systems are experienced based, and limited modifications have been made since the mid 1970's. For both wire mesh and cable net systems on slopes less than 75 feet high, anchors are spaced at 50-foot intervals; spacing is reduced to 25 feet, for slope heights greater than 75 feet. Anchors in rock include either a 1" diameter, Grade 60, threaded bar or a 3/4" diameter wire rope placed between 4 to 6 feet in depth. Prior to 1997, 1/2" diameter anchor rods were allowed for rock applications, but their use was terminated in 1997 after numerous anchor failures occurred during installation of a large cable net system (Tumwater Canyon). Details for deadman-type anchors are provided in the contract plans for soil conditions, although most contractors submit their own anchor designs for approval by WSDOT. For wire mesh and cable net systems, both soil and rock anchors must achieve a 20,000 lb vertical pullout capacity. Anchors, as well as the top of the mesh/nets, are located a minimum of 10 to 15 feet beyond actively eroding slope crests. No midslope anchors are used.

The mesh/nets are suspended on a grid of 5/8" – 3/4" diameter, vertical wire ropes 25 or 50 feet wide and horizontal ropes spaced at 50 feet. Due to problems with debris accumulation along horizontal ropes located between the mesh and the slope, the support grid has been placed on the outside of the mesh/nets after their hanging, raising questions about the utility/value of the all but the top horizontal suspension rope.

For double twist mesh, a 12" overlap is specified between panels fastened with Spenax™, Tiger-Tite™, or 9 gage (minimum) lacing wire on roughly 2" intervals (each cell). Cable nets are butted flush, laced with 1/4"-5/16" diameter wire rope, and backed with either chain link or double twist mesh.

### **Typical WM and CN applications:**

Washington State has a wide range of climates, geologic conditions, and slope morphology that yield a gamut of rockfall problems. Wire mesh/cable net is most typically used on eroding, coarse surficial deposits (i.e., alluvium, colluvium, glacial deposits) and highly fractured and generally poor quality rock masses. Wire mesh is used on slopes where block sizes generally do not exceed 2 feet in diameter; on steep slopes,

larger block sizes (~ 3 ft) are commonly contained causing little to no damage to the mesh. Cable nets have proven effective on high slopes with maximum block sizes ranging between 3 to 5 feet. On flatter slopes where the mesh/cable nets are in intimate contact with the slope or other instances where large kinetic energies are unlikely to develop, these systems have contained larger block sizes. Generally, WSDOT applies other stabilization measures (i.e., scaling, rock anchors, shotcrete) where blocks sizes exceed 3-5 feet, prior to placement of a draped system.

WSDOT has used wire mesh/cable net systems on slope heights approaching 300 feet and on slopes ranging in orientation from around 40° to near vertical. On slopes where a significant snowpack can develop (up to around 55° to 60°), consideration is given to reduced anchor spacing and upsizing system components.

**Design problems or failures of installations:**

Localized and global failures of systems have occurred due to excess debris accumulation behind installations and snow loading on top of installations. Horizontal support cables placed inside the mesh often cause accumulation of debris. Snow has also created problems that accumulates or where snowplows pile snow against the bottom of an installation, resulting in the inability of the debris to clear from behind the mesh. Installations on moderately inclined slopes generally seem to experience greater damage than those on steep slopes. Problems associated with these raised systems include debris accumulation at abrupt slope convexities, lifting of lightweight installations, and occasionally puncturing of wire mesh fabric.

**Applications exposed to significant horizontal impact energy:**

About one quarter of WSDOT's systems mitigate rockfall that originates upslope of the installation; thus, systems are exposed to sub-horizontal impact energy. These systems are anchored on promontories adjacent to chutes or raised on posts.

**Applications exposed to snow or avalanche loads:**

A number of installations are located in areas where significant winter snowpack develops. Failures have occurred on moderately inclined slopes that accumulate snow when standard anchor spacings have been used. Anchor spacing/capacity have been designed for anticipated snow loads for several installations.

**Other related information/experience:**

Vertical and horizontal support cables in the field of mesh are often slack, indicating load is generally not being transferred below the top horizontal support rope.

Design for snow loads requires some accounting of interface friction, which is a difficult parameter to assess.

## WYOMING DEPARTMENT OF TRANSPORTATION

Jim Coffin

### **Usage of both WM and CN for rockfall protection:**

WM has been used on 13 individual projects, with an average of 5 individual backslope locations per project for a total of approximately 275,000 square yards installed to date. Approximately 95% of the mesh installed is the double twist type. Currently, WYDOT has one CN drapery site (100 feet high) and also three other sites that incorporate CN's as fences and as elevated catchment draperies.

WYDOT's oldest WM installations were a series of chain link mesh draperies installed in 1980 on Highway 14A, in the Big Horn Mountains (North Central Wyoming). Approximately 80% of all WYDOT's mesh drapery systems have been installed within the last 10 years.

### **Typical WM and CN design components and significant design modifications:**

#### Anchors and anchor spacing/locations

Typically in Wyoming unstable slopes protected with wire mesh consist of unconsolidated colluvial or glacial soil, gravel and boulders or highly weathered rock overlying fractured to massive rock. These ground conditions lend themselves well to installing a driven (soil) or drilled (rock) 1-inch diameter bar approximately 5 to 7 feet into the ground approximately 20 to 25 feet beyond the top of slope (outside the active zone of erosion). If the Contractor is driving anchors in soil and hits a section of moderate to hard rock, the same type of bar as for the colluvium is used, except the holes are drilled, centralizers are added, the anchor is grouted, and a pull test is conducted. Both driven and drilled anchors are spaced the same distance apart, 5.5 feet, which provides an anchor approximately at the edge and center of mesh rolls. Due to Wyoming's low average precipitation (8 to 15 inches/year) corrosion is generally not a problem. However, the anchor bars are epoxy coated and grouted in place for drilled anchor locations. Face anchors have been used on five sites to pin the mesh to the slope for revegetation enhancement. The face anchors are usually driven bars, ½ inch to 1 inch in diameter and range from 3 to 5 feet in length.

WYDOT's only cable net drapery site has anchors spaced the width of the cable mesh panel (24' apart). The anchors were set back 20 to 30 feet beyond the edge of slope. The anchors are ¾ inch wire rope anchors grouted into rock 6 to 7 feet deep and were required to be pull tested to 10 tons.

#### Support cables

Vertical and horizontal support cables for WM installations (besides the horizontal top anchor cable) have only been used on one project and consisted of 3/8 inch diameter, wire rope. The vertical cables were used to attach 20-foot long cables to connect the mesh to the anchors. Horizontal cables were spaced approximately 25 feet apart.

Anchors for CN installations were connected to the cable nets with 20 to 30 foot long, ¾ inch diameter wire rope vertical support ropes to insure that the anchors are placed outside the zone of erosion and into competent rock.

### Fabric

Galvanized chain link fence has been used on one project in the early 1980's. Since then, double twist mesh, either plain galvanized and more commonly PVC color coated, has been used exclusively. Many of WYDOT's meshed slopes are located within U.S. Forest Service corridors (environmentally sensitive areas), and it is often a requirement to use the PVC color coated wire to blend in with the surrounding rock slope. WYDOT has one slope on Interstate 80 east of Laramie where the PVC coating faded from tan to white 1 year after installation. WYDOT's only cable net site incorporated 12 x 12 inch CN's with WM fastened to the nets between the slope and the CN's.

### Connection details

For wire mesh installations, a ½ inch wire rope top cable is installed at the top of the mesh, and attached by overlapping the mesh 12 inches over the cable and then held with fasteners on 6 inch centers. The top cable is attached to the anchors by wrapping the ½ inch top cable one circumference around the anchor. The anchor is attached to the mesh with an 8 inch x 8 inch steel plate over the mesh followed by a steel washer and nut. Mesh is overlapped at all the seams 12 inches and secured with fasteners on a 6-inch spacing.

Cable nets are attached to the anchors as per the manufacturer's recommendations. The vertical support ropes are attached to the top horizontal support ropes with a thimble and 4 cable clamps. All seams are laced together with 5/16-inch diameter wire rope.

### **Typical WM and CN applications:**

For wire mesh installations, slope heights (vertical change) range from approximately 40 to 200 feet with 80 feet being the average. Slope angles range from near vertical to 38 degrees. The cable net installation slope heights range from 60 to 100 feet and are 75 degrees to near vertical.

For both WM and CN installations, rockfall source areas include talus chutes, mixtures of colluvial or glacial soil, gravel, and boulders and moderately to highly fractured sandstone, limestone, volcanic breccia and granite. Rockfall events generally consist of individual rocks 6 to 36 inches in diameter and/or rock debris events 1 to 3 cubic feet in size.

WYDOT's anchor design was initially based on guidelines in the Maccaferri anchor design section of their Hexagonal Mesh Design Manual. Rock or soil slopes that are a hazard are evaluated in detail using aerial photos, DTM mapping, ditch design charts, maintenance history, CRSP Computer Program, and field mapping including the driving of test anchors. In addition, all of the WYDOT's soil and rock slopes have been evaluated with a Rock Hazard Rating System. The ratings are used as a guideline for

proposed new construction projects and for existing problem slopes. Currently, approximately \$1 million is spent per year for mitigation of slopes.

**Design problems or failures of installations:**

Three WM drapery sites experienced failure of face anchors. The face anchors consisted of 3 to 5 foot long steel bars, installed to help secure the mesh to the slope and enhance revegetation. Sloughing of soil and highly weathered rock that the anchors were installed in along the slope interface led to the failures. The face anchors were not reinstalled after the failures. Face anchors currently are not generally used because of these problems.

Failure of top support anchors occurred at two locations. The anchors were not installed far enough beyond the zone of erosion at the top of slope, and this resulted in a loss of a portion of the top anchors. New anchors were then installed in a stable area beyond the active erosion area at one location.

Horizontal support cables have been installed on one project, and created problems by allowing rock to be caught behind the mesh, preventing the rock from falling into the ditch. Horizontal cables are not used on current projects for this reason.

During the spring, prior to complete thaw of the ground while the bottom half of the mesh is still frozen to the slope but the upper half is not, loose rock has collected behind the mesh into pockets or pillows at some sites. This has resulted in a few tears in the mesh, approximately 6 to 12 inches wide, and failure of seams when fasteners pulled apart.

**Applications exposed to significant horizontal impact energy:**

An elevated CN drapery installed in a talus chute was impacted with a combination of snow and rock debris, failing an anchor. The CN and the anchor were reset.

**Applications exposed to snow or avalanche loads:**

Two WM sites on State Highway 22 on Teton Pass and one in Snake River Canyon have avalanche chutes located directly above the meshed slopes and have been impacted with avalanches. Only minor damage has occurred at one of the sites due to snow avalanches (see CN drapery anchor failure above).

**Other related information/experience:**

We have used WM at approximately 6 locations combined with coconut mat, face anchors (few locations), fertilizer, seed and tree plantings to provide a fabric that enhances revegetation and possibly adds to the stability of the slope. We have determined that this works best when the coconut mat is attached directly to the mesh.

Besides a few minor failures that were repaired, WM and CN installations in Wyoming have all been a success to date.



**APPENDIX B**  
**FABRIC TEST REPORTS**



**Report No. WMEL 03-043**

**Tensile Capacity Testing of Twisted Wire Mesh and Cable Net  
Mesh for Use as Rock Fall Protection**

**Prepared  
For**

**Balasingam Muhunthan  
Washington State University  
Department of Civil and Environmental Engineering  
Sloan 26  
Pullman, WA 99164-2910**

**By  
Wood Materials and Engineering Laboratory  
Washington State University  
April 28, 2004**

**Report No. WMEL 03-043**  
**Tensile Capacity Testing of Twisted Wire Mesh and Cable Net**  
**Mesh for Use as Rock Fall Protection**  
**For**  
**Balasingam Muhunthan**  
**Washington State University**  
**Department of Civil and Environmental Engineering**  
**Sloan 26**  
**Pullman, WA 99164-2910**

## **1. Introduction**

The Wood Materials and Engineering Laboratory (WMEL) at Washington State University in Pullman, WA, performed a series of tests on twisted wire mesh and cable net mesh for use as rock fall protection. A total of 16 tension tests were conducted on 8 twisted wire meshes and 8 cable net meshes, at the request of the client, B. Muhunthan. The WMEL received 4 separate shipments of material which were tested as described below. This report includes descriptions of specimens, test methods and testing apparatus, descriptions of failures, and tabulated results of test data. While testing was conducted using ASTM A 975 *Standard Specification for Double-Twisted Hexagonal Mesh Gabions and Revet Mattresses (Metallic-Coated Steel Wire or Metallic-Coated Steel Wire with Poly (Vinyl Chloride) (PVC) Coating)* as a general guideline, the results of these tests are not intended for code approval of these products.

## **2. Test Specimens**

Table 1 provides information on the different types of specimens that were tested. All specimens were tested as delivered, although it was necessary to bend the untested portions of the Mac Double Galv1 and the Mac Double Coat in order to get these specimens to fit into the testing apparatus. Differences among the twist mesh specimens were not apparent, therefore the descriptions of those meshes were based on appearance. The meshes described as Double meshes had two layers of twisted wire mesh, both of which were fixed to the testing apparatus and contributed to the load carrying capacity. Meshes described as having a coating were made from wires which were coated all the way around with a PVC coating in either gray or brown. I was informed by a

representative of Maccaferri that the difference in colors of the coatings was strictly for aesthetic purposes. Meshes describes as Narrow were approximately 34.5 inches wide (perpendicular to the direction of loading), while the remaining twist mesh specimens ranged from 40.0 inches to 71.0 inches wide. Specific information on GeoBrugg specimens was provided by the manufacturer of the specimens and is provided in Appendix A.

**Table 1. Description of Tested Specimens**

<b>Specimen</b>	<b>Description</b>
GeoBrugg Twist 1	Twist wire mesh made by GeoBrugg
GeoBrugg Twist 2	Twist wire mesh made by GeoBrugg
GeoBrugg Twist 3	Twist wire mesh made by GeoBrugg
Mac Double Galv1	Doubled twist wire mesh, galvanized, made by Maccaferri
Mac Double Coat	Doubled twist wire mesh, gray coating, made by Maccaferri
Mac Double Narrow	Doubled twist wire mesh, narrow, made by Maccaferri
Mac Narrow Coat1	Twist wire mesh, narrow, brown coating, made by Maccaferri
Mac Narrow Coat2	Twist wire mesh, narrow, brown coating, made by Maccaferri
GeoBrugg Square 1	Square woven cable mesh made by GeoBrugg
GeoBrugg Square 2	Square woven cable mesh made by GeoBrugg
GeoBrugg Diagonal 1	Diagonally woven cable mesh made by GeoBrugg
GeoBrugg Diagonal 2	Diagonally woven cable mesh made by GeoBrugg
Mac Cable 1	Cable mesh made by Maccaferri
Mac Cable 2	Cable mesh made by Maccaferri
Mac Cable 3	Cable mesh made by Maccaferri
Mac Cable 4	Cable mesh made by Maccaferri

### 3. Testing Methods

Based on photographs taken from a report entitled “TECCO Mesh G-65 and G-80 Mechanical Properties and Simulation Models for Surface Support Determination in Slope Stabilization Applications” that was provided by B. Muhunthan, the test fixture shown in Figure 1 was designed, fabricated and bolted to the reaction floor inside the WMEL’s structural testing facility. The intent of the test fixture was to load the meshes in tension at the two edges perpendicular to the direction of loading while restraining the edges parallel to the direction of loading from constricting as loads were applied. Loads were applied utilizing a 100,000 lbs capacity hydraulic actuator with a stroke of 10 inches that was controlled using an MTS 407 Controller, which received actuator displacement

feedback using a string potentiometer. Load data were obtained using a 100,000 lbs capacity load cell placed in line with the loading apparatus. Linear variable differential transformers (LVDT's) and string potentiometers were used to monitor displacement of the loading head with respect to the base of the test apparatus in order to get an accurate record of the distance the meshes moved through the first 2 inches of displacement. These data were used in determining the elastic modulus of the meshes. Load data and displacement data from the string potentiometer and the 2 LVDT's were recorded using LabVIEW version 6.1 software.

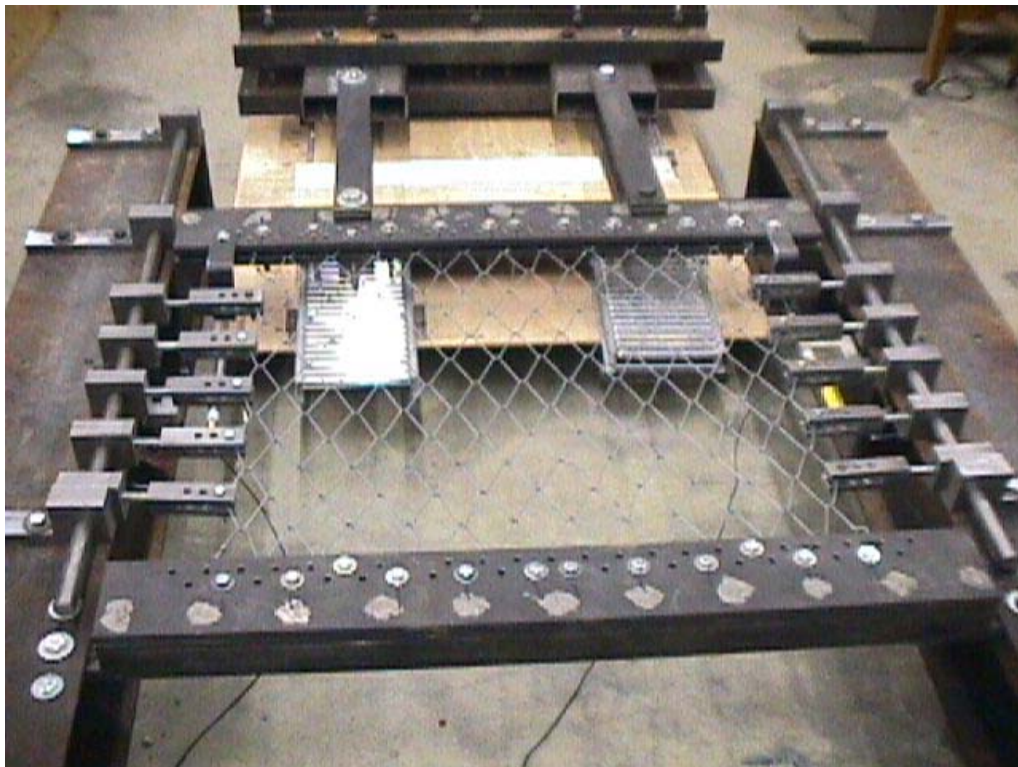


**Figure 1. Mesh Testing Apparatus**

Differences in dimensions of the meshes made it necessary to attach the specimens to the test apparatus slightly differently. As shown in Figure 1, the twisted wire mesh specimens manufactured by GeoBrugg were pinned to the loading plates and side restraints through holes machined in the steel components. All of the twisted mesh specimens manufactured by Maccaferri were pinned through holes in the side restraints, but were attached to the loading plates with bolts placed in the holes in the plates and that extended far enough above the plates to capture the mesh, as shown in Figure 2. It was

also necessary to fold the portions of the Mac Double Galv1 and Mac Double Coat meshes that extended beyond the lateral restraints, also seen in Figure 2. Attachment of the loading plates was done far enough in from the ends of the meshes so that the wires would not unwind or come undone prior to failure of the specimens. Longer segments of threaded rod were required to attach the lateral restraints to the meshes described as Narrow. The square woven cable net meshes manufactured by GeoBrugg were attached to the end plates and lateral restraints in the same manner as were the GeoBrugg twisted wire mesh specimens, except that segments of steel plate were attached to the lateral restraints to maintain the distance between parallel cables, as shown in Figure 3A. The diagonally woven cable net meshes manufactured by GeoBrugg were attached to each end plate with 2 bolts and long threaded rod segments were utilized on the lateral restraints in order to maintain the shape of the nets, as shown in Figure 3B. All specimens were placed in the fixture in such a way that as much slack could be taken out of the specimens as possible to ensure that there would be enough deformation of the specimens to cause failure. In general there was very little load applied to these specimens as they were installed in the test fixture. Cable net mesh specimens manufactured by Maccaferri were approximately 75 inches long, parallel to the direction of loading, which made it necessary to remove the loading plate closest to the actuator and some of the steel linkages so that the mesh could be directly attached to the loading apparatus connected to the load cable, as shown in Figure 4. Four lateral restraints were used on each side based on the shape of the Maccaferri cable net mesh.

All specimens were secured in the test frame and then the LVDT's or string potentiometers were installed such that the maximum amount of displacement data could be recorded before the instruments ran out of stroke on the plunger or extension of the string. Following installation of the displacement measuring devices, the data acquisition program was started and the hydraulic actuator was put into action. Load was induced by the hydraulic actuator which ran at 0.25 inches per minute under displacement control. All specimens were loaded to the full stroke of the actuator, with the exception of the cable net meshes, which failed distinctly prior to reaching the entire distance. Testing results and descriptions of failure for the various specimens are presented in the following section. Following each test, specimens were removed from the test apparatus, regions of failure were documented and specimens stored on a pallet for disposal.

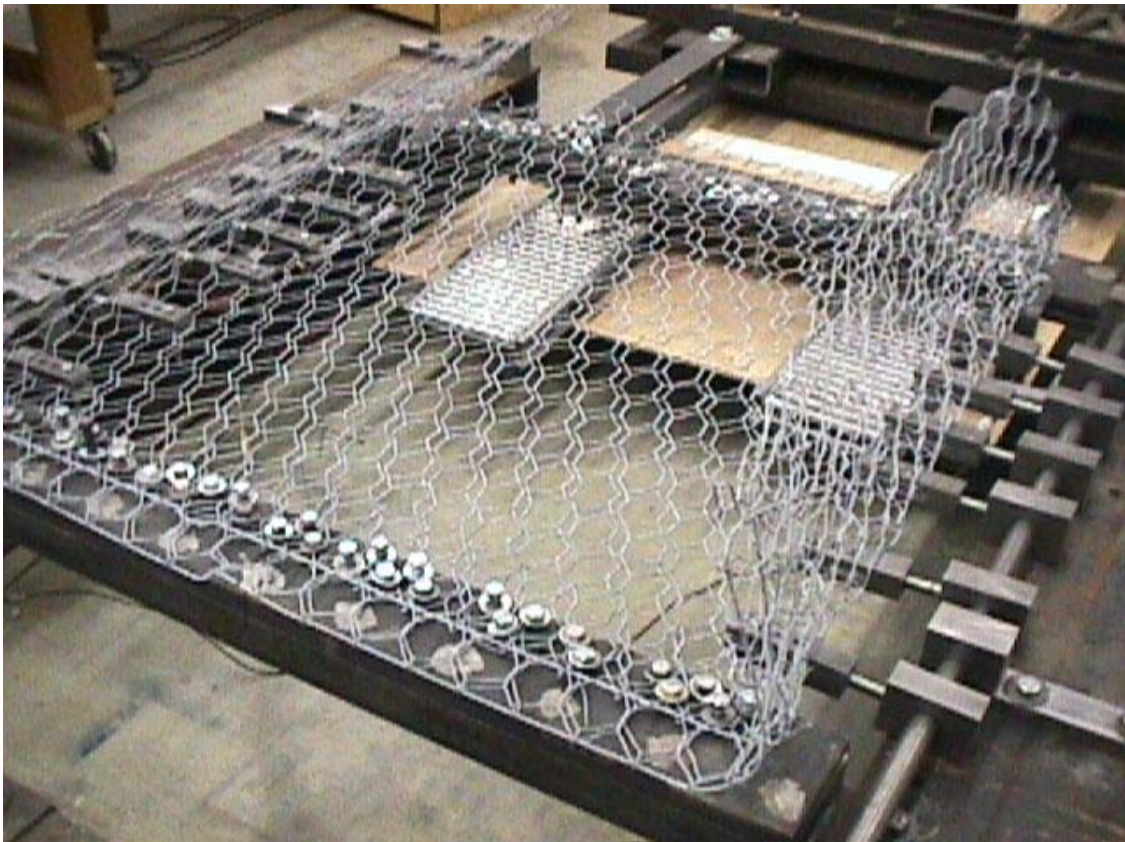


**Figure 2. Testing Setup for Twisted Wire Mesh with Bolts Extended Above the Loading Plates**

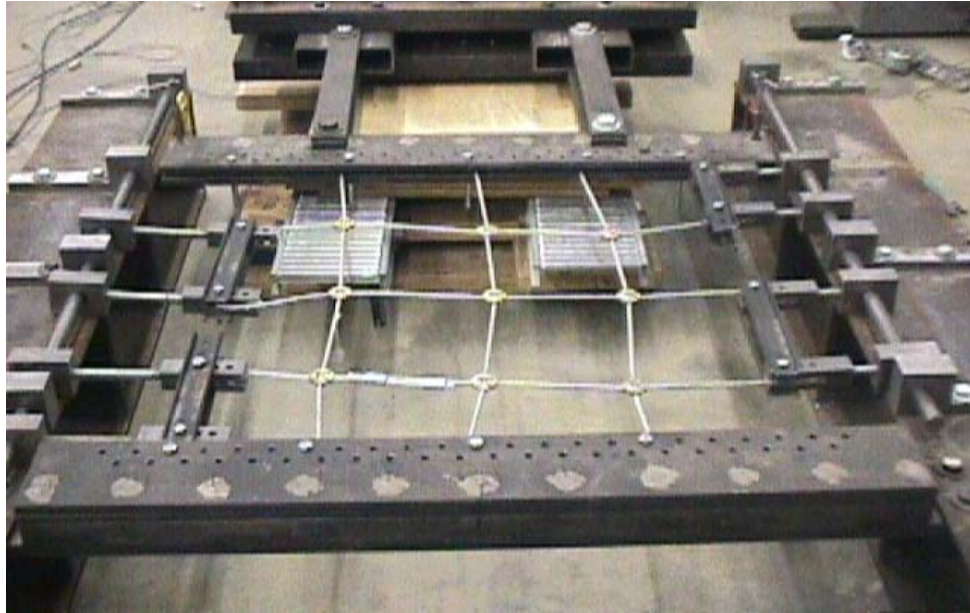


**Figure 3A. Testing Setup for Square Woven Cable Net Mesh from GeoBrugg**

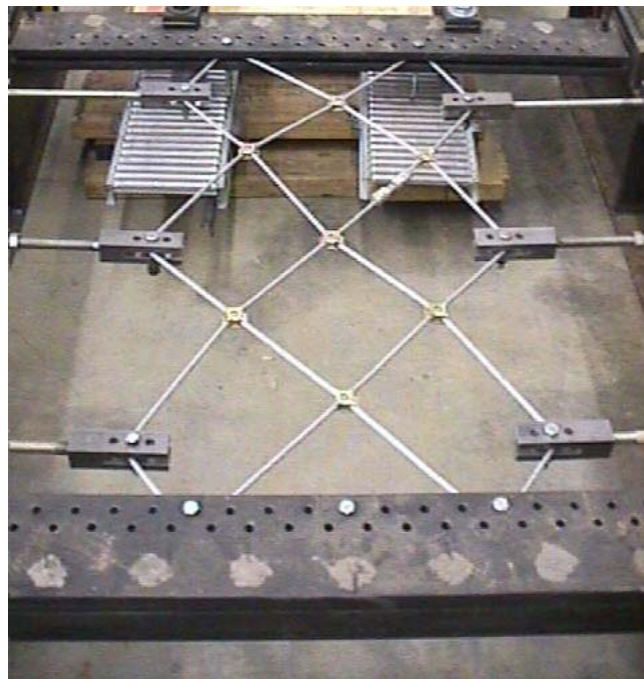


**Figure 3B. Testing Setup for Diagonally Woven Cable Net Mesh from GeoBrugg**

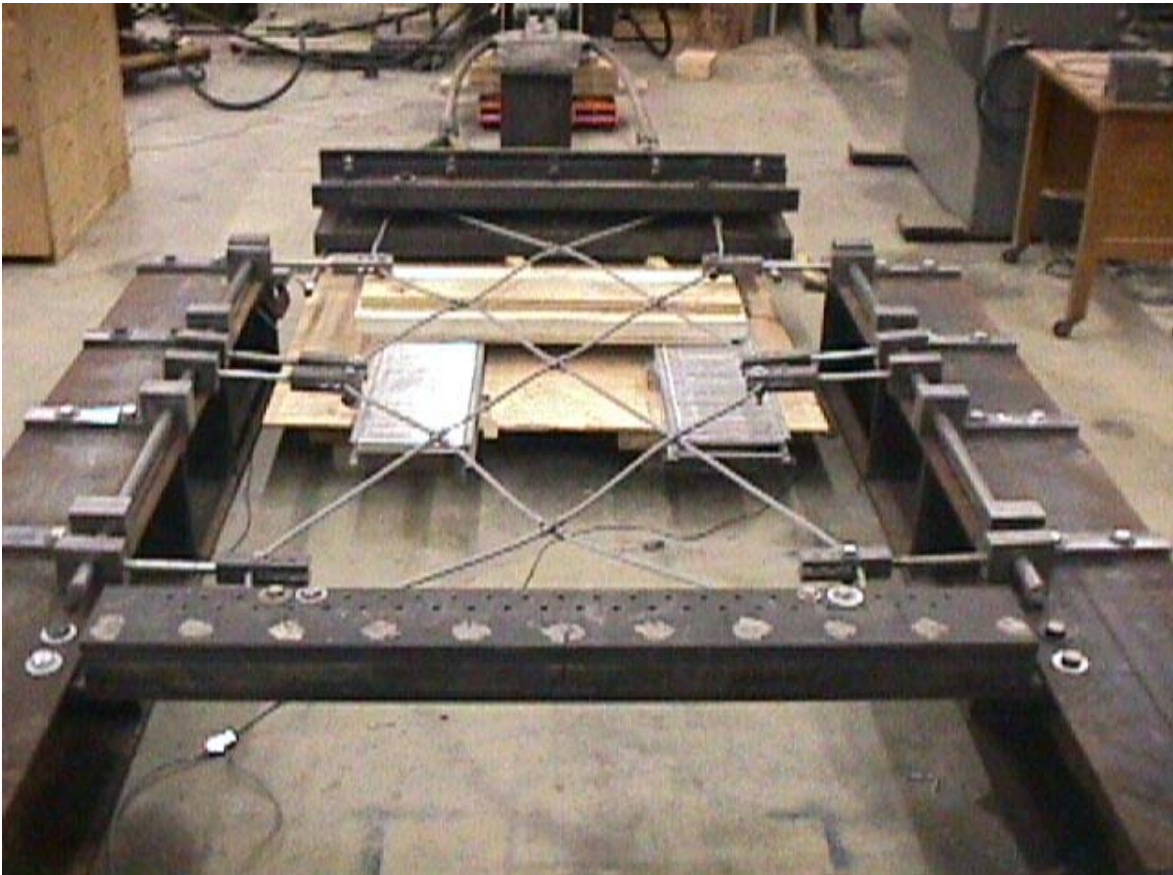


**Figure 4. Testing Setup for Cable Net Mesh from Maccaferri Utilizing Modified Test Apparatus**

## 4. Testing Results

### 4.1. Introduction

Provided in the following sections are results of the tension testing conducted on 16 specimens, which included 8 twisted wire meshes and 8 cable net meshes. Test results are tabulated and descriptions of failures and other relevant information are provided. All testing was conducted as described above, using ASTM A 975 *Standard Specification for Double-Twisted Hexagonal Mesh Gabions and Revet Mattresses (Metallic-Coated Steel Wire or Metallic-Coated Steel Wire with Poly(Vinyl Chloride) (PVC) Coating)* as a general guideline.

### 4.2 Tension Test Results

Testing to determine tensile load test capacity was conducted as described above for each of the provided steel meshes. Figure 5 shows an example of a typical load versus displacement curve from which elastic modulus values were obtained. It should be noted that the data from the initial portions of the load versus displacement curves were neglected when determining elastic modulus values because the initial data was erratic for most specimens due to settling of the specimens within the test fixture as loads were applied. Table 2 provides data on specimen name, ultimate load, elastic modulus, and dimensions used to calculate the elastic modulus for each specimen. Because different specimen types failed in different manners, Section 4.3 provides descriptions of the failures for the steel meshes. Table 3 provides average test values for cases where more than one specimen was tested for the type of mesh tested.

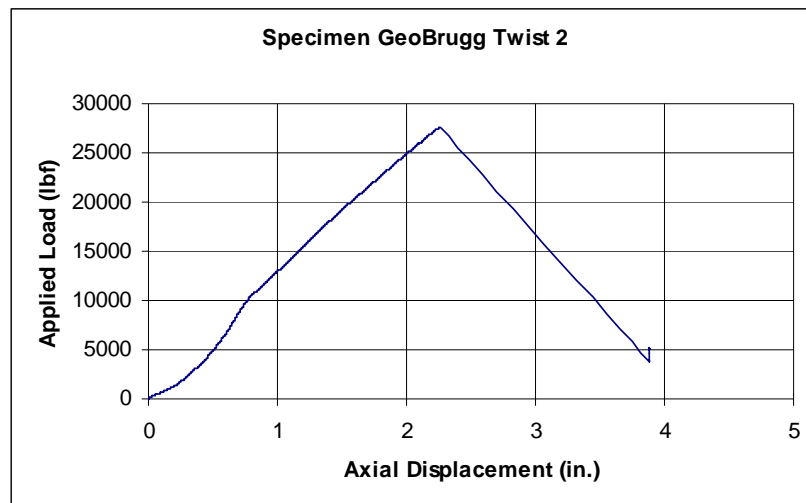


**Figure 5. Testing Typical Load Versus Displacement Plot for Determining Elastic Modulus Values**

**Table 2. Results from Steel Mesh Tension Testing**

<b>Specimen</b>	<b>Ultimate (Maximum) Load (lbs)</b>	<b>Initial Mesh Width (in.)</b>	<b>Initial Mesh Length (in.)</b>	<b>Elastic Modulus (lbs/in.)</b>
GeoBrugg Twist 1	25,500	40.0	40.0	9,880
GeoBrugg Twist 2	28,200	40.0	40.0	12,400
GeoBrugg Twist 3	27,800	40.0	40.0	11,600
Mac Double Galv1	13,000	45.0	42.0	3,820
Mac Double Coat	14,800	45.0	42.0	2,970
Mac Double Narrow	14,100	35.0	43.5	6,010
Mac Narrow Coat1	8,700	35.0	42.5	3,070
Mac Narrow Coat2	7,040	35.0	42.5	1,670
GeoBrugg Square 1	21,400	40.0	40.0	15,900
GeoBrugg Square 2	22,300	40.0	40.0	19,900
GeoBrugg Diagonal 1	19,200	24.0	39.0	11,200
GeoBrugg Diagonal 2	18,800	24.0	39.0	12,000
Mac Cable 1	33,800	31.0	75.5	11,800
Mac Cable 2	32,300	31.0	75.5	12,600
Mac Cable 3	35,200	31.0	75.5	14,900
Mac Cable 4	33,000	31.0	75.5	9,540

**Table 3. Results Averages from Steel Mesh Tension Testing**

<b>Specimen</b>	<b>Ultimate (Maximum) Load (lbs)</b>	<b>Elastic Modulus (lbs/in.)</b>
GeoBrugg Twist	27,200	11,300
GeoBrugg Square	21,900	17,900
GeoBrugg Diagonal	19,000	11,600
Mac Narrow Coat	7,870	2,370
Mac Cable 1	33,600	12,200

### 4.3 Failure Descriptions

Several different failure modes were observed for the different mesh types. The GeoBrugg Twist specimens resisted load steadily then failed due to a breaking of a wire which resulted in a fabric rupture like that shown in Figure 6, at which point a dramatic drop in load was observed and this was considered failure of the specimens. Fabric

rupture for all three GeoBrugg Twist specimens occurred near the ends of the mesh, close to one of the loading plates. All of the Maccaferri twist meshes failed due to breakage of multiple wires making up the meshes. In general, the Maccaferri twist meshes would steadily acquire load up to the maximum, then breakage of individual wires could be heard and the load would drop with each breakage. While there was not a dramatic drop in load for each wire, by the time the actuator reached the maximum stroke length a hole would be visible in the mesh, like that shown in Figure 7. Wire breakage and the subsequent fabric rupture occurred near the ends of the mesh, close to one of the loading plates. The GeoBrugg Cable specimens settled into the test fixture as load was applied and resisted load steadily up to the maximum load. Failure in both square woven specimens and diagonally woven specimen 2 was due to breaking of the cable near the end plate, while diagonally woven specimen 1 failed due to the cable slipping out of the crimps holding the ends of the cable together. Failures for GeoBrugg cable net meshes are shown in Figures 8 and 9. The Maccaferri Cable specimens all failed dramatically at the maximum loads when the cable fractured near the point of attachment to the loading steel as shown in Figure 10. While some of the connections where the cables crossed each other were stretched, there was no evidence of failure to the cable crimps or slippage of the cable through the crimps that hold the cable ends together.



**Figure 6. Typical Failure for GeoBrugg Twist Meshes**

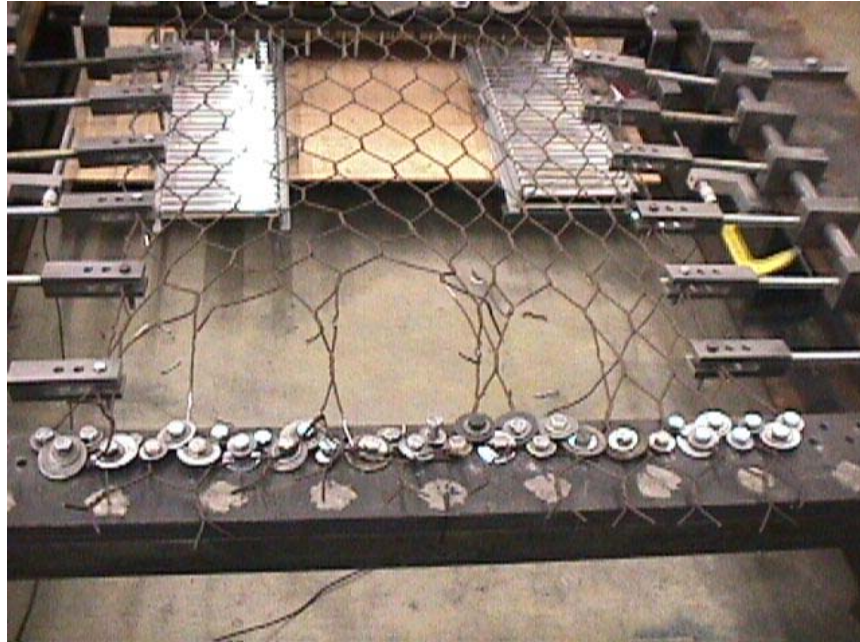


**Figure 7. Typical Failure for Maccaferri Twist Meshes**

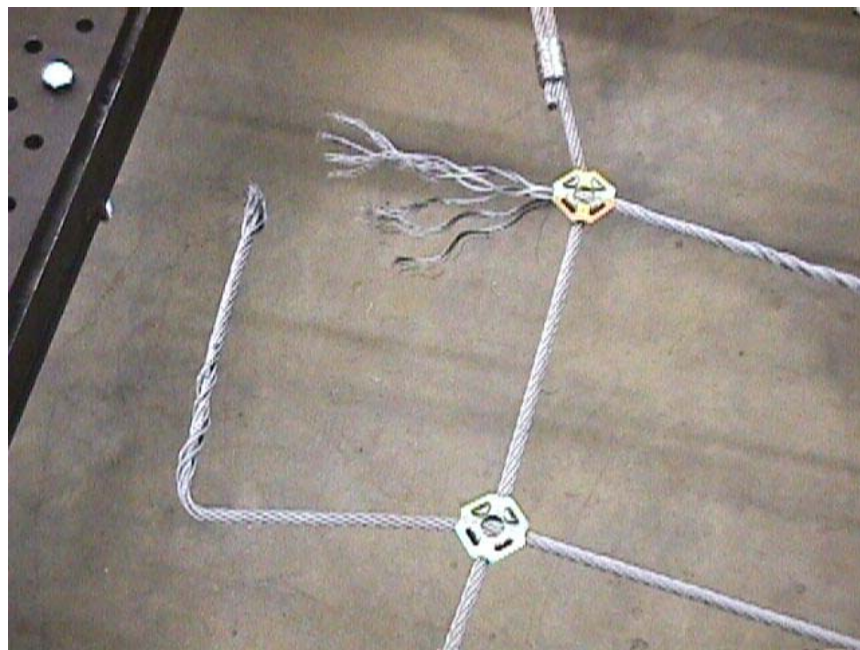


**Figure 8. Cable Breaking Failure of GeoBrugg Cable Specimens**

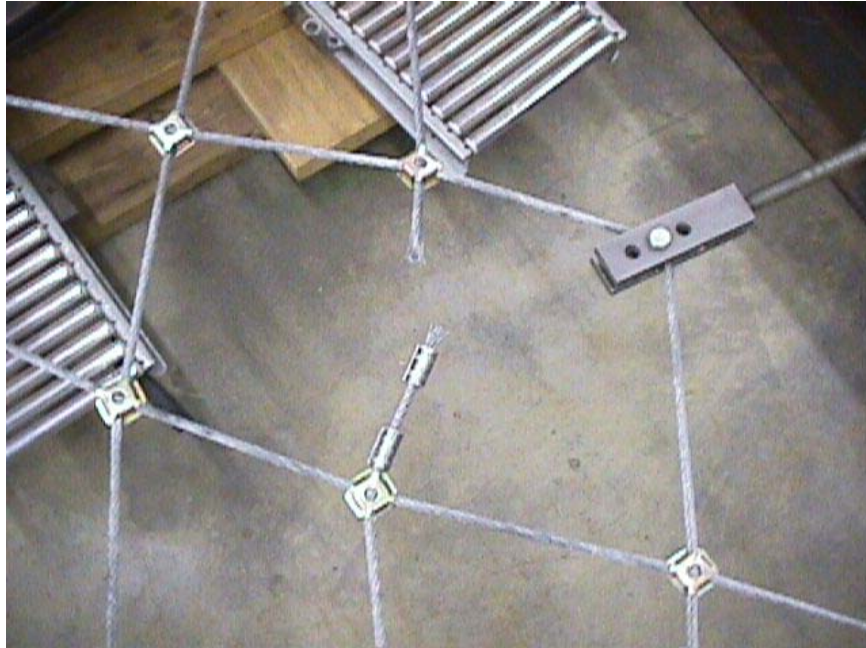


**Figure 9. Cable Slippage Failure of GeoBrugg Cable Specimen**

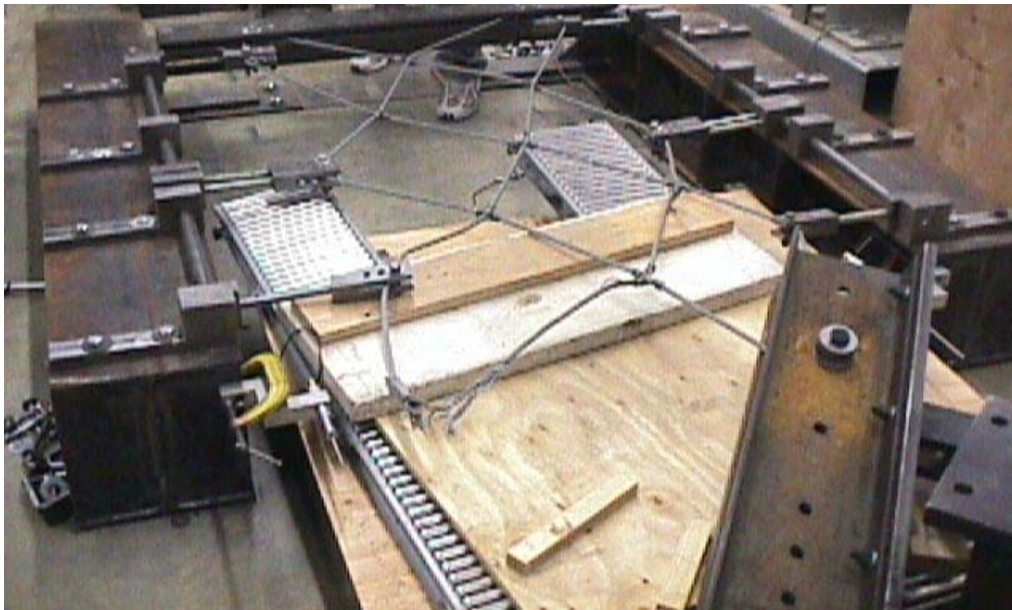


**Figure 10. Typical Cable Failure of Maccaferri Cable Net Specimens**

## 5. Summary

The Wood Materials and Engineering Laboratory (WMEL) at Washington State University in Pullman, WA, performed a total of 16 tension tests on twisted wire mesh and cable net mesh for use as rock fall protection as described above. All specimens were loaded to failure and sufficient data were obtained to determine the ultimate load capacity and modulus of elasticity for the various steel meshes, as provided in the tables above.

Testing was conducted by David M. Carradine with the assistance of Robert W. Duncan, Scott R. Lewis, David F. Dostal, Charles Underwood and Bill Elliot. Testing of the Maccaferri cable meshes was witnessed by Steve Sullivan, a Technical Manager for Maccaferri, Inc. on February 10, 2004. Testing of the GeoBrugg cable meshes was witnessed by Steve Mumma, a Regional Manager for GeoBrugg North America, LLC on April 20, 2004.

Report prepared by:



David M. Carradine, Ph. D.  
Technical Manager

## Report No. WMEL 03-043

# Tensile Capacity Testing of Twisted Wire Mesh and Cable Net Mesh for Use as Rock Fall Protection

## Appendix A

### 1. Introduction

Presented in this appendix are data provided by GeoBrugg regarding the specifications of the twisted wire mesh and cable net mesh specimens tested for the previously discussed testing program at the Washington State University WMEL.

### 2. Material Specifications

#### 2a. GeoBrugg Twist

The twisted wire mesh referred to in the previous report at GeoBrugg Twist was a product the manufacturer labeled as TECCO© steel wire mesh G65/3mm. Provided in Figure A1 below is a data sheet provided by Erik Rorem of GeoBrugg containing the technical specifications for the material tested.

#### 2b. GeoBrugg Square Woven and Diagonally Woven Cable Net

The square woven and diagonally woven cable nets manufactured by GeoBrugg were fabricated utilizing 5/16" diameter Galvanized Aircraft Cable, of 7x19 construction, with a nominal breaking strength of 9,800 lbs, and standard zinc galvanization of 0.10 oz./ft<sup>2</sup>. The square woven nets were based on a 12" x 12" straight weave (square shaped) opening size construction and were made with no perimeter rope. The diagonally woven nets were based on a 12" x 12" diagonal weave (diamond shaped) opening size construction, and were also manufactured with no perimeter rope. The cross-clips which were installed where perpendicular cables crossed one another were fabricated from cold-rolled steel, annealed 0.0940 (min.) x 2.6000, with zinc electroplate coating per ASTM B633, type II SC 3 0.0005 (min.), yellow chromate. The stop sleeves for splices, referred to as cable end crimps in the previous report, were fabricated using 6063-T42 aluminum. Unit weights for both types of nets are typically considered to be 0.503 lbs/ft<sup>2</sup>.

Author: ol  
 Visa: AK  
 Date: 14.01.04  
 Page: 1 / 1

**TECCO® steel wire mesh**  
**G65 / 3 mm**



**TECCO® steel wire mesh G65**

High-performance mesh from high-tensile steel wire for slope stabilizations.

**Technical data**

**TECCO® mesh**

Mesh shape:	diamond
Mesh size:	$x \cdot y = 83 \cdot 143 \text{ mm (+/-3\%)}$
Incircle diameter of mesh:	$D_i = 65 \text{ mm (+/-3\%)}$
Angle of mesh:	$\epsilon = 49 \text{ degrees}$
Total height of mesh:	$h_{tot} = 12.5 \text{ mm (+/-1 mm)}$
Clearance of mesh:	$h_i = 6.5 \text{ mm (+/-1 mm)}$
No. of meshes longitudinal:	$n_l = 7 \text{ pcs/m}$
No. of meshes transversal:	$n_t = 12 \text{ pcs/m}$

**TECCO® steel wire**

Wire diameter:	$d = 3.0 \text{ mm}$
Tensile strength:	$f_y \geq 1770 \text{ N/mm}^2$
Material:	high-tensile carbon steel
Tensile strength of a wire:	$Z_w = 12.5 \text{ kN}$

**TECCO® corrosion protection**

Corrosion protection:	GEOBRUGG SUPERCOATING®
Compound:	95% Zn / 5% Al
Coating:	150 g/m <sup>2</sup>

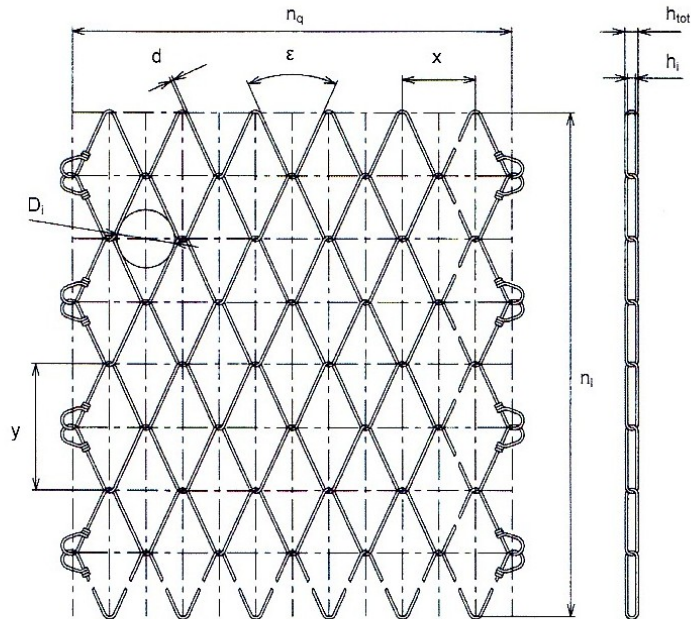
**Load capacity**

Tensile strength of mesh longitudinal:	$z_l = 150 \text{ kN/m'}$
Tensile strength of mesh transversal:	$z_t = 60 \text{ kN/m'}$
Bearing resistance against puncturing:	$D_R = 180 \text{ kN}$
Bearing resistance against shearing-off:	$P_R = 90 \text{ kN}$
Bearing resistance against slope-parallel tensile strain:	$Z_R = 30 \text{ kN}$

**TECCO® mesh standard roll**

Roll width:	$b_{Roll} = 3500 \text{ mm}$
Roll length:	$l_{Roll} = 30 \text{ m}$
Total surface per roll:	$A_{Roll} = 105 \text{ m}^2$
Weight per m <sup>2</sup> :	$g = 1.65 \text{ kg}$
Weight per mesh roll:	$G_{Roll} = 175 \text{ kg}$
Mesh edges:	mesh ends nodded

G65, 3 mm



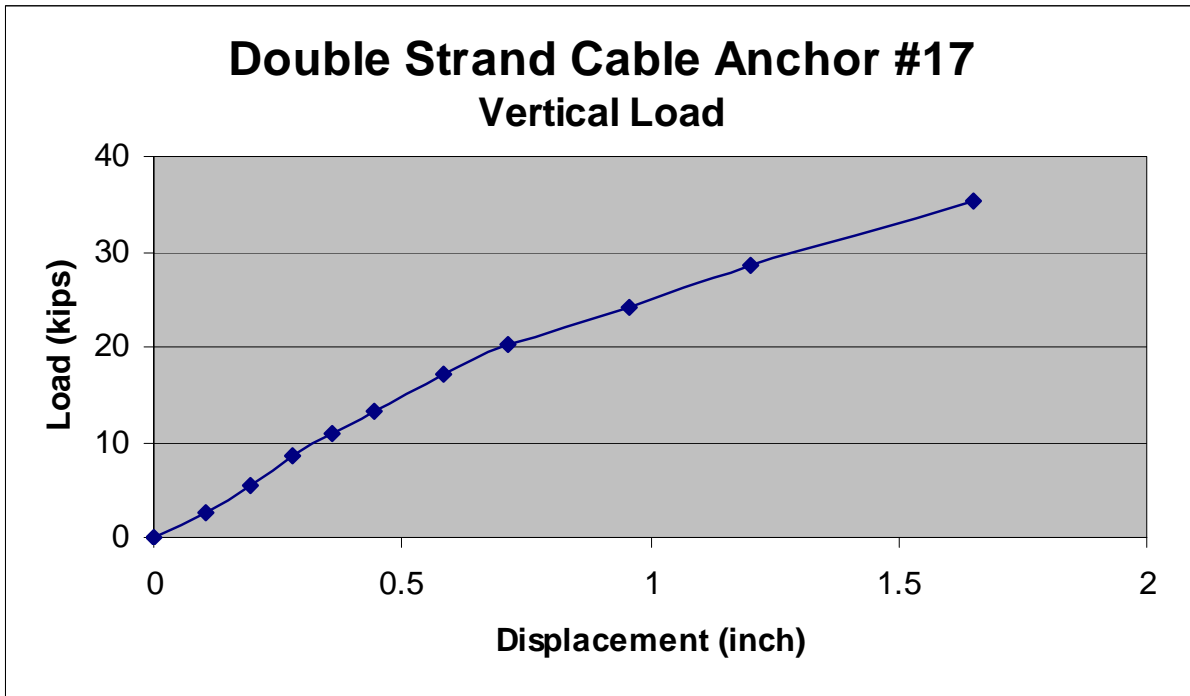
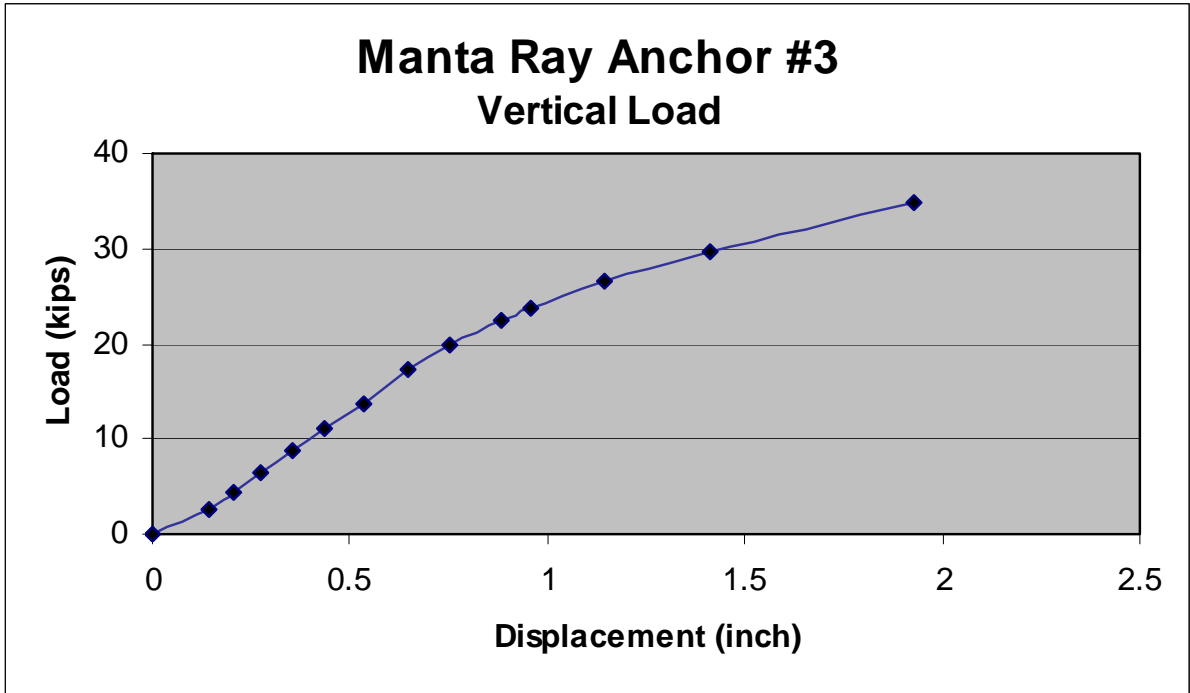
TECCO G65 3mm\_TechData\_140104\_e

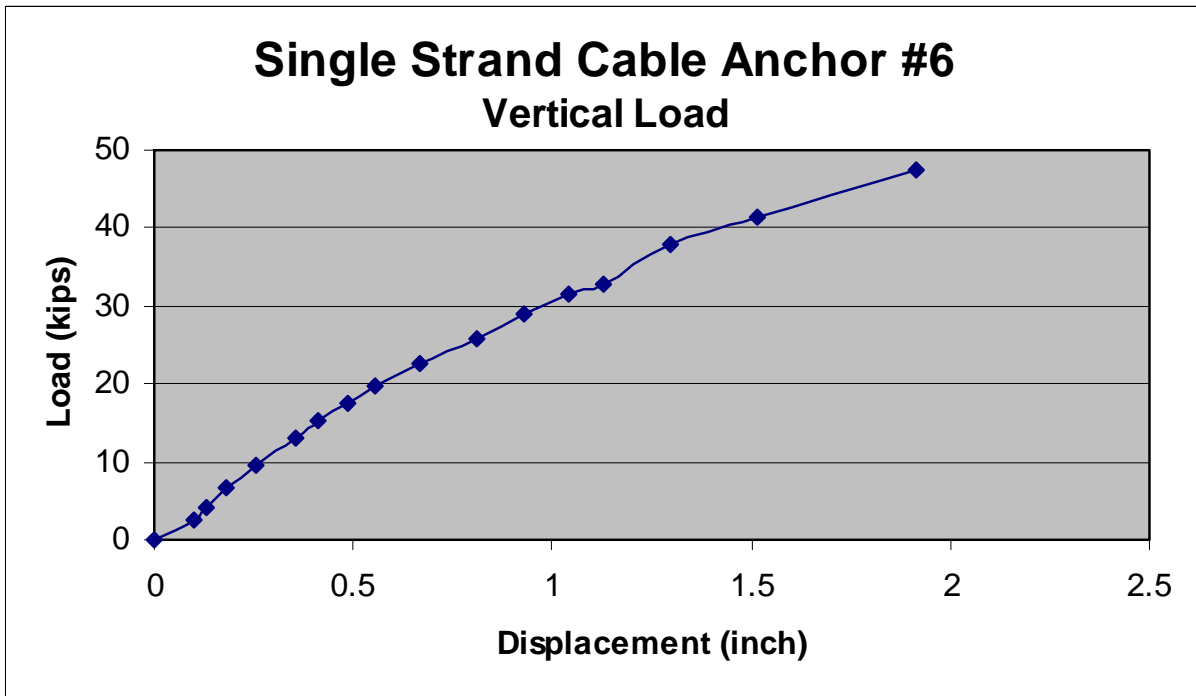
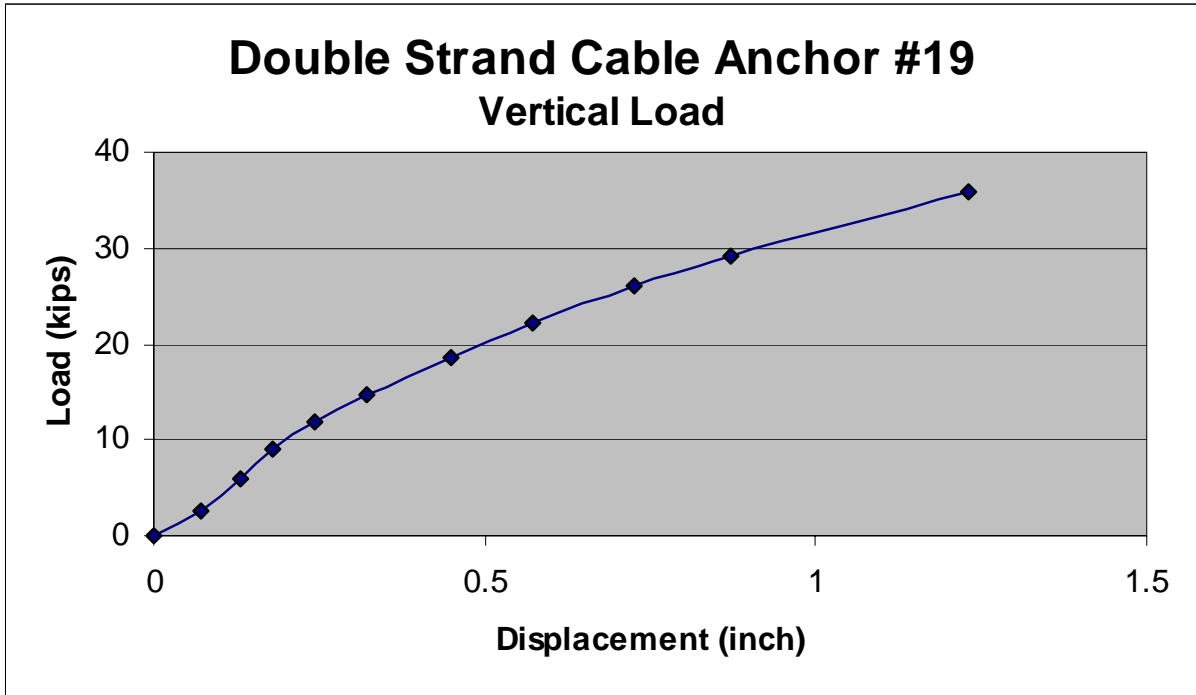
**Figure 1A. Technical Data Sheet Provided by Manufacturer for TECCO® steel wire mesh G65/3mm**

**APPENDIX C**  
**ANCHOR LOAD TEST DATA**

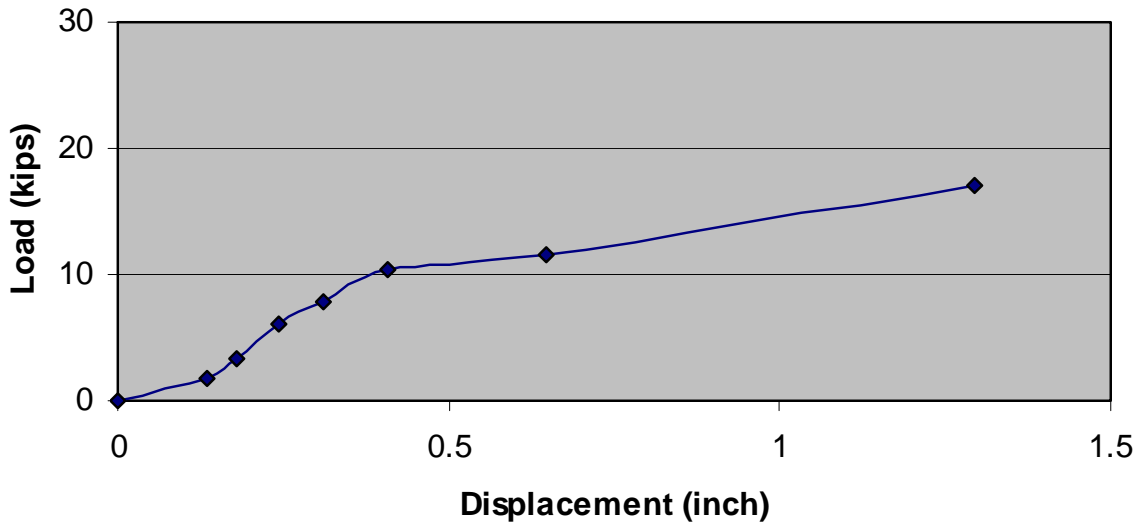
## CONTENTS

Manta Ray Anchor #3 Vertical Load .....	C-3
Double Strand Cable Anchor #17 Vertical Load.....	C-3
Double Strand Cable Anchor #19 Vertical Load.....	C-4
Single Strand Cable Anchor #16 Vertical Load .....	C-4
Single Strand Cable Anchor #15 Vertical Load .....	C-5
Deformed Steel Threaded Bar #7 Vertical Load .....	C-5
HI-TECH Anchor #11 Vertical Load .....	C-6
HI-TECH Anchor #12 Vertical Load .....	C-6
Manta Ray Anchor #2 Horizontal Load.....	C-7
Manta Ray Anchor #4 Horizontal Load.....	C-7
Double Strand Cable Anchor #5 Horizontal Load.....	C-8
Double Strand Cable Anchor #16 Horizontal Load.....	C-8
Single Strand Cable Anchor #18 Horizontal Load .....	C-9
Single Strand Cable Anchor #20 Horizontal Load .....	C-9
Deformed Steel Threaded Bar #9 Horizontal Load .....	C-10
Deformed Steel Threaded Bar #10 Horizontal Load .....	C-10
HI-TECH Anchor #13 Horizontal Load .....	C-11
HI-TECH Anchor #14 Horizontal Load .....	C-11

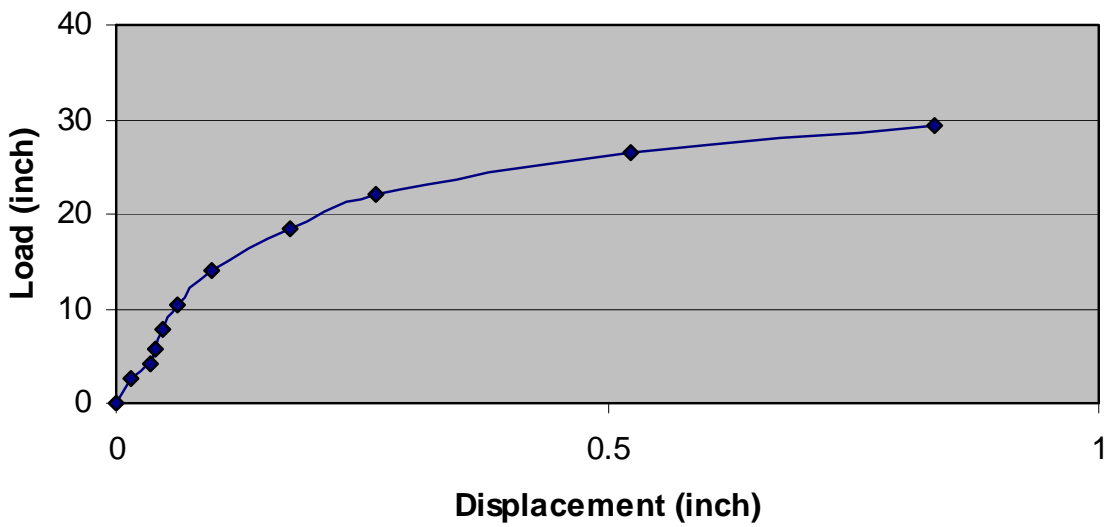


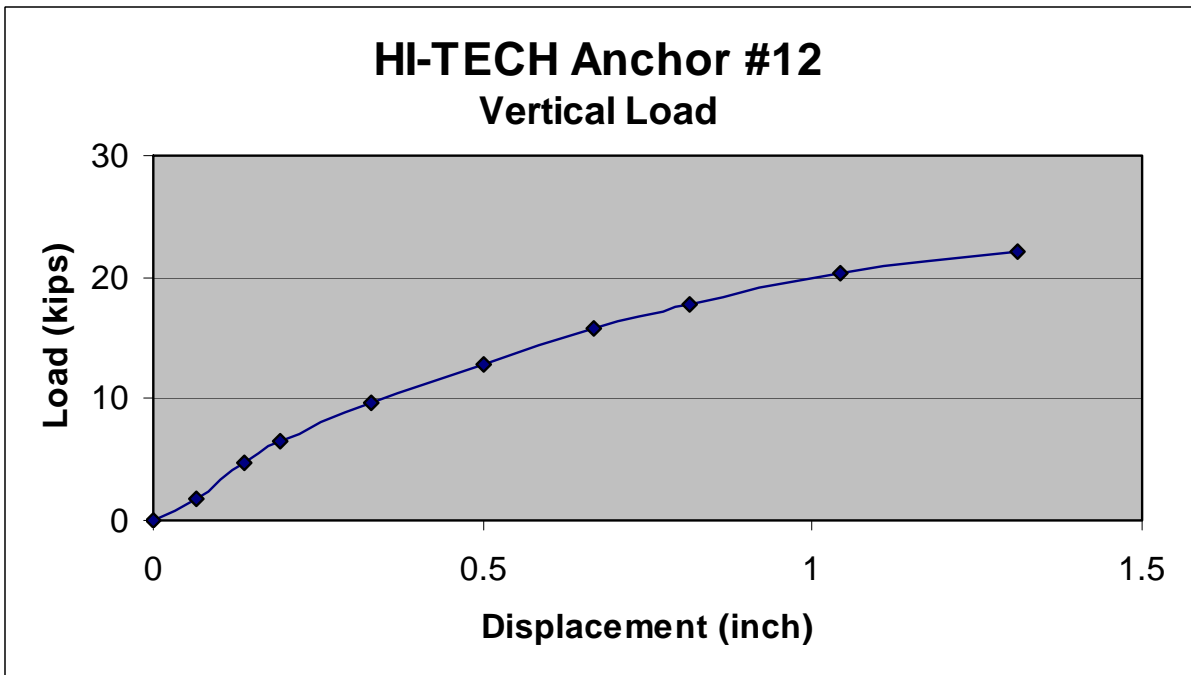
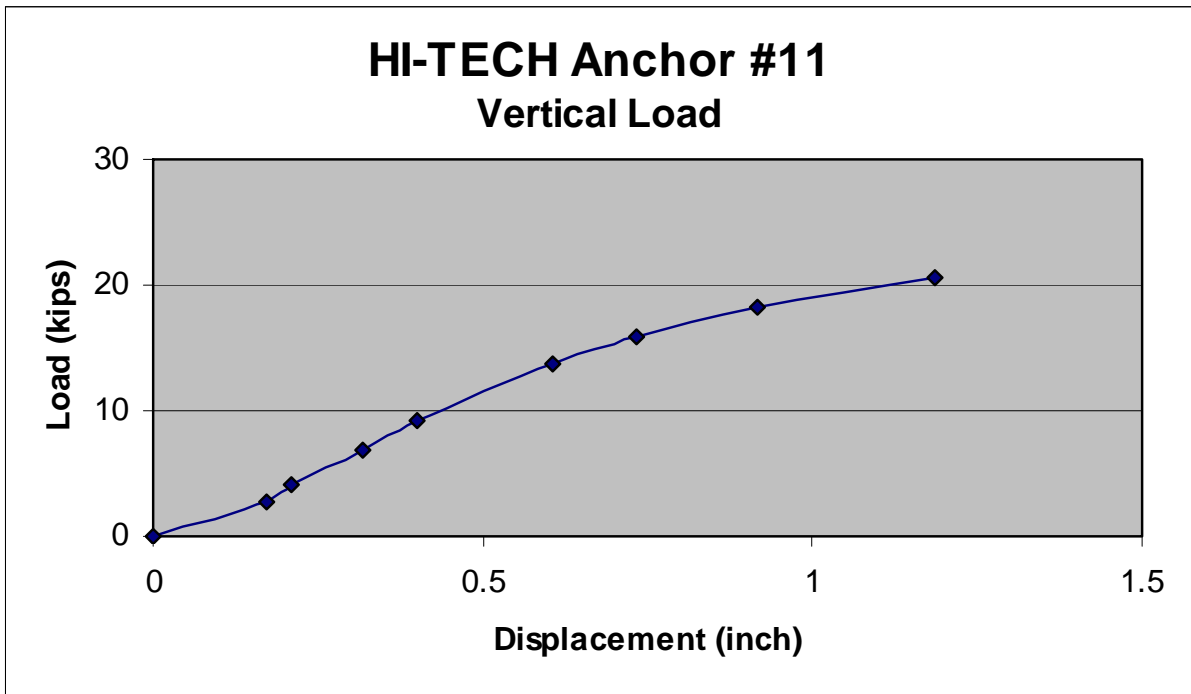


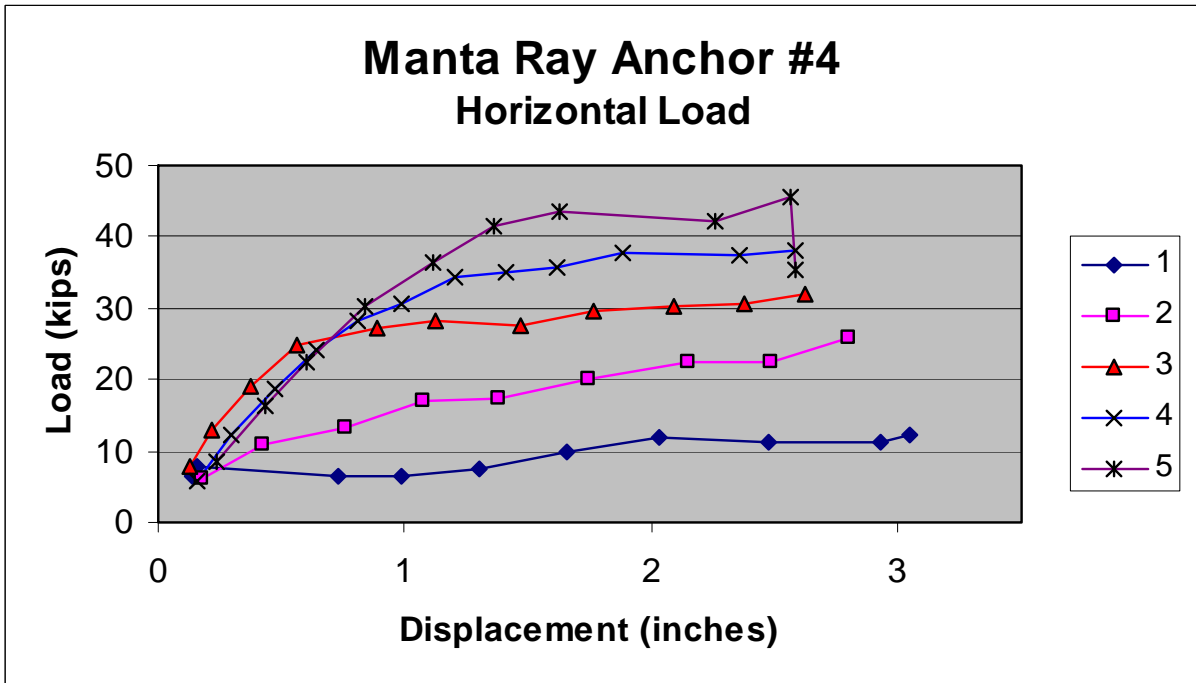
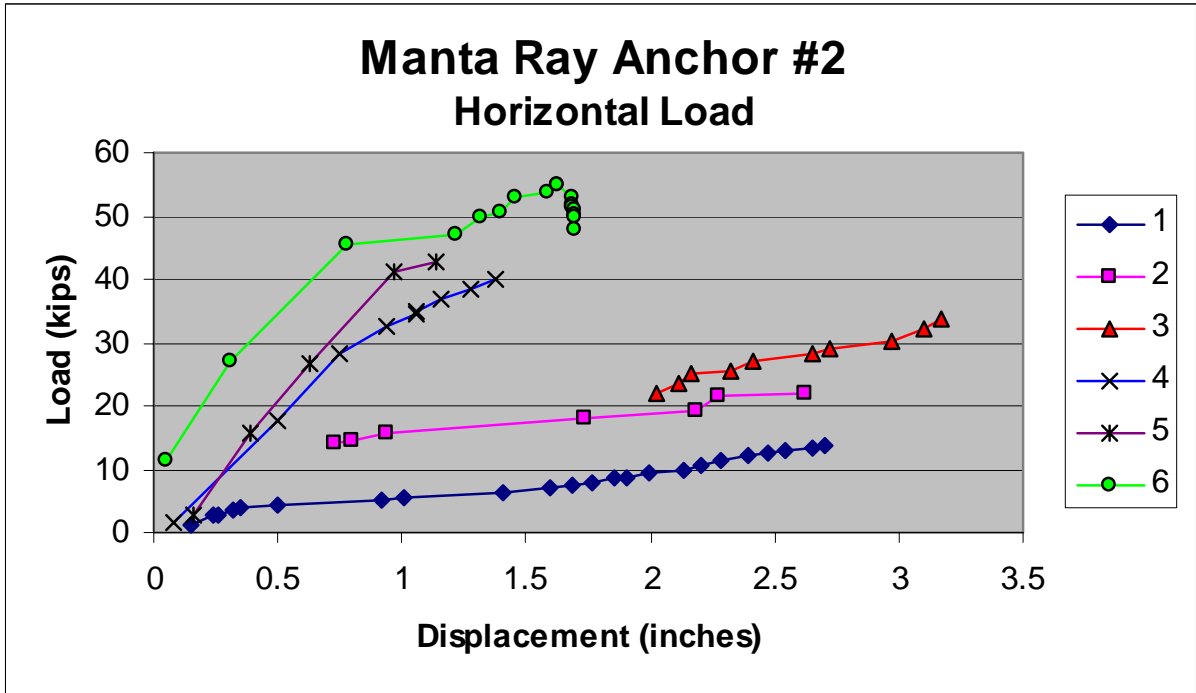
### Single Strand Cable Anchor #15 Vertical Load



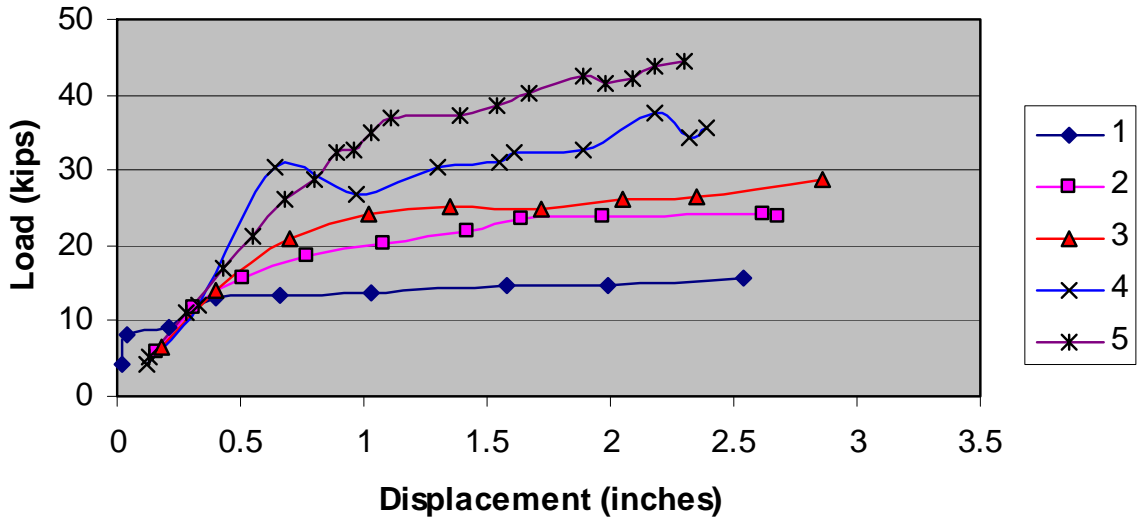
### Deformed Steel Threaded Bar #7 Vertical Load



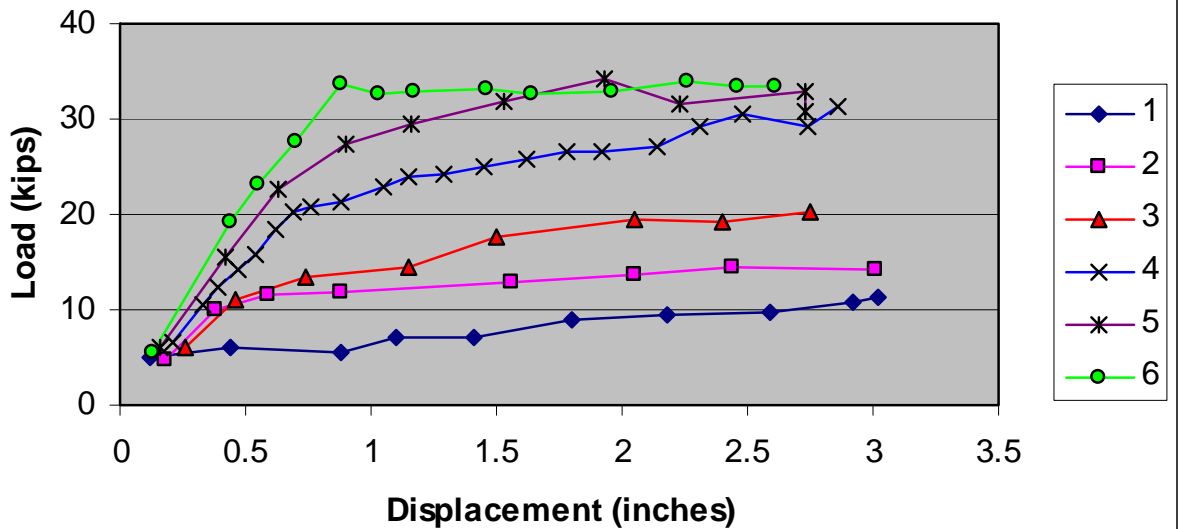




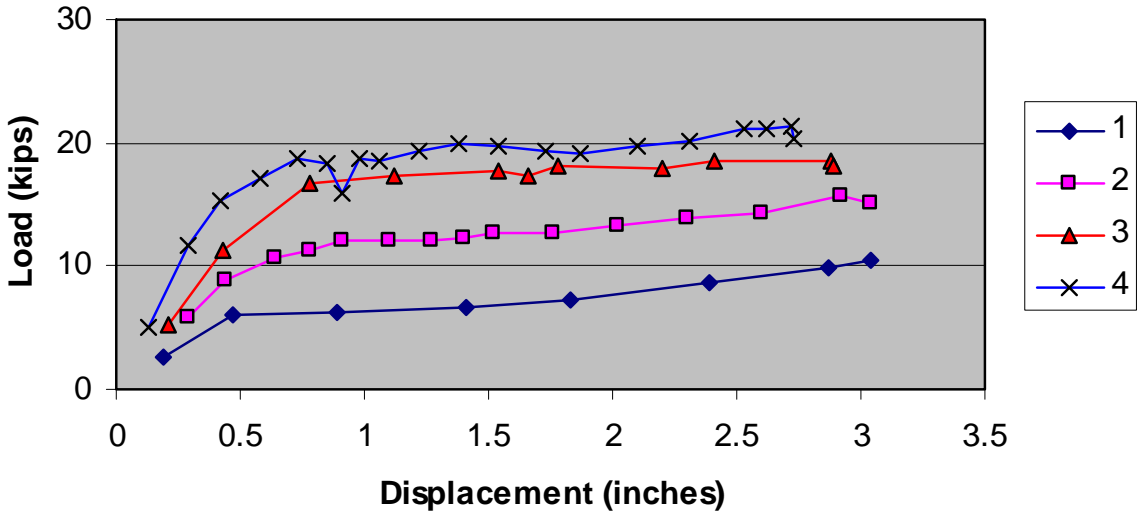
### Double Strand Cable Anchor #5 Horizontal Load



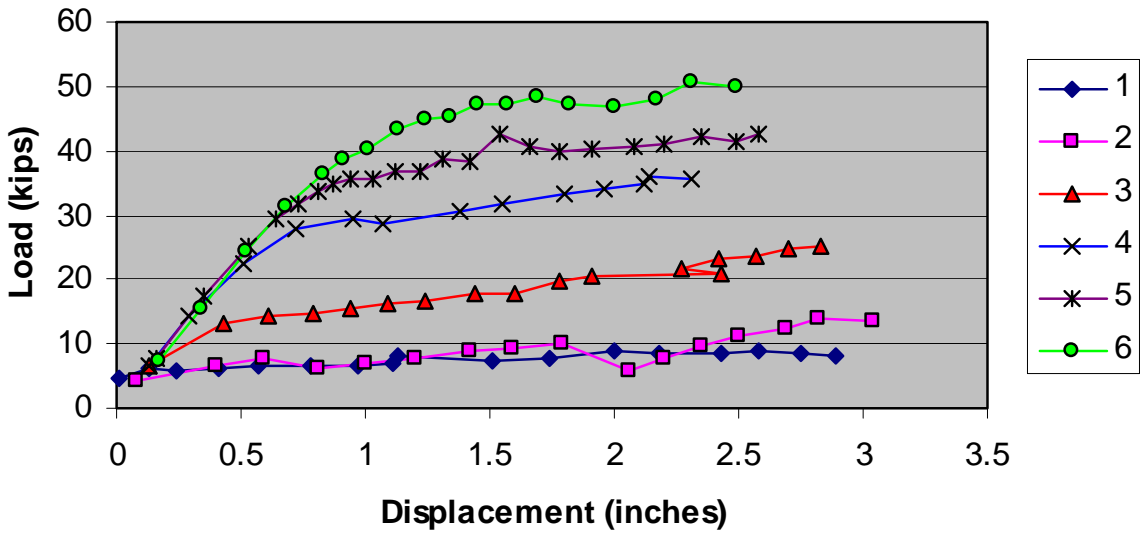
### Double Strand Cable Anchor #16 Horizontal Load

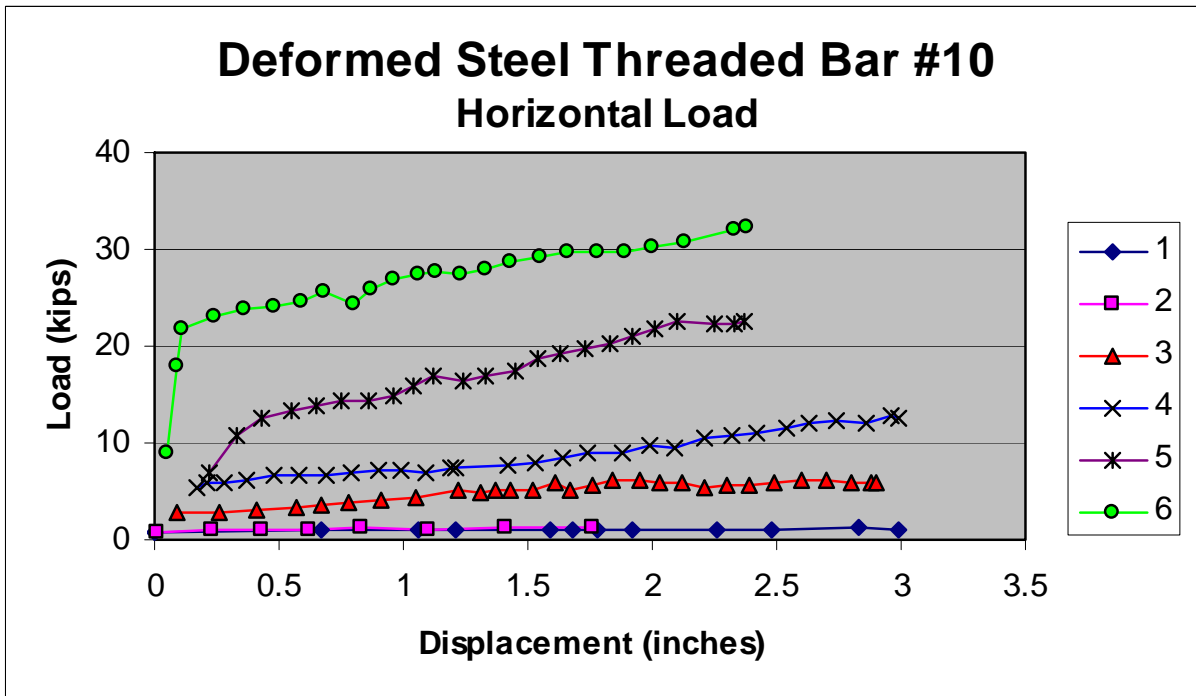
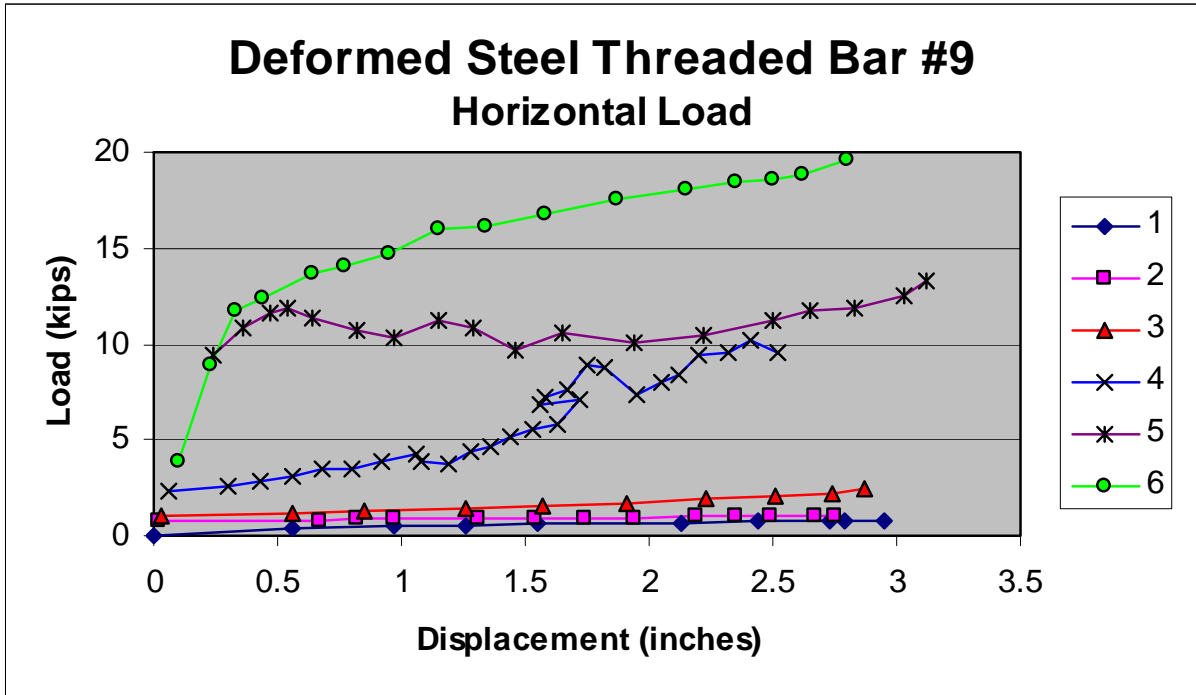


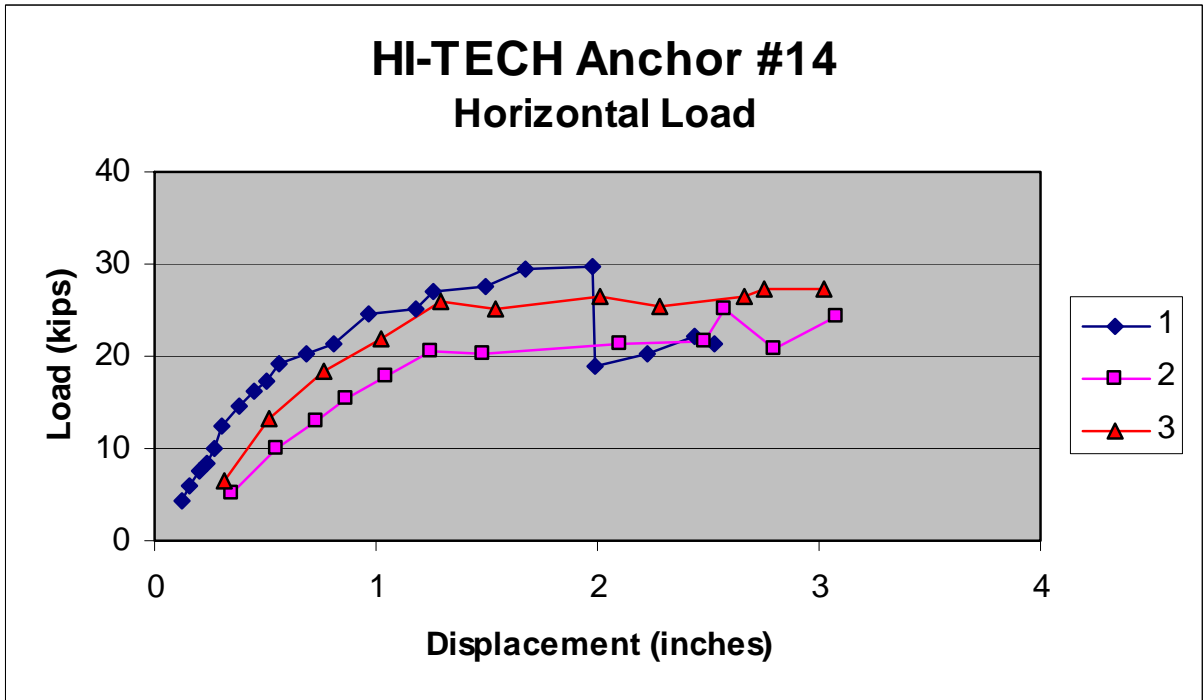
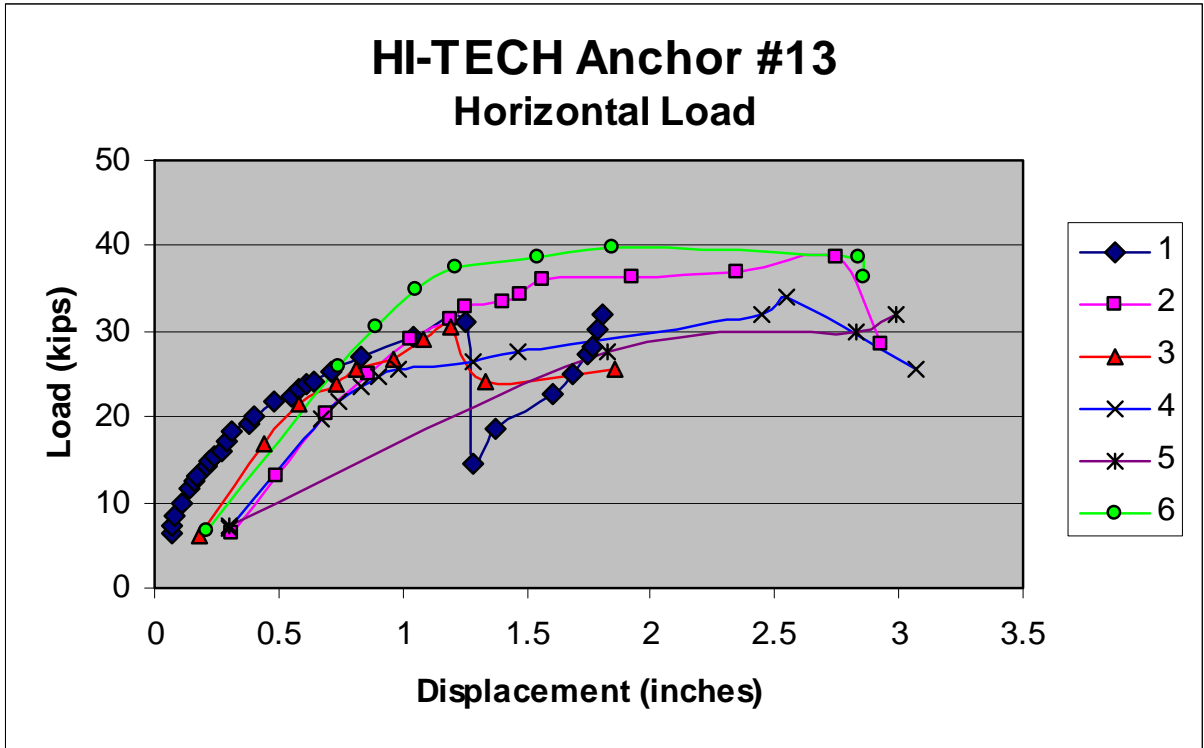
### Single Strand Cable Anchor #18 Horizontal Load



### Single Strand Cable Anchor #20 Horizontal Load









## **APPENDIX D**

### **ANCHOR SPACING/LOAD CHARTS**

## CONTENTS

<i>Figure</i>	<i>Page</i>
D-1 Graph plots anchor load <i>v.</i> spacing for double-twisted hexagonal wire mesh for a planar, 45° slope ranging in height from 50 to 300 ft (15 to 90 m).....	D-3
D-2 Graph plots anchor load <i>v.</i> spacing for double-twisted hexagonal wire mesh for a planar, 60° slope ranging in height from 50 to 300 ft (15 to 90 m).....	D-3
D-3 Graph plots anchor load <i>v.</i> spacing for double-twisted hexagonal wire mesh for an undulating, 45° slope ranging in height from 50 to 300 ft (15 to 90 m)	D-4
D-4 Graph plots anchor load <i>v.</i> spacing for double-twisted hexagonal wire mesh for an undulating, 60° slope ranging in height from 50 to 300 ft (15 to 90 m)	D-4
D-5 Graph plots anchor load <i>v.</i> spacing for double-twisted hexagonal wire mesh for a rough, 45° slope ranging in height from 50 to 300 ft (15 to 90 m) .....	D-5
D-6 Graph plots anchor load <i>v.</i> spacing for double-twisted hexagonal wire mesh for a rough, 60° slope ranging in height from 50 to 300 ft (15 to 90 m) .....	D-5
D-7 Graph plots anchor load <i>v.</i> spacing for TECCO <sup>®</sup> mesh for a planar, 45° slope ranging in height from 50 to 300 ft (15 to 90 m).....	D-6
D-8 Graph plots anchor load <i>v.</i> spacing for TECCO <sup>®</sup> mesh for a planar, 60° slope ranging in height from 50 to 300 ft (15 to 90 m).....	D-6
D-9 Graph plots anchor load <i>v.</i> spacing for TECCO <sup>®</sup> mesh for an undulating, 45° slope ranging in height from 50 to 300 ft (15 to 90 m).....	D-7
D-10 Graph plots anchor load <i>v.</i> spacing for TECCO <sup>®</sup> mesh for an undulating, 60° slope ranging in height from 50 to 300 ft (15 to 90 m).....	D-7
D-11 Graph plots anchor load <i>v.</i> spacing for TECCO <sup>®</sup> mesh for a rough, 45° slope ranging in height from 50 to 300 ft (15 to 90 m).....	D-8
D-12 Graph plots anchor load <i>v.</i> spacing for TECCO <sup>®</sup> mesh for a rough, 60° slope ranging in height from 50 to 300 ft (15 to 90 m).....	D-8
D-13 Graph plots anchor load <i>v.</i> spacing for cable nets for a planar, 45° slope ranging in height from 50 to 300 ft (15 to 90 m).....	D-9
D-14 Graph plots anchor load <i>v.</i> spacing for cable nets for a planar, 60° slope ranging in height from 50 to 300 ft (15 to 90 m).....	D-9
D-15 Graph plots anchor load <i>v.</i> spacing for cable nets for an undulating, 45° slope ranging in height from 50 to 300 ft (15 to 90 m).....	D-10
D-16 Graph plots anchor load <i>v.</i> spacing for cable nets for an undulating, 60° slope ranging in height from 50 to 300 ft (15 to 90 m).....	D-10
D-17 Graph plots anchor load <i>v.</i> spacing for cable nets for a rough, 45° slope ranging in height from 50 to 300 ft (15 to 90 m).....	D-11
D-18 Graph plots anchor load <i>v.</i> spacing for cable nets for a rough, 60° slope ranging in height from 50 to 300 ft (15 to 90 m).....	D-11

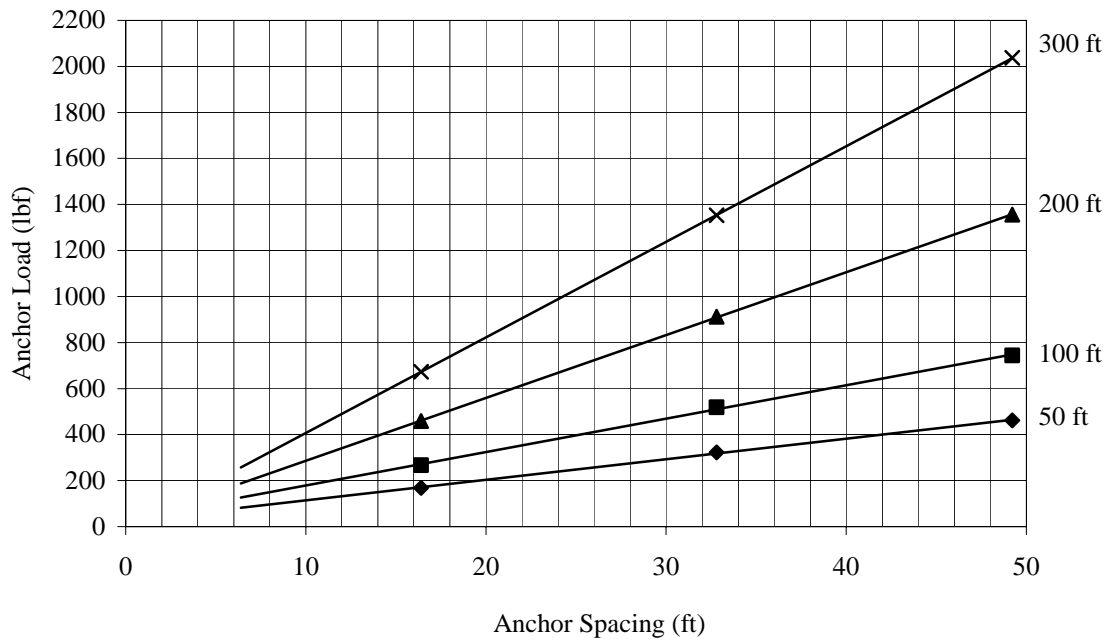


Figure D-1. Graph plots anchor load v. spacing for double-twisted hexagonal wire mesh for a planar, 45° slope ranging in height from 50 to 300 ft (15 to 90 m).

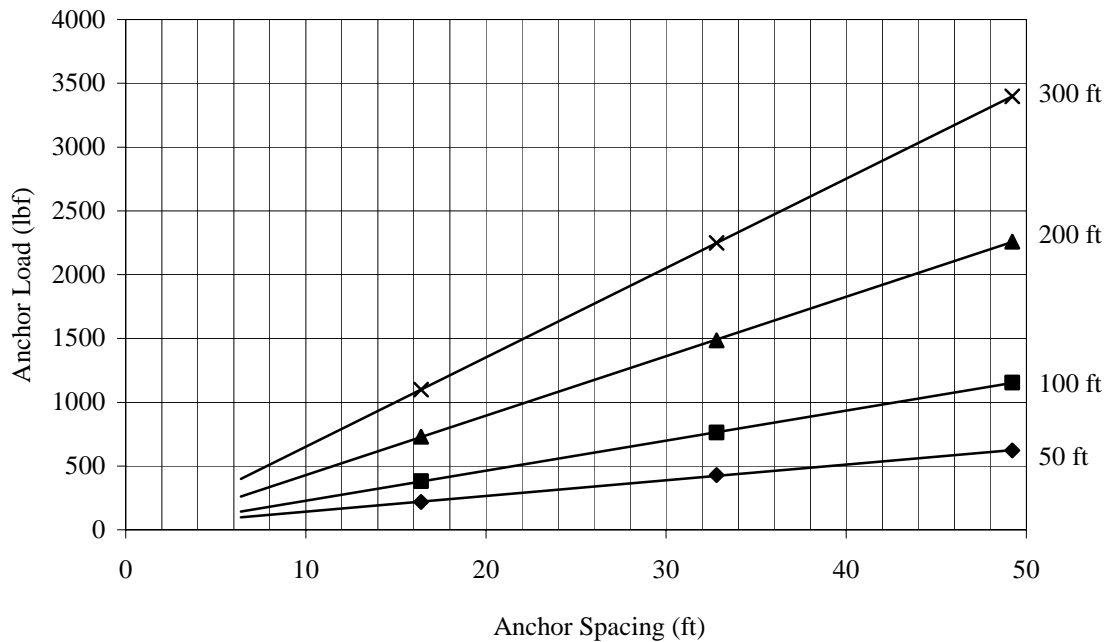


Figure D-2. Graph plots anchor load v. spacing for double-twisted hexagonal wire mesh for a planar, 60° slope ranging in height from 50 to 300 ft (15 to 90 m).

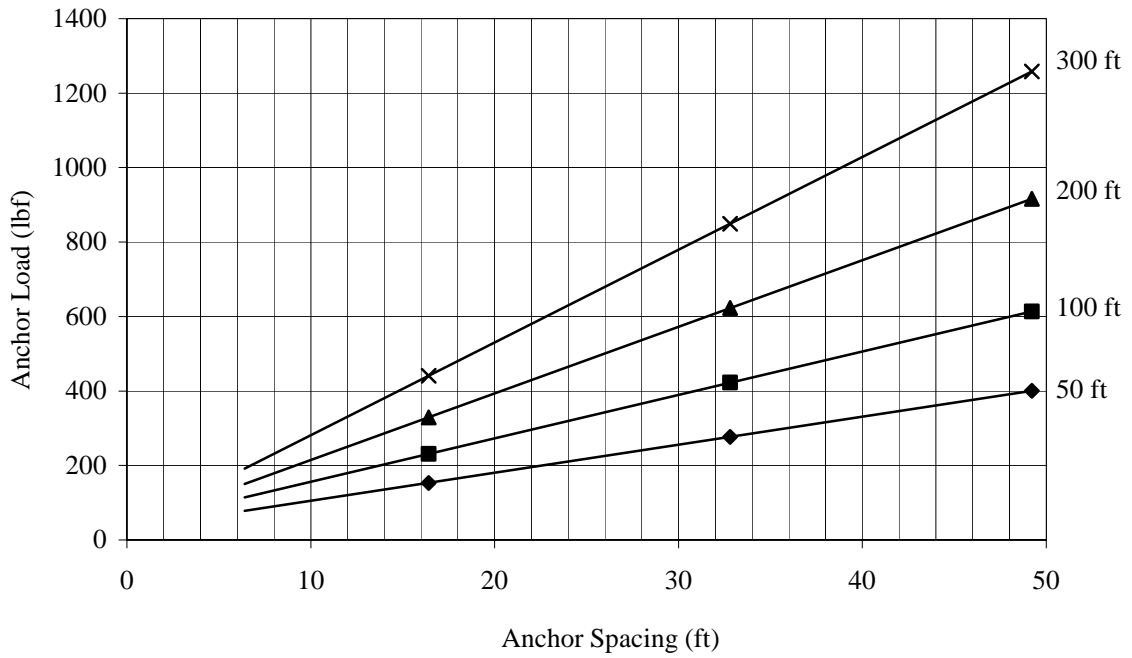


Figure D-3. Graph plots anchor load v. spacing for double-twisted hexagonal wire mesh for an undulating, 45° slope ranging in height from 50 to 300 ft (15 to 90 m).

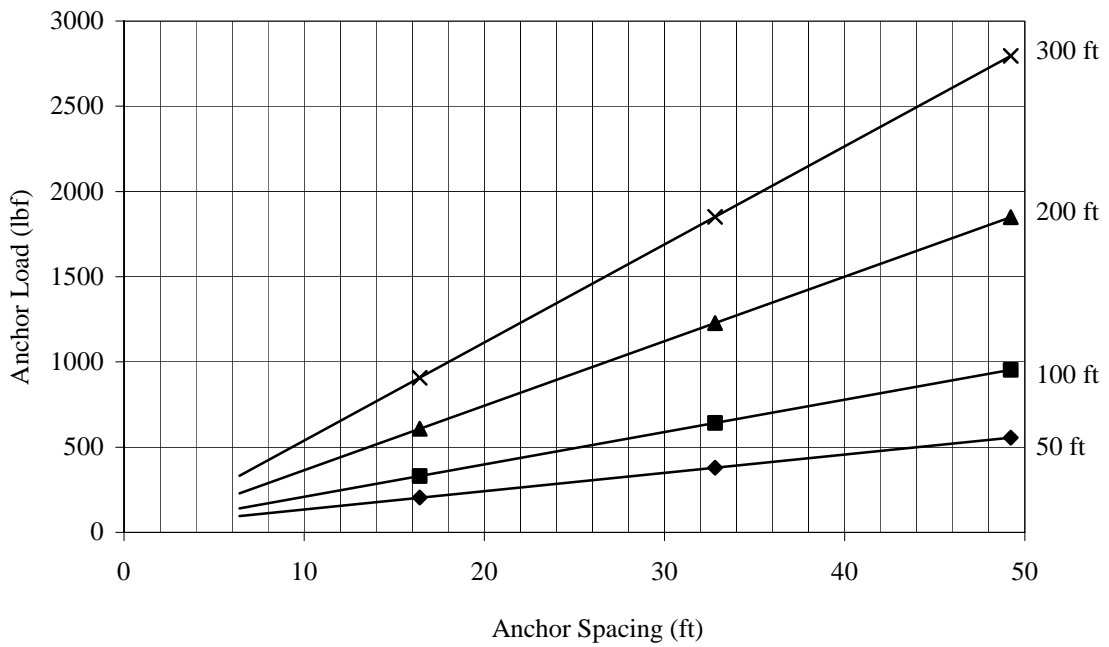


Figure D-4. Graph plots anchor load v. spacing for double-twisted hexagonal wire mesh for an undulating, 60° slope ranging in height from 50 to 300 ft (15 to 90 m).

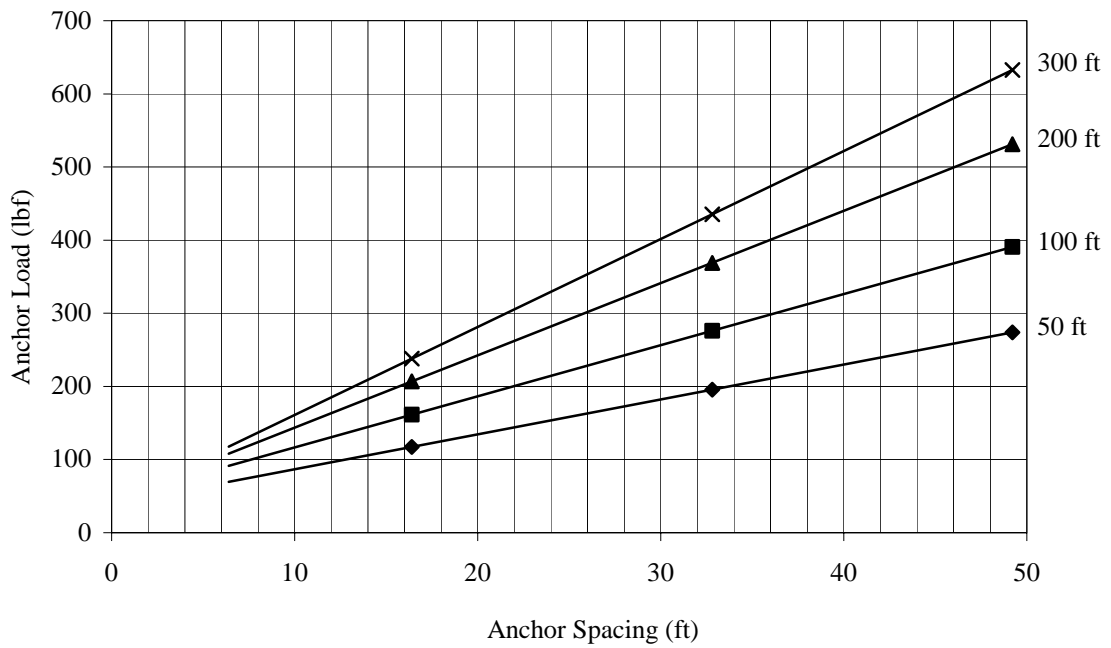


Figure D-5. Graph plots anchor load v. spacing for double-twisted hexagonal wire mesh for a rough, 45° slope ranging in height from 50 to 300 ft (15 to 90 m).

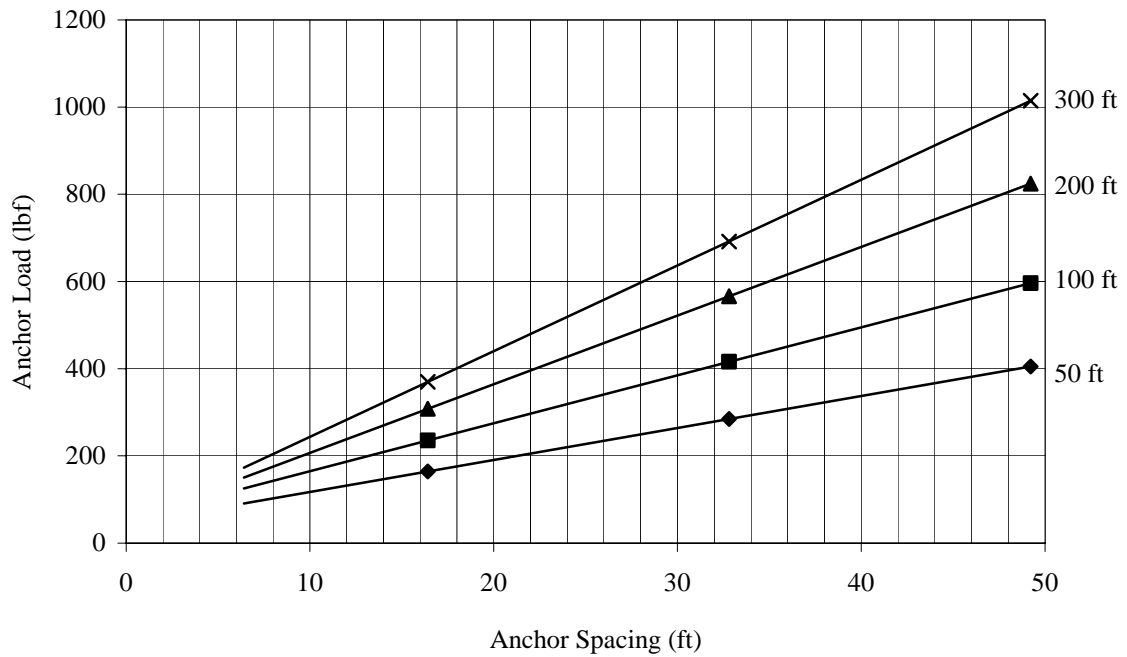


Figure D-6. Graph plots anchor load v. spacing for double-twisted hexagonal wire mesh for a rough, 60° slope ranging in height from 50 to 300 ft (15 to 90 m).

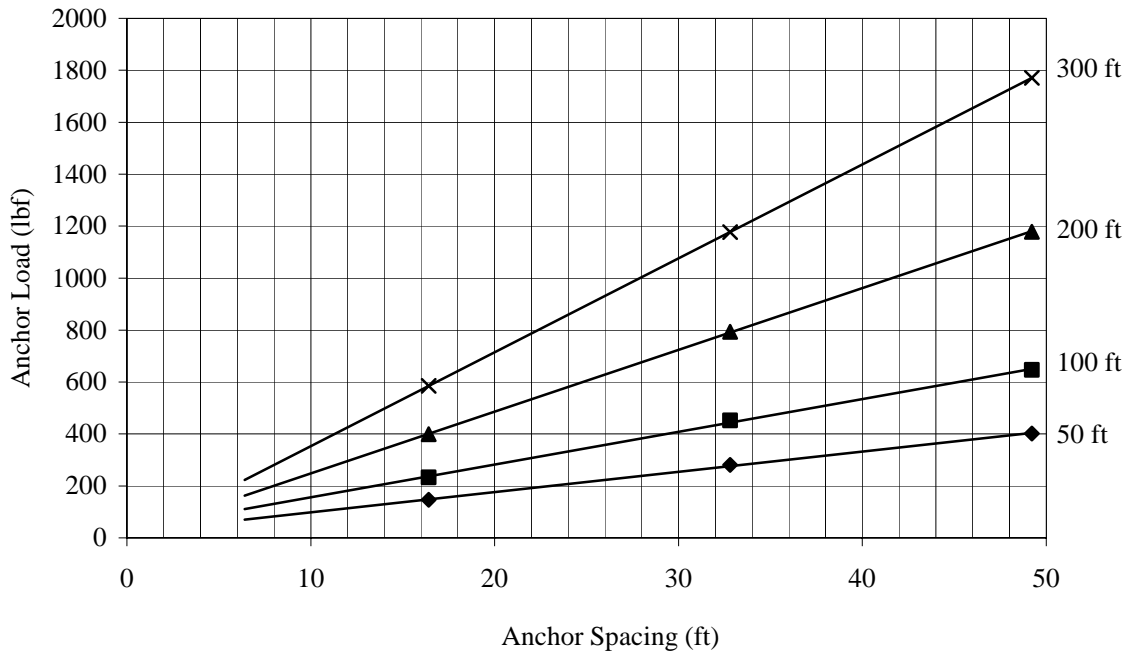


Figure D-7. Graph plots anchor load v. spacing for TECCO® mesh for a planar, 45° slope ranging in height from 50 to 300 ft (15 to 90 m).

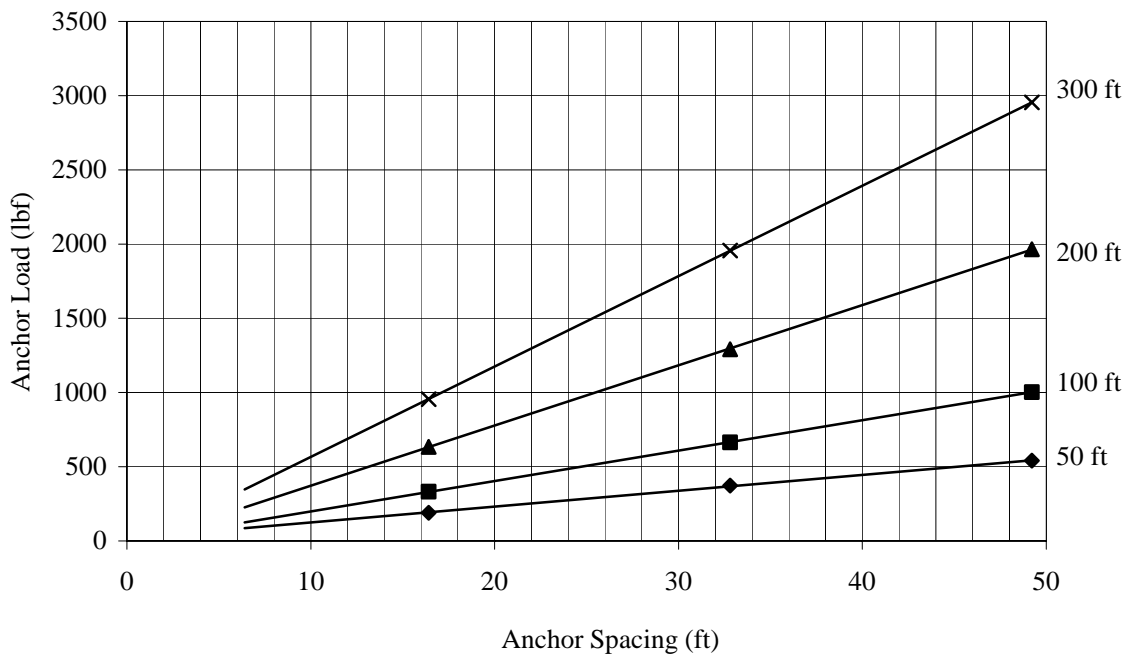


Figure D-8. Graph plots anchor load v. spacing for TECCO® mesh for a planar, 60° slope ranging in height from 50 to 300 ft (15 to 90 m).

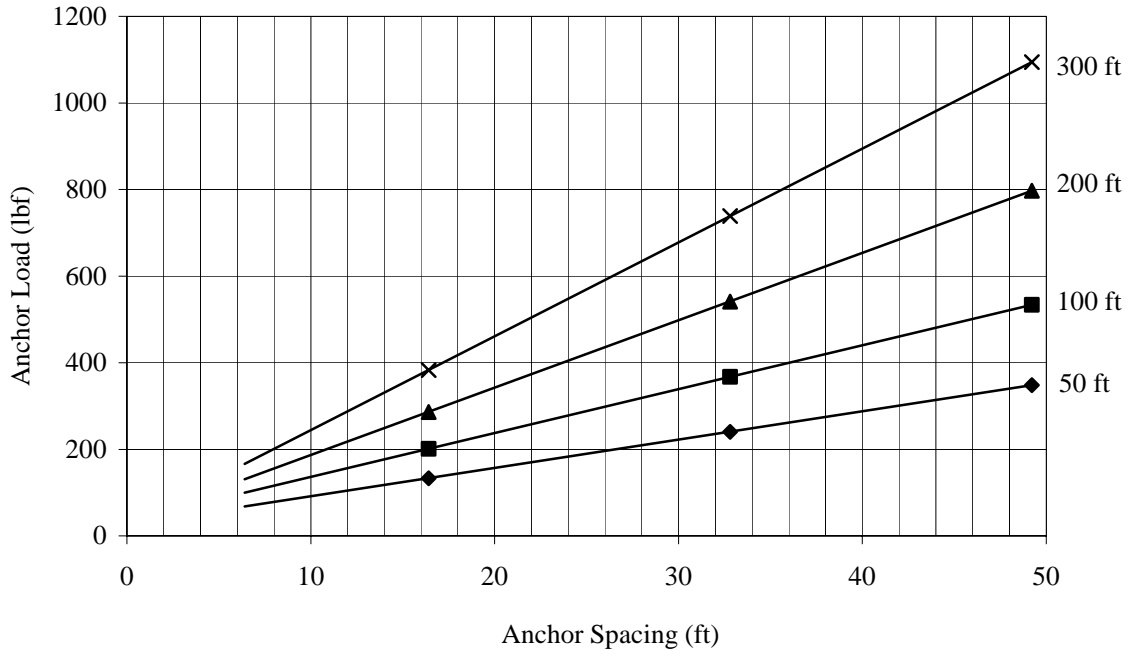


Figure D-9. Graph plots anchor load v. spacing for TECCO® mesh for an undulating, 45° slope ranging in height from 50 to 300 ft (15 to 90 m).

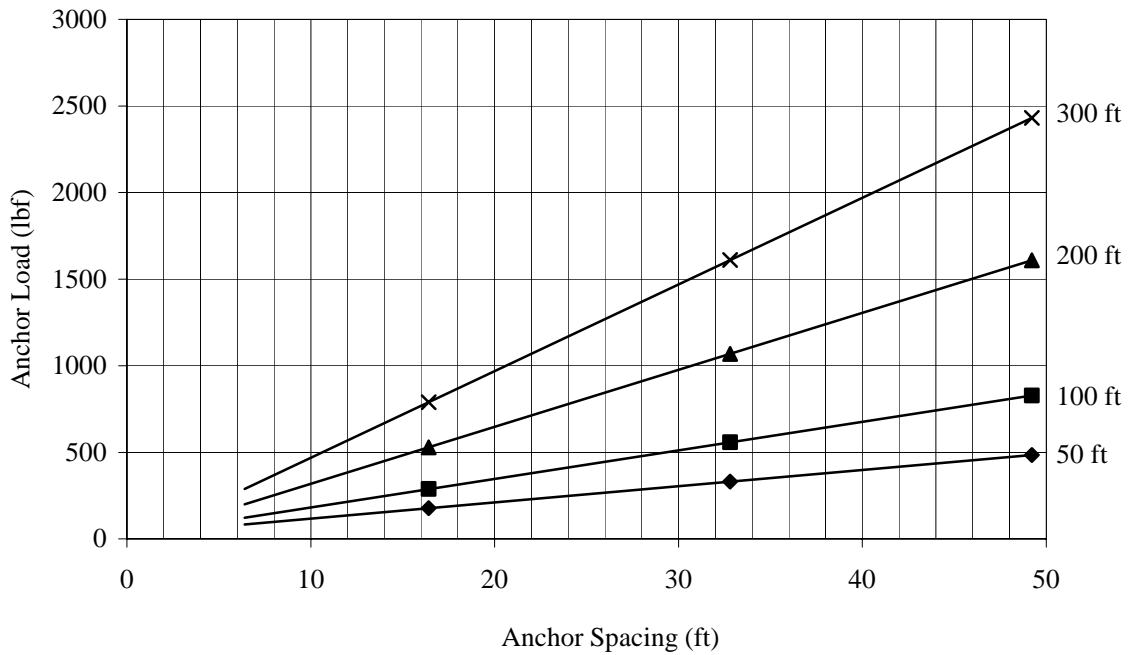


Figure D-10. Graph plots anchor load v. spacing for TECCO® mesh for an undulating, 60° slope ranging in height from 50 to 300 ft (15 to 90 m).

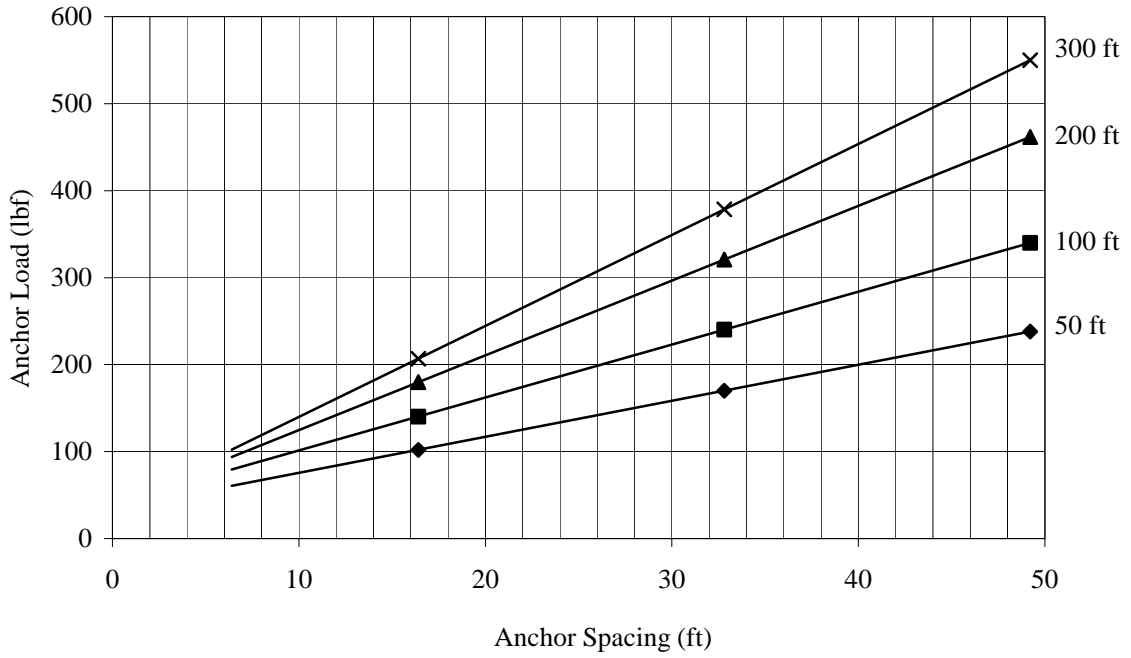


Figure D-11. Graph plots anchor load v. spacing for TECCO® mesh for a rough, 45° slope ranging in height from 50 to 300 ft (15 to 90 m).

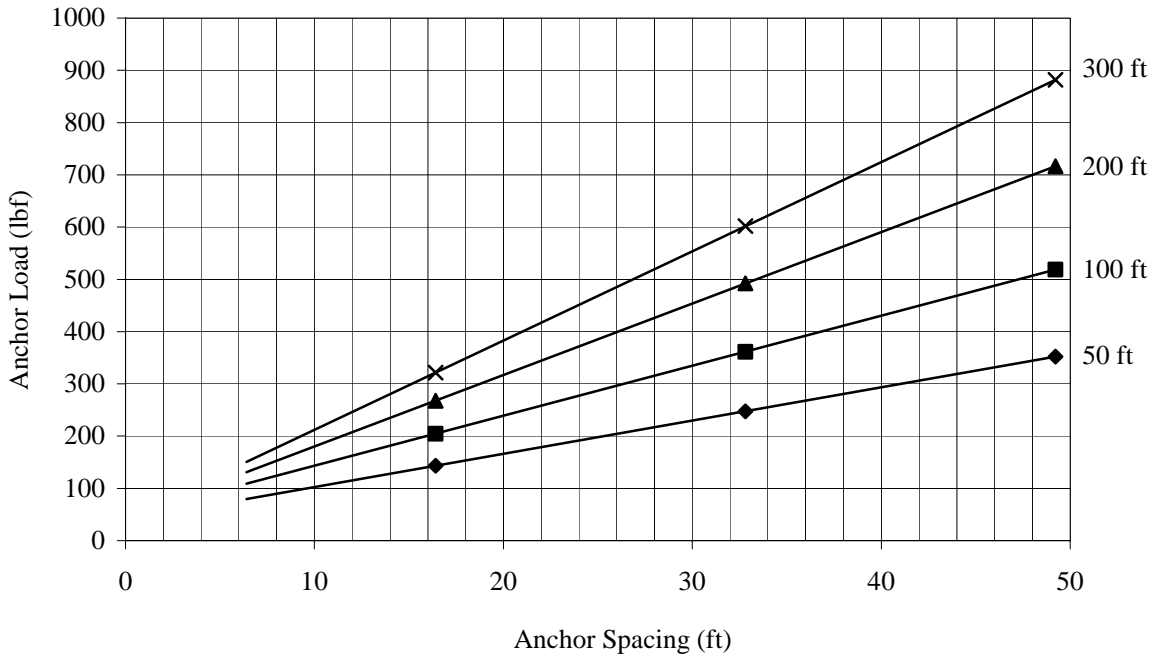


Figure D-12. Graph plots anchor load v. spacing for TECCO® mesh for a rough, 60° slope ranging in height from 50 to 300 ft (15 to 90 m).

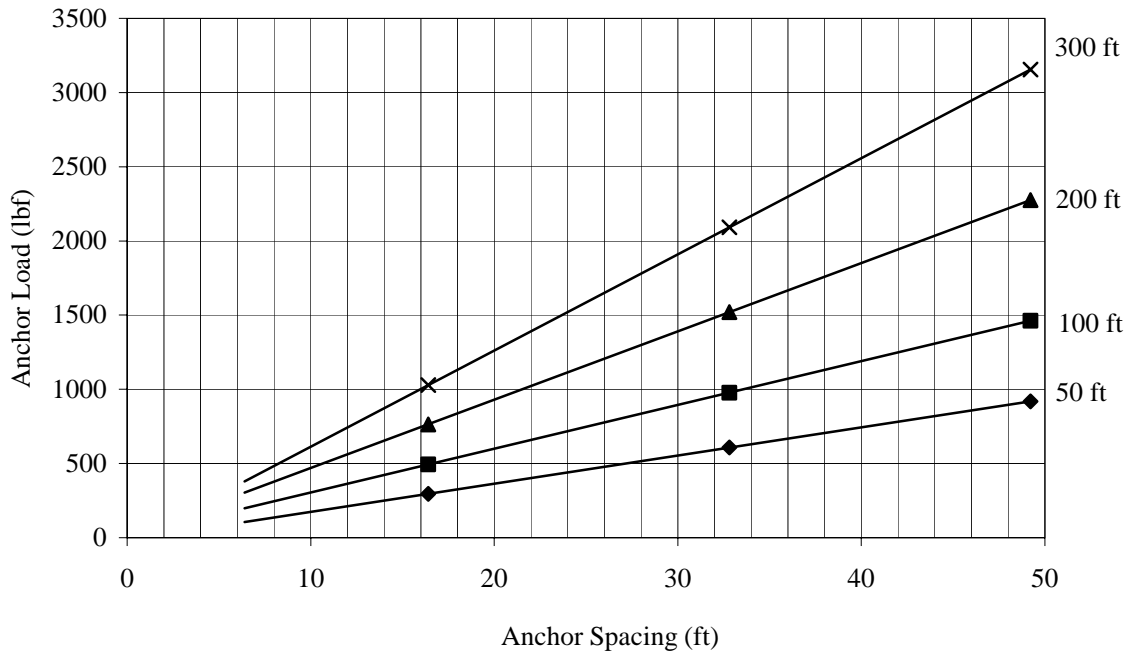


Figure D-13. Graph plots anchor load v. spacing for cable nets for a planar, 45° slope ranging in height from 50 to 300 ft (15 to 90 m).

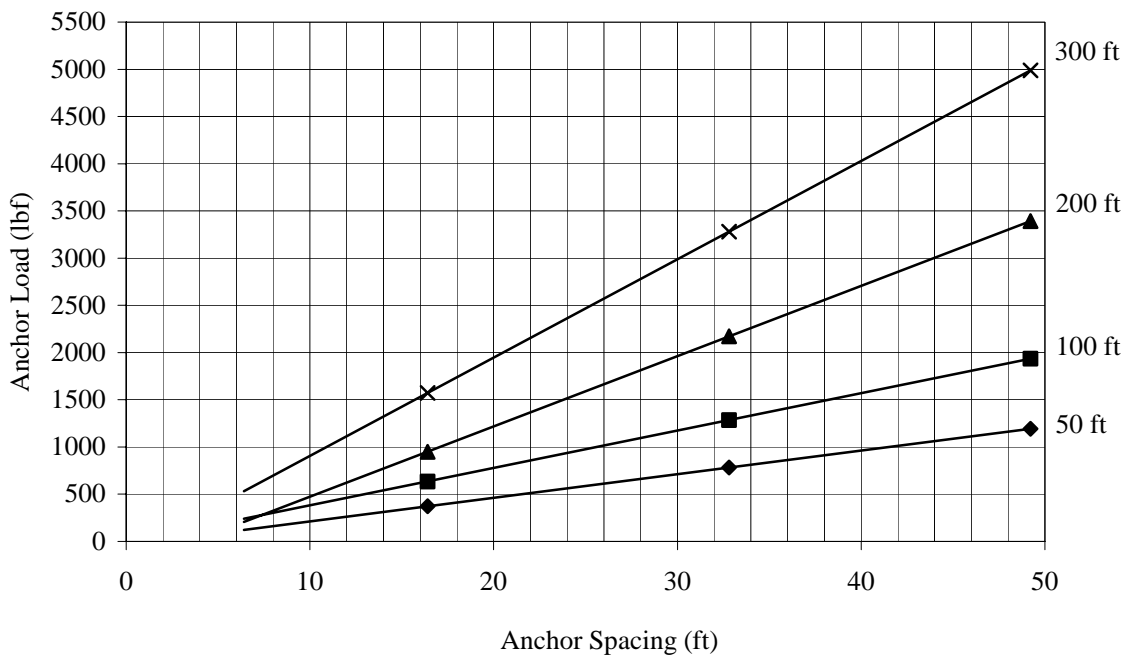


Figure D-14. Graph plots anchor load v. spacing for cable nets for a planar, 60° slope ranging in height from 50 to 300 ft (15 to 90 m).

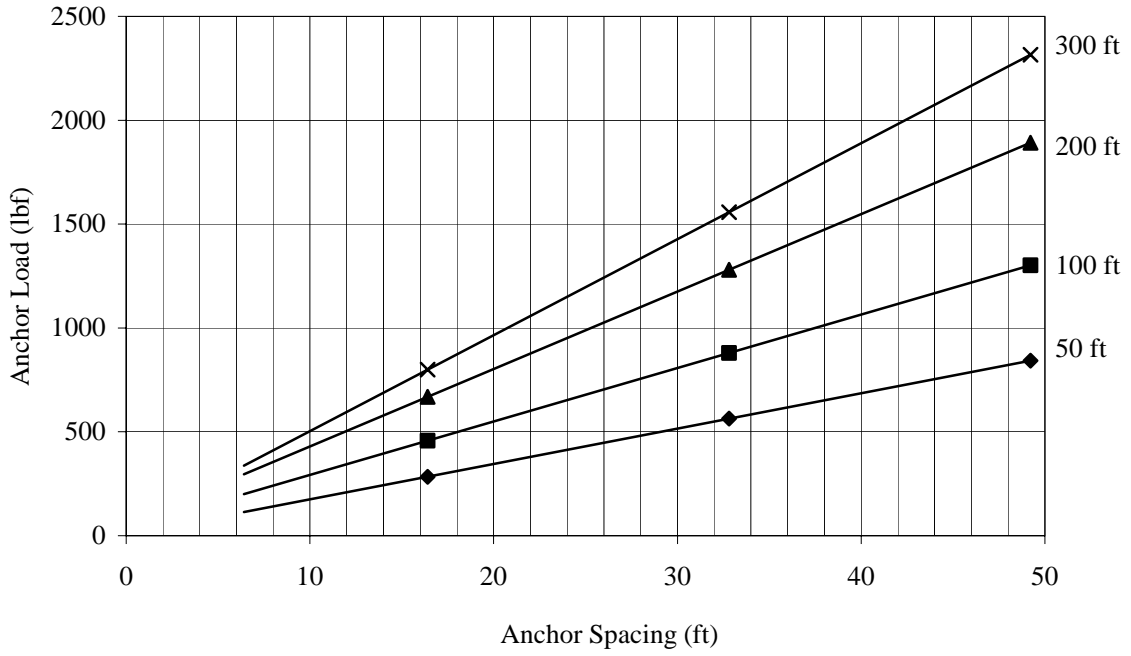


Figure D-15. Graph plots anchor load v. spacing for cable nets for an undulating, 45° slope ranging in height from 50 to 300 ft (15 to 90 m).

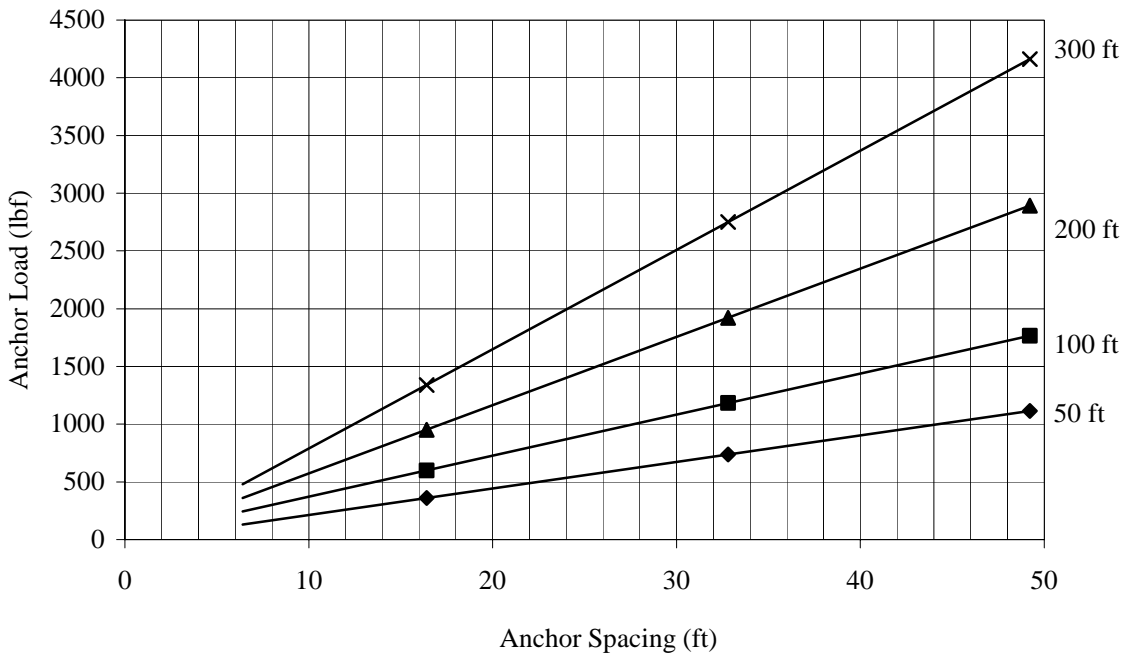


Figure D-16. Graph plots anchor load v. spacing for cable nets for an undulating, 60° slope ranging in height from 50 to 300 ft (15 to 90 m).

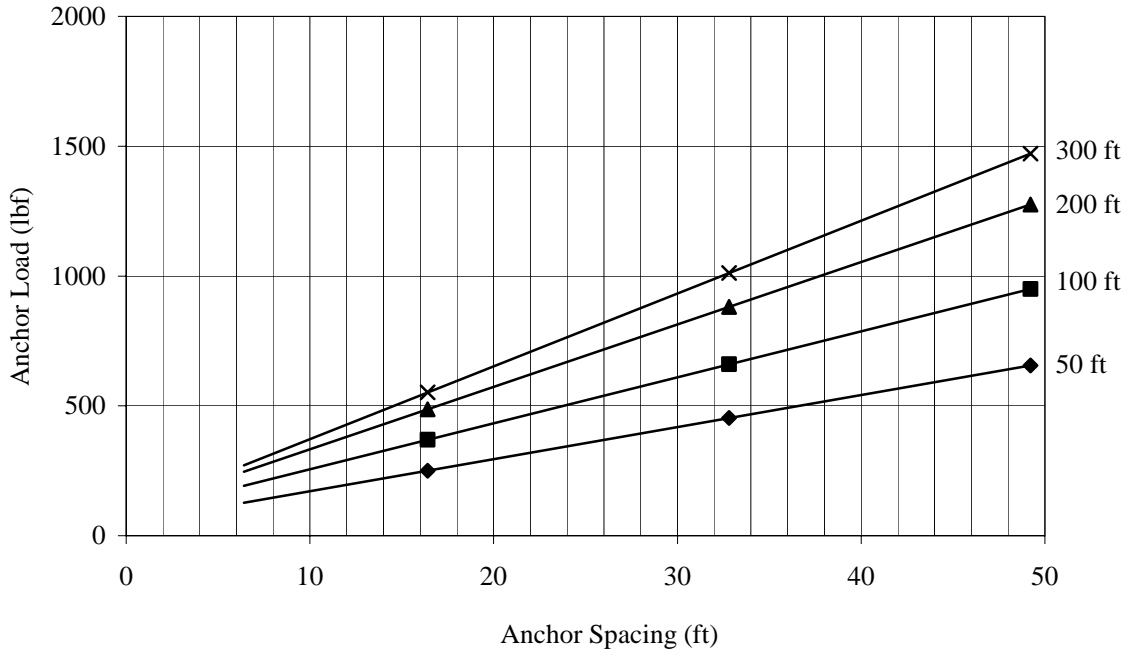


Figure D-17. Graph plots anchor load v. spacing for cable nets for a rough, 45° slope ranging in height from 50 to 300 ft (15 to 90 m).

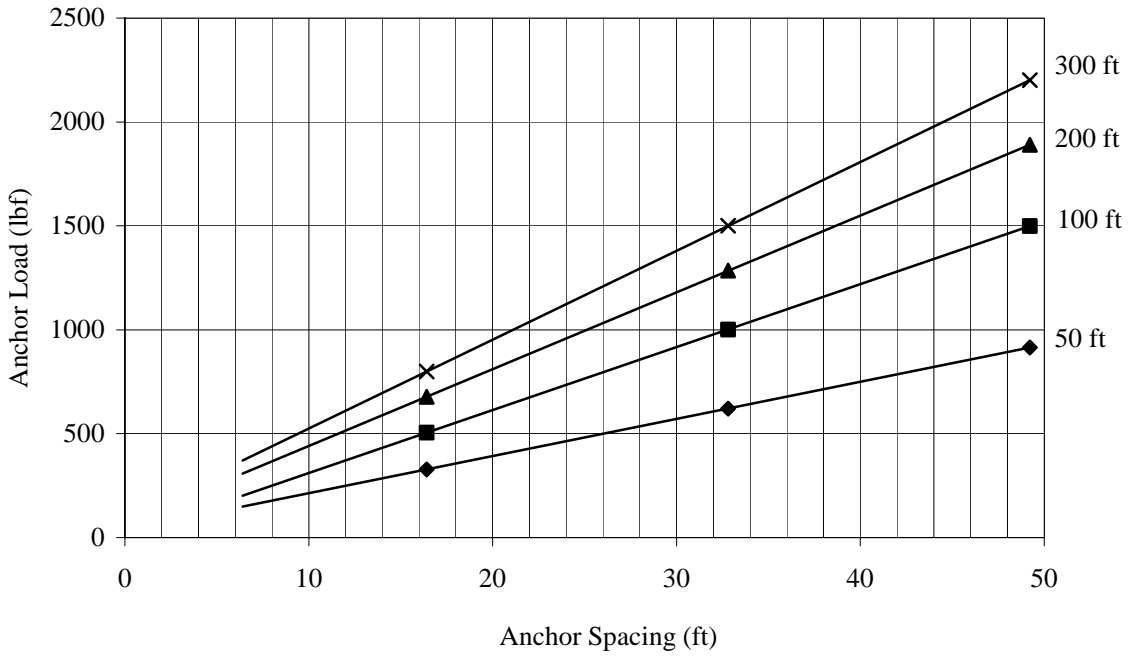


Figure D-18. Graph plots anchor load v. spacing for cable nets for a rough, 60° slope ranging in height from 50 to 300 ft (15 to 90 m).



**APPENDIX E**  
**PLAN SHEETS**

## **CONTENTS**

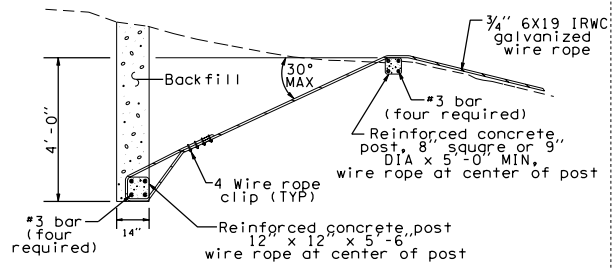
Wire Mesh/Cable Net Anchors

Cable Net Slope Protection

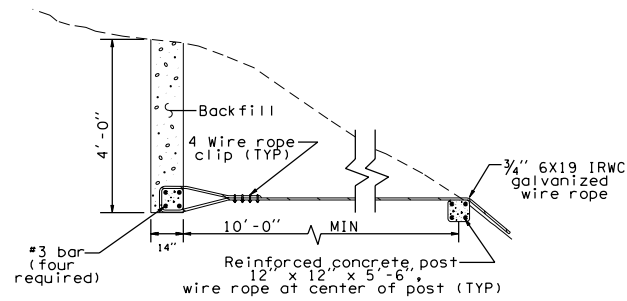
Wire Mesh Slope Protection

# Wire Mesh/Cable Net Anchors

## Soil Anchor Details

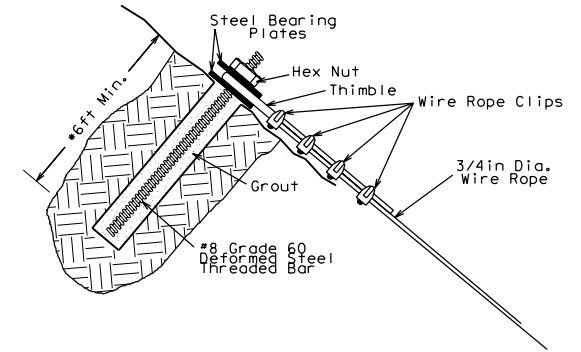


**Deadman Type 1**  
(for use in soil)

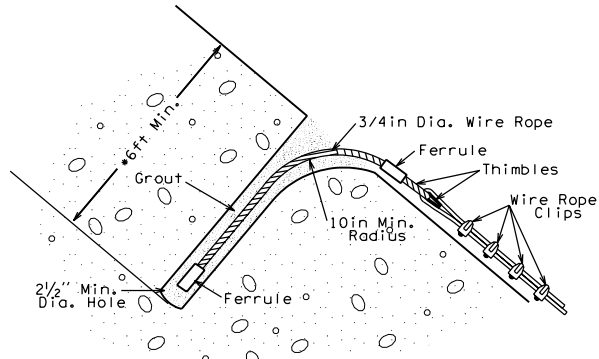


**Deadman Type 2**  
(for use in soil)

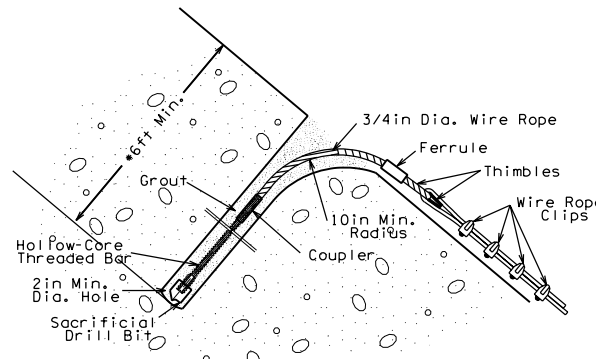
## Rock Anchor Details



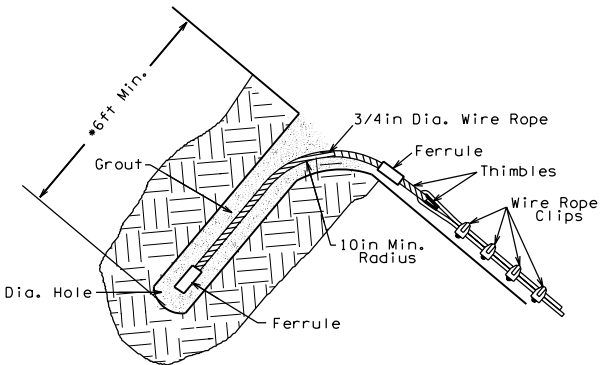
**Deformed Steel Threaded Bar**  
(for use in rock)



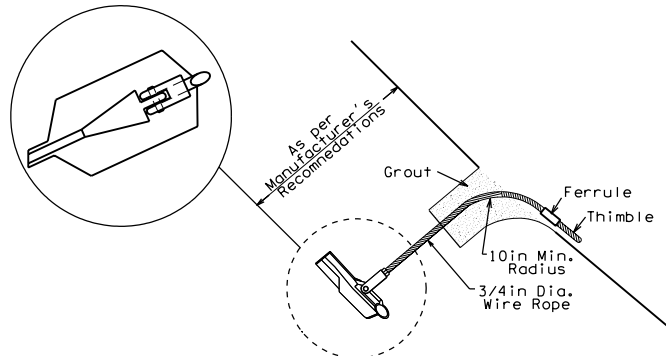
**3/4" Wire Rope**  
(for use in soil)



**Drillable-Groutable**  
(for use in soil)



**3/4" Wire Rope**  
(for use in rock)

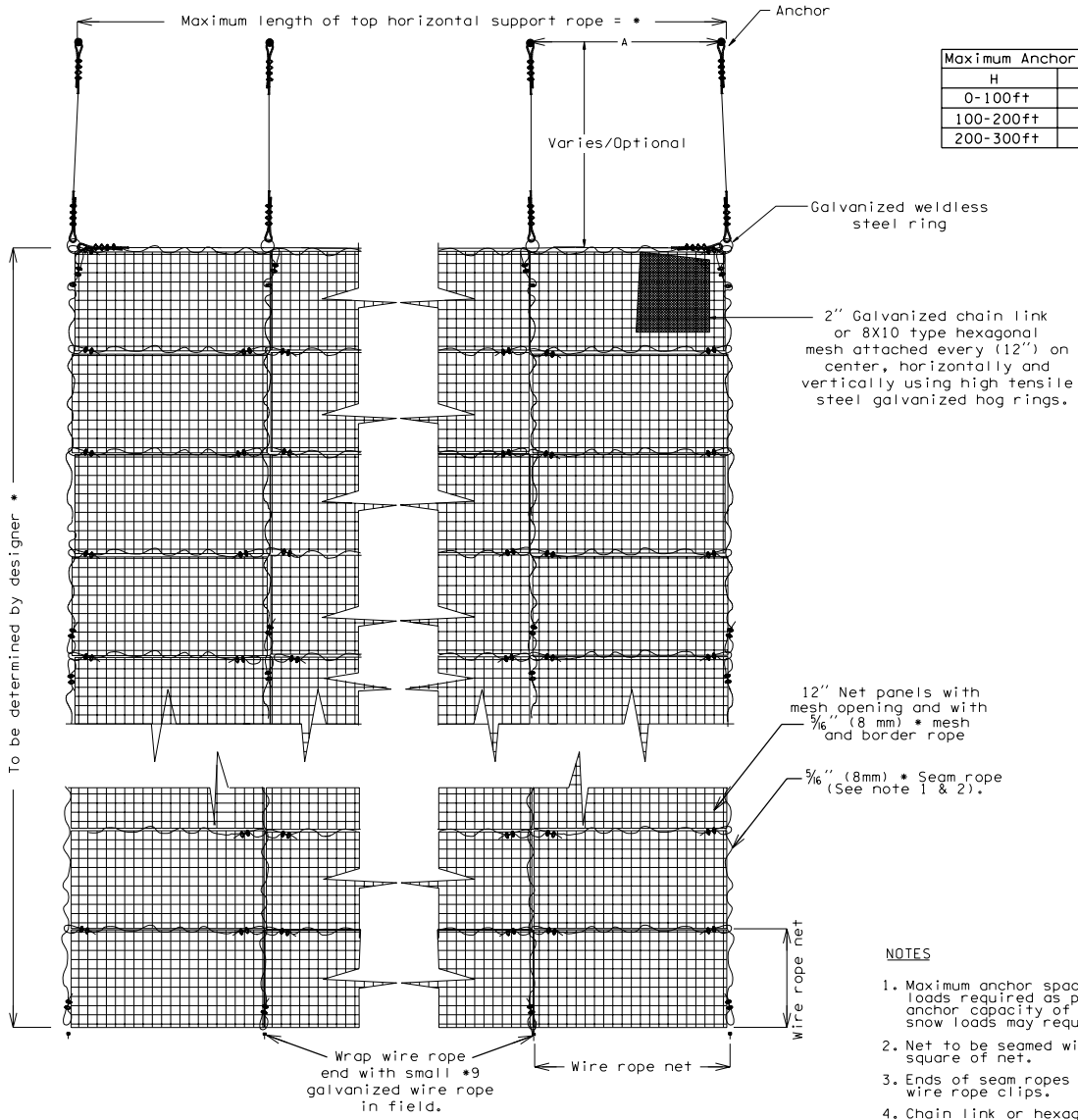


**Manta Ray®**  
(for use in soil)

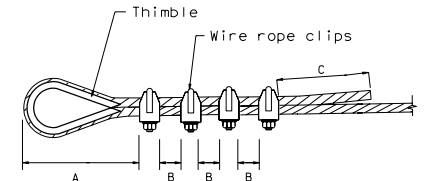
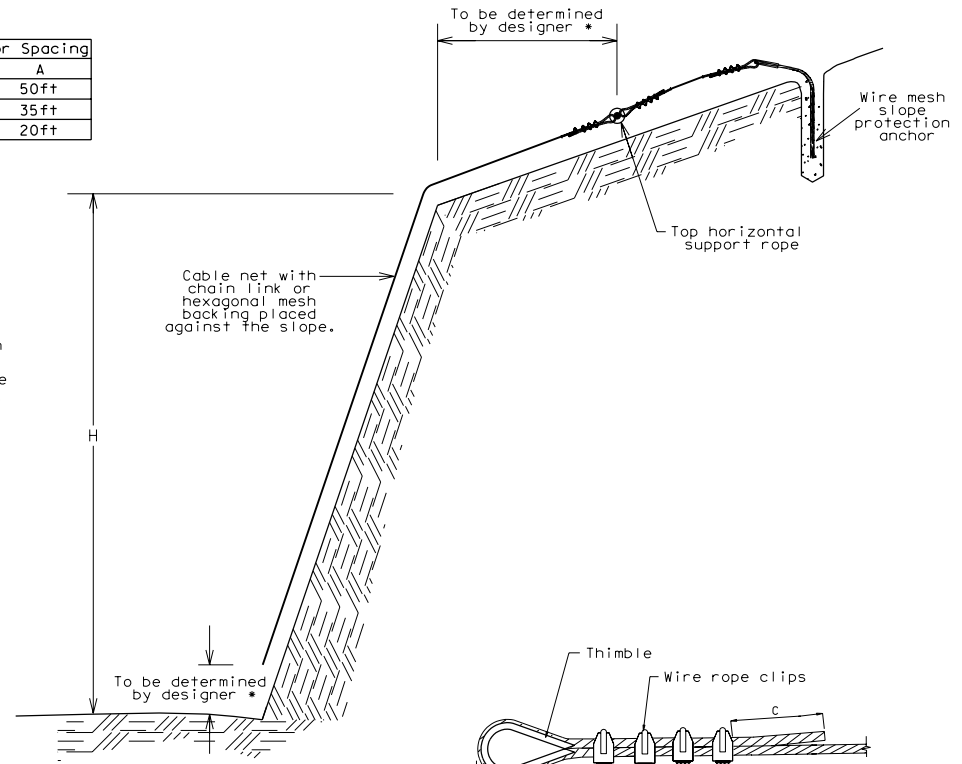
• Suggested minimum depth

• Suggested minimum depth

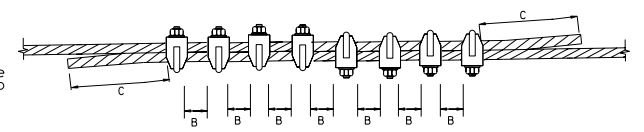
# Cable Net Slope Protection



Maximum Anchor Spacing	
H	A
0-100ft	50ft
100-200ft	35ft
200-300ft	20ft



WIRE ROPE DETAIL "AA"  
Distances A,B,C and torque to comply with manufacturer's specifications



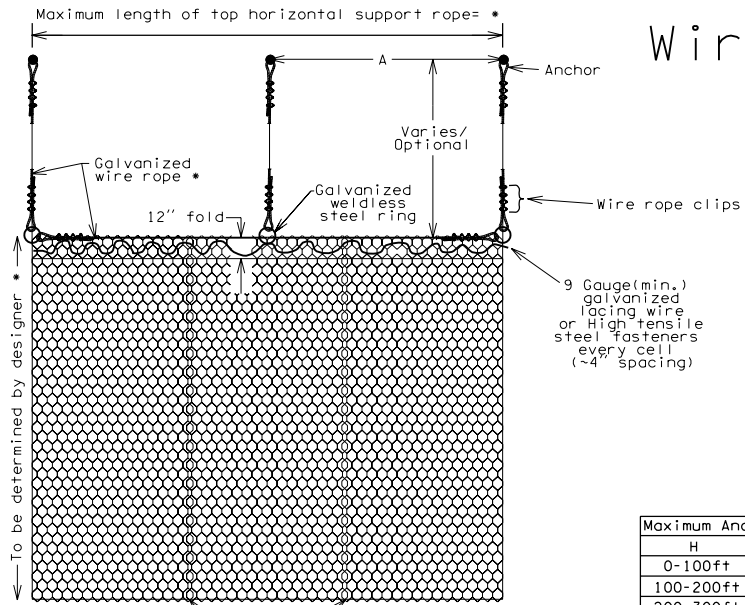
WIRE ROPE DETAIL "BB"  
WIRE ROPE SPLICING

## NOTES

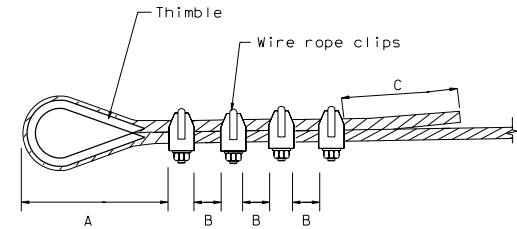
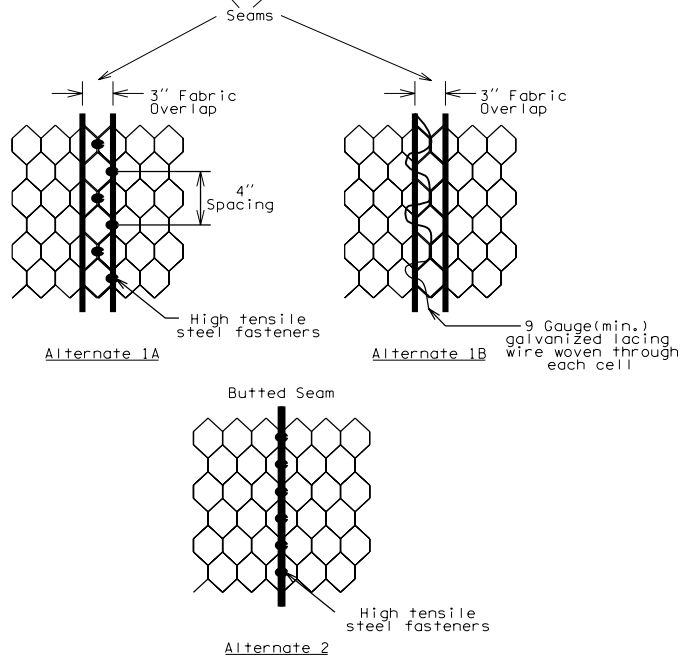
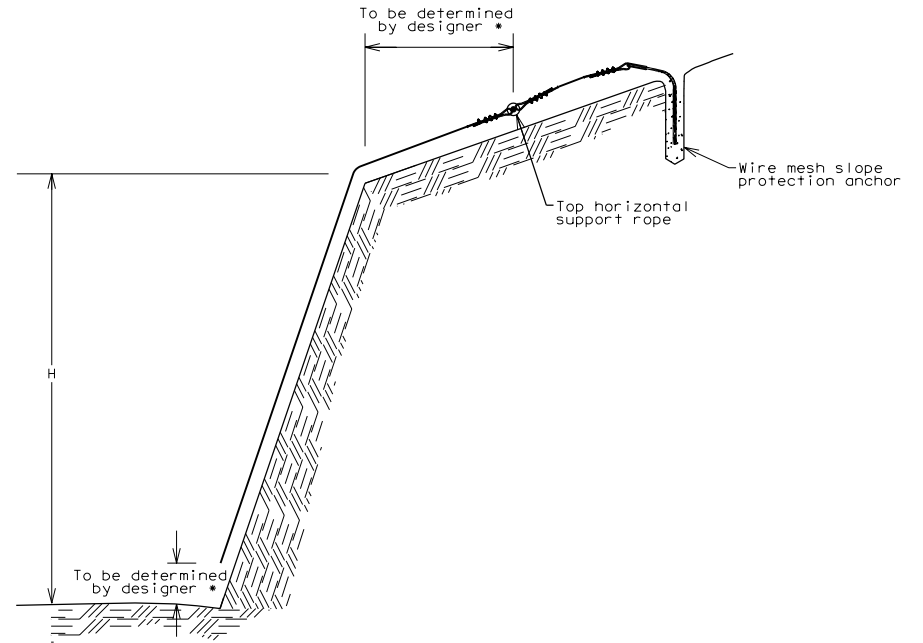
1. Maximum anchor spacing (A) for debris and impact loads required as per table for a minimum allowable anchor capacity of 20,000lbf. Systems subjected to snow loads may require narrower maximum spacing.
2. Net to be seamed with 5/8" wire ropes through each square of net.
3. Ends of seam ropes are to be terminated with (2) 5/8" wire rope clips.
4. Chain link or hexagonal mesh backing must be fastened to the cable net prior to placement on the slope.
5. \* See chapter 7 design guidelines.

FRONT SLOPE ELEVATION

# Wire Mesh Slope Protection



Maximum Anchor Spacing	
H	A
0-100ft	50ft
100-200ft	35ft
200-300ft	20ft



Distances A,B,C and torque to comply with manufacturer's specifications

## NOTES

1. Maximum anchor spacing (A) for debris and impact loads required as per table for a minimum allowable anchor capacity of 20,000lbf. Systems subjected to snow loads may require narrower maximum spacing.
2. \* See chapter 7 design guidelines.